

In compliance with the
Canadian Privacy Legislation
some supporting forms
may have been removed from
this dissertation.

While these forms may be included
in the document page count,
their removal does not represent
any loss of content from the dissertation.

**MOLECULAR ELECTROPHYSIOLOGY UNDERLYING
REPOLARIZATION IN CANINE CARDIAC PURKINJE CELLS:
CHARACTERIZATION AND SIGNIFICANCE**

by

Wei Han

Department of Pharmacology and Therapeutics

Faculty of Medicine

McGill University, Montreal

A thesis submitted to the Faculty of Graduate Studies and Research

McGill University, Montreal, Canada

In partial fulfillment of the requirements for the degree of

Doctor of Philosophy

© Wei Han December, 2002



National Library
of Canada

Bibliothèque nationale
du Canada

Acquisitions and
Bibliographic Services

Acquisisitons et
services bibliographiques

395 Wellington Street
Ottawa ON K1A 0N4
Canada

395, rue Wellington
Ottawa ON K1A 0N4
Canada

Your file *Votre référence*

ISBN: 0-612-88485-6

Our file *Notre référence*

ISBN: 0-612-88485-6

The author has granted a non-exclusive licence allowing the National Library of Canada to reproduce, loan, distribute or sell copies of this thesis in microform, paper or electronic formats.

L'auteur a accordé une licence non exclusive permettant à la Bibliothèque nationale du Canada de reproduire, prêter, distribuer ou vendre des copies de cette thèse sous la forme de microfiche/film, de reproduction sur papier ou sur format électronique.

The author retains ownership of the copyright in this thesis. Neither the thesis nor substantial extracts from it may be printed or otherwise reproduced without the author's permission.

L'auteur conserve la propriété du droit d'auteur qui protège cette thèse. Ni la thèse ni des extraits substantiels de celle-ci ne doivent être imprimés ou autrement reproduits sans son autorisation.

Canada

This thesis is dedicated to:

*my husband, Jian Lin, and my lovely son, Shaohan Lin
for their love, understanding, patience and support.*

ABSTRACT

Cardiac Purkinje fibers (PFs) play a very important role in cardiac electrophysiology. They are crucial for assuring appropriate timing and sequence of ventricle contraction and play an important role in cardiac arrhythmogenesis, largely via abnormalities in repolarization. Little work has been done to define the molecular electrophysiology of cardiac Purkinje cells (PCs). The primary hypothesis of this thesis was that PCs have unique molecular determinants of repolarization. The specific objectives were to characterize the repolarizing currents in isolated canine PCs, to clarify the molecular basis for these currents and to study role of PC current remodeling in a cardiac disease state. To achieve these goals, we used approaches at three different levels: the cellular level (with microelectrode techniques), the ionic level (with whole-cell patch clamp techniques) and molecular level (with competitive RT-PCR, Western blot analysis and immunocytochemistry).

We first optimized PC isolation techniques, which allowed us to characterize repolarizing currents and to visualize channel protein distribution by immunolocalization in cardiac PCs. We then characterized an important repolarizing current, the transient outward current (I_{to}) in canine PCs. We found that Purkinje I_{to} has some unique properties compared to those of atrial and ventricular I_{to} , suggesting a different molecular basis. We therefore characterized the expression of α -subunits encoding I_{to} -like currents and the K⁺-channel interacting protein 2 (KChIP2) β -subunit. We demonstrated important differences in the expression of Kv3.4, encoding a TEA-sensitive I_{to} channel, and of KChIP2, that might play an important role in the specific molecular composition of Purkinje I_{to} . We also characterized another important repolarizing current, the delayed rectifier (I_K) that had been reported to be absent or small in PCs. We found that I_K in PCs has properties typical of those observed in other regions of the heart; and I_K channel subunits ERG, KvLQT1 and minK were more sparsely expressed in PCs than in ventricular muscle (VM), potentially explaining the tendency of PCs to generate arrhythmias due to abnormal repolarization. We also noted important differences in the expression of the Ca²⁺-channel subunits (Ca_v1.2, Ca_v3.1, 3.2 and 3.3), the Na⁺/Ca²⁺-exchanger subunit NCX1 and the hyperpolarization-activated channel subunits HCN1, 2 and 4. Studies in human PCs confirmed that some of the unique PC ionic properties observed in dogs are also present in man. Finally, we showed that an experimental cardiac disease paradigm (congestive heart failure) causes characteristic ionic remodeling in PCs that may explain their role in potentially lethal arrhythmias associated with heart failure.

Our findings support the hypothesis of a unique and important molecular basis for the control of repolarization in cardiac PCs.

ABRÉGÉ FRANÇAIS

Les fibres de Purkinje (FP) jouent un rôle très important dans l'électrophysiologie cardiaque. Elles assurent aux ventricules une contraction séquentielle dans un espace temps approprié. Elles sont également responsables de la genèse des arythmies par l'intermédiaire d'anomalies au niveau de la repolarisation du potentiel d'action cardiaque. Très peu d'études ont été entreprises pour définir les caractéristiques moléculaires de l'électrophysiologie cardiaque des cellules de Purkinje (CP). L'hypothèse principale de cette thèse était de démontrer que les CP ont des propriétés moléculaires uniques dans la repolarisation cardiaque. Les objectifs spécifiques étaient de caractériser les courants repolarisants dans des CP isolées de chien, de clarifier la base moléculaire de ces courants et d'étudier leur modification d'expression (remodelage) dans un cas de pathologie cardiaque. Afin de répondre à ces objectifs, nous avons utilisé des approches à trois différents niveaux: Au niveau cellulaire (techniques de microélectrodes), au niveau ionique (techniques de patch clamp en configuration cellule entière) et au niveau moléculaire (competitive RT-PCR, analyse de Western blot et immunocytochimie).

Nous avons tout d'abord optimisé les techniques d'isolation de CP, nous permettant ainsi de caractériser les courants repolarisants et de visualiser la distribution protéique des canaux par immunolocalisation dans les CP cardiaques. Nous sommes attachés plus particulièrement à la caractérisation d'un important courant repolarisant, le courant transitoire sortant (I_{to}) dans les CP de chien. Nous avons déterminé que le courant I_{to} dans les FP avait des propriétés uniques comparé à celles du même courant dans les cellules auriculaires et ventriculaires, suggérant une base moléculaire différente. Par conséquent, nous avons caractérisé l'expression des sous unités alpha encodant des courants de type I_{to} ainsi que la sous unité β (protéines interagissant avec les canaux K^+ ou KChIP2). Nous avons démontré des différences importantes dans l'expression de Kv3.4, portant un courant I_{to} sensible au TEA, ainsi que dans celle de KChIP2. Ceux-ci peuvent jouer un rôle important dans la composition moléculaire spécifique de I_{to} dans les FP. Nous avons également caractérisé un autre courant repolarisant important, le courant retardé à rectification sortante (I_K), reporté comme étant absent ou très petit dans les CP. Nous avons trouvé que I_K dans les CP a des propriétés typiques de celles observées dans d'autres régions du coeur. Nous avons mis en évidence que les sous unités codant pour I_K , soit HERG, KvLQT1 et minK, étaient exprimées de façon plus parsemée dans les CP que dans le muscle ventriculaire (ceci pouvant expliquer la tendance des CP à provoquer des arythmies dues à une repolarisation anormale). Nous avons également noté des différences dans l'expression de sous unités de canaux calciques ($Ca_v1.2$, $Ca_v3.1$, 3.2 and 3.3), de la sous unité NCX1 de l'échangeur Na^+/Ca^{2+} , et de sous unité du canal activé par hyperpolarisation HCN1,2 et 4. Des études dans les CP humaines ont confirmé que certaines des propriétés ioniques uniques des CP observées chez le chien étaient également présentes chez l'humain. Finalement, nous avons démontré qu'un état pathologique cardiaque expérimental (insuffisance cardiaque) causait un remodelage ionique caractéristique dans les CP, pouvant ainsi expliquer leur rôle dans des arythmies léthales associées à l'insuffisance cardiaque.

Nos résultats supportent l'hypothèse d'une base moléculaire unique et importante dans le contrôle de la repolarisation des CP cardiaques.

ACKNOWLEDGMENTS

I am heartily indebted to my supervisor, Dr. Stanley Nattel. Were it not for his extraordinary supervision, persistent encouragement, invaluable support, enthusiastic inspiration, pertinent guidance, constructive criticism, creative discussion, careful proof-reading and correcting of all the manuscripts and this thesis, my graduate studies and this thesis would never have been completed.

I am sincerely indebted to Dr. Zhiguo Wang, for his hands-on training in molecular and patch-clamp methods, for his constructive and helpful suggestions and also for his strong recommendation in my application for studentship and fellowship training.

I am deeply and especially grateful to a wonderful couple, Dr. Lixia Yue and Jianlin Feng, for their unforgettable help in my molecular and patch-clamp studies, for their suggestions and friendship.

My special thanks go to the Department of Pharmacology and Therapeutics for giving me the opportunity to pursue my graduate studies in this wonderful department, to the Montreal Heart Institute for its wonderful milieu and nice people.

My deep thanks go to Dr. Alvin Shrier and Dr. Daya Vama, for their strong recommendations in my application for studentship and fellowship funding.

I would like to extend my thanks to Dr. Céline Fiset, Dr. Terence Hebert, and Dr. Bruce Allen, for their knowledge and useful suggestions in my studies; as well as Chantal St-Cyr, Evelyn Landry, Chantal Maltais, Xiaofan Yang and Nathalie L'Heureux for their excellent technique assistance.

I wish to express my sincere gratitude to all my colleagues with whom I have spent time in the lab, including Liming Zhang, Weishen Bao, Denis Chartier, Gernot Schram, Danshi Li, Marc Pourrier, Jim Kneller, Pang Li, Hong Han, Renqiang Zou for their collaboration, friendship and assistance in different aspects of my life and laboratory work.

I would like to express my special thanks to Marc Pourrier, for his generous and careful translation of the abstract from English into French.

In my personal life, I am blessed with a wonderful family. Family members whose love I treasure always include my parents and my brothers.

Special thanks go to the Heart and Stroke Foundation of Canada for its financial support from 2001-2002.

PREFACE

Note on the format of this thesis:

In accordance with the Faculty of Graduate Studies and Research the candidate has the option of including as part of the thesis the text of original papers already published by learned journals, and original papers submitted or suitable for submission to learned journals. The exact wording relating to this option is as follows:

Candidates have the option of including, as part of the thesis, the text of one or more papers submitted or to be submitted for publication, or the clearly-duplicated text of one or more published papers. These texts must be bound as an integral part of the thesis.

If this option is chosen, connecting text that provide logical bridges between the different papers are mandatory. The thesis must be written in such a way that it is more than a mere collection of manuscripts; in other words, results of a series of papers must be integrated.

The thesis must still confirm to all other requirements of the “Guideline for Thesis Preparation”. The thesis must include: a table of content, an abstract in English and French, an introduction which clearly states the rationale and objectives of the study, a review of the literature, a final conclusion and summary, and a thorough bibliography or reference list.

Additional material must be provided where appropriate (e.g. appendices) and in sufficient detail to allow a clear and precise judgment to be made of the importance and originality of the research reported in the thesis.

In the case of manuscripts co-authored by the candidate and others, the candidate is required to make an explicit statement in the thesis as to who contribute to such work and to what extent. Supervisors must attest to the accuracy of such statement at the doctoral oral defense. Since the task of the examiners is made more difficult in these cases, it is in the candidate's interest to make perfectly clear the responsibilities of co-authored papers.

This thesis consists of the following published papers and submitted papers co-authored by myself and others:

1. **Wei Han**, Zhiguo Wang and Stanley Nattel. A comparison of transient outward currents in canine cardiac Purkinje cells and ventricular myocytes. *Am. J. Physiol. Heart Circ Physiol.* 2000; 279(2): H466-H474.
2. **Wei Han**, Zhiguo Wang and Stanley Nattel. Slow delayed rectifier current and repolarization in canine cardiac Purkinje cells. *Am. J. Physiol Heart Circ Physiol.* 2001; 280(3): H1075-H1080.
3. **Wei Han**, Denis Chartier, Danshi Li and Stanley Nattel. Ionic remodeling of cardiac Purkinje cells by congestive heart failure. *Circulation.* 2001; 104(17): 2095-2100.
4. **Wei Han**, Weishen Bao, Zhiguo Wang and Stanley Nattel. Comparison of ion-channel subunit expression in canine cardiac Purkinje fibers and ventricular muscle. *Circ. Res.* 2002; 91(9): 790-7.
5. **Wei Han**, Liming Zhang, Gernot Schram and Stanley Nattel. Properties of potassium currents in Purkinje cells of failing human hearts. *Am. J. Physiol. Heart Circ Physiol.* 2002; 283(6): H2495-503.

STATEMENT OF AUTHORSHIP

The following is a statement regarding the contributions of co-authors and myself to the papers included in this thesis.

Paper 1. I established the Purkinje cell isolation technique and made the initial findings. I designed and performed the experiments and analyzed all of data and wrote the manuscript. Zhiguo Wang helped me designing the protocol and solved some problems in the patch clamp set-up. Dr. Nattel provided close supervision in all aspects, generating the initial idea, clarifying the thoughts, and producing the final version of the manuscript

Paper 2. The idea came in discussion with my supervisor. I performed all of the experimental work and data analysis, made the initial findings and wrote the manuscript. Zhiguo Wang provided me with the protocol for AP clamp and technical suggestions. Dr. Nattel provided close supervision in all aspects, clarifying the ideas, reorganizing the data and producing the final version of the manuscript

Paper 3. The idea was based on previous work done in our lab. I designed and completed all of the ionic current studies and data analysis, and wrote the manuscript. Denis Chartier conducted AP studies, analyzed the corresponding data, and the Figure 7. Danshi Li provided tissues from dogs with congestive heart failure. Dr. Nattel provided overall supervision, clarified the ideas, and produced the final version of the manuscript.

Paper 4. The work was suggested by my supervisor. I designed and performed the experiments in human cardiac Purkinje cells and analyzed all of the data and wrote most of the manuscript. Liming Zhang conducted the I_{to} recordings in human ventricular myocytes and Gernot Shram did the I_{K1} experiments in human ventricular myocytes. Dr. Nattel closely supervised, clarified the ideas, reorganized the data and produced the final version of the manuscript.

Paper 5. The idea was based on my previous work. I performed all of experiments and data analysis, and wrote the manuscript. Weishen Bao prepared some solutions and did some experiments for me. Dr. Wang taught me competitive RT-PCR techniques and provided some technical suggestions. Dr. Nattel closely supervised, clarified the ideas, reorganized the data and produced the final version of the manuscript.

LIST OF ABBREVIATION

Anatomical aspect:

SA	Sino-atrial
AV	Atrial-ventricular
PF(s)	Purkinje Fiber(s)
PC(s)	Purkinje Cell(s)
VM	Ventricular Myocytes/Muscle
VC(s)	Ventricular Myocyte(s)
Midmyocardial	M
Left (right) atria	L(R)A
Left (right) ventricle	L(R)V
SR	Sarcoplasmic Reticulum

Electrophysiological aspect:

AP(s)	Action Potential(s)
APA	Action Potential Amplitude (mV)
APD	Action Potential Duration (ms)
APD20	Action Potential Duration to 20% Repolarization (ms)
APD50	Action Potential Duration to 50% Repolarization (ms)
APD70	Action Potential Duration to 70% Repolarization (ms)
APD90	Action Potential Duration to 90% Repolarization (ms)
APD95	Action Potential Duration to 95% Repolarization (ms)
V_{\max}	Maximal Upstroke Velocity
EC coupling	Excitation-Contraction Coupling
I_{Na}	Inward Na^{2+} Current
I_{Ca}	Inward Ca^{2+} Current
$I_{\text{Ca.L}}$	L-type Ca^{2+} Current
$I_{\text{Ca.T}}$	T-type Ca^{2+} Current
$I_{\text{f}}, I_{\text{(h)}}$	Funny, hyperpolarization-activated Inward Current

I_A	A-type Transient Outward K^+ Current
I_{to} (I_{to1})	Transient Outward K^+ Current
I_{to2} ($I_{Cl,Ca}$)	Ca^{2+} -activated Cl^- current
I_K	Delayed Rectifier K^+ Current
I_{Kr}	Rapidly-activated Delayed Rectifier K^+ Current
I_{Ks}	Slowly-activated Delayed Rectifier K^+ Current
I_{Kur}	Ultrarapidly-activated Delayed Rectifier K^+ Current
I_{sus}	Sustained Depolarization-induced Outward K^+ Current
I_{KI}	Inward Rectifier K^+ Current
I_{KACh}	ACh-induced Inward Rectifier K^+ Current
I_{KATP}	ATP-induced Inward Rectifier K^+ Current
I_{NCX}	Na/Ca Exchanger Current
I_p	Na/K Pump Current
$I_{Cl,basal}$	Background Cl^- Conductance
$I_{Cl,PKA}$	PKA-induced Cl^- Current
$I_{Cl,PKC}$	PKC-induced Cl^- Current
$I_{Cl,swell}$	Swelling-activated Cl^- Current
E_{rev}	Reversal Potential
HP	Holding Potential
TP	Test Potential
I-V relation	Current-voltage Relation
C_m	Membrane Capacity
R_s	Series Resistance
R_i	Internal Resistance
R_m	Membrane Resistance
$V_{1/2}$	Half maximal voltage for activation or inactivation
κ	Slope factor
P	Pulse
pA	Picoampere
pF	Picofarad
τ	Time Constant

τ_1 (τ_{fast})	Fast Component Time Constant
τ_2 (τ_{slow})	Slow Component Time Constant

Signal transductional and pharmacological aspects:

AC	Adenylate Cyclase
ACh	Acetylcholine
AKAPs	A-Kinase-Anchoring Proteins
Ang-II	Angiotensin II
ACE	Angiotension Converting Enzyme
cAMP	Adenosine-3, 5,-cyclic Monophosphate
CaMKII	Ca ²⁺ /Calmodulin-dependent protein kinase II
DAG	Diacylglycerol
G _α	α-subunits of G-protein
G _{βγ}	β- and γ- subunits of G-protein
G _i	PTX-sensitive G-protein
G _q	PTX-insensitive G-protein
G _s	Stimulatory G-protein
IP ₃	Inositol 1, 4, 5-triphosphate
PKA	Protein Kinase A
PKC	Protein Kinase C
PLC	Phospholipase C
PTX	Pertussis Toxin
4AP	4-aminopyridine
BDS	Blood-depressing Substance
DTX	Dendrotoxin
DIDS	4,4'-Diisothiocyanatostilbene-2,2'-disulfonic Acid
DHP	Dihydropyridines
H ₂ O ₂	Hydrogen Peroxide
ISO	Isoproterenol
PE	Phenylephrine
PMA	Phorbol 12-myristate 13-acetate

STX	Saxitoxin
TEA	Tetraethylammonium
TTX	Tetrodotoxin

Molecular biological aspects:

EB	Ethidium Bromide
NBD	Nucleotide Binding Domain
PCR	Polymerase Chain Reaction
RT	Reverse Transcription

Pathophysiological aspects:

EAD(s)	Early Afterdepolarization(s)
DAD(s)	Delayed Afterdepolarization(s)
CHF	Congestive Heart failure
MI	Myocardium Infraction
TdP	Torsade de Pointes

LIST OF FIGURES AND TABLES

Chapter 1

- Figure 1 Schematic representation of the heart (left panel) and action potential waveforms recorded in different regions of the heart.
- Figure 2 Cable-like cell and its electrical analogue.
- Figure 3 Organization of connexins into connexons, intercellular channels, and gap junctions.
- Figure 4 Phylogenetic relationships by maximum parsimony analysis of rat sodium channels $\text{Na}_v1.1$ - $\text{Na}_v1.9$ and Na_x .
- Figure 5 Schematic depiction of the Na channel topology (A) and aligned P-loop amino acid sequences for all four domains of cardiac Na channel (top) and skeletal muscle Ca channel (lower) (B).
- Figure 6 A topology model of Ca^{2+} channel composed of α_1 and associated auxiliary subunits of β , α_2 and δ .
- Figure 7 Schematic representation of the structural classification of K^+ channel subunits
- Figure 8 Model of the Na/Ca exchanger.
- Figure 9 Ion channels underlie cardiac excitability.
- Figure 10 Schematic depiction of ion channel regulation by G-protein-mediated PKA and PKC signaling pathways via stimulation of cardiac membrane receptors.
- Table 1 Mammalian Na^+ channel α subunits.
- Table 2 Subunit composition and function of Ca^{2+} channel types.
- Table 3 Classification of cloned K^+ channels
- Table 4 HCN channel subunits

Chapter 2

Paper 1

- Figure 1 Purkinje cell action potential on the onset of stimulation at 2Hz.
- Figure 2 Purkinje cell I_{to} and its I-V relations of activation and inactivation.

- Figure 3 Time-dependent inactivation of I_{to} in Purkinje cells and ventricular myocytes.
- Figure 4 A comparison of I_{to} recovery and frequency-dependence in Purkinje cells and ventricular myocytes
- Figure 5 Inhibition of Purkinje cell and ventricular myocyte by 4AP
- Figure 6 Effects of TEA on Purkinje cell and ventricular myocyte I_{to} .
- Figure 7 Effects of flecainide on Purkinje cell and ventricular myocyte I_{to} .
- Figure 8 Effects of H_2O_2 on I_{to} inactivation in Purkinje cells and ventricular myocytes.
- Figure 9 Effects of blood-depressing substance and dendrotoxin on Purkinje cell I_{to} .
- Figure 10 Effects of 4AP and TEA on APs of Purkinje cells.

Paper 2

- Figure 1 Photomicrographs of human cardiac Purkinje cells (left) and Ventricular myocytes (right) at comparable magnifications.
- Figure 2 Comparison of human Purkinje cell and ventricular myocyte I_{K1} .
- Figure 3 I_H in human Purkinje cells.
- Figure 4 Comparison of human Purkinje cell and ventricular myocyte I_{to} .
- Figure 5 Recovery and rate-dependence of human Purkinje cell and ventricular myocyte I_{to} .
- Figure 6 4AP and TEA effects on human Purkinje cell and ventricular myocyte I_{to} .
- Figure 7 4AP and TEA effects on human Purkinje cell I_{sus} .
- Table 1 Patient characteristics.

Chapter 3

Paper 3

- Figure 1 I_{to} subunit mRNA-expression.
- Figure 2 Protein expression and immunolocalization of Kv4.3.
- Figure 3 Protein expression and immunolocalization of Kv3.4.
- Figure 4 mRNA and protein expression of I_K subunits.
- Figure 5 mRNA and protein expression of $Ca_v1.2$ subunit and NCX1.
- Figure 6 mRNA and protein expression of HCN isoforms.

Figure 7 mRNA expression of Cav3 subunits.

Table 1 Conditions used for competitive RT-PCR.

Chapter 4

Figure 1 Delayed rectifier current (I_K) in isolated single canine cardiac Purkinje cells.

Paper 4

Figure 1 Concentration-dependent effects of Iso on I_{Ks} .

Figure 2 Iso effects on the kinetics and V_{50} of I_{Ks} .

Figure 3 Influence of 293 B, Iso, and 293B + Iso on action potential.

Figure 4 Currents affected by Iso and 293B, as indicated by AP-clamp methods.

Figure 5 Effects of Iso and 293B on Purkinje cell action potentials in the absence of I_{to} .

Chapter 5

Paper 5

Figure 1 CHF effects on I_{Ks} .

Figure 2 CHF effects on I_{to} .

Figure 3 CHF effects on I_K .

Figure 4 CHF effects on I_{CaL} .

Figure 5 CHF effects on I_{CaT} .

Figure 6 CHF effects on I_{NCX} .

Figure 7 CHF effects on action potentials.

Table 1 Comparison of AP properties in control and CHF Purkinje cells at 1 Hz.

Chapter 6

Figure 1 Ionic determinants of the Purkinje cell repolarization.

TABLE OF CONTENTS

TITLE.....	i
DEDICATION.....	ii
ABSTRACT.....	iii
ABRÉGÉ FRANÇAIS.....	iv
ACKNOWLEDGMENTS.....	v
PREFACE.....	vi
STATEMENT OF AUTHORSHIP.....	viii
LIST OF ABBREVIATION.....	x
LIST OF FIGURES AND TABLES.....	xiv
TABLE OF CONTENTS.....	xvii
CHAPTER 1. INTRODUCTION	1
1. What is a Purkinje cell?.....	2
1.1 Gene makers and origin of Purkinje fibers.....	2
1.2 Purkinje fiber physiological functions and roles in pathological disease states (potential arrhythmogenesis).....	3
2. Classical early studies of Purkinje fiber currents	4
3. Cardiac electrophysiology-speciality of cardiac Purkinje fibers excitability.....	5
3.1 Cardiac action potential.....	6
3.2 Properties of ionic currents underlying cardiac action potentials	7
3.2.1 Depolarizing currents	8
3.2.1.1 Sodium currents (I_{Na})	8
3.2.1.1.1 Fast I_{Na}	8
3.2.1.1.2 Slow I_{Na}	10
3.2.1.2 Calcium currents (I_{Ca}).....	12
3.2.1.2.1 Functions of I_{Ca}	12
3.2.1.2.2 L-type and T-type Ca currents	13
3.2.1.3 Hyperpolarization-activated current (I_f).....	14
3.2.2 Repolarizing currents	15
3.2.2.1 Potassium currents.....	16
3.2.2.1.1 Transient outward current (I_{to})	16
3.2.2.1.1.1 Species and regional differences.....	18
3.2.2.1.1.2 Physiological roles.....	19
3.2.2.1.2 Delayed rectifier currents (I_K).....	19
3.2.2.1.3 Ultrarapid rectifier current (I_{Kur}).....	23
3.2.2.1.4 Inward rectifier currents.....	23
3.2.2.1.4.1 Classical inward rectifier current: I_{K1}	24
3.2.2.1.4.2 I_{KACH}	25
3.2.2.1.4.3 I_{KATP}	25
3.2.2.2 Other ion transporters	26
3.2.2.2.1 Na/Ca exchanger current (I_{NCX}).....	26
3.2.2.2.2 Na/K pump	27
3.2.2.3 Other repolarizing currents.....	28
3.3 Passive properties of Purkinje fibers	29
3.3.1 Definition of passive properties	29
3.3.2 Architecture of cable-like Purkinje false tendons	30

3.3.3 Gap junctions and connexins.....	31
4. Molecular basis of cardiac ion channels.....	34
4.1 Na ⁺ channel	34
4.2 Ca ²⁺ channels.....	43
4.2.1 Molecular basis for Ca ²⁺ channels function	44
4.2.2 L-type Ca ²⁺ channel.....	45
4.2.3 T-type Ca ²⁺ channel.....	45
4.3 K ⁺ channels.....	46
4.3.1 Molecular basis of <i>I</i> _{to}	51
4.3.2 Molecular basis of <i>I</i> _K	54
4.3.3 Molecular basis of <i>I</i> _{Kur}	58
4.3.4 Molecular basis of inward rectifier currents.....	59
4.3.4.1 <i>I</i> _{K1}	59
4.3.4.2 <i>I</i> _{KACh}	60
4.3.4.3 <i>I</i> _{KATP}	61
4.4 Molecular basis of <i>I</i> _f	61
4.5 Other ion transporters.....	63
4.5.1 Na/Ca exchanger (NCX)	63
4.5.2 Molecular basis of Na/K pump	65
5. Summary of ionic and molecular basis of the cardiac action potential.....	66
6. Modulation of cardiac ionic currents	68
6.1 Ionic currents regulated by G-protein-mediated signal transduction pathways	68
6.1.1 <i>I</i> _{Na}	69
6.1.2 <i>I</i> _{Ca}	70
6.1.3 Na/Ca exchanger	71
6.1.4 <i>I</i> _{to}	72
6.1.5 <i>I</i> _K	73
6.1.6 <i>I</i> _{K1}	74
6.1.7 <i>I</i> _{Kur}	75
6.2 Ionic remodeling	75
6.2.1 <i>I</i> _{Na}	75
6.2.2 <i>I</i> _{Ca}	76
6.2.3 Na/Ca exchanger	77
6.2.4 K ⁺ currents.....	78
6.2.4.1 <i>I</i> _{to}	78
6.2.4.2 <i>I</i> _K	78
6.2.4.3 <i>I</i> _{K1}	79
7. Questions raised from above overview	80
8. Approaches to address the questions.....	81
9. References	82
CHAPTER 2. CHARACTERIZATION OF POTASSIUM CURRENTS IN CANINE AND HUMAN CARDIAC PURKINJE CELLS.....	137
CHAPTER 3. MOLECULAR CHARACTERIZATION OF ION CHANNELS UNDERLYING PURKINJE CELL REPOLARIZATION	182

CHAPTER 4. PRESENCE OF DELAYED RECTIFIER CURRENT AND POTENTIAL ROLE OF SLOW DELAYED RECTIFIER CURRENT IN ABNORMAL REPOLARIZATION-RELATED ARRHYTHMOGENESIS.....	217
CHAPTER 5. PURKINJE CELL IONIC REMODELING BY CONGESTIVE HEART FAILURE.....	226
CHAPTER 6. GENERAL DISCUSSION.....	233
6.1 Summary of novel findings in the thesis and significance of this work in context of the literature	234
6.1.1 Unique properties and potential molecular basis of Purkinje I_{to}	234
6.1.2 Characterization of some K^+ currents in human Purkinje cells.....	237
6.1.3 Demonstration of the presence of I_K in canine cardiac Purkinje cells and characterization of the expression profiles of Ca^{2+} , NCX and HCN channels	237
6.1.4 Identification of I_{Ks} and potential role of I_{Ks} in abnormal repolarization -related arrhythmogenesis	239
6.1.5 Ionic remodeling of Purkinje cells by congestive heart failure.....	239
6.2 Directions for future research.....	240
6.2.1 Purkinje I_{to} and Kv3.4	240
6.2.2 Molecular mechanisms underlying big maximal upstroke velocity (V_{max}) of Purkinje depolarization	242
6.2.3 Molecular mechanisms underlying ionic remodeling of Purkinje cells by congestive heart failure	243
6.3 General conclusions	243
6.4 References	244

CHAPTER 1. INTRODUCTION

1. What is a Purkinje cell?

Jan Evangelista Purkinje, a Czech scientist, described round or oval large pale heart cells almost devoid of myofibrils, which came therefore to be known as “Purkinje cells”(James 2001). A bunch of such cells encased by a thick connective sheath consists of Purkinje fiber(s) in longitudinally oriented patterns. In fact, Purkinje cells (PCs) are found in many sections of the cardiac conducting system (i.e., His bundles and /or their branches) and are dispersed throughout the ventricular endocardium, ramifying over the endocardial surface and then penetrating towards the epicardial surface (James 2001). PCs are specialized for rapid conduction and carry the electrical impulse quickly from the atrial-ventricular (AV) node towards the entire ventricular myocardium.

1.1 Gene makers and origin of Purkinje fibers

Purkinje fibers (PFs) are distinguished from working myocytes by a distinct pattern of gene expression. They up-regulate a conduction cell-specific gap-junction protein-Connexin 40 (Delorme et al. 1995; Gourdie et al. 1993a), and express the gene markers typical of neurons and skeletal muscle, which include glycoproteins Thy-1 and Gp120 that are expressed in human brain (Berglund et al. 1991), neurofilament antigens (Gorza and Vitadello 1989; Vitadello et al. 1990), neural crest-associated markers, HNK-1 (Gorza et al. 1988; Nakagawa et al. 1993), and EAP-300 (McCabe et al. 1995), acetylcholinesterase (Lamers et al. 1987; Lamers et al. 1990) as well as those of skeletal muscle genes that are not present in the myocardium, such as a slow twitch muscle myosin heavy chain (Gonzalez-Sanchez and Bader 1985; Sartore et al. 1978), atrial myosin heavy chain (de Groot et al. 1987) and skeletal muscle myosin binding protein H (Alyonycheva et al. 1997). Purkinje fibers also downregulate cardiac muscle specific myofibril proteins, such as cardiac myosin binding protein-C (Gourdie et al. 1998), which are essential for normal heart muscle contractility (Bonne et al. 1995; Watkins et al. 1995).

The understanding of the origin of PFs has been confounded by the coexpression of neural and muscular genes as described above. Two hypotheses regarding their origin, myogenic (Patten 1956) and neurogenic (Gorza et al. 1988; Vitadello et al. 1990) have been proposed. Recently, a series of retroviral cell lineage studies in the embryonic chick

heart have suggested that signals from coronary arteries might locally induce cardiomyocytes into PCs (Cheng et al. 1999; Gourdie et al. 1995). This hypothesis is strengthened by *in vivo* evidence demonstrating that inhibition of intramural coronary arterial development in the embryonic heart results in suppression of PF differentiation, while ectopic placement of the coronary arterial bed in the embryonic myocardium induces adjacent myocytes to differentiate into PCs (Hyer et al. 1999). Additionally, *in vitro* experiments show that recombinant endothelin-1 (ET-1), a vascular-associated cytokine, induces embryonic chick myocytes to upregulate a number of PF-specific gene products (Gourdie et al. 1998). Such an ability of ET-1 is further established by retroviral-mediated coexpression of both preproET-1 and ET converting enzyme-1 (Takebayashi-Suzuki et al. 2000). However, the optical mapping data demonstrate the appearance of a functional His-Purkinje network in the E10.5 murine heart, a stage when only the earliest signs of coronary vessel formation are present. By E13, just before the completion of ventricular septation, high-pressure blood from the aorta begins flow through the vascular bed (Viragh and Challice 1981). At this stage, a highly patterned and functional network of PCs, similar to that in adult heart, is already present in the murine heart, suggesting that, in contrast to the chick, hemodynamic factors from the coronary arterial system may not be responsible for the induction and /or organization of murine Purkinje network (Rentschler et al. 2001). The origin of PFs may therefore be species-specific. Further investigation is required.

1.2 Purkinje fiber physiological function and roles in pathological disease states (Potential arrhythmogenesis)

Heart contractility is coordinated by the specialized tissues of the cardiac conduction system. Purkinje fibers are critical for assuring appropriate timing and sequence of ventricular contraction. They rapidly conduct and distribute impulses throughout the ventricles, initiating synchronous apical-to-basal ejection of blood from both ventricular chambers cyclically.

It is well appreciated that a polymorphic ventricular tachycardia -Torsade de Pointes (TdP), occurring with acquired (Brachmann et al. 1983; Habbab and el Sherif 1990) and congenital long QT syndromes (Shimizu et al. 1991) is associated with the

generation of long action potential duration (APD)-related early afterdepolarizations (EADs) and EAD-induced triggered activity. EADs, occurring as oscillations during phase 2 or 3 of the action potential (AP) (Damiano and Rosen 1984) are potentially arrhythmogenic (Priori et al. 1990; Rubart et al. 1993). PFs are more sensitive to drug-induced long APD and EADs than working ventricular muscle (Abrahamsson et al. 1996), and consequently EADs are more easily induced in PFs (Davidenko et al. 1989; Gintant et al. 2001; Habbab and el Sherif 1990; January and Moscucci 1992; Nattel and Quantz 1988). In agreement with these observations in *vitro*, *in vivo* studies show that the initiation of EAD-induced TdP arises in PFs (Arnar et al. 1997; el Sherif et al. 1996; Gilmour, Jr. and Moise 1996; Kuboki et al. 1999). Therefore, Purkinje fibers appear to play a particularly important role as a generator of EADs in TdP arrhythmias associated with long QT syndromes. In addition, much evidence has shown that PFs are involved in intraventricular reentry (Chalvidan et al. 2000; Lai et al. 1998; Markowitz et al. 1995), and play an important role in the early development of ventricular fibrillation (Arnar et al. 1997; Koller et al. 1998). An electrophysiologic study in 48 patients reported that 98% of patients presented ventricular tachycardia with a mechanism of (left) bundle-branch reentry due to conduction delay in the His-Purkinje system (Blanck and Akhtar 1993). Recently, a study has reported that PCs significantly participate in malignant ventricular tachyarrhythmias via delayed afterdepolarizations (DADs) (Verkerk et al. 2000).

2. Classical early studies of Purkinje fiber currents

Hodgkin and Huxley (1952) developed the basis for understanding the action potentials of nerve by use of a negative feedback technique that allowed them to control the membrane potential-voltage clamp. The concept of the voltage clamp is that the membrane potential is monitored and current is passed across the membrane uniformly so that the value of the membrane potential is directly adjustable by the investigator. Unfortunately, no method for truly uniform voltage control in heart muscle has been found that is comparable to that used with squid axon. Furthermore, the method of inserting a pair of wires along the axis of the cylindrical “giant” axon used by Hodgkin and Huxley is not possible in heart muscle, because the myocytes are too small.

Attempts to apply the voltage clamp technique to study of the electrical activity of the heart began in the 1960s. Deck et al (1964) and Hecht et al (1964) were the first to introduce current through a second micropipette into a short strand of sheep PFs. Even though this electrode forms a point source, fair uniformity of voltage change can be achieved because of favorable fiber geometry. The sheep PF is a long column of closely packed cells about 100 μm in diameter overall and encased by a connective tissue sheath. The cells are each about 50 μm in diameter and 150 μm long and are well connected to each other electrically, so that the column behaves to a first approximation as a single long cell. Furthermore, when the fiber is cut or damaged, the injured ends ‘seal’, developing a high resistance. Due to the advantage of the axial symmetry of PFs, PF ionic currents had been among the first to be studied in the heart. Classical studies of the role and properties of inward rectifier current I_{K1} , delayed rectifier current I_K , transient outward current I_{to} , pacemaker currents I_h or I_f , Ca^{2+} current I_{Ca} and Na^+ current I_{Na} were all performed in multicellular PF preparations (for details, see below). However, the inherent limitations of classical voltage clamp techniques and problems achieving rapid and spatially-complete voltage control, as well as the risk of ion accumulation and depletion in intercellular clefts, distort the true properties of membrane currents and leave many important questions unanswered.

3. Cardiac electrophysiology -speciality of cardiac Purkinje fiber excitability

In the heart, millions of well structurally and functionally-coupled cells produce characteristic regenerative depolarization and repolarization, namely, action potentials (APs), and propagate in a strictly controlled sequence to allow synchronized contraction and effective cardiac output.

During the normal cardiac cycle, action potentials that originate at the sinoatrial (SA) node are conducted via specialized conducting tracts throughout the atria until they converge at the atrial-ventricular (AV) node and delay a little while, then pass through the bundle of His and the PF fiber networks, and eventually excite the working myocytes in the ventricles. Coordination of these cellular events is ensured by the unique electrical properties of these five primary distinct regions. The unique electrical properties of each region are attributable to the cells within the region that possess different types and

densities of ion channels, and consequently have different action potential morphologies and duration (Fig 1) (Nerbonne 2000).

3.1 Cardiac action potential

Unlike the action potentials (APs) in nerve cells that last only a few milliseconds, cardiac APs can last several hundred milliseconds, exhibiting the signature plateau that distinguishes the cardiac AP from others. This long action potential duration is essential for normal excitation-contraction (EC) coupling, and renders the myocytes relatively refractory to premature excitation.

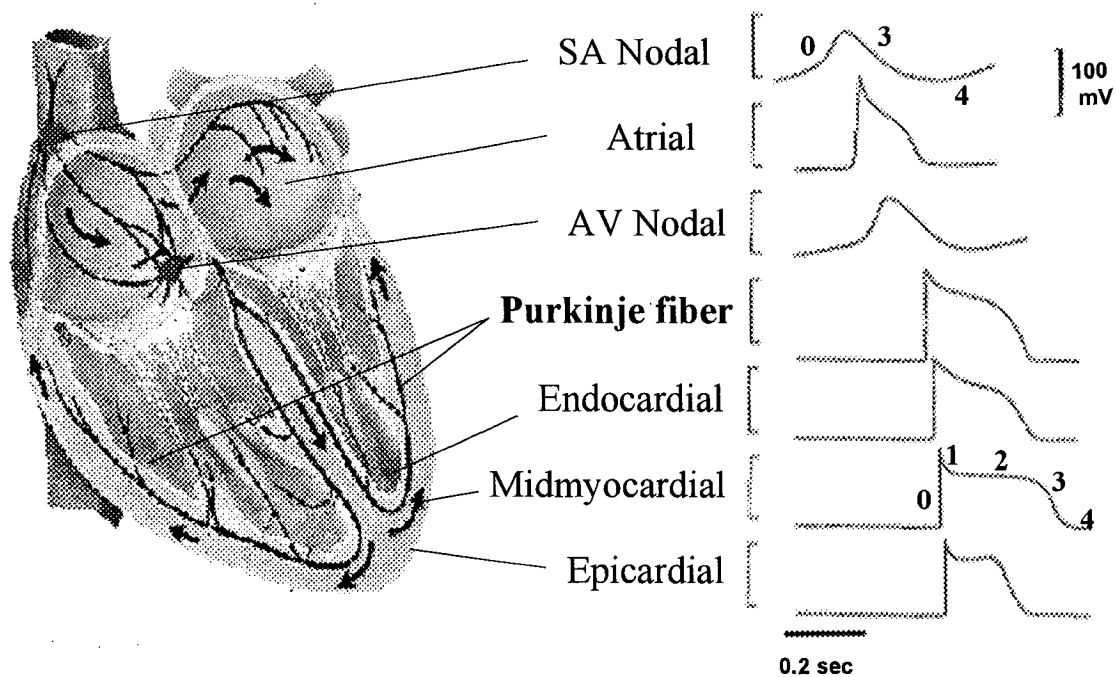


Figure 1. Schematic representation of the heart (left panel) and action potential waveforms recorded in different regions of the heart (right panel). SA, sino-atrial; AV, atrial-ventricular. Five phases of the AP are designated from 0 to 4 [adapted from Nerbonne (2000) with modification].

A typical cardiac AP consists of 5 phases (Fig.1): the sudden depolarization upon a stimulus that brings the membrane to threshold triggers the onset of the AP. This part is called the upstroke or phase 0. An important characteristic of the upstroke is the maximal

upstroke velocity, $(dV/dt)_{\max}$ or V_{\max} . Purkinje fibers (PFs) have a very larger V_{\max} (500 V/sec) (Fozzard 1993). Phase 1 is the early rapid repolarization that occurs within a few milliseconds. This is especially pronounced in ventricular epicardium and midmyocardium, and PFs. Phase 0 and 1 together are also sometimes called the spike, an alternative name taken from the nerve AP. After this brief repolarization, the membrane potential stabilizes at the plateau, called phase 2. Phase 2 is the most prominent characteristic of cardiac AP that distinguishes it from others (i.e., nerve AP) and also a main factor for much longer AP duration (APD) than that of nerve. It begins often with a notch, a slight depolarization after the end of phase 1, and lasts several hundreds milliseconds. When the notch is prominent, the AP is sometimes referred to as showing a “spike and dome” configuration. PFs have a more negative plateau, generally in the range of -10 to -30 mV, compared to the ventricular muscle of around $+20$ mV (Balati et al. 1998). Phase 3 is the terminal rapid repolarization phase, during which the potential rapidly returns to the stable resting potential (phase 4) and the action potential is terminated for ventricular muscle. In Purkinje cells and other pacemaker tissue, the cells do not remain at the resting level, but begin a slow depolarization. This is called the pacemaker potential, also referred to as phase 4 in these cells. The slope of phase 3 is generally slower in PFs than in ventricular muscles, and PFs have longer APDs.

3.2 Properties of ionic currents underlying cardiac action potentials

A number of diverse inward and outward ionic currents, corresponding to depolarizing and repolarizing currents, and along with ion pumps such as Na/K ATPase and Na/Ca exchanger, work in concert to generate the AP. The introduction of two techniques—single cell isolation (Powell and Twist 1976) and patch-clamp (Neher and Sakmann 1976) in the 1970s, revolutionized the study of ionic currents, by virtue of the ability to achieve effective voltage clamps in a wide variety of single cells, including cardiac cells from various regions of the heart. Paradoxically, although much of the classical knowledge about cardiac membrane ionic currents was obtained in PF preparations, single-cell voltage clamp studies of cardiac Purkinje cells (PCs) have been quite limited because of difficulties in PC isolation and limited quantity of PFs.

3.2.1 Depolarizing currents

Depolarization, a reduction in the degree of electronegativity in a resting cell, occurs when Na^+ and/or Ca^{2+} enter the cytosol to generate inward ionic currents. The depolarizing currents carried by these two types of ions have different roles in different regions of the heart. In the fast-reaction cells including working atria, ventricles and His-Purkinje system, the depolarization is caused by the fast opening of Na^+ channels; while Ca^{2+} channels in these cells generate smaller secondary inward currents mainly responsible for the plateau of action potential. In the slow-reaction cells including SA and AV nodes, the depolarization depends on the slower opening of smaller conductance Ca^{2+} channels, leading to a slower conduction velocity than that in the tissues using Na^+ as the depolarizing cation.

3.2.1.1 Sodium currents (I_{Na})

Two types of I_{Na} in terms of their rate of inactivation, fast and slow I_{Na} , are present in the heart. In contrast to well-recognized and characterized fast I_{Na} , slow I_{Na} has received relatively little attention, and its structural basis has remained unclear. With the finding that a large slow I_{Na} is associated with the Long QT syndrome 3 (LQT3) due to Na^+ channel mutations, research on slow I_{Na} has become resurgent.

3.2.1.1.1 Fast I_{Na}

Among many known membrane currents, fast I_{Na} was one of the earliest currents to be characterized and has been of special importance in the history of physiology. Elucidation of its fundamental properties in the squid axon by Hodgkin and Huxley (1952) launched modern channel theory.

Weidmann (1951) was the first to show that sodium ion is the inward charge carrier during the rising phase and initial spike of the cardiac action potential, and presented evidence for the similarities of the kinetics of sodium inward currents in cardiac PFs and squid axons (Weidmann 1951). Fast I_{Na} activates quickly and generates a large inward current that exceeds any other cardiac membrane current, causing depolarization at 100-500 V/sec and producing a rapid conduction velocity (0.5-1.5 m/sec) (Fozzard and Hiraoka 1973). Initial efforts to measure cardiac fast I_{Na} by voltage clamp had been

unsuccessful because the complex multicellular organization of cardiac muscle made it difficult to establish control of membrane potential rapidly and uniformly, especially for intense currents like fast I_{Na} (Beeler and McGuigan 1978; Fozzard and Beeler, Jr. 1975). Colatsky and Tsien (1979) were first able to achieve the best voltage control in a multicellular preparation by using a short Purkinje strand from the rabbit, which has rather wide intercellular spaces, and by using low temperature to slow the current kinetics and low extracellular Na^+ concentrations ($[Na^+]_o$) to reduce the size of current, which minimized the voltage non-uniformity. They first demonstrated that cardiac I_{Na} generally resembled I_{Na} in the squid giant axon. However, the relative slowness of the voltage clamp in their study hampered them to determine kinetic details, especially of activation. Furthermore, abnormal conditions (low temperature and $[Na^+]_o$) raised concerns about the applicability of the results to the physiological state.

The successful voltage clamp of cardiac fast I_{Na} was achieved with the application of single cell isolation technique (Benndorf et al. 1985; Bodewei et al. 1982; Brown et al. 1981; Bustamante and McDonald 1983; Lee et al. 1979) because single cells are so amenable to rapid and nearly uniform voltage control that a voltage step can be completed within about 100 μ sec, which is at least an order of magnitude improvement over that of multicellular preparations (Fozzard et al. 1985). The canine cardiac PCs were also considered to have advantages over other cardiac cells for voltage clamping because its larger diameter and lack of t-tubules (Mathias et al. 1985) result in a smaller R_s . Similar to the previous description of I_{Na} in both nerve (Frankenhauser 1963) and working myocytes (Brown et al. 1981; Kunze et al. 1985; Patlak and Ortiz 1985), canine PC I_{Na} displayed the sigmoid onset and multiexponential decay, but with a greatly increased I_{Na} density than ventricular (Bodewei et al. 1982; Brown et al. 1981) and atrial cells (Bustamante and McDonald 1983). The high density of fast I_{Na} may relate to the rapid conduction velocity in PCs. However, the problem of this study was that the threshold potential and voltage at peak I_{Na} continued to shift to more negative potentials during the duration of the experiment, though the shape of the Na^+ channel availability curve relation did not change with time.

Studies of fast I_{Na} with patch clamp from other regions of different species (Brown et al. 1981; Follmer et al. 1987; Mitsuiye and Noma 1992; Schneider et al. 1994)

revealed a similarity not only in the properties of voltage dependence, but also in the basic kinetic properties. In single human atrial myocytes (Sakakibara et al. 1992), fast I_{Na} is activated at a voltage threshold of -70 to -60 mV, and peak inward current is at approximately -30 mV (holding potential, -140 mV). The reversal potential of fast I_{Na} varies by approximately 57 mV at $17 \pm 1^\circ\text{C}$ with a 10-fold change in $[\text{Na}^+]_o$. The I-V relations of activation and inactivation are sigmoidal with the half-activation at -38.9 ± 0.9 mV and a slope factor of 6.5 ± 0.1 mV, and with the half-inactivation at -95.8 ± 0.9 mV and a slope factor of 5.3 ± 0.1 mV. The overlap of the inactivation and activation curves in most models of fast I_{Na} predicts a small steady-state component (Beeler and Reuter 1977; DiFrancesco and Noble 1985; McAllister et al. 1975), which is called (Na^+) “window” current. Biophysically, window current is time-invariant, whereas slow I_{Na} is slowly-inactivating.

Fast I_{Na} inactivates rapidly relative to slow I_{Na} . Compared with Na^+ channels in nerve cells that inactivate within 10 ms, the cardiac Na^+ channels are kinetically slower. The time course of inactivation is voltage dependent and generally biexponential, with time constants from 2 ms to 70 ms and the contribution of the slow component from 1% to 15% (Hanck and Sheets 1992; Makielski et al. 1987; Schneider et al. 1994). Recovery from inactivation is also voltage dependent and best fitted by biexponential function with time constants of 16 ± 10 ms and 53 ± 33 ms at -95 mV (Schneider et al. 1994).

The most important properties that distinguish cardiac from nerve I_{Na} are that cardiac fast I_{Na} is relatively resistant to TTX and STX; complete block requires micromolar concentrations of TTX, whereas nerve I_{Na} is sensitive to TTX and STX and can be completely blocked by nanomolar concentrations (Brown et al. 1981; Rogart 1981; Rogart 1986). In addition, cardiac I_{Na} is more sensitive to the blocking effects of divalent ions such as Cd^{2+} and Zn^{2+} (Frelin et al. 1986) and the local anaesthetic lidocaine (Hanck et al. 1994; Wright et al. 1997).

3.2.1.1.2 Slow (late) I_{Na}

Fast (-inactivated) Na^+ channels normally remain quiescent during the action potential plateau and rapidly recover from inactivation during the hyperpolarized diastolic interval between stimuli. However, during sustained depolarization, Na^+ channels may enter

stable, nonconducting conformational states that require a prolonged period of hyperpolarization to recover (slow inactivation) (Veldkamp et al. 2000). The classical slowly-inactivating I_{Na} has a recovery time constant > 1 second and is induced by much longer depolarizations (≈ 60 seconds) (Rudy 1978). Although cardiac Na^+ channels are less prone to occupy this ultra-stable state than their skeletal muscle counterparts (Richmond et al. 1998), the cardiac channels do exhibit a more prominent intermediate kinetic component of slow inactivation that is induced by shorter depolarization periods (Nuss et al. 2000), well within the length of the cardiac AP.

Coraboeuf et al (1979) first reported that TTX shortened the AP plateau in dog PFs at concentrations (10^{-7} M) that did not affect the V_{max} (corresponding to fast I_{Na}) and proposed the existence of a second population of Na^+ channels that lacked the property of inactivation. This was supported by demonstration of a small, slowly inactivating component of I_{Na} in another study of canine PFs (Gintant et al. 1984) and in rabbit PFs (Carmeliet 1987).

Slow I_{Na} have been also described in cardiac pacemaker cells from toad sinus venosus (Ju et al. 1996) and ventricular myocytes from rabbit (Grant and Starmer 1987), chick embryo (Liu et al. 1992), guinea pig (Sakmann et al. 2000) and dog (Zygmunt et al. 2001). It shows threshold activation at -80 mV and peak activation around -55 to -40 mV, and can be abolished by $5 \mu\text{M}$ TTX (Eskinder et al. 1993). Kiyosue and Arita (1989) found no appreciable differences between the conductance of channels active at the beginning of a depolarizing step and those exhibiting sustained reopenings. Liu et al (1992) reported that a separate collection of Na^+ channels with the same voltage dependence, single channel conductance and TTX-sensitivity as the fast Na^+ channels remained open throughout the plateau and early repolarization phase. Patlak and Ortiz (1985) thought Na^+ channels could enter different modes, the fast-inactivation, intermediate 1 and 2, and slow and persistent modes. Opposite to these findings, Saint et al (1992) found that fast and slow I_{Na} in rat ventricular myocytes had a different voltage dependence and sensitivity to TTX. They proposed that two populations of different channels might exist.

The observation that low concentrations of lidocaine that have little effect on V_{max} (corresponding to fast I_{Na}) can reduce the APD of canine ventricular myocytes indicates

the importance of slow or late Na conductance in maintenance of the AP plateau (Wasserstrom and Salata 1988). The best support for this functional role of slow I_{Na} has been obtained from the observation that the specific Na^+ channel blocker TTX decreases APD (Zygmunt et al. 2001). Recent studies show that there is transmural heterogeneity in slow I_{Na} (Sakmann et al. 2000; Zygmunt et al. 2001), which may contribute to transmural dispersion of repolarization (Antzelevitch 2000) and development of cardiac arrhythmias, particularly under conditions in which I_{Kr} and I_{Ks} are reduced (e.g., Long QT syndrome, hypertrophic cardiomyopathy, chronic infarction and heart failure) (Marban 1999; Tomaselli and Marban 1999).

3.2.1.2 Calcium currents (I_{Ca})

3.2.1.2.1 Functions of I_{Ca}

The membrane Ca^{2+} channels (L- and T-type Ca^{2+} channels) in cardiac myocytes serve to bring Ca^{2+} into the cell in response to APs and sub-threshold depolarizing signals. This Ca^{2+} influx generates an inward current, which plays an important role in diastolic depolarization of pacemaker cells in SA node, conduction through the AV node and shaping action potential morphology. Furthermore, Ca^{2+} influx serves as an electrical signaling, initiating intracellular events such as Ca^{2+} induced Ca^{2+} -release from sarcoplasmic reticulum (SR) that results in cardiac contraction and regulatory changes in gene expression. Intracellular $[Ca^{2+}]$ can also modulate the conductance of Ca^{2+} -activated K^+ and Cl^- currents.

Reuter (1967) observed in thin, short strands of PFs from sheep and calf that propagated APs were replaced with non-propagated regenerative membrane depolarizations in Na^+ -free solution, and these responses were dependent on $[Ca^{2+}]_0$ and eliminated in Ca^{2+} -free solution. Subsequent voltage clamp experiments with cardiac PFs in Na^+ -free solution demonstrated a slow Ca^{2+} -sensitive inward current. However, the kinetic properties of this current in PFs had not been worked out very well because of the complications arising from a rapidly rising and slowly decaying outward current that is activated at potentials positive to -20 mV. Therefore, the initial outward current which is much larger than the slow inward current conceals the latter over a wide potential range, which interfered with the analysis.

It had first been recognized that at least two different kinds of Ca channel currents were present in the same cell of neurons (Llinas and Yarom 1981) and noncardiac tissues (Fukushima and Hagiwara 1983; Hagiwara et al. 1975; Hagiwara and Ohmori 1983). In the heart, the evidence for two major types of Ca channel currents (I_{Ca}) was initially documented in canine atrial myocytes (Bean 1985) and guinea pig ventricular myocytes (Mitra and Morad 1986; Nilius et al. 1985), and later in rabbit SA node cells (Hagiwara et al. 1988) and canine PFs (Hirano et al. 1989; Tseng and Boyden 1989).

3.2.1.2.2 L-type and T-type Ca currents

There are two main classes of Ca current (I_{Ca}) in cardiac myocytes (Bean 1985; Bean 1989; Nilius et al. 1985). The L-type (“long lasting” and “large”) I_{Ca} ($I_{Ca,L}$) activates and inactivates at less negative membrane potentials. $V_{1/2}$ for activation and inactivation is about -10 mV and -30 mV respectively, and the peak current appears at $+10$ mV. The inactivation of $I_{Ca,L}$ is slow, particularly when Ba^{2+} is the current carrier. It has a large single-channel Ba^{2+} conductance and is sensitive to dihydropyridines (DHP) (Tsien et al. 1987a; Tsien et al. 1987b). By contrast, the T-type (“transient” and “tiny”) I_{Ca} ($I_{Ca,T}$) activates and inactivates at more negative membrane potentials. $V_{1/2}$ for activation is generally $20\sim 40$ mV more negative than for $I_{Ca,L}$ and for inactivation is around -70 mV, and the peak current is generally at 30 mV more negative than that of $I_{Ca,L}$ (Bean 1985; Hirano et al. 1989). $I_{Ca,T}$ is more transient with Ba^{2+} as the charge carrier. It has a smaller single-channel Ba^{2+} conductance and is less sensitive to DHP (Nowycky et al. 1985), but more sensitive to block by Ni or mibefradil than $I_{Ca,L}$.

The relative amounts of $I_{Ca,L}$ and $I_{Ca,T}$ are different from region to region in the heart. $I_{Ca,L}$ appears to be prominent throughout the heart. $I_{Ca,L}$ is pivotal for EC coupling (Nargeot et al. 1997) and maintains the plateau phase of the AP (Bean 1989). By contrast, $I_{Ca,T}$ is much more variable. Purkinje cells seem to have the largest $I_{Ca,T}$ (Hirano et al. 1989), pacemaker cells and some atrial myocytes also have significant amounts (Bean 1989; Hagiwara et al. 1988), whereas ventricular myocytes either have less (guinea pig) or none (rat, cat, rabbit, ferret and calf) $I_{Ca,T}$ (Bean 1989; Nuss and Houser 1993; Yuan et al. 1996). A significant $I_{Ca,T}$ is found in embryonic cardiomyocytes (Wetzel et al. 1993), neonatal rat ventricular myocytes in culture and hypertrophied ventricular myocytes

(Nuss and Houser 1993). This phenomenon has led to the speculation that $I_{Ca,T}$ plays an important role in pacemaker activity and arrhythmogenesis (Hagiwara et al. 1988; Mitra and Morad 1986; Wu and Lipsius 1990). In addition, a recent study indicates an important contribution of $I_{Ca,T}$ to Ca^{2+} signaling and atrial natriuretic factor secretion during postnatal development (Leuranguer et al. 2000).

3.2.1.3 Hyperpolarization-activated current (I_f)

The rhythmical pacing of the heart (automaticity) arises from a slow membrane depolarization between the APs (DiFrancesco 1993; Irisawa et al. 1993). Analysis of the mechanisms of this slow membrane depolarization was begun in mammalian PFs (Weidmann 1951), and was not extended to the natural pacemaker region of the heart—SA node (Brown et al. 1977; Noma and Irisawa 1976a; Noma and Irisawa 1976b) until the success in the method of voltage clamping very small preparations of mammalian SA node in the 1970s (Tsien and Carpenter 1978). In discussing the ionic basis of the pacemaker depolarization, Weidmann put forward three possible mechanisms: a) a time-dependent increase of Na conductance, b) a time-dependent decrease of K conductance, or c) a time-dependent decrease in activity of an electrogenic pump. Subsequent voltage clamp experiments (Noble and Tsien 1968; Peper and Trautwein 1969; Vassalle 1966) favored explanation b. A decade later, direct evidence presented by DiFrancesco et al (DiFrancesco 1981; DiFrancesco and Ojeda 1980) showed that the pacemaker current in PFs (originally denoted as I_{K2}) is not, as previously thought, a pure K^+ current deactivated by hyperpolarization (Noble and Tsien 1968; Peper and Trautwein 1969), but is an inward current activated by hyperpolarization (abbreviated I_h ; h for hyperpolarization activated) negative to the threshold of about $-50 \sim -60$ mV. The properties of this current in PFs are identical to those of pacemaker current- I_f (f for funny because of its peculiar characteristics) (Brown et al. 1979a) described in the SA node (Brown and DiFrancesco 1980; DiFrancesco and Ojeda 1980). This was confirmed by a straightforward demonstration of the I_f current in isolated PCs (Callewaert et al. 1984), in which extracellular K accumulation and depletion processes (distorting the time course of I_f) cannot be as severe as in multicellular preparations and inward ionic nature of the

pacemaker current became apparent even without using Ba^{2+} to block inward rectifier I_{K1} (DiFrancesco 1985).

I_f is a time- and voltage- dependent inward current upon hyperpolarization, starting at potentials between -50 and -60 mV and being fully activated at -100 mV (Cerbai et al. 1999). The $V_{1/2}$ for activation is around -80 mV. The rate constants of I_f activation and deactivation are also strongly voltage-dependent, with more negative voltages resulting in faster activation and positive voltages resulting in fast deactivation. With 5.4 mM $[\text{K}^+]_o$, the reversal potential of I_f is between -20 and -30 mV. I_f is Cs^+ sensitive (Isenberg 1976), but largely Ba^{2+} insensitive (Yanagihara and Irisawa 1980). It is permeable to monovalent cations, allowing both Na^+ and K^+ ion to pass through with the selectivity being fourfold higher for K^+ than Na^+ (Ho et al. 1994; Wollmuth and Hille 1992).

I_f plays an important role both in normal rhythmic activity (Bouman and Jongasma 1986; DiFrancesco 1995) and in mediating the responses to sympathetic (Hauswirth et al. 1968) and parasympathetic neurotransmitters (DiFrancesco and Tromba 1988a). Addition of adrenaline causes a substantial and reversible increase in I_f and accelerates the activation of I_f by stimulation of beta-adrenergic receptors (Brown et al. 1979b), while acetylcholine inhibits I_f via muscarinic receptors (DiFrancesco and Tromba 1988a; DiFrancesco and Tromba 1988b). Both modulations are involved in a mechanism that depends on direct channel activation by intracellular cyclic-adenosine-monophosphate (cAMP) (DiFrancesco and Tortora 1991). I_f has been observed in right atrium (Zhou and Lipsius 1992) and neonatal ventricular myocytes (Cerbai et al. 1999). The occurrence and density of I_f in the ventricles is development-related; both the proportion of cells with I_f and density of I_f decrease progressively during development with other characteristics unchanged (Cerbai et al. 1999). During severe hypertrophy (Cerbai et al. 1996) and heart failure (Cerbai et al. 1997; Yu et al. 1995), I_f is reexpressed in the ventricles or increased, suggesting it may be important in disease-related arrhythmias (Hart 1994).

3.2.2 Repolarizing currents

Repolarization, the return to resting potential, occurs when outward currents, largely generated by K^+ efflux, restore the membrane potential to its resting level of electronegativity. Delayed repolarization is the main feature of cardiac APs. The

repolarizing currents in the heart include K^+ currents, Cl^- currents and transport currents such as Na/Ca exchanger and Na/K pump currents.

3.2.2.1 Potassium currents (K^+ currents)

Diverse K^+ currents with different time and voltage dependencies and pharmacological properties function in concert to regulate the heart rate by setting the resting membrane potential, amplitude, and duration of the AP and its refractoriness (Barry and Nerbonne 1996; Roden and Kupersmidt 1999; Snyders 1999). They are mediators for neurohormonal control of cardiac function and potential targets for antiarrhythmic agents. Based on their functional and biophysical characteristics, cardiac K^+ currents can be classified into four families: 1) transient or A-type currents (I_{to}); 2) delayed rectifiers-rapid and slow (I_{Kr} and I_{Ks}); 3) ultrarapid delayed rectifier (I_{Kur}); 4) inward rectifying currents including classic inward rectifying current I_{K1} , ACh-sensitive and ATP-sensitive inward rectifying currents (I_{KACh} and I_{KATP}).

3.2.2.1.1 Transient outward current (I_{to})

Transient outward current refers to the outward K^+ current with rapidly activating and inactivating kinetics upon sustained membrane depolarization. This current was originally found in neurons, and named A type current I_A (Hagiwara 1961). The cardiac equivalence to I_A was first investigated by Dudel et al (1967) with two-microelectrode voltage-clamp techniques in shortened PF strands and later by Fozzard and Hiraoka (1973). Initial studies on I_{to} lacked quantitative assessment due to the limitations of techniques and multicellular PF preparations (Kenyon and Gibbons 1979a; Kenyon and Gibbons 1979b). Furthermore, the studies of the composition of I_{to} in the heart produced conflicting results regarding the charge-carrying species (Kenyon and Gibbons 1979a; Kenyon and Gibbons 1979b; Siegelbaum and Tsien 1980; Zygmunt and Gibbons 1991; Zygmunt and Gibbons 1992). Now it is commonly accepted that there are two components of cardiac I_{to} : one is a 4-aminopyridine (4-AP) sensitive Ca^{2+} -independent K^+ current $-I_{to1}$ (or I_{to} : for simplicity, I_{to} instead of I_{to1} stands for the transient outward K^+ current and will be used in the rest of this thesis) and the other is a 4-AP resistant Ca^{2+} -

activated Cl⁻ current I_{to2} (or $I_{Cl,Ca}$) (discussed in the section of “other repolarizing currents”).

Cardiac I_{to} has been extensively characterized in considerable detail in the ventricular myocytes of cat (Furukawa et al. 1990), dog (Litovsky and Antzelevitch 1988; Tseng and Hoffman 1989), ferret (Campbell et al. 1993a; Campbell et al. 1993b), human (Amos et al. 1996; Kaab et al. 1998; Konarzewska et al. 1995; Nabauer et al. 1996; Wettwer et al. 1993; Wettwer et al. 1994), mouse (Xu et al. 1999a) and rat (Apkon and Nerbonne 1991; Himmel et al. 1999; Wickenden et al. 1999a; Wickenden et al. 1999b) as well as in the atrial cells from dog (Yue et al. 1996a), rat (Boyle and Nerbonne 1991; Boyle and Nerbonne 1992), human (Amos et al. 1996; Escande et al. 1987; Fermini et al. 1992; Shibata et al. 1989), and mouse (Xu et al. 1999b). In these different cardiac cell types of different species, the general properties of I_{to} are similar in voltage dependence of activation and inactivation, and 4AP-sensitivity, but the diversity of I_{to} is also seen in terms of region- and species- dependence.

Although guinea pig ventricular myocytes reportedly lack I_{to} (Sanguinetti and Jurkiewicz 1990; Sanguinetti and Jurkiewicz 1991), an I_{to} -like outward K⁺ current is detectable in these cells once $[Ca^{2+}]_o$ is removed (Inoue and Imanaga 1993).

Gating properties

Voltage-dependence of activation and inactivation I_{to} shows a linear current-voltage relationship in the physiological voltage range. The threshold for activation is in the range of $-40 \sim +10$ mV; the $V_{1/2}$ ranges from -12 to $+22$ mV (Nabauer et al. 1993; Shibata et al. 1989; Yue et al. 1996a). Voltage-dependent steady-state inactivation develops between -70 mV and -10 mV. The $V_{1/2}$ for inactivation is between -50 mV and -15 mV (Nabauer et al. 1993; Shibata et al. 1989; Yue et al. 1996a). The single channel conductance of I_{to} ranges from 4 to 20 pS in different studies (Campbell et al. 1993b; Nakayama and Irisawa 1985).

Time-dependent activation and inactivation The characteristic property of I_{to} compared to other K⁺ currents is its rapid activation and inactivation. The values of time to peak (refers to as activation kinetics) are on the order of milliseconds to tens of

milliseconds, depending on the voltage steps (Yue et al. 1996a). Both mono- and bioexponential functions have been reported to fit I_{to} decay (Campbell et al. 1993b; Li et al. 1998; Nabauer et al. 1996). The time constants for inactivation generally are on the order of tens of milliseconds for the fast portion and hundreds of milliseconds for the slow portion at 37 °C (Campbell et al. 1995).

Reactivation and rate-dependence The recovery of I_{to} from inactivation shows very striking variations in different species and different regions of the same species (see below). The recovery of I_{to} is voltage dependent; with less negative holding potentials, recovery slows (Han et al. 2000; Li et al. 2000). For I_{to} with slow recovery kinetics, such as atrial and ventricular I_{to} in rabbit (Giles and Imaizumi 1988), endocardial and Purkinje I_{to} in dog (Tseng and Hoffman 1989) and sheep Purkinje I_{to} (Boyett 1981a; Boyett 1981b), they also show very strong frequency dependence: I_{to} amplitude decreases as stimulation frequency increases.

3.2.2.1.1.1 Species and regional differences

Significant differences in I_{to} density and kinetics have been observed in different species and different regions within the heart. The slow reactivation kinetics of I_{to} in rabbit is distinct from I_{to} in other species (Fermini et al. 1992; Wang et al. 1999). For the fast component of I_{to} recovery, the time constants are on the order of 10-100 ms in ferret, rat and human (Campbell et al. 1993b; Fermini et al. 1992; Josephson et al. 1984; Nabauer et al. 1996). For the slow component, the time constants range from hundreds of milliseconds to seconds in rabbit, dog and human (Antzelevitch et al. 1991; Clark et al. 1988; Fermini et al. 1992; Li et al. 1998). I_{to} density in rat, rabbit and human is substantially larger in atrial than in ventricular myocytes (Boyle and Nerbonne 1992; Giles and Imaizumi 1988; Varro et al. 1993), whereas I_{to} density in mouse shows the opposite (Xu et al. 1999b). In rat, atrial I_{to} also shows significant differences from ventricular I_{to} in the rates of inactivation and recovery (Apkon and Nerbonne 1991; Boyle and Nerbonne 1992). In dog and human, I_{to} density of epicardial and endocardial myocytes is higher in the right than in the left ventricle (Di Diego et al. 1996; Volders et al. 1999a) and transmural heterogeneity of I_{to} exists in both right and left ventricles (Li et

al. 1998; Liu et al. 1993). I_{to} in epicardial myocytes has higher peak current density and faster recovery kinetics than that in endocardial myocytes in the left ventricle of human (Kaab et al. 1998; Nabauer et al. 1996), dog (Liu et al. 1993) and ferret (Brahmajothi et al. 1999). These regional differences in I_{to} contribute importantly to the regional differences in AP morphology and APD.

3.2.2.1.1.2 Physiological roles

I_{to} is responsible for the early repolarization (phase 1) of the AP. The spike and dome morphology of the AP has been attributed to the rapid activation and inactivation of I_{to} , followed by rapid activation of I_{CaL} (Boyett 1981a; Boyett 1981b; Giles and Imaizumi 1988). I_{to} also influences the overall duration of the AP via its interaction with other ionic currents such as I_{CaL} and delayed rectifier currents, thereby modulating both myocardial repolarization and contractility, as well as EC coupling (Courtemanche et al. 1998; Greenstein et al. 2000; Hoppe et al. 2000; Sah et al. 2001; Volk et al. 1999; Winslow et al. 1998). I_{to} heterogeneity contributes to regional variations of AP profiles (Li et al. 1998; Liu et al. 1993). This in turn leads to a more synchronous repolarization throughout ventricles (Antzelevitch et al. 1991; Baker et al. 2000; Burgess 1979). In addition, regional differences in the sensitivity to drugs and reactions to insults such as ischemia have been also documented to be attributable to the heterogeneity of I_{to} (Litovsky and Antzelevitch 1988).

3.2.2.1.2 Delayed rectifier currents (I_K)

The delayed rectifier K^+ current (I_K) was originally designated as “delayed” to distinguish the slow onset of this current from rapidly activating Na^+ current. Noble and Tsien (Noble and Tsien 1969) were the first to describe a slowly activating, non-inactivating outward current, which they initially called I_x , in the plateau range of the AP in sheep PFs. They observed that I_x could be well fit as the sum of two exponentials, corresponding to distinct components I_{x1} and I_{x2} . Later studies suggested that I_{x2} may have been an artifact due to K^+ accumulation in restricted extracellular spaces of PFs (Attwell et al. 1979) and that I_K represents the activation of a single population of channels with multiple closed states (Bennett et al. 1985). Following the application of

single cell isolation and patch clamp techniques in the late 1990's, two distinct components of I_K , a rapid component I_{Kr} and a slow one I_{Ks} , were again distinguished in isolated guinea pig cardiac myocytes based on pharmacology and distinct properties of time- and voltage dependence (Sanguinetti and Jurkiewicz 1990; Sanguinetti and Jurkiewicz 1991). I_{Kr} and I_{Ks} can also be distinguished at the microscopic level: in symmetrical K^+ ; the single channel conductances of I_{Kr} and I_{Ks} channels are 10-13 and 3-5 pS (Balsler et al. 1990; Veldkamp et al. 1993). Similar components have been described in single isolated myocytes from different regions of the heart and from different species, including node cells of rabbit (Howarth et al. 1996; Ono and Ito 1995; Shibasaki 1987) and guinea pig (Anumonwo et al. 1992), atrial myocytes of guinea pig (Sanguinetti and Jurkiewicz 1991), dog (Gintant 1996; Yue et al. 1996a) and human (Wang et al. 1994), ventricular myocytes of cat (Follmer and Colatsky 1990), feline (Barajas-Martinez et al. 2000), rabbit (Salata et al. 1996), guinea pig (Sanguinetti and Jurkiewicz 1990), dog (Gintant 1996; Liu and Antzelevitch 1995) and human (Li et al. 1996a), and Purkinje cells of rabbit (Cordeiro et al. 1998; Scamps and Carmeliet 1989) and dog (Gintant et al. 1985).

Voltage-dependence of activation and inactivation I_{Kr} has an activation threshold of -40 to -30 mV that is more negative than the value of -20 mV for I_{Ks} (Sanguinetti and Jurkiewicz 1990). The I-V relation of I_{Kr} is not linear, peaking at 0 to +10 mV and rectifying inwardly at more positive potentials, whereas I_{Ks} has a linear I-V relation. The $V_{1/2}$ and slope factor of I_{Kr} are \sim -20 mV and 7.5 mV respectively, while corresponding values for I_{Ks} are +24 mV and 15.7 mV (Sanguinetti and Jurkiewicz 1990), showing more positive activation and less steep slope for I_{Ks} than for I_{Kr} .

Kinetics For activation, I_{Kr} is more rapid than I_{Ks} . Depending on the species, the time constants (τ s) of I_{Kr} activation range from 40 ms of guinea pig atrial cells to 600 ms of canine ventricular myocyte at 0 mV (Tseng 2001). By contrast, the time course of I_{Ks} activation is extremely slow and may not achieve steady state during 10-second pulse (Freeman and Kass 1993a). For deactivation, I_{Kr} is variable among species, either fast (30 ms, in guinea pig atrial cells) (Sanguinetti and Jurkiewicz 1991) or slow (250 ms, in

rabbit ventricular myocyte) (Clay et al. 1995) at -60 mV. For both activation and deactivation rates of I_{Kr} , guinea pig I_{Kr} is relatively fast; rabbit, cat and canine I_{Kr} are slow and human I_{Kr} is in between. For I_{Ks} deactivation, τ values are in the range of hundred milliseconds to seconds at -40 mV (Varro et al. 2000).

The inactivation of I_{Kr} is faster than its activation at voltages positive to 0 mV, account for I_{Kr} 's typical inward rectification (Shibasaki 1987). As the membrane repolarizes to below 0 mV, I_{Kr} rapidly recovers from inactivation, contributing importantly to phase 3 repolarization. By contrast, I_{Ks} does not show a time-dependent inactivation.

Pharmacological sensitivity Selective I_{Kr} blockers are the methanesulfonanilide class III antiarrhythmic agents E-4031, dofetilide, almokalant, and D-sotalol (Mounsey and DiMarco 2000). E-4031 and dofetilide are widely-used experimental tools to dissect out the physiological contribution of I_{Kr} . I_{Kr} is also sensitive to the other antiarrhythmic agents such as the class 1A drug quinidine (Balsler et al. 1991; Roden et al. 1988) and the class 1C drug flecainide (Follmer and Colatsky 1990), as well as the class 1B agent mexiletine (Mitcheson and Hancox 1997). I_{Ks} is reported to be selectively blocked by the chromanol 293B (Busch et al. 1996), the benzodiazepine L-735,821 (Jurkiewicz et al. 1996), and the diuretic indapamide (Turgeon et al. 1994). Some class III antiarrhythmic agents such as amiodarone have been shown to block both I_{Kr} and I_{Ks} (Balsler et al. 1991).

I_{Kr} is paradoxically increased by $[K^+]_o$, which decreases the driving force (Sanguinetti and Jurkiewicz 1992; Shibasaki 1987). This has been attributed to a positive shift in the voltage dependence of channel inactivation without change in the voltage dependence of activation (Wang et al. 1996). This phenomenon may explain why I_{Kr} -blocking drug induced Long QT Syndromes occur much more commonly during hypokalemia. It has also been the basis of a therapeutic strategy- in patients with Long QT Syndrome 2 (caused by mutations in the gene encoding I_{Kr} channels) a therapeutically-induced increase of serum $[K^+]$ by 1.4 mEq/L shortened the QTc interval by 24% (Compton et al. 1996).

Divalent cations can modulate the magnitude of I_{Ks} . Elevated $[Ca^{2+}]_i$ increases I_{Ks} while increased $[Mg^{2+}]_i$ decreases I_{Ks} (Nitta et al. 1994).

Physiological roles I_K is the major repolarizing current determining plateau duration and APD in most cell types. The inward rectification of I_{Kr} limits the amount of outward current during the initial plateau phase of AP, and a progressive increase in its magnitude as the membrane repolarizes below 0 mV initiates and contributes to phase 3 repolarization. I_{Kr} also plays an important role in pacemaker cells, as demonstrated by the finding that E-4031 attenuates the maximum diastolic potential, decreases AP amplitude, and slows the rate of repolarization in rabbit SA node cells (Ono and Ito 1995). The role of I_{Ks} is unclear because of its slow kinetics and positive activation voltage. Small I_{Ks} is thought to contribute to the relatively long APD of ventricular midmyocardial (M) cells (Liu and Antzelevitch 1995). Increased I_{Ks} at rapid heart may contribute to rate-dependent APD abbreviation (Jurkiewicz and Sanguinetti 1993). Recently, I_{Ks} is suggested to play little role in normal dog ventricular muscle, but to be important in counteracting I_{Kr} -blocker induced APD prolongation (Varro et al. 2000). In addition, the decline of I_{Ks} is reported to be partially responsible for the slow diastolic depolarization of SA node cells in guinea pig (Anumonwo et al. 1992), while in rabbit, I_{Ks} is small, and I_{Kr} modulates pacemaker activity (Ono and Ito 1995; Shibasaki 1987). The important role of I_{Kr} and I_{Ks} in cardiac normal repolarization is underscored by the finding that mutations in the genes encoding these channels prolong the QTc interval and predispose affected individuals to potentially lethal ventricular arrhythmias (see molecular basis of I_K).

I_K is a major target for class III antiarrhythmic drugs. It has been recognized that most I_K -blocking class III drugs, including E4031 and dofetilide, selectively inhibit I_{Kr} and produce reverse frequency-dependent prolongation of APD (Heath and Terrar 1996; Jurkiewicz and Sanguinetti 1993). This phenomenon limits their therapeutic potential because of limited effectiveness in terminating tachycardias and a tendency to produce EADs at slow heart rates. The selective I_{Ks} blocker chromanol 293B has been reported to prolong APD in a frequency-independent manner in guinea pig and human ventricular myocytes (Bosch et al. 1998). This favourable characteristic has led to speculation that specific I_{Ks} blockers might have an antiarrhythmic effect on tachyarrhythmias with reduced risks of ventricular proarrhythmia at slow heart rates (Hondeghem and Snyders

1990). However, a recent study showed that blockade of I_{Ks} in rabbit ventricular myocytes increases APD in a reverse frequency-dependent manner, as does blockade of I_{Kr} (Lu et al. 2001).

3.2.2.1.3 Ultrarapid rectifier current (I_{Kur})

A nearly instantaneous activating and slowly inactivating K^+ current has been described in rat (Boyle and Nerbonne 1991; Boyle and Nerbonne 1992), human (Wang et al. 1993) and dog atrial myocytes (Yue et al. 1996b), and guinea pig ventricular myocytes (Yue and Marban 1988). This current has also been referred to as the steady-state (I_{ss}), sustained (I_{sus}), ultra-rapid (I_{Kur}), and the persistent, plateau (I_{Kp}) current. They are now often referred to as I_{Kur} (Nerbonne 2000).

I_{Kur} is an outwardly rectifying K^+ current upon membrane depolarization. Depending on species, the specific properties may be different, with differences reflected in: 1) the inactivation rate, with human atria > rat atria > canine atria > guinea pig ventricle (non-inactivating); 2) pharmacological profiles, human atrial I_{Kur} being blocked by 4AP (IC50 \approx 50 μ M), relatively insensitive to TEA, Ba^{2+} and several peptide toxins (Fedida et al. 1993; Firek and Giles 1995; Wang et al. 1993), rat atrial I_{Kur} less sensitive to 4AP (IC50 \approx 0.6 mM); canine atrial I_{Kur} most sensitive to 4AP (IC50 \approx 1 μ M) and TEA (IC50 \approx 0.3 mM); guinea pig ventricular I_{Kur} sensitive to Ba^{2+} . These different properties suggest diversity in the molecular composition of channels underlying macroscopic currents.

I_{Kur} contributes to the repolarization in these preparations to a different degree. In human atria, I_{Kur} is thought to be predominant delayed rectifier current because half blockade of I_{Kur} by 4AP prolongs APD by 66% (Wang et al. 1993).

3.2.2.1.4 Inward rectifier currents

Inward rectifier currents are distinct from those discussed above in that they conduct predominantly in the inward direction and carry little current in the outward direction, a property referred to as “inward rectification”. Three types of inward rectifier currents have been described in cardiac cells: I_{K1} , I_{KACH} and I_{KATP} . They differ in their regulation by acetylcholine (I_{KACH}) or intracellular ATP (I_{KATP}) and in the degree of inward

rectification ($I_{K1} > I_{KACH} > I_{KATP}$). They also display different single-channel properties, which suggests distinct underlying molecular entities (Barry and Nerbonne 1996).

3.2.2.1.4.1 Classical inward rectifier current: I_{K1}

I_{K1} is responsible for setting cardiac resting potential and contributes to terminal cardiac repolarization, thereby helping to shape the AP. It was first described in PFs by Weimann in 1955. Since then, it has been characterized in atrial and ventricular myocytes of guinea pig (Hume and Uehara 1985), rabbit (Giles and Imaizumi 1988), canine (Yue et al. 1996a), and humans (Heidbuchel et al. 1990; Varro et al. 1993), and PCs of canine (Pinto and Boyden 1998) and rabbit (Cordeiro et al. 1998) by patch clamp. The properties of the current in these preparations are similar in that they are K^+ -selective, blocked by extracellular Cs^+ and Ba^{2+} , modulated by external K^+ , and strongly rectifying.

Strong inward rectification in I_{K1} is of pivotal importance in determining membrane excitability in cardiac myocytes. The underlying mechanism is voltage-dependent blockade of the channel by intracellular cations (Lopatin et al. 1994; Matsuda et al. 1987; Matsuda 1993; Matsuda and Cruz 1993). Small ions, such as Mg^{2+} , block the channel with fast kinetics; polyamines, such as spermine and spermidine, account for a slower component of rectification (Ishihara et al. 1989; Lopatin et al. 1994).

The heterogeneity of I_{K1} is pronounced. Different myocardial cell types have very different current densities. Generally, I_{K1} is prominent in ventricular myocytes (Giles and Imaizumi 1988) and Purkinje cells (Cordeiro et al. 1998) but is small in atrial myocytes and absent in node cells (Giles and Imaizumi 1988; Noma et al. 1984). In addition, different myocardial cell types may also display distinct properties; for example, I_{K1} inactivates during maintained hyperpolarization in ventricular, but not in atrial, myocytes, and elevation of $[K^+]_o$ substantially increases the magnitude of the outward currents through ventricular I_{K1} channels, but has little effect on atrial I_{K1} channels (Hume and Uehara 1985). There are also data suggesting that the mean open time of ventricular I_{K1} channels is significantly longer ($\tau \sim 1$ s) than that of atrial I_{K1} channels ($\tau \sim 220$ ms) (Hume and Uehara 1985). These results suggest the interesting possibility that the molecular composition of atrial and ventricular I_{K1} channels is not identical.

3.2.2.1.4.2 I_{KACH}

Acetylcholine (ACh), released on vagal stimulation, produces negative inotropic and chronotropic effects that are mediated through the activation of M2 muscarinic acetylcholine receptors (mAChRs) (Kurachi 1995). The negative chronotropic effect arises partially from the membrane hyperpolarization by opening of a distinct class of inwardly rectifying K^+ channels (I_{KACH}) (Noma et al. 1979; Noma and Trautwein 1978). I_{KACH} was initially characterized in nodal and atrial cells of many species (Sakmann et al. 1983; Heidbuchel et al. 1990; Ito et al. 1992; Soejima and Noma 1984) and later was also described in cardiac Purkinje fibers and ventricular myocytes (Heidbuchel et al. 1990). All cell types from various species have similar single-channel conductance and kinetic properties (Koumi and Wasserstrom 1994), suggesting the same molecular basis for I_{KACH} in different species and different cell types in the same species.

Application of ACh to preparations activates channels with a large single conductance of 40 pS in symmetrical K^+ (Heidbuchel et al. 1990; Soejima and Noma 1984). Intracellular GTP is required for I_{KACH} channel activation through a pertussis toxin-sensitive G protein (Kurachi et al. 1986; Kurachi et al. 1992; Pfaffinger et al. 1985). Subsequent work has demonstrated that $\beta\gamma$ subunits of heterotrimeric G proteins directly activate I_{KACH} (Logothetis et al. 1987; Wickman et al. 1994).

3.2.2.1.4.3 I_{KATP}

I_{KATP} is an inwardly rectifying current activated by intracellular ADP and inhibited by intracellular ATP (Terzic et al. 1994; Terzic et al. 1995), thus linking cellular metabolism (reflected by the ADP/ATP ratio) to membrane excitability (Baukrowitz 2000). The current has been identified in a variety of tissues, including pancreatic β -cells (Amoroso et al. 1990), skeletal muscle (Spruce et al. 1987), and arterial smooth muscle (Standen et al. 1989). I_{KATP} was first discovered in the heart (Noma 1983) and has been extensively described in various cardiac cells of different species including atrial and ventricular myocytes from rat (Nichols and Lederer 1991), guinea pig (Faivre and Findlay 1990), rabbit (Nichols et al. 1991), dog (Horie et al. 1987) and human (Heidbuchel et al. 1990), and AV node cells as well as Purkinje cells from rabbit and canine (Kakei and Noma 1984; Light et al. 1999).

Once activated, cardiac I_{KATP} is active at every potential, displaying “weak” rectification, allowing substantial outward current to flow at positive potentials (Nichols and Lederer 1991). It is largely time- and voltage independent. The underlying single channel opens in bursts separated by long closed gaps (Heidbuchel et al. 1990; Terzic et al. 1995; Horie et al. 1987). With symmetrical 150 mM K^+ , the unitary conductance is 70-90 pS (Standen et al. 1989; Noma 1983), larger than those of I_{K1} and I_{KACh} (Kurachi et al. 1986; Sakmann and Trube 1984a).

Unlike I_{KATP} channels in pancreatic β -cells, which are open under normal conditions, cardiac I_{KATP} channels are generally closed at normal resting cardiac intracellular ATP levels. However, under hypoxia or ischemia the intracellular ATP may fall below a critical level, leading to opening of the channels (Noma 1983), increased K^+ efflux (Gasser and Vaughan-Jones 1990), and shortening of the APD (Faivre and Findlay 1990; Isenberg et al. 1983). Increased K^+ efflux and shortening of APD contribute to predisposing the heart to the development of reentrant arrhythmias (Wilde 1993; Wilde and Janse 1994). On the other hand, mitochondrial I_{KATP} plays an important role in cardioprotection and ischemia-related preconditioning (Garlid et al. 1997; Liu et al. 1998).

3.2.2.2 Other ion transporters

3.2.2.2.1 Na/Ca exchanger current (I_{NCX})

In 1968 Reuter and Seitz first identified a Na^+ -dependent influx and efflux of Ca^{2+} in cardiac muscle. It is now known that Na/Ca exchange plays an important role in controlling levels of $[Ca^{2+}]_i$ and maintaining Ca^{2+} homeostasis (Philipson and Nicoll 2000).

The Na/Ca exchanger is a membrane transporter catalyzing the countertransport of three Na^+ ions for one Ca^{2+} ion, thus producing an ionic current (I_{NCX}) (Fujioka et al. 2000a; Fujioka et al. 2000b) that can influence cardiac AP shape. Depending on the membrane potential, $[Na^+]_i$ and $[Ca^{2+}]_i$, the Na/Ca exchanger can operate in both a forward mode (Ca^{2+} out, Na^+ in, generating an inward I_{NCX}) and a reverse mode (Na^+ out, Ca^{2+} in, generating an outward I_{NCX}). High $[Ca^{2+}]_i$ favors Ca^{2+} efflux, generating inward I_{NCX} , whereas positive membrane potential and high $[Na^+]_i$ favor outward I_{NCX} . On

repolarization of the AP, the negative membrane potential and high $[Ca^{2+}]_i$; drive a large inward I_{NCX} and this causes Ca^{2+} extrusion from the cell. Under physiological conditions the Na/Ca exchanger works mainly in the Ca^{2+} extrusion mode, but it can also work in Ca^{2+} influx mode, triggering Ca^{2+} release in some circumstances (Dipla et al. 1999).

The first whole-cell patch-clamp study of I_{NCX} was conducted by Kimura et al in guinea pig ventricular myocytes (Kimura et al. 1986; Kimura et al. 1987). Subsequent studies have been done in many species. The amplitude of I_{NCX} is largest in hamster, smallest in rat, with guinea pig and human myocytes having intermediate values, and the Ca^{2+} extruding activity of Na/Ca exchanger follows the order of hamster \geq guinea pig \geq human \geq rat. The kinetics of the Na/Ca exchanger also varies among species. These differences imply the differences in the expression of the exchanger or species-dependent variability in spatial distribution of Na/Ca exchanger with respect to the SR (the ryanodine receptor) (Sham et al. 1995). More recently, spatial heterogeneity of I_{NCX} in the canine ventricle has been reported. I_{NCX} is large in M cells, and significantly smaller in endocardial myocytes, implying possible transmural differences in EC coupling (Zygmunt et al. 2000). Finally, the activity of the Na/Ca exchanger is development-related: in rabbit, I_{NCX} density is high at birth and declines postnatally (Haddock et al. 1998). In humans, NCX mRNA and protein expression is greater at early fetal compared to adult stages, consistent with reports of NCX mRNA and protein development in other species (Qu et al. 2000). The functional significance of this temporal change remains to be determined.

3.2.2.2.2 Na/K pump

The Na/K pump is a membrane-bound, Na^+ - and K^+ -activated ATPase that establishes and maintains the high internal K^+ and low internal Na^+ typical of most animal cells. By using the energy from the hydrolysis of one molecule of ATP, it transports three Na^+ out of the cell in exchange for two K^+ in, thus generating a small outward pump current (I_p) (Glitsch 2001). The Na/K pump is Mg^{2+} and ATP-dependent, activated by intracellular Na^+ and extracellular K^+ , and regulated by autonomic transmitters and hormones. The generation and maintenance of Na^+ and K^+ gradients across the cell membrane are prerequisites for the maintenance of the resting potential and the generation and

propagation of APs. The Na/K pump can also contribute directly to the resting potential through its electrogenic function. During the AP, an increased I_p would be expected according to the cardiac I_p -V relationship, due to the increased $[Na^+]_i$ caused by Na^+ influx during phase 0 of AP. Therefore, the Na/K pump can affect the shape and duration of AP under some circumstances. Indeed, activation of the pump in Purkinje fibers following a short period of increased stimulation frequency or in K^+ -free solution considerably shortens the APD (Hiraoka and Kawano 1987), whereas inhibition of the pump by cardiac glycosides prolongs the APD (Isenberg and Trautwein 1974). In addition, the Na/K pump is particularly critical to control steady-state cytoplasmic Na^+ concentration. As such, it has an important role in regulating cell volume, cytoplasmic pH, Ca^{2+} levels and Ca^{2+} associated muscle contraction through the Na/H and Na/Ca exchangers, respectively (Therien and Blostein 2000).

3.2.2.3 Other repolarizing currents

Calcium-activated Cl^- currents (I_{to2}) ($I_{Cl,Ca}$) $I_{Cl,Ca}$ is a Ca^{2+} -dependent, 4AP-insensitive transient outward Cl^- current. The presence of $I_{Cl,Ca}$ has been demonstrated in atrial and ventricular myocytes, and Purkinje fibers (cells) of rabbit and dog hearts (Verkerk et al. 2000; Siegelbaum and Tsien 1980; Zygmunt and Gibbons 1991; Wang et al. 1995a; Kawano et al. 1995; Yue et al. 1996a; Sipido et al. 1993; Zygmunt 1994). $I_{Cl,Ca}$ has a threshold voltage of 20 - 0 mV, and the current amplitude increases with membrane depolarization, with a peak at + 40 mV followed by a prominent decay, exhibiting a bell-shaped I-V curve. $I_{Cl,Ca}$ is blocked by the anion channel blockers (i.e., DIDS) and niflumic acid. It is believed that $I_{Cl,Ca}$ mainly contributes to the early rapid repolarization phase 1 of the AP. During high frequency stimulation, increased $I_{Cl,Ca}$ contributes to APD shortening (Hiraoka and Kawano 1989; Kawano and Hiraoka 1991). In addition, $I_{Cl,Ca}$ is involved in the generation of delayed afterdepolarizations (DADs) (Verkerk et al. 2000).

Other Cl^- currents There are other Cl^- currents, including the protein kinase A- and C-activated Cl^- currents ($I_{Cl,PKA}$ and $I_{Cl,PKC}$), the stretch- or swelling-activated Cl^- current ($I_{Cl,SWELL}$) and sustained Cl^- conductance ($I_{Cl,basal}$). Only $I_{Cl,basal}$ is active under basal

conditions. However, under pathological conditions, these Cl^- currents significantly contribute to the regulation of APD and cell volume, and may be involved in arrhythmias (Hiraoka et al. 1998).

3.3 Passive properties of Purkinje fibers

The conduction of the cardiac impulse depends on both sarcolemmal ionic currents as described above and passive electrical properties determined by the myocardial tissue architecture and specialized gap junctions responsible for electrical coupling between adjacent cells. The influence of myocardial architecture on conduction is determined by the size and shape of individual cardiomyocytes (Spach 1999; Spach et al. 2000; Spach and Heidlage 1995) and their packing geometry in the myocardium (Saffitz et al. 1994). The role of gap junctions is dependent on their constituent connexin isoforms, as well as on the size, number and spatial distribution of these junctions.

3.3.1 Definition of passive properties

The electrical properties of excitable cells are divided into passive and active properties (Fozzard and Arhsdorf 1992). The passive system responds to a stimulus proportionally and does not add energy, while the active system can respond out of proportion to the stimulus, thereby adding energy from sources such as the electrochemical gradient in $[\text{Na}^+]$ (Fozzard 1977).

The membrane itself, being surrounded by electrically conductive extracellular and intracellular fluid, possesses capacitance and resistance, and can be modeled in terms of an electrical analogue containing resistors and capacitors (Fig.2), with properties resembling those described by Kelvin in his study of cables (Cranefield 1983). The cable properties actually are attributes of electrically conducting cells of any shape (Cranefield 1983).

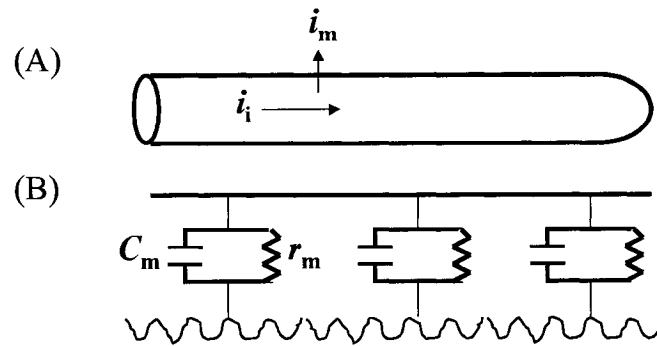


Figure 2. Cable-like cell and its electrical analogue. A: The cell has longitudinal current i_i and transmembrane current i_m . B: The cell membrane is modeled as a parallel set of unit membranes, each consisting of a capacitor (C_m) and a resistor (r_m). The interior of the cell is shown as a resistance (r_i). The exterior of the cell is presumed to have little resistance because of the large volume of bathing solution. [adapted from Fozzard and Arhdsdorf (1992)].

Changes in ionic concentration caused by normal accumulation and depletion, as well as by abnormal factors such as hypoxia and ischemia, can affect cell to cell coupling. The cable properties of cardiac cells are dynamically changeable, especially under abnormal conditions, which can have an important impact on cardiac AP conduction and arrhythmogenesis.

3.3.2 Architecture of cable-like Purkinje false tendons

The prototype of a cable-like structure in the heart is the Purkinje false tendon in which a bundle of well-connected cells form a long cable resembling a nerve. They are 50-300 μm in diameter, have 2-30 cells in cross-section, and are surrounded by a dense connective tissue sheath (Fozzard 1977).

The cells of Purkinje false tendons are larger than other cardiac cells-as much as 50 μm in diameter and therefore have a larger capacitance. They contain little contractile filaments or sarcoplasmic reticulum, and transverse tubules are rare. Furthermore, Purkinje cells have fewer lateral intercalated discs and 1-2 large gap junctions at the ends (Zhang et al. 1996) so that they behave like one large cell for the purpose of current spread.

The connective tissue sheath has an insulating function, as implied by Curran (1909) and endorsed by Field (1951). They can be compared to the myelin that surrounds nerve axons, thus increasing conduction velocity and preventing decay of the impulse over large distances. Moreover, the sheath prevents the transmission of the impulse from PFs to neighboring myocytes and from neighboring myocytes to PFs, allowing transmission to the myocardium only at the Purkinje-ventricular muscular junction. In addition, the sheath protects PCs from stresses and strains produced by myocardial contraction.

3.3.3 Gap junctions and Connexins

The gap junction is a specialization of the membrane that allows intracellular communication and mediates transport of small molecules and ions between cells. At gap junctions, the membranes of neighbouring cells are $\sim 30 \text{ \AA}$ from each other and are linked by hydrophilic channels that connect their interiors. Electrical connection is mediated by a hexagonal grouping of protein subunits (called connexins) surrounding the central pore (Fozzard and Arhsdorf 1992). The conductance of gap junctions is modulated by transjunctional voltage, by $[\text{H}^+]_i$, $[\text{Mg}^{2+}]_i$, and $[\text{Ca}^{2+}]_i$, by the phosphorylation state of the connexins, and by extracellular fatty acid composition (Jongsma and Wilders 2000).

At least 14 members of the connexin protein family have been cloned and sequenced (Kumar and Gilula 1996). All connexins are predicted to have four hydrophobic membrane-spanning domains (M1 through M4); N- and C- termini are within the cytoplasmic compartment. The C-terminus region plays an important role in channel regulation by pH and phosphorylation. Six connexin subunits assemble into a hemichannel (termed connexon) that spans the lipid bilayer (Fig.3) (White and Paul 1999).

In the mammalian heart, at least three connexins (Cx) important for impulse propagation are expressed -Cx43, Cx45 and Cx40. Each of them has unique voltage dependence (Hellmann et al. 1996; Moreno et al. 1994a), single channel conductance (Beblo et al. 1995; Bukauskas et al. 1995; Moreno et al. 1994b), permeability properties (Beblo et al. 1995; Beblo and Veenstra 1997; Steinberg et al. 1994; Valiunas et al. 1997; Veenstra et al. 1994), and spatial distribution (Gourdie et al. 1993b; Gros et al. 1994).

Cx43 is present throughout most of the heart, including atrial and ventricular muscle and most components of the conduction system (Gros and Jongma 1996). In contrast, Cx40, which generates channels with high conductance (Beblo and Veenstra 1997), is mainly expressed in the fast-conducting tissue of the His-Purkinje fibers, being nested within the Cx45 expression domain (Coppen et al. 1999; Gourdie et al. 1993b). In the PFs of the peripheral conducting system, Cx 43 is coexpressed with Cx40 (Gourdie et al. 1993b).

The expression of multiple connexins by individual cells in a given tissue raises the distinct possibility that single channels may be composed of more than one connexin. Because each cell's contribution to a complete channel consists of a hemi-channel (referred to as a connexon) containing six connexin subunits, the potential number of unique hybrid connexon and channels is vast (Fig 3) (Kumar and Gilula 1996; White and Paul 1999). Little is known about the natural occurrence or biological significance of hybrid channels *in vivo*. Cardiac tissues that conduct rapidly, such as working myocardium and His-Purkinje fibers, have numerous, large gap junctions, whereas tissues that conduct slowly, such as the SA and AV nodes, contain myocytes that are interconnected by considerably fewer and smaller junctions (Davis et al. 1994; Gourdie et al. 1993b; Oosthoek et al. 1993a; Oosthoek et al. 1993b; Saffitz et al. 1997).

Insights into connexin function have been gained recently through studies of mice in which the expression of one and more connexins has been manipulated genetically. Modest slowing of ventricular conduction velocity has been observed in adult mice that are heterozygous for a Cx43 null mutation (Cx43^{+/-} mice) (Thomas et al. 1998). No slowing of atrial conduction was observed in these mice, even though both atrial and ventricular muscle express Cx43 abundantly in roughly equal amounts and the levels of Cx43 are reduced by approximately 50% in both tissues. These observations suggest that Cx40, present in atrial but not the ventricles of adult mice, is a major electrical coupling protein in the atria whereas Cx43 solely fulfills this role in the ventricle. This prediction has been substantiated by recent studies in Cx40 knockout mice, which exhibit conduction disturbances in atria and the proximal bundles (Hagendorff et al. 1999).

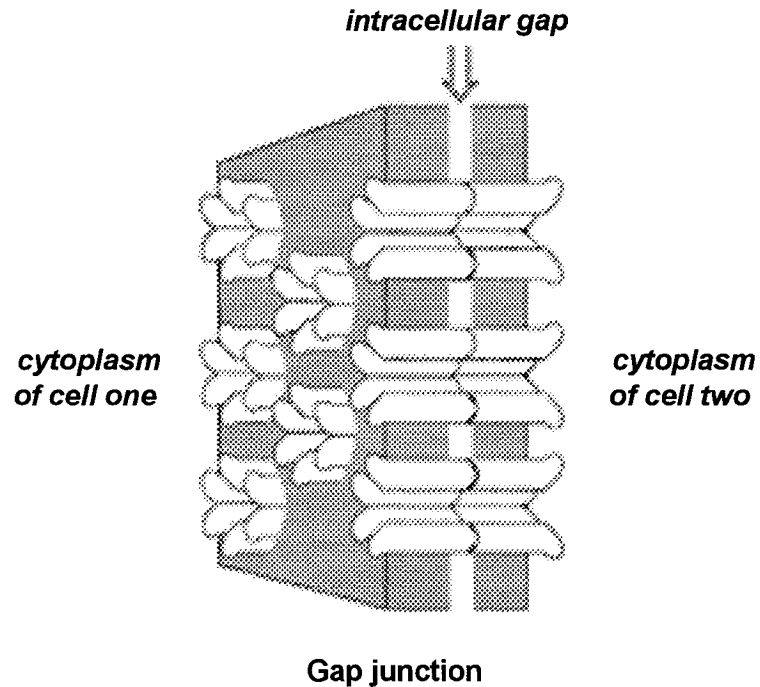
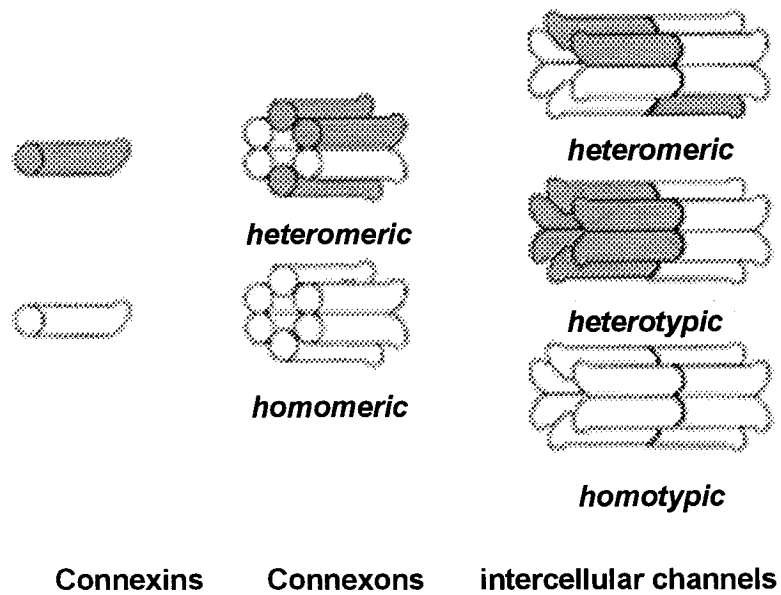


Figure 3. Organization of connexins into connexons, intercellular channels, and gap junctions. Connexin proteins oligomerize into connexons that are homomeric if they have one type of connexin or heteromeric if they contain multiple connexins. Connexons from adjacent cells align to form complete intercellular channels that span two plasma membranes. Each cell can contribute different types of connexons—giving rise to either homotypic, heterotypic, or heteromeric intercellular channels—that cluster in specialized membrane regions called gap junctions [adapted from White and Paul (1999)].

Diverse connexin expression patterns and channel composition are not the only determinants of intercellular communication in the heart. Increasing evidence implicates changes in protein phosphorylation in the regulation of many aspects of connexin biology including intracellular trafficking and assembly of protein into channels at cell surface, single channel properties including unitary conductance and channel open state probability, and connexin degradation and turnover kinetics (Musil and Goodenough 1991).

An altered pattern of Cx40 distribution resulting in microheterogeneities in conduction is found in pacing-induced persistent atrial fibrillation and thought to contribute to the initiation and maintenance of atrial fibrillation (AF) (van der Velden et al. 1998). Cell coupling changes in the ventricles of hypertrophied and failing heart; either via a redistribution of Cx43 (Emdad et al. 2001; Peters et al. 1997), a decline in junctional conductance, or an increase in gap junctional resistance (Carey et al. 2001), leading to conduction abnormalities that are central to arrhythmogenesis (Kleber 1999).

4. Molecular basis of cardiac ion channels

4.1 Na⁺ channels

Na⁺ channels were the first voltage-gated ion channels to be cloned (Noda et al. 1984). With radio-labelled toxin as a probe for Na⁺ channels, a 260-280 kDa glycoprotein (referred to as α subunit) was identified as the major component of Na⁺ channels from eel electroplax (Agnew et al. 1980), chick heart (Lombet and Lazdunski 1984) and rat brain (Noda et al. 1986). Functional mammalian Na⁺ channels are believed to consist of a principal pore-forming α -subunit and one or more auxiliary β -subunits.

Nomenclature Based on the nomenclature for voltage-dependent K⁺ (K_v) channels that is now in common use, a comparable nomenclature has been proposed for voltage-gated Na⁺ channels (Goldin et al. 2000). The name consists of the chemical symbol of the principal permeating ion (Na) with the principal physiological regulator (voltage) indicated as a subscript (Na_v). The number following the subscript indicates the gene subfamily (currently only Na_v1), and the number following the decimal point identifies the specific channel isoform (e.g., Na_v1.1). That isoform number has been assigned

according to the approximate order in which each gene was identified. Splice variants of each family member are identified by lowercase letters following the numbers (e.g., $\text{Na}_v1.1a$). Nine different α subunit isoforms of Na_v1 subfamily and three β subunits (β_1 to β_3) that modify channel gating and kinetics have been identified. Another subfamily (Na_x) closely related Na^+ channel-like proteins has been cloned from mouse, rat and human but has not yet been functionally expressed. The phylogenetic relationships of voltage-gated Na^+ α channel subunits and other information are shown in Fig 4 and table 1.

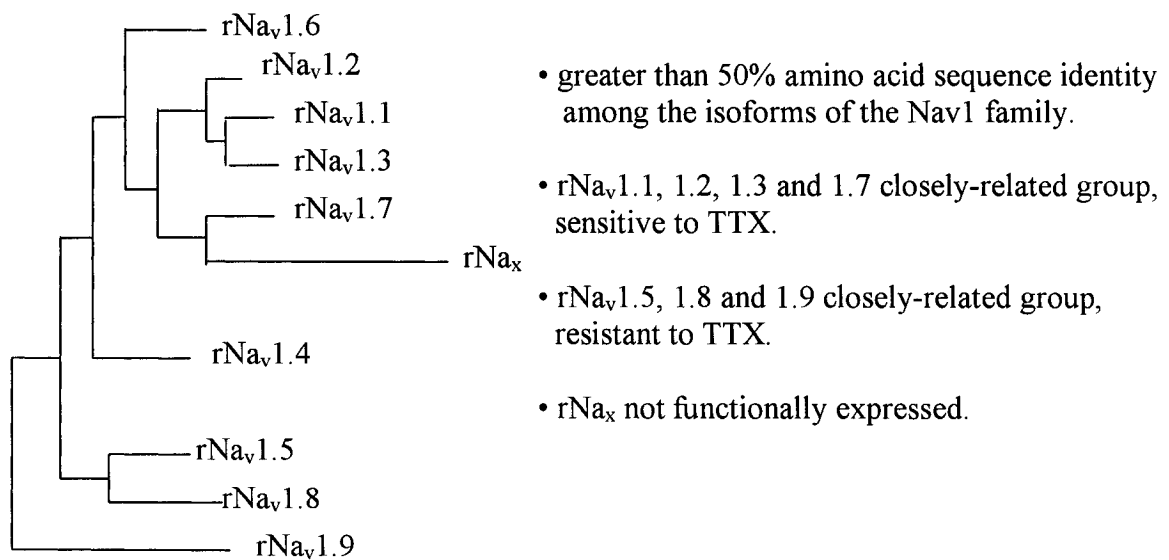


Figure 4. Phylogenetic relationships by maximum parsimony analysis of rat sodium channels $\text{Na}_v1.1$ - $\text{Na}_v1.9$ and Na_x . To perform the analysis, the amino acid sequences for all of the isoforms were aligned using Clustal W [adapted from Goldin (2000) with modification].

Table 1. Mammalian Na⁺ channel α subunits [modified from Goldin (2000)].

Type	Former name	Gene symbol	Chromosomal location	Splice variants	Tissue location	Accession number ^a
Na _v 1.1	rat 1	SCN1A	Mouse 2	Na _v 1.1a	CNS	X03638 (r)
	HBSCI NaCh I		Human 2q24		PNS	X65362(h)
Na _v 1.2	rat II	SCN2A	Mouse 2	Na _v 1.2a	CNS	X03639(r)
	HBSC II HBA		Human 2q23-24			X61149(r) X65361(h)
Na _v 1.3	rat III	SCN3A	Mouse 2	Na _v 1.3a Na _v 1.3b	CNS	Y00766 (r)
			Human 2q24			
Na _v 1.4	SkM1	SCN4A	Mouse 11		sk. muscle	M26643(r)
			Human 17q23-25			M81758(h)
Na _v 1.5	SkM2 rH1 hH1	SCN5A	Mouse 9		uninnervated sk	M27902(r)
			Human 3p21			muscle, heart
Na _v 1.6	NaCh6 PN4 Scn8a	SCN8A	Mouse 15	Na _v 1.6a	CNS, PNS	L39018(r)
			Human 12q13			AF049239(r) AF049240(r)
Na _v 1.7	NaS hNE-Na PN1	SCN9A	Mouse 2		PNS Schwann cells	U35238(rb)
			Human 2q24			X82835(h) U79568(r)
Na _v 1.8	SNS PN3 NaNG	SCN10A	Mouse 9		DRG	X921184(r)
			Human 3p22-24			U53833(r) Y09108(m)
Na _v 1.9	NaN SNS2 PN5 NaT SCN12A	SCN11A	Mouse 9	Na _v 1.9a	PNS	AF05930(r)
						AJ237852(r)
						AF118044(m)
						AB031389(m) AF126739(h)
Na _x	Na _v 2.1	SCN7A	Mouse 2		heart, uterus, sk.muscle	M91556(h)
	Na-G	SCN6A	Human 2q21-23			M96578(r)
	Na _v 2.3	^b				heart, DRG

^a The letter in parentheses after each accession number indicates the species of origin for the sequence, as follows: h, human; r, rat; rb, rabbit; m, mouse. ^b This gene was originally assigned symbols SCN6A and SCN7A, which were mapped in human and mouse, respectively. The two most likely represent the same gene, and the SCN6A symbol will probably be deleted.

Architecture and features of Na⁺ channels Mammalian brain Na⁺ channels are believed to consist of 1 α and 2 β subunits (Catterall 2000a). The structure of cardiac Na⁺ channels has not been as well defined. A relatively huge α subunit is enough to constitute functional Na⁺ channels, i.e., to permit Na⁺ permeation, voltage-dependent activation, inactivation and the receptors for neurotoxin and drug binding (Marban et al. 1998). The α -subunit has four structurally similar domains (DI-DIV), each domain having six helical transmembrane segments S1-S6 (Figure 5A). The S4 segments in each domain contain large numbers of positively charged residues that serve as voltage sensors for channel activation and coupled inactivation (Kontis et al. 1997; Kontis and Goldin 1997; Mitrovic et al. 1998). The channel pore is formed by the P-loop region connecting S5 and S6 segments in each domain and is highly conserved among species- and tissues-specific isoforms. Inspection of the primary structure of the P-loops in each domain reveals that each is unique, as shown in Fig 5B, which differs from Ca²⁺ channels for which each is the same. In domain II of the Na⁺ channel, a lysine in the selectivity filter region critically selects for Na⁺ over Ca²⁺ (Heinemann et al. 1992). Residues in the P-loop of domain I also mediate divalent cation binding, as well as isoform-specific toxin affinity (Backx et al. 1992; Satin et al. 1992). A cysteine that is one position C-terminal to the selectivity filter residue in domain I renders the cardiac channel insensitive to blockade by TTX or STX, but sensitive to Cd²⁺ or Zn²⁺. Conversely, an aromatic residue at the equivalent position (the skeletal muscle or neuronal isoforms) renders the channel TTX sensitive, but Cd²⁺ insensitive. The S6 segment of Domain IV forms part of the local anaesthetic receptor and specific residues in this region are critical in use-dependent blockade by local anaesthetics.

Cardiac α subunit isoforms There have been intermittent electrophysiological reports suggesting the presence of multiple isoforms in cardiac myocytes (Ju et al. 1994). At least 2 α -subunits, Na_v1.1 and Na_v1.5 have been identified in the hearts of rat, rabbit and mouse (Rogart et al. 1989; Baruscotti et al. 1997; Dhar et al. 2001; Petrecca et al. 1997). High- and low-affinity populations of STX receptors, presumably corresponding to Na_v1.1 and Na_v1.5, have been reported in adult rat heart, with high-affinity receptors estimated to make up 25% to 50% of the total population of Na⁺ channels (Rogart et al.

1989). A TTX-sensitive component was also found to be involved in Purkinje fiber APs of guinea pig (Aomine 1989).

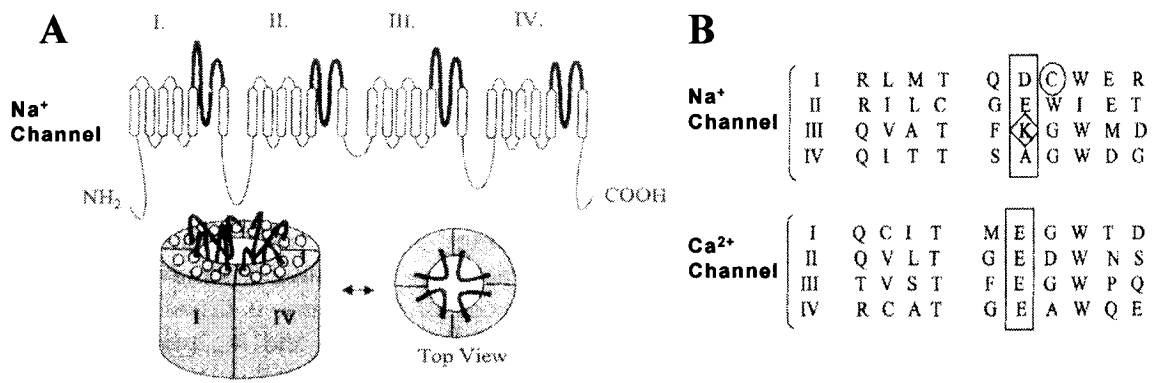


Figure 5. Schematic depiction of the Na channel topology (A) and aligned P-loop amino acid sequences for all four domains of cardiac Na channel (top) and skeletal muscle Ca channel (lower) (B). □ Putative selectivity filter/Ca²⁺ binding sites. ○ isoform-specific TTX/Cd²⁺ sensitivity. ◇ Na/Ca permeability [adapted from Balsler (1999)].

Rogart et al (1989) first cloned a cardiac-specific and TTX-resistant Na⁺ channel isoform of α subunits from rat heart (designated rH1). They found that the corresponding mRNA species were abundant in newborn and adult rat hearts, but not detectable in brain and innervated skeletal muscle. Later on, Gellens et al (1992) cloned the human counterpart (designated hH1, or SCN5A or Na_v1.5). Their Northern blot analysis demonstrated hH1 expression in human atrial and ventricular tissue but not adult skeletal muscle and brain. Moreover, when expressed in *Xenopus* oocytes, hH1 exhibits rapid activation and inactivation kinetics similar to those of native cardiac Na⁺ channels and is resistant to block by TTX (IC₅₀ = 5.7 μ M). More importantly, recent studies reveal that mutations in SCN5A (hH1) cause chromosome 3-linked LQT (Wang et al. 1995b) or Brugada syndrome (Chen et al. 1998) or both (Bezzina et al. 1999), or conduction defects and AV block (Lupoglazoff et al. 2001; Tan et al. 2001).

Na_v1.5 (SCN5A), as the prominent cardiac α subunit, is heterogeneously expressed in the heart: Northern blots, with higher expression in left atrium (LA), right atrium (RA),

and left ventricle (LV) than PFs and the right ventricle (RV), and more in endocardium than epicardium in sheep heart; Western blots show higher expression in LA and LV than RA and RV (Fahmi et al. 2001). The distribution of $\text{Na}_v1.5$ across different regions of rat heart has been localized to the surface and t-tubular system, and expression is seen at the intercalated disks of ventricular myocytes. This localization is likely responsible for fast conduction in ventricular myocardium (Cohen 1996). A gradient of sodium channel expression has been reported in the enclosed rabbit AV node; lower levels in the central compact node perhaps underlies the slower conduction through this region (Petrecca et al. 1997).

$\text{Na}_v1.1$, encoding TTX-sensitive Na^+ channel, was cloned from rat brain and is expressed in adult rat brain and heart (Noda et al. 1986; Schaller et al. 1992). In both brain and heart, there are two isoforms of NaCh I ($\text{Na}_v1.1$), NaCh I and NaCh Ia (Schaller et al. 1992). Huang et al (2001) recently reported an increased expression of $\text{Na}_v1.1$ protein in post-myocardium infarction (MI) myocytes with reversion of NaCh Ia:NaCh I isoform ratio toward the fetal phenotype, but the predominant $\text{Na}_v1.5$ subtype remained unchanged in post-MI myocytes. By applying immunocytochemistry, Dhar et al (2001) showed that $\text{Na}_v1.1$, $\text{Na}_v1.5$, $\beta 1$ and $\beta 2$ subunits are localized in adult rat and mouse cardiac myocytes along z-lines.

Very recently, a comprehensive study by the Catterall group showed that the principal cardiac pore-forming α -subunit in mouse heart ($\text{Na}_v1.5$) is also preferentially localized in intercalated disks, whereas the brain isoforms $\text{Na}_v1.1$, $\text{Na}_v1.3$, and $\text{Na}_v1.6$ are localized in the transverse tubules (Maier et al. 2002). Although currents carried by these highly-TTX-sensitive Na^+ channels were small and only detectable after activation with β scorpion toxin, they played an important role in coupling depolarization of the cell surface membrane to contraction, because low TTX concentrations (that do not affect $\text{Na}_v1.5$) reduced left ventricular function. It was therefore suggested that $\text{Na}_v1.5$ in the intercalated disks is primarily responsible for AP conduction between cells, whereas brain isoforms in the transverse tubules play a role in coupling electrical excitation to contraction in cardiac muscle (Maier et al. 2002).

Two isoforms with similar sequences (Shimizu et al. 1991) have been found to be expressed abundantly in the heart and uterus: one is $\text{hNa}_v2.1$ isolated from human heart

(George, Jr. et al. 1992), the other is mNa_v2.3 cloned from a mouse atrial tumor cell line (Felipe et al. 1994). The transcript levels of mNa_v2.3 in the heart, brain, and skeletal muscle are differentially regulated during development and in the heart are greatest immediately after birth (Felipe et al. 1994). These two isoforms have been considered atypical Na⁺ channels because they differ in two major regions shown to be critical for normal Na⁺ channel function (George, Jr. et al. 1992). First, there are significantly fewer charges in the S4 region, which are essential for voltage-sensitive gating (Stuhmer et al. 1989; Yang and Horn 1995). Second, the interdomain III-IV linker that is involved in fast inactivation (Patton et al. 1992; West et al. 1992) is poorly conserved. In particular, the critical Ile-Phe-Met (IFM) residues that form the nucleus of the inactivation particle have been replaced with Ile-Phe-Ile (IFI). It is not possible to evaluate the functional significance of these channels because none of them has been able to be functionally expressed in a heterologous system (Akopian et al. 1997; Felipe et al. 1994). The reason for the inability to observe functional currents may be because the channels require presently unidentified accessory subunits to function, because the full-length sequences may contain cloning errors or because they represent pseudo-genes (Goldin 2001).

β-subunits Instead of forming the ion conducting pore, β-subunits modulate channel gating and regulate the level of cell surface expression. More recently, they have been shown to function as cell adhesion molecules in terms of interaction with extracellular matrix and cytoskeleton, regulation of cell migration and cellular aggregation (Isom 2001). Three auxiliary subunits β1 (Isom et al. 1992; Makita et al. 1994), β2 (Isom et al. 1995) and β3 (Morgan et al. 2000) with at least one alternative splicing isoform of β1 (β1A) (Malhotra et al. 2000) have been reported. They consist of a single transmembrane domain, a small intracellular C-terminal region and a large extracellular N-terminal domain with an immunoglobulin-like fold (Stevens et al. 2001). All of them have been found to be expressed in the heart and to assemble with α-subunits to form a heterooligomeric, glycosylated protein modulating the gating and /or current amplitude of Na⁺ channels (Dhar et al. 2001; Gordon et al. 1988; Malhotra et al. 2000; Wollner et al. 1988).

$\beta 1$ was initially cloned from rat brain (Isom et al. 1992) and later from human, mouse and rabbit brain (Belcher and Howe 1996; Grosson et al. 1996; McClatchey et al. 1993). Coexpression of rat brain α subunits with $\beta 1$ in *Xenopus* oocytes increases peak current and accelerates activation and inactivation (Isom et al. 1992). Although $\beta 1$ mRNA is detected in the heart (Makita et al. 1994; Qu et al. 1995), in addition to brain, spinal cord and skeletal muscle (Isom et al. 1992; Makita et al. 1994), it has been controversial whether $\beta 1$ -subunits contribute to native cardiac I_{Na} . Makita et al (1994) reported no change in phenotype, while Qu et al (1995) reported an increase in current amplitude as the major effect by coexpression of the rH1 α -subunits in *Xenopus* oocytes. Nuss et al (1995) reported that the effects of $\beta 1$ subunit on currents carried by co-expressed human cardiac α -subunits were similar to those with the brain α -subunit. In cardiac muscle, $\beta 1$ has been assumed to contribute to the gating properties observed in mature cells, while gating behaviour of channels in immature cells is believed caused by a lack of $\beta 1$ subunits (Kupersmidt et al. 1998). In line with this notion, mouse atrial tumour (AT-1) cells exposed to anti- $\beta 1$ antisense oligonucleotides displayed an immature I_{Na} phenotype with smaller I_{Na} that activated and inactivated more slowly and had more negative voltage dependence of inactivation than mature I_{Na} (Kupersmidt et al. 1998). Recently, it has also been demonstrated that disturbed association of $\beta 1$ with the cardiac hH1 isoform occurs in congenital long QT3 syndrome (An et al. 1998). In addition, association with $\beta 1$ has been reported to change the pharmacological profile of cardiac Na^+ channels (Bonhaus et al. 1996; Makielski et al. 1996).

A splice variant of $\beta 1$, termed $\beta 1A$ with an apparent intron retention event, has recently been cloned from an adrenal gland cDNA library (Malhotra et al. 2000). It is structurally homologous to $\beta 1$ with a single transmembrane domain. $\beta 1A$ mRNA expression is developmentally regulated in rat brain such that it is complementary to $\beta 1$. $\beta 1A$ mRNA is expressed during embryonic development, and then undetectable after birth, concomitant with the onset of appearance of $\beta 1$. Western blot analysis reveals that $\beta 1A$ protein is expressed in the heart, skeletal muscle and adrenal gland but not in adult brain or spinal cord. Immunocytochemical analysis of $\beta 1A$ expression shows selective expression in the heart and spinal cord neurons, with high expression in the heart and all

dorsal root ganglia neurons. Co-expression of $\beta 1A$ with $Na_v1.2$ in heterologous systems results in a 2.5-fold increase in current density and subtle differences in channel activation and inactivation compared with $Na_v1.2$ expression alone.

The $\beta 2$ subunits have been cloned from rat and human brain, and found to be expressed in the heart (Eubanks et al. 1997; Isom et al. 1995). The role of $\beta 2$ is more controversial. Although recent studies suggest that it does not have a significant functional role in the heart (Dhar et al. 2001), it does coimmunoprecipitate and colocalize with $Na_v1.1$, $Na_v1.5$ and $\beta 1$.

The $\beta 3$ subunits have recently been cloned and are expressed widely in excitable and nonexcitable tissues (Stevens et al. 2001). Very recently, Fahmi et al (2001) reported that $\beta 3$ is expressed heterogeneously in sheep heart, with highest levels in ventricles, moderate levels in PFs and minimal expression in atria by either Northern blot or Western blot analysis. This is in contrast to the uniform expression of $\beta 1$ throughout the heart. Co-expression of $\beta 3$ with cardiac-specific SCN5A in *Xenopus* oocytes resulted in three-fold increases in current density (similar to that observed with $\beta 1$ and SCN5 α co-expression), and a significant depolarizing shift in steady-state inactivation with little difference in activation compared to SCN5A alone or SCN5A + $\beta 1$. In addition, the rates of inactivation for SCN5A co-expression with either β subunit were not significantly different from those for SCN5A alone. However, recovery from inactivation at -90 mV was significantly faster for SCN5A + $\beta 1$ compared to SCN5A + $\beta 3$, and both were significantly faster than SCN5A alone.

The heterogeneity of functional Na^+ channel density among different regions of the heart has been long recognized and recently described in detail by Li and Shrier (2001). Whether different β subunits and/or different levels of expression of these subunits underlie such heterogeneity remains unclear, but it was suggested that differences in the levels of SCN5 α expression may be more important (Fahmi et al. 2001). Both $Na_v1.5$ and $Na_v1.1$ associate with $\beta 1$ and $\beta 2$ and are expressed in cardiac myocytes (Dhar et al. 2001), thus the distribution of α or β subunit may contribute to Na^+ channel heterogeneity.

4.2 Ca²⁺ channels

Ca²⁺ channels are structurally more complex and thus functionally more diverse than Na⁺ channels. A model of Ca²⁺ channel composition based on purification studies and biochemical analysis consists of a principal pore-forming α_1 subunit of 190 kDa in association with a disulfide-linked dimer of $\alpha_2\delta$ (170 kDa), an intracellular phosphorylated β subunit of 55 kDa, and a transmembrane γ subunit of 33 kDa (Fig 6).

Ten different isoforms of the α_1 subunit have been defined. They are responsible for the functional differences among different types of Ca²⁺ currents. As shown in the table 2 below (Catterall 2000b), a nomenclature dividing the channels into three structurally and functionally related families (Ca_v1, Ca_v2 and Ca_v3) has been recently proposed (Ertel et al. 2000). The basis of multiple types of Ca²⁺ channels and their corresponding currents, as defined by physiological and pharmacological criteria (Bean 1989; Hess et al. 1986; Llinas et al. 1992) are now clear.

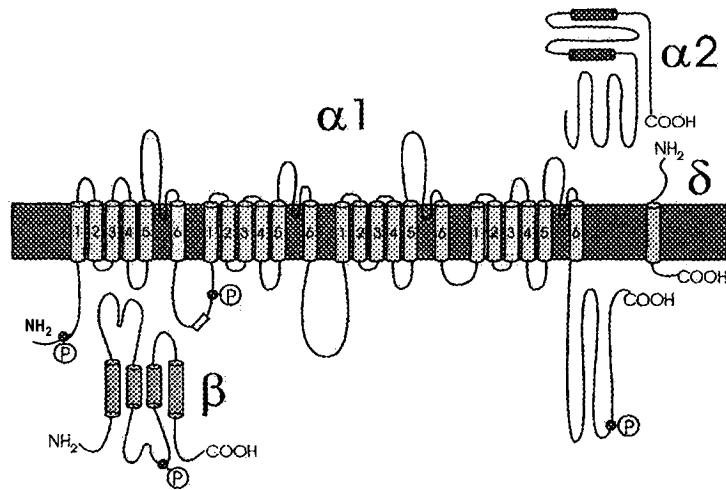


Figure 6. A topology model of Ca²⁺ channel composed of α_1 and associated auxiliary subunits of β , α_2 and δ . P in circle represents phosphorylation sites [adapted from Keef et al. (2001) with modification].

Table 2. Subunit composition and function of Ca²⁺ channel types

Ca ²⁺ channel	I _{Ca} types	α subunit names	Primary locations	Specific blockers	Functions
Ca _v 1.1	L	α _{1S}	Skeletal muscle	DHPs	EC-coupling, Ca homeostasis, Gene regulation
Ca _v 1.2	L	α _{1C}	Cardiac muscle Endocrine Neurons	DHPs	EC-coupling, Hormone secretion, Gene expression
Ca _v 1.3	L	α _{1D}	Endocrine Neurons	DHPs	Hormone secretion, Gene regulation
Ca _v 1.4	L	α _{1F}	Retina		Tonic neurotransmitter release
Ca _v 2.1	P/Q	α _{1A}	Nerve terminals Dendrites	ω-Agatoxin	Neurotransmitter release, Dendritic Ca ²⁺ transient
Ca _v 2.2	N	α _{1B}	Nerve terminals Dendrites	ω-CTx-GVIA	Neurotransmitter release, Dendritic Ca ²⁺ transient
Ca _v 2.3	R	α _{1E}	Cell bodies Dendrites	None	Ca ²⁺ dependent AP
Ca _v 3.1	T	α _{1G}	Nerve terminals Cardiac muscle Skeletal muscle Neurons	None	Neurotransmitter release, Repetitive firing
Ca _v 3.2	T	α _{1H}	Cardiac muscle Neurons	None	Repetitive firing
Ca _v 3.3	T	α _{1I}	Cardiac muscle Neurons	None	Repetitive firing

Adapted from Catterall (2000b) with modification

4.2.1 Molecular basis for Ca²⁺ channel function

As for the pore-forming subunits of voltage-gated Na⁺, K⁺ channels, α₁ subunits of all types of Ca²⁺ channels are essential for channel function. They contain four repetitive domains (I-IV), each consisting of six transmembrane α helices (S1-S6) and a membrane-associated loop between S5 and S6 (P-loop). The S4 segments of each homologous domain serve as the voltage sensors for activation, moving and rotating under the influence of the electric field and initiating a conformational change that opens the pore. The P-regions of each domain contain a pair of glutamine residues that are required for Ca²⁺ selectivity. The inner pore lined by the S6 segments of each domain forms the binding sites for dihydropyridines (DHPs).

4.2.2 L-type Ca^{2+} channel

Cardiac L-type Ca^{2+} channels were initially purified from chick (Cooper et al. 1987) and porcine heart (Haase et al. 1991). They are heterooligomeric complexes consisting of an α_{1C} (~240 kDa) and an accessory $\alpha_{2\delta}$ (~175 kDa) and β subunit (~60 kDa). As the prominent subunit of channel, α_{1C} subunit is encoded by the gene of $\text{Ca}_v1.2$ and highly expressed in cardiac muscle. It comprises more than 80% of L-type channel-associated subunits in mammalian heart and vascular smooth muscle (Safayhi et al. 1997). The human α_{1C} gene has been mapped to the chromosome 12p13.3 (Schultz et al. 1993). The auxiliary β subunits modulate channel expression and gating (Lacerda et al. 1991; Singer et al. 1991) and also control targeting of α_{1C} subunits to the plasma membrane (Gerster et al. 1999). They are encoded by four different genes (β_1 to β_4). β_2 is not the only β cDNA that has been cloned from the heart, β_1 and β_3 variants have also been detected (Collin et al. 1993; Hullin et al. 1992), but β_2 is found at the highest density in the heart muscle and has been reproducibly shown to form cardiac Ca^{2+} channels (Gao et al. 1997a; Pichler et al. 1997). The $\alpha_{2\delta}$ subunit is ubiquitously expressed in all types of high voltage-dependent Ca^{2+} channels (Takagishi et al. 2000). Three isoforms have been defined, with isoform 1 and 2 expressed in the heart (Klugbauer et al. 1999). However, their function remains undefined.

L-type Ca^{2+} channels are localized on the surface of the plasma membrane and T-tubules in both rabbit and rat myocytes, but in rat the labeling is more intense in T-tubules than on the surface of the membrane (Takagishi et al. 2000).

4.2.3 T-type Ca^{2+} channels

Three α_1 subunits of low voltage-activated T-type channels were recently cloned, α_{1G} , α_{1H} and α_{1I} (Cribbs et al. 1998; Lee et al. 1999; McRory et al. 2001; Perez-Reyes et al. 1998). The location of these genes on human and mouse chromosomes was also mapped. The α_{1G} gene was localized to human chromosome 17q22, α_{1H} gene to 16p13.3 and α_{1I} gene to 22q 12.3-13.1. The channels encoded by these genes are similar in structure to high voltage-activated L-type channels. However, their overall amino acid sequence homology to L-type channels is quite low (< 25%). The β -subunit binding region found

in α_{1C} is not found in α_{1H} . Expression of any of α_{1G} , α_{1H} and α_{1I} subunits alone produces the classic T-type Ca^{2+} channel current, suggesting that the expression of T-type channels does not require auxiliary subunits.

The α_{1G} cDNA was cloned from rat brain and is most highly expressed in brain (Perez-Reyes et al. 1998). Although α_{1H} was cloned from an adult human heart library, much more mRNA appears to be expressed in kidney and liver (Cribbs et al. 1998). α_{1I} was also cloned from rat brain (Lee et al. 1999), but no expression of α_{1I} in the heart has been reported until recently. The exact α_1 subunit composition of cardiac T-type channels is still an open question.

4.3 K^+ channels

K^+ channels are the largest and most diverse family of ion channels, and the voltage-gated K^+ channels (Kv channels) constitute the largest group. In cardiac myocytes, many types of K^+ channels act in concert to determine the configuration and duration of the action potential (AP). The presence of multiple overlapping K^+ currents also contributes to the heterogeneity of AP configuration and duration throughout the heart.

Channel diversity and classification Since the first gene encoding a K^+ channel was cloned from *Drosophila* (Papazian et al. 1987), more than 200 genes encoding a variety of K^+ channels have been identified, all containing a pore segment selective for K^+ ions (Hartmann et al. 1991; Yellen et al. 1991). K^+ channels are divided into families with groups containing six, four and two putative transmembrane segments (Fig 7); namely: 1) voltage-gated K^+ (Kv) channels containing six transmembrane regions (S1-S6) with a single pore (6-TM); 2) inward rectifier K^+ channels containing only two transmembrane regions and a single pore (2-TM); 3) two-pore K^+ channels containing four transmembrane regions with two pore regions (4-TM) (Snyders 1999). Table 3 lists a generalized classification of K^+ channel subunits (Shieh et al. 2000).

Table 3. Classification of cloned K⁺ channels [modified from Shieh (2000)].

Type	Gene	Nomenclature	Modulators	Tissue Expression
Kv channels (Shaker)	<i>KCNA1</i>	Kv1.1	α-DTX, HgTX1	Neurons, heart,
	<i>KCNA2</i>	Kv1.2	CTX, α-DTX	Brain, heart
	<i>KCNA3</i>	Kv1.3	AgTX2, α-DTX	Lymphocytes
	<i>KCNA4</i>	Kv1.4	UK78282	Brain, heart
	<i>KCNA5</i>	Kv1.5	4AP, clofilum	Brain, heart
	<i>KCNA6</i>	Kv1.6	α-DTX	Brain
	<i>KCNA7</i>	Kv1.7	4AP, capasicin	Heart,
β subunits (Kv channels)	<i>KCNAB1</i>	Kvβ1		Brain (Kvβ1.1) Heart (Kvβ1.2)
	<i>KCNAB2</i>	Kvβ2		Brain, heart,
	<i>KCNAB3</i>	Kvβ3		Brain
Kv channel (<i>Shab</i>)	<i>KCNB1</i>	Kv2.1-2	Hanatoxin, TEA	Brain, heart, Kidney, retina,
Kv channel (<i>Shaw</i>)	<i>KCNC1</i>	Kv3.1	4-AP, TEA	Brain, muscle,
	<i>KCNC1</i>	Kv3.2	4-AP, TEA	Brain
	<i>KCNC1</i>	Kv3.3	4-AP, TEA	Brain, liver,
	<i>KCNC1</i>	Kv3.4	4-AP, TEA	Brain, muscle,
Kv channel (<i>Shal</i>)	<i>KCND1</i>	Kv4.1	4-AP	Brain, heart,
	<i>KCND2</i>	Kv4.2	4-AP, PaTX	Brain, heart
	<i>KCND3</i>	Kv4.3	4-AP, PaTX	Heart, brain
Ether-a-go-go Human EAG	<i>KCNH1</i>	ERG		Brain
	<i>KCNH2</i>	hERG	E4031, dofetilide	Brain, heart
	<i>KCNH3</i>	BEC1		Brain
	<i>KCNH4</i>	BEC2		Brain
minK	<i>KCNE1</i>	minK		Kidney, heart,
	<i>KCNE2</i>	MiRP1		Heart
	<i>KCNE3</i>	MiRP2		Muscle
KvLQT1	<i>KCNQ1</i>	KvLQT1	Chromanol-293B	Heart, kidney,
	<i>KCNQ2</i>	KvLQT2	TEA, L735,821	Brain, neuron
	<i>KCNQ3</i>	KvLQT3	TEA, linopirdine	Brain, neuron
	<i>KCNQ4</i>	KvLQT4		Outer hair cell,
	<i>KCNQ5</i>	KvLQT5	Linopirdine	Brain, s.k.muscle
Inward rectifier	<i>KCNJ1</i>	Kir1.1-1.3	Ba ²⁺	Kidney,
	<i>KCNJ2</i>	Kir2.1	Ba ²⁺ , spermine, Mg ²⁺	Heart, brain
	<i>KCNJ3</i>	Kir3.1	Ba ²⁺	Heart, cerebellum
	<i>KCNJ4</i>	Kir2.3	Ba ²⁺	Heart, brain
	<i>KCNJ5</i>	Kir3.4	Ba ²⁺ , Cs ⁺	Heart, pancreas
	<i>KCNJ6</i>	Kir3.2	Ba ²⁺ , Cs ⁺	Cerebellum,
	<i>KCNJ9</i>	Kir3.3	Ba ²⁺ , Cs ⁺	Brain
	<i>KCNJ12</i>	Kir2.2	Ba ²⁺ , Cs ⁺	Heart
<i>KCNJ14</i>	Kir2.4	Ba ²⁺ , Cs ⁺	Brain, retina	

Characteristic structure of Kv channels Kv channels include four *Shaker*-related families (*Shaker*, *Shab*, *Shaw* and *Shal*), human *ether-a-go-go*-related K⁺ channels (HERG), Ca²⁺-activated K⁺ channels and KCNQ channels.

Kv channels conserve the K⁺-selective signature motif of G(Y/F)G in the P-loop. Four of the P-loop domains form a functional K⁺-conducting pore (MacKinnon 1991). Kv channels are thought to be tetramers of four pore loop-containing α subunits (MacKinnon 1995; MacKinnon and Doyle 1997). The outer mouth of the pore that is composed of portions of the P-loop and adjacent residues in S5 and S6 segments serves as the binding sites for toxins and K⁺ channel blockers (Yellen et al. 1991; Goldstein and Miller 1993; MacKinnon et al. 1988; MacKinnon and Yellen 1990; Pascual et al. 1995), while the inner mouth consisting of residues from S5 and S6 segments serves as binding sites for compound such as 4-aminopyridine (4AP), tetraethylammonium (TEA) and quinidine.

A regularly spaced array of 5-7 positive charges in S4 constitutes the major component of the voltage sensor for gating, though negative charges in S2 and S3 may also contribute (Seoh et al. 1996). Depolarization of the membrane causes a physical (outward) movement of S4, which in turn induces further conformational changes that open the channel and selectively conduct K⁺ ions.

After activation, most Kv channels undergo a stable nonconducting state, termed inactivation. The mechanisms of inactivation have been associated with distinct molecular domains of the channel. The N-terminus of the *Shaker* K channel is essential for the fast “ball and chain” reaction called N-type inactivation. The N-terminus moves into the internal mouth to occlude the pore after the channel has opened (Hoshi et al. 1990; Isacoff et al. 1991). In contrast to this fast process of inactivation, the C- and P-type processes existing in most K⁺ channels involve a slower rearrangement of outer mouth and specific residues in the pore, respectively (De Biasi et al. 1993; Liu et al. 1996a; Yellen et al. 1994).

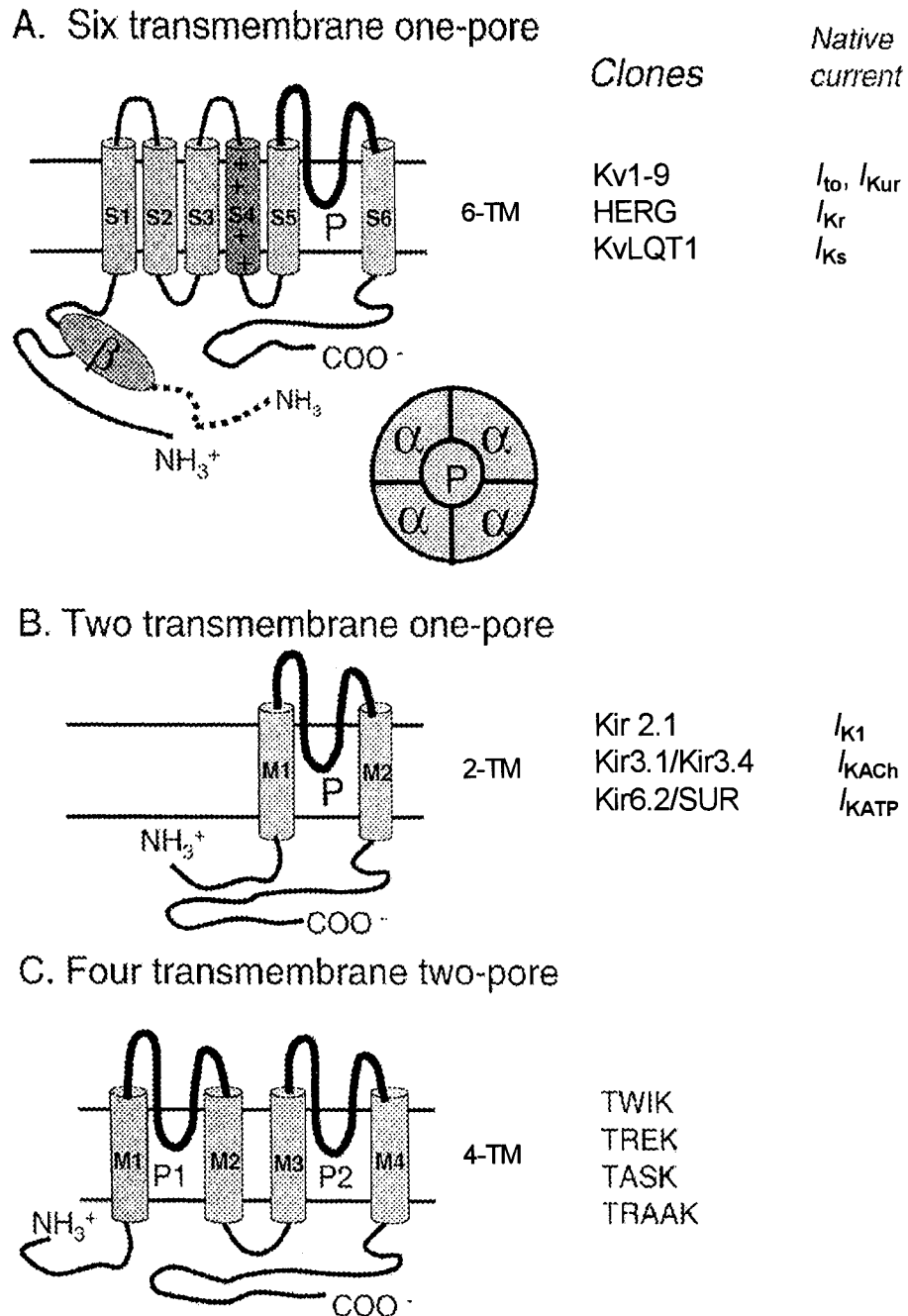


Figure 7. Schematic representation of the structural classification of K^+ channel subunits. **A**, 6-TM subunits. The voltage-gated K^+ channels are composed of four subunits, each containing six transmembrane segments (S1-S6) and a conducting pore (P) between S5 and S6 with a voltage sensor (positive charge of amino acid residues) located at S4. Some of the voltage-gated K^+ channels include an auxiliary β -subunit ($Kv\beta$), which is a cytoplasmic protein with binding site located at the N terminus of the α -subunit. The inset shows the general assembly of K^+ channels. The homotetrameric K^+ channel

consists of four identical subunits while different α -subunits form heterotetrameric K^+ channels. **B**, 2-TM subunits. The inward rectifier K^+ channels belong to a superfamily of channels with four subunits each containing two transmembrane segments (M1 and M2) with a P-loop in between. **C**, 4-TM subunits. This represents a class of K^+ channels that has four transmembranes with two P-loops. TWIK, two-pore weak inward rectifier; TASK, TWIK-related acid-sensitive K^+ channel; TRAAK, TWIK-related arachidonic acid-stimulated K^+ channel are in this group [adapted from Shieh (2000) with modification].

Accessory subunits Accessory subunits contribute to the diversity of Kv channel function. Although they are not involved in forming the pore, the accessory subunits play roles as diverse as modulation of gating properties, cell surface expression, and /or trafficking of the ion channel complex, and binding sites for endogenous and exogenous ligands.

Kv β 1.1 and Kv β 2.1 belong to a family of cytoplasmic subunits that encode proteins of 360-400 amino acids with 85% homology between the C terminal residues (Deal et al. 1996; Rettig et al. 1994). Differences in the N-terminus of these two subunits cause different modulation of channel function. Kv β 1.1 inactivates the delayed rectifier Kv1.1 with a ball-chain mechanism (Morales et al. 1995), while Kv β 2.1 induces more subtle kinetic changes (Uebele et al. 1996). Several splice variants of the Kv β 1.1 isoform have been cloned from the heart (Deal et al. 1996; England et al. 1995a; England et al. 1995b; Majumder et al. 1995).

Kv β 1- β 3 family subunits associate with Kv1 subunits, while Kv β 4 associates with the Kv2 family (Fink et al. 1996). Certain other Kv channels, such as Kv5, Kv6, Kv8 and Kv9 do not form functional channels themselves but associate with Kv2.1 channels to alter their biophysical properties (Kramer et al. 1998; Salinas et al. 1997). A classical β subunit, minK, is associated with KvLQT1 to generate the current most close to endogenous I_{Ks} by regulating channel surface expression and gating. minK-related peptide1 (MiRP1) not only modulates HERG channel gating (Abbott et al. 1999; Sesti et al. 2000), but also enhances HCN expression and activation kinetics (Yu et al. 2001). Recently, chaperone proteins, such as Kv channel associating protein (KChAP), regulating the function and expression of Kv2.1, Kv1.3 and Kv4.3, have been reported

(Kuryshv et al. 2000); Kv channel interacting proteins (KChIPs) increase the current density of Kv4 subunits (An et al. 2000) and contribute to the heterogeneity of I_{to} density across canine and human ventricular free walls (Rosati et al. 2001).

Given the diversity of K^+ channel subunits (α and β) and the potential to form heteromeric channel complexes with specific expression, cellular targeting, biophysical and pharmacological properties, understanding the precise composition of channel complexes *in vivo* remains a big challenge.

Criteria for assigning cloned channel subunits to native cardiac currents With many cDNAs cloned from mammalian heart, the assignment of the gene(s) encoding specific endogenous currents has become a significant issue. The following criteria have been used (Deal et al. 1996):

- (1) The basic biophysiological properties (kinetics and their voltage-dependence, conductance, rectification, ion selectivity) should be in reasonable agreement.
- (2) The pharmacology of compounds known to interact directly with the channel pore, e.g., dendrotoxin, TEA, quinidine, should be similar.
- (3) Immunohistochemistry with isoform-specific antibodies made against the cloned subunits should confirm that channel protein is present in the cardiac myocytes.
- (4) Affinity-purification from native tissue should confirm the protein composition of the native channel in terms of accessory subunits and heterotetramer formation.
- (5) Deletion of the cloned channel using *in vitro* antisense approaches or *in vivo* suppression should further confirm the identity of the current that this gene supports.
- (6) Refined versions of these techniques should be used to identify the exact splice variant(s) of relevant K^+ channel subunits involved in the native channel.

4.3.1 Molecular basis of I_{to}

I_{to} varies widely in density and kinetics among different species and different cardiac cell types. Two potential explanations of this variability have been proposed: (1) the I_{to} in different regions is produced by more than one α -subunit gene product, or (2) the α subunits for I_{to} channels are modified by association with accessory subunits or other factors (McKinnon 1999). I_{to} can broadly be classified into two separate types – fast and

slow I_{to} ($I_{to,f}$ and $I_{to,s}$) in terms of rates of inactivation and recovery (Nerbonne 2000; Barry and Nerbonne 1996; Brahmajothi et al. 1999; Nabauer et al. 1996; Guo et al. 2000). A number of Kv α -subunits such as Kv1.4, Kv3.4, Kv4.2 and Kv4.3, known for generating I_{to} -like currents when heterologously expressed, have become primary candidates for cardiac I_{to} . These clones are all expressed in the myocardium. Based on their biophysical properties, Kv4.2 and /or Kv4.3 contribute to cardiac $I_{to,f}$, while Kv1.4 shares many properties with $I_{to,s}$ (Beck et al. 1998). Antisense oligonucleotides targeted against Kv1.4, Kv4.2 or Kv4.3 (Bou-Abboud and Nerbonne 1999; Fiset et al. 1997; Wang et al. 1999) and transgenic knockouts of Kv1.4 or Kv4.2 (Guo et al. 2000; London et al. 1998; Wickenden et al. 1999c; Barry et al. 1998) suggest that Kv4.2 is involved in encoding $I_{to,f}$ in rodents such as mouse, rat, and ferret, Kv4.3 is more responsible for $I_{to,f}$ in dog and human, while Kv1.4 primarily contributes to a small and slow component of I_{to} . Supporting evidence comes from studies examining the relationship of the expression patterns of Kv1.4, 4.2 and 4.3 with the magnitude of $I_{to,f}$ and $I_{to,s}$. For example, in rat left ventricle, Kv4.3 and Kv1.4 mRNA expression has been found to be uniform across the ventricular wall, whereas Kv4.2 shows a marked gradient, with higher expression levels in epicardial than endocardial cells (Dixon et al. 1996; Dixon and McKinnon 1994), paralleling I_{to} density across the ventricular wall (Dixon and McKinnon 1994; Wickenden et al. 1999b). Similarly, in ferret left ventricle, regional differences in the expression of Kv1.4 and Kv4.2/Kv4.3 are related to regional differences in $I_{to,f}$ and $I_{to,s}$ (Brahmajothi et al. 1999).

Nevertheless, the electrophysiological properties of Kv1.4 and Kv4 currents are still somewhat different from those in native cells. Although the characteristic properties of rabbit I_{to} are consistent with those of Kv1.4 (Wickenden et al. 1999a; Giles and Imaizumi 1988; Petersen and Nerbonne 1999), treatment of cultured rabbit atrial myocytes with antisense against Kv1.4 results in only partial reduction of I_{to} , with even larger I_{to} reductions by antisenses targeted against Kv4.2 and Kv4.3 (Wang et al. 1999). Kv β 2 and 3 subunits specifically increase the rate of inactivation of human and ferret Kv1.4 currents (Morales et al. 1995; Majumder et al. 1995), while Kv β 1 and 2 increase Kv4.3 current density and Kv4.3 protein expression without affecting channel gating (Yang et al. 2001).

KChAP is a member of the transcription factor binding protein family. It has been found that coexpression with KChAP increases the amplitude currents carried by many Kv α -subunits including Kv4.3, without affecting channel gating and kinetics (Kuryshv et al. 2000; Wible et al. 1998). Complexes of KChAP with Kv4.3 have been coimmunoprecipitated from rat heart (Kuryshv et al. 2000).

KChIPs are Ca²⁺-binding proteins that interact with the cytoplasmic amino termini of Kv4 subunits and increase current density, slow inactivation and accelerate recovery from inactivation, while shifting activation and inactivation voltage-dependence (An et al. 2000; Decher et al. 2001). They also colocalize and coimmunoprecipitate with native Kv4 channels (An et al. 2000). KChIP2 is specifically expressed in hearts of rats (Ohya et al. 2001), mice (Ohya et al. 2001), dogs (Rosati et al. 2001) and humans (Ohya et al. 2001; Rosati et al. 2001). Coexpression of rat or human Kv4.2/4.3 and KChIP2 generates the currents that closely resemble I_{to} recorded in rat myocytes (Wickenden et al. 1999a; An et al. 2000 ; Bou-Abboud and Nerbonne 1999) and human epicardial I_{to} (Decher et al. 2001). The steep gradient of KChIP2 mRNA concentration across the canine and human ventricular free wall parallels that of I_{to} (Rosati et al. 2001), while Kv4.3 mRNA is expressed uniformly across the ventricular wall. Kou et al (2001) used a gene-targeting approach to generate KChIP2-deficient mice (KChIP2^{-/-}) found that although the hearts of KChIP2^{-/-} mice had no obvious structural abnormalities and no arrhythmias, single-cell electrophysiology revealed nearly complete elimination of I_{to} and prolonged APs. Programmed stimulation provoked nonsustained polymorphic ventricular tachycardia in 8 of 12 KChIP2^{-/-} mice, but not in wild-type mice. Thus, loss of I_{to} can confer a genetic susceptibility to ventricular tachycardia-one of the most lethal forms of ventricular arrhythmia (Sanguinetti 2002).

In addition, frequenin (KChIP-related Ca²⁺ binding protein) is expressed in the heart, increases I_{to} density and alters inactivation properties (Nakamura et al. 2001). The cytoskeleton has been shown to regulate Kv4.2 currents by interacting with a scaffold protein, filamin that is directly linked to Kv4.2 channels (Petrecca et al. 2000).

4.3.2 Molecular basis of I_K

Genes and heterologous expression of I_{Kr} channels HERG, the human *ether-a-go-go*-related gene, was initially isolated by screening a human hippocampus cDNA library with a mouse homologue of *ether-a-go-go* (*eag*), a *Drosophila* K^+ channel gene (Warmke and Ganetzky 1994). *Eag* was also found to be strongly expressed in the heart (Warmke and Ganetzky 1994). Shortly thereafter, HERG was identified as the gene involved in chromosome 7-associated long QT syndrome (LQT2) (Curran et al. 1995). Although the overall amino acid identity with K_v α subunits is low (10-15%), each HERG subunit contains six transmembrane α -helices, with S4 and pore regions that contain a slightly modified version of the “signature sequence” of K^+ selective pores (Heginbotham et al. 1994; Doyle et al. 1998), consistent with the formation of functional K^+ channels (Zhong and Wu 1991; Zhong and Wu 1993). When expressed heterologously, HERG channels produce a current with biophysical and pharmacological properties similar, but not identical, to native I_{Kr} . These properties include voltage dependence of activation and rectification, sensitivity to methanesulfonanilides, and a single channel conductance of 10-12 pS (Trudeau et al. 1995; Hancox et al. 1998; Kiehn et al. 1996; Sanguinetti et al. 1995; Spector et al. 1996a; Zhou et al. 1998; Zou et al. 1997).

The inward rectification of I_{Kr} is due to inactivation at a rate much faster than activation (Shibasaki 1987). Mutagenesis reveals that the inactivation of HERG channel is not affected by truncation of its N-terminal region (Spector et al. 1996b; Schonherr and Heinemann 1996), indicating that inactivation is not caused by the N-type mechanism typical for the *Shaker* family; instead, inactivation can be disrupted by mutations in the pore loop (Smith et al. 1996), suggesting HERG inactivation involves conformational changes in the outer vestibule of the pore. This mechanism is similar to C-type inactivation in *Shaker*-related channels (Hoshi et al. 1990; Lopez-Barneo et al. 1993; Panyi et al. 1995).

Mutation studies also reveal that S4-S5 linker and C-terminal half of S6 have profound impacts on the voltage-dependence and activation and deactivation kinetics (Holmgren et al. 1998; Lees-Miller et al. 2000; Sanguinetti and Xu 1999), and the N-terminal domain of HERG plays a key role in deactivation. Deleting amino acids 2-354

(Spector et al. 1996b; Wang et al. 1998a) or 2-373 (Schonherr and Heinemann 1996) from the N-terminal domain causes a ten-fold acceleration of HERG deactivation.

Although homomultimeric HERG channels carry a current resembling native I_{Kr} , apparent discrepancies have been noted (Sanguinetti et al. 1995). Alternatively spliced variants of HERG have been discovered (Lees-Miller et al. 1997; London et al. 1997) and the channels encoded by these splicing genes activate and deactivate with a time course similar to that of myocyte I_{Kr} (London et al. 1997). Heteromultimeric channels can be formed by spliced isoforms and the full-length isoform (HERG) (London et al. 1997), and it has been proposed that differential expression or heteromultimeric assembly of HERG isoforms may underlie the region- and species-variations as well as developmental changes in gating kinetics (Barajas-Martinez et al. 2000). However, Western blot analysis reveals that only full-length HERG protein is detected in rat, mouse and human heart, questioning the contribution of alternatively spliced HERG variants to functional I_{Kr} (Pond et al. 2000).

The first clue that HERG channels can be modulated by regulatory β subunits came from the observation of I_{Kr} reduction by antisense oligonucleotides against minK in a mouse atrial cell line (Yang et al. 1995). Later experiments of minK knockout (Kupershmidt et al. 1999) and the immunoprecipitation demonstration of a stable complex of minK and HERG *in vitro* (McDonald et al. 1997) reinforce the notion that minK can augment the I_{Kr} amplitude and modulate its gating kinetics. Very recently, minK-related peptides (MiRPs) have been identified, and these MiRPs, along with minK, constitute the KCNE family (KCNE1 to KCNE4 are correspondingly minK, MiRP1 to MiRP3) (Abbott et al. 1999). It has been shown that co-expression of HERG with MiRP1 reconstitutes properties of native I_{Kr} such as accelerated deactivation, and more positive voltage-dependence of activation compared to HERG alone (Abbott et al. 1999). More importantly, MiRP1 mutations have been linked to congenital LQT syndrome 6 (LQT6) (Abbott et al. 1999; Sesti et al. 2000; Splawski et al. 2000). MiRP1 was thus suggested to be the subunit of native I_{Kr} channel in cardiac myocytes. However, the discrepancies that remain between the MiRP1 co-expressed current and native I_{Kr} (Abbott et al. 1999; Weerapura et al. 2002) and a lack of biochemical evidence for the association between MiRP1 and HERG *in vivo* leave the issue open.

Genes and heterologous expression of I_{Ks} channels It is now clear that two genes – KvLQT1 (KCNQ1) and minK (KCNE1) are required to produce I_{Ks} . In 1988, a gene (minK), encoding a small (129 amino acids) protein was cloned from kidney (Takumi et al. 1988) and later isolated from neonatal rat (Folander et al. 1990) and mouse heart (Honore et al. 1991), guinea pig heart (Zhang et al. 1994) and human lymphocyte (Attali et al. 1992) libraries. When expressed in oocytes, minK channels induced a very slowly activating delayed rectifier K^+ current with many properties similar to I_{Ks} . Furthermore, mutations in minK alter the properties of expressed current, suggesting that minK contributes to the K^+ -selective pore (Takumi et al. 1988; Goldstein and Miller 1991). However, expression of minK in mammalian cells failed to produce detectable current, implying that an endogenous factor might exist in oocytes but be lacking in mammalian cells (Lesage et al. 1992). Further evidence to support the notion that current resulted from the interaction of minK with an endogenous protein came from the observation that the amplitude of minK current saturated at a small amount of cRNA injection, even though injection of large amounts of cRNA produced substantial minK proteins at the plasma membrane (Blumenthal and Kaczmarek 1994; Freeman and Kass 1993b). These findings suggested that minK coassembled with a protein that is endogenously expressed in oocytes, but not in mammalian cells, to form I_{Ks} (Tai et al. 1997; Mitcheson and Sanguinetti 1999).

The mysterious protein partner of minK, KvLQT1, was identified by a positional cloning approach in 1996 (Barhanin et al. 1996; Sanguinetti et al. 1996). KvLQT1 is a typical K^+ channel α -subunit of 676 amino acids that consists of six transmembrane domains and a typical pore loop with a potassium signature sequence. Heterologous expression of KvLQT1 generated a voltage-gated K^+ current that did not match any known K^+ currents recorded from cardiac myocytes. This led to the hypothesis that KvLQT1 might assemble with other subunits to form K^+ channels with recognizable biophysical characteristics (Mitcheson and Sanguinetti 1999). Since minK and KvLQT1 mRNA have a similar tissue distribution, being most abundant in the heart and kidney (Barhanin et al. 1996) and minK current bears some known properties with native I_{Ks} , minK became an obvious choice for the hypothesized ancillary subunits. This hypothesis was confirmed when KvLQT1 and minK were coexpressed in mammalian cells, and the

resulting current activated slower and at more positive potentials, and was several-fold larger, than the current produced by KvLQT1 alone (Barhanin et al. 1996; Sanguinetti et al. 1996), resembling native I_{Ks} . The discovery that mutations in the minK gene on chromosome-21 cause LQT5 reinforces the idea that minK is a necessary subunit for functional I_{Ks} (Barhanin et al. 1996; Sanguinetti et al. 1996; Splawski et al. 1997).

The structural determinants and stoichiometry of KvLQT1/minK interaction are still poorly understood. It seems that four KvLQT1 α -subunits coassemble to form a pore structure and that one or more minK subunits stabilize the heteromultimeric channel (Mitcheson and Sanguinetti 1999).

In addition, MiRP1 and MiRP2 have been reported to interact with KvLQT1, modifying gating properties dramatically (Bianchi et al. 1999; Schroeder et al. 2000). MiRPs seem to be involved in the regulation of many K^+ channels; for example, MiRP1 affects the behavior of HERG (Abbott et al. 1999; Sesti et al. 2000; Cui et al. 2001), KvLQT1 (Bianchi et al. 1999; Schroeder et al. 2000) and the function of Kv4 channels (Zhang et al. 2001); while MiRP2 alters the function of KCNQ1 (KvLQT1) and 3, HERG, and Kv3.4 (Schroeder et al. 2000; Abbott et al. 2001; Bianchi et al. 1999).

Heterogeneity of I_{Kr} and I_{Ks} channel expression Heterogeneity of AP configuration and APD in different regions of the heart and across the ventricular free wall are partially attributable to differences in I_{Kr} or I_{Ks} density (Li et al. 2001; Liu and Antzelevitch 1995). In the ferret, HERG mRNA transcripts and protein levels are higher in epicardial than endocardial cell layers (Brahmajothi et al. 1996). Macroscopic I_{Kr} has a higher density in epicardial cells with similar single channel open probability and conductance to those in the other layer cells, suggesting that the differences in current density across the wall are not due to a different molecular composition but to higher expression of the same channel protein (Furukawa et al. 1992a). Similarly, in guinea pig left ventricle, both I_{Kr} and I_{Ks} are smaller in sub-endocardial than in mid-myocardial or sub-epicardial cells (Bryant et al. 1998). In canine atria, Li et al (2001) reported a larger I_{Kr} in left than right atrium, contributing to the shorter left atrial APD. HERG protein expression parallels I_{Kr} density in these regions. In canine left ventricle, Liu et al (1995) described a smaller I_{Ks} in M cells compared to cells isolated from the endocardium or epicardium, without differences

in I_{Kr} density and kinetics, contributing to longer APD in M cells. Similar I_{Ks} distribution is found across the right ventricle free wall, but I_{Ks} is larger in right than left ventricular midmyocardium (Volders et al. 1999a). To investigate small I_{Ks} in M cells at the molecular levels, Péréon et al (2000) used RNase protection assays to determine KvLQT1 and minK message expression across the human right and left ventricular wall. They found that all layers of left and right ventricles had a similar expression of minK and total KvLQT1, but M cells had a higher percentage of an endogenous N-terminal truncated KvLQT1 splice variant, referred to as KvLQT1 isoform 2, which has dominant negative effects on isoform 1 (KvLQT1) (Demolombe et al. 1998; Jiang et al. 1997). Coinjection of isoform 1 with isoform 2 in COS 7 cells at the “midmyocardium ratio” (more isoform 2) resulted in only 25% current amplitude of the expressed I_{Ks} at “epicardium ratio” (less isoform 2), without changes in kinetics. This study suggests that an endogenous dominant negative-like mechanism may underlie the variation of I_{Ks} density across the ventricular wall (Pereon et al. 2000).

4.3.3 Molecular basis of I_{Kur}

Striking differences in properties of I_{Kur} between species suggest a different molecular basis. Human atrial I_{Kur} have many properties similar to Kv1.5 clone, which is originally cloned from rat and human ventricle (Roberds and Tamkun 1991; Tamkun et al. 1991). Northern blot analysis demonstrates that Kv1.5 mRNA is predominantly expressed in adult human heart with little expression elsewhere (Tamkun et al. 1991) and is at least ten-fold more abundant in human atrium than in ventricle (Tamkun et al. 1991). Furthermore, the Kv1.5 protein has been detected in human atrial and ventricular tissue, (Mays et al. 1995) and Kv1.5 specific antisense oligonucleotides suppress the native I_{Kur} by 50% in human atrial myocytes without altering expression of other currents. Immunofluorescence studies reveal Kv1.5 protein in human and rat myocytes, and in high density at the intercalated disks. Similar findings regarding Kv1.5 in rat atria suggest that rat atrial I_{Kur} has the same molecular identity as human (Barry et al. 1995; Bou-Abboud and Nerbonne 1999). The molecular basis for I_{Kur} is less certain in other species. Kv3.1 underlies canine atrial I_{Kur} (Yue et al. 1996b); while the molecular entity underlying guinea pig ventricular I_{Kur} is unknown.

4.3.4 Molecular basis of inward rectifier currents

In 1993, the first members [Kir1.1a (RomK1), Kir2.1 (IRK1), and Kir3.1 (GIRK1)] of the new Kir channel family were cloned and expressed in *Xenopus* oocytes (Dascal et al. 1993a; Dascal et al. 1993b; Ho et al. 1993; Kubo et al. 1993a; Kubo et al. 1993b). Kir subunits, similar to Kv subunits, are composed of tetramers of four identical (homomeric) or related (heteromeric) subunits. Kir subunits each have two transmembrane domains (2-TM) linked by a pore loop retaining a K⁺ channel signature sequence with either a GYG (Gly-Tyr-Gly) or a GFG (Gly-Phe-Gly) motif (Doupnik et al. 1995; Nichols and Lopatin 1997; Yamada et al. 1998). There are now at least six Kir channel subfamilies, sharing ~40% amino acid identity, individual members within each subfamily, sharing ~60% identity. The nomenclature of Kir channels is provided in the above Table 3 (Shieh et al. 2000; Reimann and Ashcroft 1999).

The property of inward rectification is believed to result principally from a voltage-dependent block of outward currents by cytoplasmic cations, chiefly Mg²⁺ and polyamines, which enter the pore under the influence of the membrane voltage field and impede K⁺ efflux. These cations interact with negatively charged residues in TM2 and /or the C- terminus to induce inward rectification (Reimann and Ashcroft 1999).

4.3.4.1 I_{K1}

The channels carrying I_{K1} belong to a subfamily of 2-TM K⁺ channels with inward rectification, the Kir2 subfamily. Since the first member of the Kir2 subfamily was cloned from mouse macrophages in 1993 (Kubo et al. 1993b), Kir2.1 (originally named IRK1) has been considered a major candidate gene for cardiac I_{K1} . Kir2.1 channels are K⁺ selective, with a single channel conductance of 20 to 29 pS (Kubo et al. 1993b; Choe et al. 2000; Morishige et al. 1993) (~30 pS for native human homologue) (Raab-Graham et al. 1994). These conductances are very close to those of native I_{K1} channels {22 pS and 27 pS in guinea pig ventricular myocytes (Matsuda 1988; Sakmann and Trube 1984b); 28 pS in rat ventricular myocytes (Burnashev and Zilberter 1986)}. Antisense targeted against Kir2.1 mRNA in rat ventricular myocytes significantly reduced whole-cell I_{K1} and the frequency of detection of 21 pS channels greatly diminished (Nakamura et al.

1998). However, other single channel events were not obviously affected, suggesting the contribution of other subunit types to native I_{K1} .

The hypothesis has been raised that heterotetrameric assemblies of different Kir2.x subunits may contribute to cardiac I_{K1} and its heterogeneity. Wang et al (1998b) first reported that Kir2.1-3 subunits are all expressed in dog atria and ventricles; Melnyk et al (2002) extended the study with Western blot and immunocytochemical methods. They found that the protein levels of these subunits paralleled those of mRNA; but their immunolocalization was different in atria from ventricles. Kir2.1 and Kir2.2 knockout mice die very soon after birth, potentially from complications of a cleft palate; neonatal ventricular myocytes from Kir2.1 $-/-$ homozygous mice show complete absence of I_{K1} currents, indicating an essential role of Kir2.1 (Zaritsky et al. 2001). I_{K1} density was also reduced by about 50% in the cells of Kir2.2 $-/-$ homozygous mice, suggesting a contribution of this gene, possibly in heteromeric complexes with Kir2.1.

4.3.4.2 I_{KACH}

I_{KACH} channel activation is mediated by pertussis toxin -sensitive G proteins via a direct membrane-delimited pathway. The Kir3 channel subunit family is the only inward rectifier family that expresses G protein-coupled receptor activated inwardly rectifying K^+ channels (GIRK). Both GIRK1 (Kir3.1) channels and endogenous I_{KACH} channels can be modulated directly by the $\beta\gamma$ subunits of heteromeric G proteins, suggesting that GIRK1 underlies I_{KACH} (Kurachi 1995; Logothetis et al. 1987; Wickman et al. 1994). The presence of an accessory subunit-CIR (Cardiac inward rectifier, now referred to as Kir3.4) that may account for the differences was subsequently demonstrated by coimmunoprecipitation with antibodies against GIRK1 (Krapivinsky et al. 1995). Subsequent heterologous expression of GIRK1 (Kir3.1) with CIR (Kir3.4) expressed currents with properties undistinguishable from native I_{KACH} , in agreement with the suggestion that functional I_{KACH} channels are heteromultimers of Kir3.1 and Kir3.4.

4.3.4.3 I_{KATP}

K_{ATP} channels are composed of a tetramer of the pore-forming subunits (either Kir6.1 or Kir6.2) and a co-assembled tetramer of regulatory subunits, termed sulfonylurea receptors (SUR), which belong to the family of ATP binding cassette transporters (Aguilar-Bryan et al. 1998; Babenko et al. 1998; Shyng and Nichols 1997).

The Kir6.x subunit shows the prototypic transmembrane topology of Kir channels, including hydrophilic N- and C-termini and two hydrophobic transmembrane segments (TM1 and TM2) flanking a well-conserved pore domain. Four Kir6.x subunits form the pore and determine single channel conductance and block by magnesium and polyamines (Tucker et al. 1997; Shyng et al. 1997a). Four SURs surrounding symmetrically the pore act as regulatory subunits endowing the K_{ATP} channel with sensitivity to sulfonylureas, channel openers and Mg-ADP (Inagaki et al. 1996; Inagaki et al. 1995a; Gribble et al. 1997; Shyng et al. 1997b; Schwanstecher et al. 1998). Three types of SURs (SUR1, SUR2A and SUR2B) have been discovered. SUR2A mRNA is highly expressed in the heart and skeletal muscle (Inagaki et al. 1996). SUR2B is uniformly expressed throughout various organs (Inagaki et al. 1995b). As the pore-forming subunit of surface K_{ATP} channels, Kir6.2 is also ubiquitously expressed in rat tissues, including pancreatic islets, pituitary, skeletal muscle, and the heart (Inagaki et al. 1995b). Co-expression of Kir6.2 with SUR2A generates cardiac and skeletal muscle K_{ATP} channels (Gribble et al. 1998); while co-expression of Kir6.2 with SUR2B and SUR1 forms the types of K_{ATP} channels in vascular smooth muscle and pancreatic β -cells, respectively (Gribble et al. 1998; Isomoto et al. 1996). All types of K_{ATP} channels show a similar sensitivity to the blocking effect of antidiabetic sulfonylureas and are target of a series K^+ channel openers.

4.4 Molecular basis of I_f

Santoro et al (1997) first detected a brain cDNA clone (BCNG-1), expression of which carries a cyclic nucleotide-sensitive cation current resembling I_f , by using yeast hybrid screen with the SH3 (Src homology 3) domain of a neural specific isoform of Src tyrosine kinase family. Based on the idea that I_f channels, like cyclic nucleotide-gated (CNG) channels (Zagotta and Siegelbaum 1996) would contain a cyclic nucleotide-binding domain (CNBD), Ludwig et al (1998) screened the expressed sequence tag (EST)

database for sequences related to the CNBD of CNG channels and identified an EST sequence. With this EST sequence as a probe, they isolated three homologous full-length cDNAs (HAC1-3) from mouse brain. The fourth full-length cDNA encoding hyperpolarization-activated cation channels was recently isolated from rabbit (HAC4) and human hearts (HCN4) (Ishii et al. 1999; Ludwig et al. 1999). The unifying nomenclature for these cDNAs is now designated as hyperpolarization-activated and cyclic nucleotide-gated (HCN) channel (Biel et al. 1999; Clapham 1998) instead of the original names of HAC and BCNG (table 4 below).

Table 4. HCN channel subunits

Type	Original name	Tissue location	Activation constants	Reference number ^α
HCN1	mBCNG-1/HAC2	Brain, heart	100-300 ms	1, 2, 3, 4
	hBCNG-1			3
	HCN1			5
	HCN1 α			6
HCN2	mBCNG-2/HAC1	Brain, heart	200-500 ms	2, 3, 7
	HBCNG-2 ^a /hHCN2			3, 7, 8
	HCN2			5, 6
	HCN2 ^a			6
HCN3	mBCNG-4a/HAC3	Brain	n.d	2, 3
	HCN3			5
	HCN3 ^a			6
HCN4	mBCNG-3	Brain, heart	660-3000 ms	3, 5, 7, 9
	hHCN4			7, 9
	HCN4			5
	HCN4 ^b /HCN4 ^a			5, 6

^a partial CDNA sequence; ^b probably represents a partial clone that is lacking of the N-terminal region. Reference number: 1 (Santoro et al. 1997), 2 (Ludwig et al. 1998), 3 (Santoro et al. 1998), 4 (Santoro et al. 2000), 5 (Ishii et al. 1999), 6 (Shi et al. 1999), 7 (Ludwig et al. 1999), 8 (Vaccari et al. 1999), 9 (Seifert et al. 1999). Modified from Kaupp and Seifert (2001).

HCN channels (HCN1-4) belong to the superfamily of voltage-gated K⁺ channel with six transmembrane domains and are likely to assemble as tetramers (Clapham 1998). The four isoforms share a homology of ~60% in amino acid sequence identity (Ludwig et al. 1999) and differ in tissue localization and biophysical properties. Initially, Northern blot

analysis showed that only HCN2 and HCN4 are expressed in the human heart. Both generate I_f -like currents with properties similar to cardiac I_f (DiFrancesco et al. 1986; Liu et al. 1996b; Maruoka et al. 1994). Hence, HCN2 and HCN4 were considered potential components for cardiac HCN channels (Seifert et al. 1999; Moroni et al. 2000). Further RT-PCR work showed that HCN2 and HCN4 mRNA expression in humans is comparable in atria and ventricles (Ludwig et al. 1999). A detailed analysis in rabbits showed that total HCN message in SA node is around 140 times the HCN message of the ventricle and 25 times that of PFs (Shi et al. 1999). These results are consistent with the fact that the SA node is the primary pacemaker and PFs are potential pacemakers, while reduced HCN message in ventricles and atria may explain the limited automaticity seen in these regions.

4.5 Other ion transporters

4.5.1 Na/Ca exchanger

The NCX gene was first cloned from dog heart muscle in 1990 (Nicoll et al. 1990). Since then, three members (denoted NCX1-3) of the NCX family have been identified from different species, including human (Komuro et al. 1992), rat (Furman et al. 1993; Li et al. 1994; Low et al. 1993; Nicoll et al. 1996), rabbit (Kofuji et al. 1994), guinea pig (Oshima et al. 1997) and mouse (Kraev et al. 1996). The locations of NCX1, NCX2 and NCX3 genes on chromosome are dispersed, being mapped to mouse chromosome 17, 7 and 12 by linkage analysis, respectively (Nicoll et al. 1996). These three genes share a striking degree of sequence identity, especially in transmembrane domains. They encode proteins of less than 1000 amino acids with an approximate molecular weight of 120 kDa that function as NCX. No distinct differences in functional properties have been observed among these three gene products (Iwamoto and Shigekawa 1998; Linck et al. 1998).

The topology of NCX is believed to include two sets of hydrophobic domains consisting of 9 transmembrane segments separated by a large intracellular loop of about 550 amino acids (Fig8). The N-terminal hydrophobic domain has 5 transmembrane segments and the N-terminus is extracellular and glycosylated. The C-terminal hydrophobic domain has 4 transmembrane segments and the C-terminus is intracellular.

The ninth hydrophobic segment is speculated to be a reentrant membrane loop similar to the pore-forming region of ion channels. It has a GIG sequence in the center.

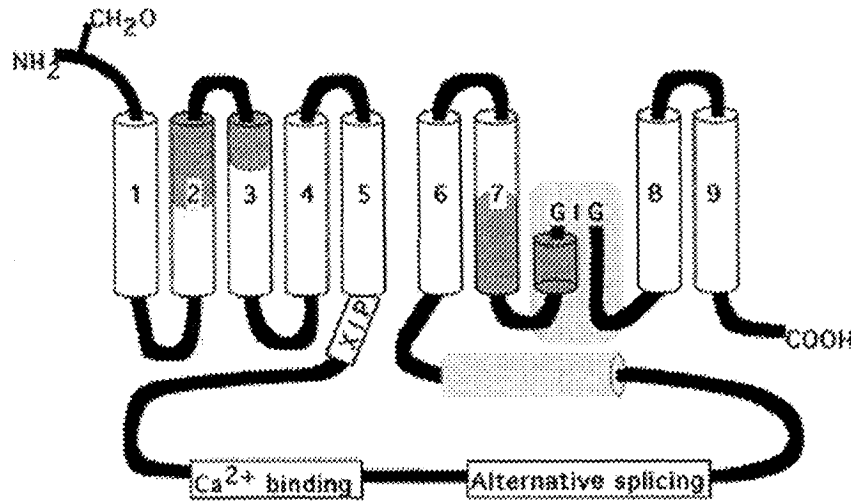


Figure 8. Model of the Na/Ca exchanger. On the large intracellular loop are the endogenous exchange inhibitory peptide domain (XIP), the binding site for regulatory Ca²⁺, and the region where extensive alternative splicing occurs [adapted from Philipson and Nicoll (2000)].

NCX gene transcripts undergo alternative splicing. For NCX1, the splice variants arise from a region of the large intracellular loop encoded by six small exons (Labeled A to F) in a tissue-specific manner (Kofuji et al. 1994; Nakasaki et al. 1993; Dyck et al. 1999; Quednau et al. 1997). At least 12 splice variants have been detected. Excitable tissues usually express exon A, whereas exon B predominates in other tissues. A single combination of exons (ACDEF) predominates in cardiac muscle. For NCX2, no splicing has been detected. For NCX3, three splicing isoforms have been identified in brain and skeletal muscle (Quednau et al. 1997). The physiological and functional significance of these splice variants remains unclear.

NCX1 is expressed widely in many tissues, including the heart (Quednau et al. 1997). In contrast, NCX2 and NCX3 have been found only in brain and skeletal muscle (Li et al. 1994; Nicoll et al. 1996). In the heart, NCX1 density is high, implying an important role in normal cardiac cell function (Cheon and Reeves 1988). There is some disagreement about the distribution of NCX1 in cardiac myocytes. Kieval et al (1992)

showed that, in adult guinea pig myocytes, NCX1 is located at the intercalated disks, the transverse tubules and exterior surface of the membrane, whereas Frank et al (1992) demonstrated that, in rabbit myocytes, NCX1 appears more prominent in t-tubule membranes than in peripheral sarcolemma. Recently, the Western blots of NCX1 were reported to be significantly lower in guinea pig atria than ventricles (McDonald et al. 2000); confocal images of these isolated myocytes revealed that the majority (about 79%) of NCX1 protein is located on the surface membrane in atrial myocytes whereas in ventricular myocytes, about 50% of NCX1 protein is located within the cell, presumably at t-tubules (McDonald et al. 2000). The cellular location of NCX1 may have implications for its activity during EC coupling in cardiac muscle. As the SR Ca^{2+} -release channels are located adjacent to t-tubular invaginations, only the fraction of NCX1 located within the t-tubules would be likely to participate in reverse-mode release of SR Ca^{2+} .

4.5.2 Molecular basis of Na/K pump

The Na/K pump is Mg^{2+} -dependent, Na^+ - and K^+ -activated ATPase. The Na-K-ATPase is composed of stoichiometric amounts of at least two polypeptides, α and β subunits. The α subunit is a multispinning (probably 10 times) membrane protein with a molecular mass of ~110 kDa. It contains the binding sites for ATP, Na^+ , K^+ , cardiac glycosides, specific inhibitors of the enzyme, and the phosphorylation sites, thus being largely responsible for the catalytic, transport and pharmacological properties of the ATPase (Glitsch 2001). The β subunit has only one transmembrane domain with a molecular mass of 40-60 kDa (depending on the degree of glycosylation). It is required for the normal activity of Na-K-ATPase through modulating transport characteristics and stabilizing the correct folding of the α subunit to facilitate membrane insertion (Therien and Blostein 2000; Blanco and Mercer 1998). Four α -subunit isoforms (α 1-4) and three β -subunit isoforms (β 1-3) have been identified so far. Both α and β subunit isoforms are expressed in tissue- and species-dependent pattern (Blanco and Mercer 1998). α 1 is expressed ubiquitously, whereas α 2 is predominant in cardiac and skeletal muscle, brain and adipocytes. α 3 is abundant in neural tissues and ovary, while α 4 is only detected in

the testis (Shamraj and Lingrel 1994). Marked variations among the species exist in the expression of $\alpha 2$ and $\alpha 3$, whereas $\alpha 1$ is present in cardiac tissue of all species (Sweadner et al. 1994). $\beta 1$ is found in nearly every tissue, while $\beta 2$ is found in skeletal muscle, pineal gland, and neural tissues; $\beta 3$ is present in testis, retina, liver and lung. Diversity of isoforms and tissue-specific expression probably attributes to the different kinetic characteristics of the ATPase and consequently may meet different physiological demands (Glitsch 2001).

5. Summary of ionic and molecular basis of the cardiac action potential

Tremendous progress has been made in understanding the molecular basis of ion channels. Figure 9 provides a summary of native ionic currents underlying AP and corresponding molecular counterparts (Marban 2002).

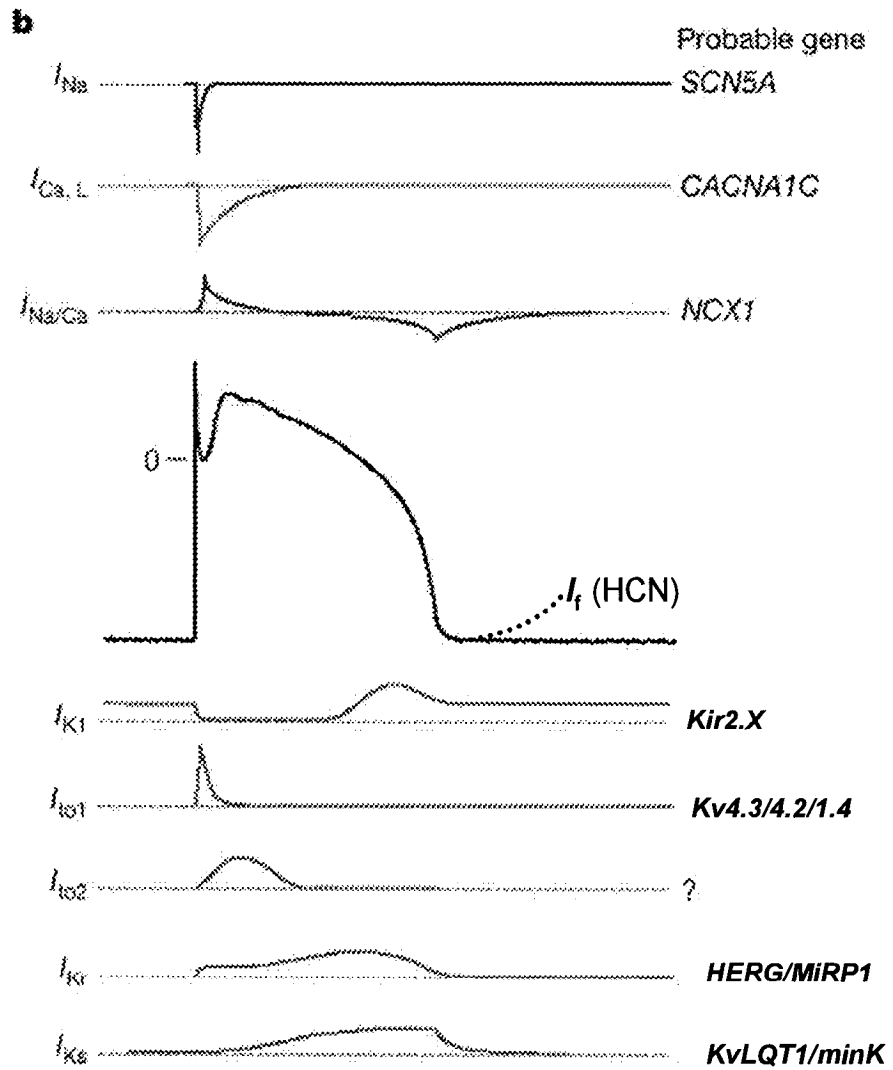
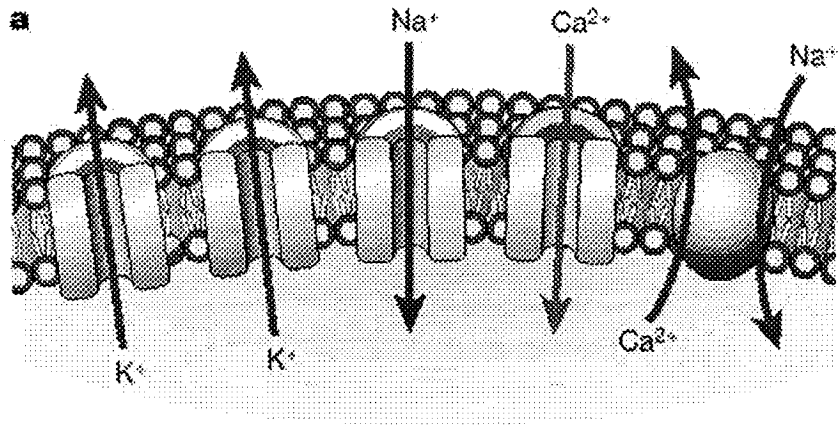


Figure 9. Ion channels underlie cardiac excitability. **a**, The key ion channels (Na^+ , Ca^{2+} , K^+ , and an electrogenic Na/Ca exchanger) in cardiac cells. **b**, Ionic currents and genes underlying the cardiac action potential. Top, depolarizing currents as functions of time, and their corresponding genes; center, a ventricular action potential; bottom, repolarizing currents and their corresponding genes [adapted from Marban (2002) with modification].

6. Modulation of cardiac ionic currents

The function of cardiac ion channels is under dynamic control by physiological regulators (such as neurotransmitters, hormones and heart rate) and can be remodeled under pathophysiological conditions such as heart failure. Modulation of ion channels may result in changes in density and/or properties (voltage dependence and kinetics) of ionic currents.

6.1 Ionic currents regulated by G-protein mediated signal transduction pathways

Heterotrimeric ($\alpha\beta\gamma$) GTP-binding proteins (G-proteins) transduce stimulatory or inhibitory signals from agonist-occupied seven-transmembrane-spanning-domain receptors. Multiple G-protein-coupled receptors in the heart act through a variety of signaling pathways, including changes in activity of protein kinase A (PKA) and C (PKC) to regulate many cellular proteins including ion channels (Fleming et al. 1992).

As shown in Figure 10, three functional classes of cardiac membrane receptors, corresponding to three major G proteins-Gs, Gi and Gq, are involved in the regulation of ion channel function (Molkentin and Dorn II 2001). In response to epinephrine and norepinephrine stimulation, β -adrenergic receptors (β_1 and β_2), primarily coupled to Gs, increase intracellular cAMP concentrations by $\text{Gs}\alpha$ -mediated activation of adenylyl cyclase (AC), this in turn activates PKA. Cardiac muscarinic acetylcholine (M) receptors activated by acetylcholine, typically coupled to Gi, lower cAMP levels by inhibition of AC and blunt the effects of PKA activation. Receptors coupled primarily to Gq include angiotensin II (At), endothelin (Et) and α -adrenergic receptors. These receptors activate phospholipase C (PLC), which cleaves phospholipids into two second messengers: inositol 1, 4, 5-triphosphate (IP_3) and diacylglycerol (DAG). IP_3 increases intracellular Ca^{2+} by IP_3 receptor-mediated release of Ca^{2+} from SR, while DAG and increased Ca^{2+} activate PKC. Increased Ca^{2+} can also modulate channel activities by activation of Ca^{2+} /

Ca²⁺-calmodulin (CaM) pathway. Both PKA and PKC can phosphorylate ion channels, altering channel function.

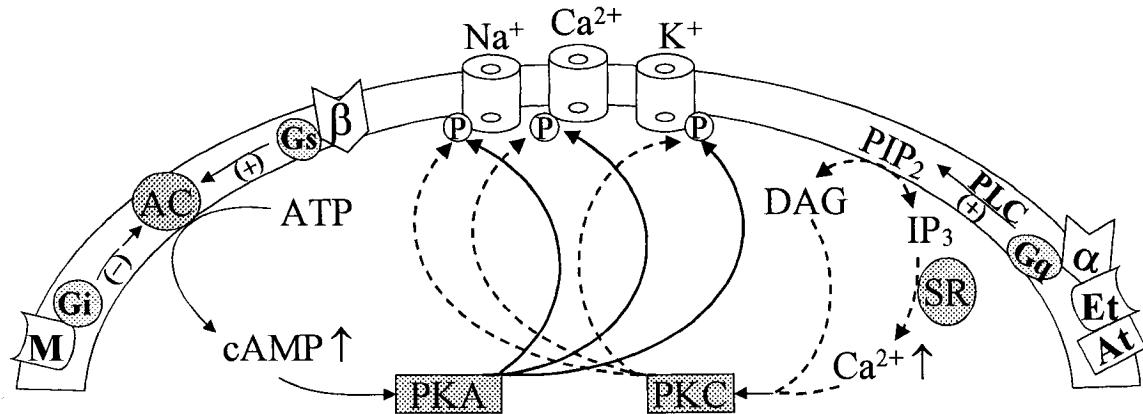


Figure 10. Schematic depiction of ion channel regulation by G-protein-mediated PKA and PKC signaling pathways via stimulation of cardiac membrane receptors. Abbreviations: α and β , adrenergic receptors; At, angiotensin receptor; Et, endothelin receptor; M, muscarinic acetylcholine receptor; SR, sarcoplasmic reticulum; AC, adenylyl cyclase; PLC, phospholipase C; IP₃, inositol 1, 4, 5-triphosphate; DAG, diacylglycerol; (+), stimulate; (-), inhibit.

6.1.1 I_{Na}

The effects of β -adrenergic receptor stimulation on cardiac Na⁺ channel function have been controversial. Earlier studies with mammalian ventricular myocytes demonstrated a reduction in cardiac I_{Na} in response to PKA activation (Schubert et al. 1989; Ono et al. 1993). However, relatively positive holding potentials were used. In subsequent investigation in which cells were held at more negative voltages (that would minimize the effects of the negative shift of inactivation), Na⁺ currents were increased by kinase stimulation (Gintant and Liu 1992; Matsuda et al. 1992). More recent studies of rat ventricular myocytes have demonstrated a consistent increase in I_{Na} with PKA stimulation (Lu et al. 1999), with similar results obtained from both rat (rH1) and human (hH1) recombinant Na⁺ channels expressed in *Xenopus* oocytes (Schreibmayer et al. 1994; Frohnwieser et al. 1997). The mechanism of this PKA-mediated increase in cardiac I_{Na} is currently unclear. Recently, Lu et al (1999) proposed that PKA stimulation increased I_{Na}

in rat ventricular myocytes by increasing the number of Na⁺ channels in the plasma membrane on the basis of single-channel recordings. Zhou et al (2000) demonstrated in recombinant human cardiac Na⁺ channels that activation of PKA caused an increase in I_{Na} and a small negative shift of voltage dependence of activation and inactivation, by both channel phosphorylation and altering trafficking to increase the number of channels in the plasma membrane.

PKC also modulates cardiac Na⁺ channels; both reduced and increased maximal channel conductances as well as altered gating have been reported (Benz et al. 1992; Moorman et al. 1989; Qu et al. 1994; Watson and Gold 1997). The reduction of I_{Na} amplitude and changes in gating are thought to be largely attributable to phosphorylation of a serine residue in the II-IV linker that is conserved in the neuronal and cardiac isoforms (Qu et al. 1996).

It is noteworthy that modulation of Na⁺ channel function by both PKA and PKC is channel isoform specific, with a molecular basis of effect that differs between channels (Frohnwieser et al. 1997; Gershon et al. 1992; Murphy et al. 1996; Murray et al. 1997; Schreibmayer et al. 1994).

6.1.2 I_{Ca}

Activation of I_{Ca} by β -adrenergic stimulation in cardiac muscle is the first described and most thoroughly studied example of I_{Ca} regulation (Reuter and Scholz 1977). Experiments in mammalian cardiac tissue (Tsien 1973; Reuter and Scholz 1977) and isolated myocytes (Osterrieder et al. 1982; Kameyama et al. 1985) showed that β -adrenergic stimulation caused a 2~4 fold increase in basal I_{Ca} and a shift in the voltage-dependence of activation and inactivation to more negative potentials through cAMP-dependent phosphorylation by PKA. This effect is responsible for most of the increase in cardiac contractility, beating rate and amplitude of the cardiac AP caused by β -agonists (Reuter 1974).

The molecular basis for regulation of I_{Ca} by PKA is still not resolved. Biochemical evidence suggested that increased activity is due to direct phosphorylation of the Ca²⁺ channel α_{1C} subunit or a tightly associated regulatory subunit. Although there are at least five consensus sites for phosphorylation by PKA within the C-terminal tail of α_{1C} , site-

directed mutagenesis has shown that only Ser-1928 is phosphorylated in *vitro* and transfected cells (Mitterdorfer et al. 1996; De Jongh et al. 1996). However, the extent of increased I_{Ca} by activation of PKA in transfected cells falls well short of the magnitude recorded in native cardiac cells (2~4 fold) (Gao et al. 1997a) and some studies with heterologously expressed α_{1C} failed to observe the expected increase upon β -adrenergic stimulation (Perets et al. 1996; Perez-Reyes et al. 1994; Zong et al. 1995). New insights into the mechanism of channel modulation by PKA have come from the finding that A-kinase-anchoring proteins (AKAPs) that help the kinase to target its specific substrate are found in the heart (Fraser et al. 1998; Gray et al. 1998). Reconstitution of PKA regulation of $Ca_v1.2$ channels in transfected cells is enhanced by co-expression of AKAP-79 (Gao et al. 1997b). The β subunits of cardiac Ca^{2+} channels are also phosphorylated by PKA in intact hearts when treated with β -adrenergic agonists (Haase et al. 1996a). However, the physiological significance of β subunit phosphorylation remains undefined.

PKC has been implicated in stimulation of cardiac Ca^{2+} channels by a variety of hormones, including angiotensin II and arginine-vasopressin as well as intracellular ATP (Striessnig 1999). PKC also mediates an inhibitory effect on cardiac Ca^{2+} channels, often following activation (Kwan and Qi 1997; Satoh 1992; Woo and Lee 1999). The N-terminal domain of cardiac α_{1C} is important for PKC regulation. Two threonine residues in PKC consensus sequences at positions 27 and 31 have been found in the cardiac, but not brain, isoform of α_{1C} subunit (Mikami et al. 1989; Snutch et al. 1991). Mutation of either of these two residues prevents regulation of cardiac channels by PKC, indicating that both residues must be phosphorylated to inhibit Ca^{2+} channel activity (McHugh et al. 2000).

The regulation of T-type Ca^{2+} channels by protein phosphorylation and G-protein pathways is much less prominent and less well studied than L-type Ca^{2+} channels (Catterall 2000b).

6.1.3 Na/Ca exchanger

PKC stimulation causes Na/Ca exchanger up-regulation in most cases through direct phosphorylation (Blaustein et al. 1996; Iwamoto et al. 1995; Iwamoto et al. 1996), but in others, like renal epithelial cells (Smith et al. 1995), a down-regulation of the Na/Ca

exchanger has been reported. Similar to PKC, PKA stimulation can both up- and down-regulate Na/Ca exchange (Fan et al. 1996; Rakotonirina and Soustre 1989). PKA regulation was reported to be temperature-dependent; at 20°C, no stimulation was observed, but stimulation was seen at 37°C (Perchenet et al. 2000). Variations in response to PKC and PKA have been assumed to arise from the expression of different isoforms (Abrahamsson et al. 1996; Ruknudin et al. 2000).

6.1.4 I_{to}

Acute application of α -adrenergic agonists causes rapid I_{to} reduction in adult rat ventricular myocytes (Apkon and Nerbonne 1988; Tohse et al. 1990; Fedida and Bouchard 1992), and rabbit atrial (Braun et al. 1990; Fedida et al. 1989; Fedida et al. 1990) and ventricular myocytes (Fedida et al. 1991). By contrast, no change (Robinson et al. 2000) and inhibition (Wang et al. 2001) of canine epicardial I_{to} and inhibition of Purkinje I_{to} (Nakayama and Fozzard 1988; Robinson et al. 2000) have been reported. The inhibitory effects can be reproduced by PKC activators, which suggests the involvement of PKC pathways (Apkon and Nerbonne 1988; Gaughan et al. 1998; Wang et al. 2001). A reduction in I_{to} by PKC activation has been also found in feline (Zhang and Ten Eick 1993) and canine (epicardial) myocytes (Wang et al. 2001). However, Braun et al (1990) found that phorbol ester (PMA) increased I_{to} despite of the reduction in I_{to} by α agonists, implying no involvement of PKC and IP_3 . A recent report suggests that the α -adrenergic agonist methoxamine can directly block I_{to} via a PKC-independent pathway (Parker et al. 1999).

Chronic exposure of cultured neonatal rat ventricular myocytes to the α -adrenergic agonist phenylephrine reduces I_{to} (Gaughan et al. 1998) in association with decreased Kv4.2 and increased Kv1.4 protein (Guo et al. 1998). Kv4.2 and Kv4.3 currents are reduced by PMA (Nakamura et al. 1997), while expressed Kv1.4 currents are increased initially, followed by a decrease (Murray et al. 1994).

The modulation of I_{to} by α -adrenergic stimulation via PKC pathway may be an important mechanism for the reduction of I_{to} in disease, since PKC inhibition has been shown to reverse the reduction of I_{to} in rat myocytes derived from hypothyroid (Shimoni and Severson 1995) and diabetic (Shimoni et al. 1998; Wang et al. 1995c) hearts.

Mediators of β -adrenergic stimulation (studied with forskolin and 8-Br-cAMP) have been reported to increase I_{to} amplitude and alter its kinetics in canine cardiac PFs (Nakayama et al. 1989), suggesting the involvement of PKA. However, activation of PKA by forskolin and isoproterenol does not affect I_{to} in feline ventricular myocytes (Zhang and Ten Eick 1993). Either I_{to} amplitude or/and kinetics can be also modulated by Ca^{2+} /Calmodulin-dependent protein kinase II (Tessier et al. 1999), Ang-II (Yu et al. 2000), thyroid hormone (Shimoni et al. 1997) and fatty acid metabolism (Xu and Rozanski 1998).

6.1.5 I_K

Studying I_{Kr} in cardiac myocytes is difficult because of its small amplitude and overlapping with a variety of other K^+ currents. Only a couple of studies show that I_{Kr} is insensitive to β -adrenergic stimulation (Sanguinetti et al. 1991; Roden et al. 1996). However, the finding of four putative cAMP-dependent PKA phosphorylation sites and a cyclic nucleotide binding domain (NBD) in the cytoplasmic regions of HERG channel imply the HERG channel is likely to be regulated by both PKA and direct cAMP binding. Indeed, recent work (Thomas et al. 1999; Cui et al. 2000) reveals that HERG current can be regulated by β -adrenergic stimulation through dual pathways. PKA-dependent phosphorylation inhibits I_{Kr} , accelerates deactivation and causes a rightward shift in voltage-dependence of activation. Direct cAMP binding to the NBD of the HERG protein in the absence of PKA phosphorylation sites negatively shifts the voltage-dependence of activation. Although this effect counterbalances the PKA-dependent shift in voltage activation, the net effect is still diminution of HERG current. When HERG is coexpressed with minK or MiRP, the relative contribution of direct cAMP effects on HERG current is accentuated (Thomas et al. 1999; Cui et al. 2000). A recent study in guinea pig ventricular myocytes demonstrates that increased I_{Kr} by β -adrenergic stimulation is mediated via PKC activation, because the increase in I_{Kr} is prevented by the blockade of Ca entry and inhibited by a selective PKC inhibitor (Heath and Terrar 2000). It remains unclear whether or how I_{Kr} in cardiac myocytes is modulated by β -adrenergic stimulation.

Enhancement of I_{Ks} by β -adrenergic stimulation is a consistent finding in cardiac tissue (Bennett et al. 1986; Tsien et al. 1972) and single cardiac myocytes (Bennett and Begenisich 1987; Giles et al. 1989; Han et al. 2001a; Walsh et al. 1991; Walsh and Kass 1988). β -adrenergic agonists increase I_{Ks} by increasing maximal conductance, accelerating activation and shifting the voltage of activation to more negative values (Han et al. 2001a; Giles et al. 1989). However, potential underlying molecular mechanisms remain unclear. Previous studies show that PKA activation by elevated cAMP increases the amplitude of minK current in oocytes (Blumenthal and Kaczmarek 1994; Blumenthal and Kaczmarek 1992; Kaczmarek and Blumenthal 1997). However, no PKA phosphorylation sites have been found on the amino acid sequence of minK, suggesting that PKA activation affects the current by phosphorylation of KvLQT1 subunits (Blumenthal and Kaczmarek 1992; Blumenthal and Kaczmarek 1994; Kaczmarek and Blumenthal 1997). In contrast to β -adrenergic modulation, the reports on α -adrenergic effects on I_{Ks} are not consistent. Stimulation of PKC by α -adrenergic agonists has been shown to enhance I_{Ks} in multicellular preparations (Bennett et al. 1986; Tsien et al. 1972) and isolated myocytes (Walsh et al. 1991; Walsh and Kass 1988), but also shown to decrease I_{Ks} in cardiac tissue (Lee and Rosen 1994) and SA node cells (Sato and Hashimoto 1988). Studies of PKC effects on minK-related currents show a species-dependent increase in guinea pig but a reduction in the rat and mouse (Varnum et al. 1993). Mutation of a key residue (Asn 102) to a Ser in the guinea pig minK protein reproduces the results observed in rat and mouse heart (Varnum et al. 1993), indicating that minK may determine the species-specific responses to PKC stimulation.

6.1.6 I_{K1}

Most studies demonstrate that both α - and β -adrenergic stimulations inhibit I_{K1} in ventricular myocytes of rabbit (Fedida et al. 1991), guinea pig (Koumi et al. 1995a; Koumi et al. 1995b), dog (Wang et al. 2001) and man (Koumi et al. 1995c), and atrial myocytes of humans (Sato and Koumi 1995). Application of isoproterenol, forskolin and dibutyryl cAMP reduces I_{K1} in guinea pig and human ventricular myocytes. This effect can be prevented by pre-treatment with a PKA inhibitor, indicating the involvement of PKA activation (Koumi et al. 1995a; Koumi et al. 1995c). Wischmeyer and Karschin

(1996) showed that the catalytic subunit of cAMP-dependent PKA causes complete inhibition of Kir 2.1. Application of methoxamine (α -agonist) and PMA (PKC activator) inhibits I_{K1} in human atrial myocytes, and this effect can be prevented in the presence of a specific PKC inhibitor, suggesting PKC involvement in α agonist -induced I_{K1} reduction (Sato and Koumi 1995). The activity of Kir2.1 channels is reduced following application of a specific activator of PKC (Fakler et al. 1994). A recent study reports that inhibition of I_{K1} by PMA in canine ventricular myocytes cannot be prevented by an inhibitor of PKC –Bisindolylmaleimide II, but is completely prevented by a potent CaMKII inhibitor –KN-93 (Wang et al. 2001).

6.1.7 I_{Kur}

I_{Kur} has been shown to undergo dual regulation by adrenergic stimulation in human atrial myocytes (Li et al. 1996b). PKA activation by isoproterenol, 8-Br-cAMP, and forskolin increases I_{Kur} ; PKC activation by phenylephrine (PE) decreases I_{Kur} . Similarly, in rat atria (Van Wagoner et al. 1996), PE activation suppresses I_{Kur} via PKC. By contrast, in canine atria, both β - and α -adrenergic stimulations increase I_{Kur} via PKA and PKC activation (Yue et al. 1999), respectively.

6.2 Ionic remodelling

Ionic remodelling can be defined as changes in ion channel function in response to a sustained anomaly in cardiac function or rhythm (Moalic et al. 1993). Dynamic changes in ion channel behaviour occur over hours to days as a result of altered gene-expression, changing ion channel synthesis and assembly (Allessie 1998).

6.2.1 I_{Na}

An early study in hypertrophied rat myocardium showed that neither the fast nor the slowly inactivating I_{Na} is altered by hypertrophy (Gulch et al. 1979). Studies in multicellular epicardial border zone (EBZ) of the infarcted heart showed V_{max} values to be reduced (Lue and Boyden 1992; Patterson et al. 1993; Ursell et al. 1985) and channel gating altered, in myocytes from EBZ (Pu and Boyden 1997). Recently, changes in Na^+ channel properties and expression in hypertrophied cardiac tissue from rats with 3- to 4-

week -old anterior myocardial infarction (MI) have been reported (Huang et al. 2001). Delayed “bursting activity”, resulting in slowed inactivation of I_{Na} , is observed. RNase protection assays reveal no change in expression of the cardiac I_{Na} isoform rH1. However, an expression pattern intermediate between control adult and fetal cardiac tissue appears in MI, causing increased cardiac membrane expression of neural TTX-sensitive channels. This may account for the slowed inactivation of I_{Na} . Undrovinas et al (1999) reported a persistent steady-state component in ventricular myocytes from dogs with congestive heart failure (CHF).

One mechanism underlying the changes in I_{Na} is recently proposed to arise from the deficient glycosylation of Na^+ channel protein in the $MLP^{-/-}$ model (a genetically engineered mouse lacking the expression of the muscle LIM protein) heart failure (Ufret-Vincenty et al. 2001).

6.2.2 I_{Ca}

Changes in Ca^{2+} channel expression and function vary with different heart diseases. A ~30% increase in L-type Ca^{2+} channel density (DHP receptor binding) has been reported in hypertrophic cardiomyopathy (Haase et al. 1996b; Wagner et al. 1989). This seems to be due to the upregulation of α_{1C} and β_2 subunits in human ventricular muscle (Haase et al. 1996b). Reports on ventricular myocyte I_{Ca} in heart failure (HF) are variable (Tomaselli and Marban 1999; Mukherjee and Spinale 1998). Overall, there seems to be no changes in $I_{Ca,L}$ density or kinetics. A detailed single-channel study of I_{Ca} in failing human ventricular myocytes showed the availability and open probability of the channel to be enhanced, resulting in an increased ensemble average current, but no increased whole-cell I_{Ca} . This indicates that the number of functional channels is lower in HF than in nonfailing myocytes, but is not evident as a decrease in whole-cell I_{Ca} (Schroder et al. 1998). In ischemia, a decrease in peak I_{Ca} and DHP binding density has been reported in relation to oxygen free radical injury in guinea pig ventricular myocytes (Coetzee and Opie 1992). Extra- or intracellular acidosis during ischemia inhibits I_{Ca} by shifting the voltage dependence of gating, reducing channel conductance and availability (Chen et al. 1996; Klockner and Isenberg 1994). The decrease in I_{Ca} may serve as a feedback mechanism to protect cardiac muscle from Ca^{2+} overload during ischemic processes.

No changes of $I_{Ca,T}$ in atrial myocytes and Purkinje cells have been reported in dog models of atrial fibrillation and congestive heart failure (Yue et al. 1997; Li et al. 2000; Han et al. 2001b). An increased $I_{Ca,T}$ has been observed in hypertrophied myocytes (Nuss and Houser 1993) and also in hypertrophy induced by growth hormone (Xu and Best 1990) and endothelin (Furukawa et al. 1992b). Recently, a study showed that $I_{Ca,T}$ reappeared in post-infarction hypertrophied rat left ventricle (LV) while it was absent in LV of sham-control rats. Expression of the T-type channel α_{1G} gene was increased by 158% compared to sham (Huang et al. 2000). Either reexpression or increased $I_{Ca,T}$ is thus proposed to be associated with arrhythmogenesis under these pathological conditions.

6.2.3 Na/Ca exchanger (NCX)

In the ischemic/reperfused heart, the ability of NCX to extrude Ca^{2+} is limited by an increased $[Na^+]_i$, leading to Ca^{2+} overload (Pike et al. 1990; Tani and Neely 1989). The Ca^{2+} overload is not only detrimental to contractile function, metabolism, and cellular integrity (Kusuoka et al. 1993), but also to cause spontaneous SR Ca^{2+} release. This in turn activates the transient inward current (I_{Ti}), of which NCX is a major component (Fedida et al. 1987). I_{Ti} is closely associated with delayed afterdepolarizations (DADs) that can cause lethal ventricular arrhythmias (Noble et al. 1996). In heart failure, an increase in I_{NCX} and the corresponding mRNA and protein levels has been noted in several animal models as well as in human tissues (Houser et al. 2000; Sipido et al. 2002). However, present data are somewhat conflicting regarding the influence of increased NCX activity on myocyte function. Litwin and Bridge (1997) reported that increased NCX would maintain SR Ca^{2+} loading through Ca^{2+} influx while O'Rourke et al (1999) thought that increased NCX activity partially compensated for reduced SR Ca^{2+} -ATPase function to maintain acceptably-low $[Ca^{2+}]_i$. In contrast to these observations, Pogwizd et al (2001) recently demonstrated that in a rabbit model of left ventricular pressure and volume overload without change in SR Ca^{2+} -ATPase and I_{Ca} , increased NCX reduced the amplitude of contraction and increased NCX-dependent currents contributed to arrhythmia generation.

6.2.4 K^+ currents

6.2.4.1 I_{to}

I_{to} remodelling is a central and consistent finding in a diversity of pathophysiological conditions including cardiac hypertrophy (see below), diabetic cardiomyopathy (Qin et al. 2001), inherited arrhythmias (Freeman et al. 1997) and atrial fibrillation (Yue et al. 1997; Li et al. 2000). Reduced I_{to} density without significant changes in kinetics or voltage dependence has been extensively documented in diverse hypertrophic or failing heart models (Kaab et al. 1996; Kaab et al. 1998; Cerbai et al. 2000; Yokoshiki et al. 1997; Lee et al. 1997; Li et al. 2000; Kaprielian et al. 1999; Tsuji et al. 2000; Rozanski et al. 1997) and in man (Nabauer et al. 1996; Bailly et al. 1997; Beuckelmann et al. 1993). Prolonged APD, as the electrophysiological hallmark of hypertrophic hearts, has been partially attributed to downregulation of I_{to} , since Kv4.2 and 4.3 are decreased at both mRNA and protein levels and associated with reduced I_{to} density and prolonged APD (Kaab et al. 1998; Gidh-Jain et al. 1996; Rozanski et al. 1998; Takimoto et al. 1997). In contrast, the mRNA and protein expression of Kv1.4 (corresponding to $I_{to,s}$) is increased in the rat infarct model at 6-8 weeks (Kaprielian et al. 1999; Gidh-Jain et al. 1996) and in renovascular hypertensive rats (Takimoto et al. 1997).

I_{to} downregulation in cardiac hypertrophy and heart failure is likely mediated by a wide array of changes in neurohumoral and paracrine factors, regulatory subunits and/or cytoskeleton and cell metabolism (Oudit et al. 2001). Examples of the importance of neurohumoral activation in mediating dysregulation of I_{to} are the ability of the angiotensin receptor antagonist, losartan, and angiotensin converting enzyme (ACE) inhibitors to reverse the changes in APD and I_{to} density in spontaneously hypertensive rats (Cerbai et al. 2000; Yokoshiki et al. 1997) as well as to completely restore Kv4.2 and 4.3 mRNA levels in renovascular hypertensive rats (Takimoto et al. 1997).

6.2.4.2 I_K

Downregulation of I_K has been reported in cardiac hypertrophy induced by pressure overload in cats (Kleiman and Houser 1989; Furukawa et al. 1994) without discriminating between I_{Kr} and I_{Ks} . In a rapid atrial pacing-induced atrial fibrillation dog model, I_{Kr} and I_{Ks} were found to be unchanged in atrial myocytes (Yue et al. 1997); while

in a rapid ventricle pacing-induced CHF dog model, I_{Ks} was reduced by 30% in atrial myocytes, with no change in I_{Kr} (Li et al. 2000). A very rapidly activating E-4031-sensitive current has been reported to increase in the 48-hour-old infarct zone of subendocardial Purkinje cells, with no classical I_K noted in either normal or infarct zone (Pinto and Boyden 1998), while in epicardial myocytes isolated from the infarct zone 5 days after a total occlusion of the left anterior descending coronary, I_{Kr} is reduced and the activation kinetics is accelerated; correspondingly, HERG mRNA level is reduced, suggesting that a decrease in HERG protein may account for the reduced I_{Kr} (but may not explain the altered I_{Kr} kinetics) (Jiang et al. 2000). Downregulation of I_{Kr} and I_{Ks} in ventricular myocytes has been also described in a rabbit tachycardia-induced heart failure model (Tsuji et al. 2000) and in a dog model of biventricular hypertrophy induced by chronically complete AV block (Volders et al. 1999b). Although the understanding of I_K remodelling is growing, experimental data on the possible changes of I_{Kr} and I_{Ks} in human ventricular hypertrophy or failure are not yet available. The potential molecular mechanisms for I_{Kr} or I_{Ks} downregulation and for variations in I_K remodelling in different models and different regions of the same model are not clear; thus further work is required.

6.2.4.3 I_{K1}

Most studies in hypertrophied or failing ventricular myocytes of animal models (Kaab et al. 1996; Pinto and Boyden 1998; Nabauer and Kaab 1998) and patients (Beuckelmann et al. 1993; Koumi et al. 1995c) show downregulation of I_{K1} (Nabauer and Kaab 1998). Some of these studies also show a slight but significant reduction in current positive to resting potentials (Kaab et al. 1996), which may affect the terminal repolarization phase of the action potential (Nabauer and Kaab 1998). No changes in I_{K1} have also been reported in a rabbit tachycardia-induced heart failure model (Rozanski et al. 1997) and in one study of failing human hearts (Koumi et al. 1995c). RNA protection assays reveal no significant changes in the mRNA level of Kir2.1 in failing human hearts (Kaab et al. 1998). In contrast to ventricular I_{K1} remodelling, no changes in I_{K1} have been observed in canine atrial myocytes of atria fast-pacing induced atrial fibrillation (AF) (Yue et al. 1997) and CHF-induced AF models (Li et al. 2000).

7. Questions raised from above overview

There has been an explosive growth of knowledge in cardiac electrophysiology and molecular biology with the development of patch clamp and molecular techniques over the past decades. The study of Purkinje fibers contributed importantly to classical electrophysiology because of their favorable anatomic structure for classical voltage clamp techniques. However, our understanding of Purkinje fiber ionic electrophysiology and ion channel molecular biology, as well as pathophysiology, lags far behind the understanding of atrium and ventricles. This is because Purkinje fibers present some important technical obstacles to the type of characterization of molecular and single cell ionic properties that has been so successful for working myocytes. Cell isolation is rendered difficult by the relatively thick connective tissue around and within false tendons, and by the requirement for the “chunk” method, rather than an arterial perfusion method for cell isolation, which tends to suppress currents (Yue et al. 1996a). In addition, the mass of Purkinje tissue in a single false tendon is extremely small, permitting the extraction of only minuscule quantities of protein or nucleic acids. Consequently, no contemporary single-cell studies have addressed in detail the ionic properties of Purkinje cells and the molecular basis of Purkinje ionic currents, as well as the potential roles of Purkinje cells in abnormal-repolarization related arrhythmias.

Considering the importance of Purkinje fibers in cardiac conduction and arrhythmogenesis, as well as the fact that Purkinje fibers are still widely-used in pharmaceutical companies for drug testing, it is therefore essential to answer the following questions:

- 1). What are the properties of ionic currents controlling cardiac Purkinje cell repolarization?
- 2). What is the molecular basis for ion channels underlying Purkinje cell repolarization?
- 3). What are the potential roles of ionic currents in abnormal repolarizing-related arrhythmias (taking I_{K_s} as an example)?
- 4). How are ionic currents remodeled by heart diseases (e.g., congestive heart failure)?

8. Approaches to address the questions

To address the above questions, we used the following approaches:

1. We optimized the isolation of cardiac Purkinje cells.
2. We used whole-cell patch clamp techniques with voltage-clamp mode to study macroscopic ionic currents and current-clamp mode to record action potentials in isolated single Purkinje cells.
3. We applied action potential waveform-clamp to evaluate relative contributions of individual currents to repolarization.
4. We used standard microelectrode techniques to investigate the AP response to specific blockers in multicellular preparations.
5. We used PCR-cloning to sequence selected segments of interesting genes.
6. We applied competitive RT-PCR to quantify ion channel mRNA concentration.
7. We used Western blot to examine ion channel protein expression.
8. We applied immunocytochemistry to examine the localization of ion channels.

9. References

- Abbott, G. W., Butler, M. H., Bendahhou, S., Dalakas, M. C., Ptacek, L. J., and Goldstein, S. A. (2001). MiRP2 forms potassium channels in skeletal muscle with Kv3.4 and is associated with periodic paralysis. *Cell* **104**, 217-231.
- Abbott, G. W., Sesti, F., Splawski, I., Buck, M. E., Lehmann, M. H., Timothy, K. W., Keating, M. T., and Goldstein, S. A. (1999). MiRP1 forms IKr potassium channels with HERG and is associated with cardiac arrhythmia. *Cell* **97**, 175-187.
- Abrahamsson, C., Carlsson, L., and Duker, G. (1996). Lidocaine and nisoldipine attenuate almodokant-induced dispersion of repolarization and early afterdepolarizations in vitro. *J.Cardiovasc.Electrophysiol.* **7**, 1074-1081.
- Agnew, W. S., Moore, A. C., Levinson, S. R., and Raftery, M. A. (1980). Identification of a large molecular weight peptide associated with a tetrodotoxin binding protein from the electroplax of *Electrophorus electricus*. *Biochem. Biophys.Res.Comm.* **92**, 860-866.
- Aguilar-Bryan, L., Clement, J. P., Gonzalez, G., Kunjilwar, K., Babenko, A., and Bryan, J. (1998). Toward understanding the assembly and structure of KATP channels. *Physiol Rev.* **78**, 227-245.
- Akopian, A. N., Souslova, V., Sivilotti, L., and Wood, J. N. (1997). Structure and distribution of a broadly expressed atypical sodium channel. *FEBS Lett.* **400**, 183-187.
- Allessie, M. A. (1998). Atrial electrophysiologic remodeling: another vicious circle? *J.Cardiovasc Electrophysiol.* **9**, 1378-1393.
- Alyonycheva, T., Cohen-Gould, L., Siewert, C., Fischman, D. A., and Mikawa, T. (1997). Skeletal muscle-specific myosin binding protein-H is expressed in Purkinje fibers of the cardiac conduction system. *Circ.Res.* **80**, 665-672.
- Amoroso, S., Schmid-Antomarchi, H., Fosset, M., and Lazdunski, M. (1990). Glucose, sulfonyleureas, and neurotransmitter release: role of ATP- sensitive K⁺ channels. *Science* **247**, 852-854.
- Amos, G. J., Wettwer, E., Metzger, F., Li, Q., Himmel, H. M., and Ravens, U. (1996). Differences between outward currents of human atrial and subepicardial ventricular myocytes. *J.Physiol* **491 (Pt 1)**, 31-50.
- An, R. H., Wang, X. L., Kerem, B., Benhorin, J., Medina, A., Goldmit, M., and Kass, R. S. (1998). Novel LQT-3 mutation affects Na⁺ channel activity through interactions between alpha- and beta1-subunits. *Circ.Res.* **83**, 141-146.
- An, W. F., Bowlby, M. R., Betty, M., Cao, J., Ling, H. P., Mendoza, G., Hinson, J. W., Mattsson, K. I., Strassle, B. W., Trimmer, J. S., and Rhodes, K. J. (2000). Modulation of A-type potassium channels by a family of calcium sensors. *Nature* **403**, 553-556.
- Antzelevitch, C. (2000). Electrical heterogeneity, cardiac arrhythmias, and the sodium channel. *Circ.Res.* **87**, 964-965.

- Antzelevitch, C., Sicouri, S., Litovsky, S. H., Lukas, A., Krishnan, S. C., Di Diego, J. M., Gintant, G. A., and Liu, D. W.** (1991). Heterogeneity within the ventricular wall. Electrophysiology and pharmacology of epicardial, endocardial, and M cells. *Circ.Res.* **69**, 1427-1449.
- Anumonwo, J. M., Freeman, L. C., Kwok, W. M., and Kass, R. S.** (1992). Delayed rectification in single cells isolated from guinea pig sinoatrial node. *Am.J.Physiol* **262**, H921-H925.
- Aomine, M.** (1989). Tetrodotoxin-sensitive component in action potential plateau of guinea pig Purkinje fibers: comparison with the papillary muscle. *Gen. Pharmacol.* **20**, 791-797.
- Apkon, M. and Nerbonne, J. M.** (1988). Alpha 1-adrenergic agonists selectively suppress voltage-dependent K⁺ current in rat ventricular myocytes. *Proc. Natl. Acad.Sci.U.S.A* **85**, 8756-8760.
- Apkon, M. and Nerbonne, J. M.** (1991). Characterization of two distinct depolarization-activated K⁺ currents in isolated adult rat ventricular myocytes. *J.Gen.Physiol* **97**, 973-1011.
- Arnar, D. O., Bullinga, J. R., and Martins, J. B.** (1997). Role of the Purkinje system in spontaneous ventricular tachycardia during acute ischemia in a canine model. *Circulation* **96**, 2421-2429.
- Attali, B., Romey, G., Honore, E., Schmid-Alliana, A., Mattei, M. G., Lesage, F., Ricard, P., Barhanin, J., and Lazdunski, M.** (1992). Cloning, functional expression, and regulation of two K⁺ channels in human T lymphocytes. *J.Biol. Chem.* **267**, 8650-8657.
- Attwell, D., Eisner, D., and Cohen, I.** (1979). Voltage clamp and tracer flux data: effects of a restricted extra- cellular space. *Q.Rev.Biophys.* **12**, 213-261.
- Babenko, A. P., Aguilar-Bryan, L., and Bryan, J.** (1998). A view of sur/KIR6.X, KATP channels. *Annu.Rev.Physiol* **60**, 667-687.
- Backx, P. H., Yue, D. T., Lawrence, J. H., Marban, E., and Tomaselli, G. F.** (1992). Molecular localization of an ion-binding site within the pore of mammalian sodium channels. *Science* **257**, 248-251.
- Bailly, P., Benitah, J. P., Mouchoniere, M., Vassort, G., and Lorente, P.** (1997). Regional alteration of the transient outward current in human left ventricular septum during compensated hypertrophy. *Circulation* **96**, 1266-1274.
- Baker, L. C., London, B., Choi, B. R., Koren, G., and Salama, G.** (2000). Enhanced dispersion of repolarization and refractoriness in transgenic mouse hearts promotes reentrant ventricular tachycardia. *Circ.Res.* **86**, 396-407.
- Balati, B., Varro, A., and Papp, J. G.** (1998). Comparison of the cellular electrophysiological characteristics of canine left ventricular epicardium, M cells, endocardium and Purkinje fibres. *Acta Physiol Scand.* **164**, 181-190.
- Balser, J. R.** (1999). Structure and function of the cardiac sodium channels. *Cardiovasc.Res.* **42**, 327-338.

- Balser, J. R., Bennett, P. B., Hondeghem, L. M., and Roden, D. M. (1991).** Suppression of time-dependent outward current in guinea pig ventricular myocytes. Actions of quinidine and amiodarone. *Circ.Res.* **69**, 519-529.
- Balser, J. R., Bennett, P. B., and Roden, D. M. (1990).** Time-dependent outward current in guinea pig ventricular myocytes. Gating kinetics of the delayed rectifier. *J.Gen.Physiol* **96**, 835-863.
- Barajas-Martinez, H., Elizalde, A., and Sanchez-Chapula, J. A. (2000).** Developmental differences in delayed rectifying outward current in feline ventricular myocytes. *Am.J.Physiol Heart Circ.Physiol* **278**, H484-H492.
- Barhanin, J., Lesage, F., Guillemare, E., Fink, M., Lazdunski, M., and Romey, G. (1996).** K(V)LQT1 and IsK (minK) proteins associate to form the I(Ks) cardiac potassium current. *Nature* **384**, 78-80.
- Barry, D. M. and Nerbonne, J. M. (1996).** Myocardial potassium channels: electrophysiological and molecular diversity. *Annu.Rev.Physiol* **58**, 363-394.
- Barry, D. M., Trimmer, J. S., Merlie, J. P., and Nerbonne, J. M. (1995).** Differential expression of voltage-gated K⁺ channel subunits in adult rat heart. Relation to functional K⁺ channels? *Circ.Res.* **77**, 361-369.
- Barry, D. M., Xu, H., Schuessler, R. B., and Nerbonne, J. M. (1998).** Functional knockout of the transient outward current, long-QT syndrome, and cardiac remodeling in mice expressing a dominant-negative Kv4 alpha subunit. *Circ.Res.* **83**, 560-567.
- Baruscotti, M., Westenbroek, R., Catterall, W. A., DiFrancesco, D., and Robinson, R. B. (1997).** The newborn rabbit sino-atrial node expresses a neuronal type I-like Na⁺ channel. *J.Physiol* **498 (Pt 3)**, 641-648.
- Baukrowitz, T. (2000).** Inward rectifier potassium channels and a multitude of intracellular gating molecules. *Eur.J.Biochem.* **267**, 5823.
- Bean, B. P. (1985).** Two kinds of calcium channels in canine atrial cells. Differences in kinetics, selectivity, and pharmacology. *J.Gen.Physiol* **86**, 1-30.
- Bean, B. P. (1989).** Classes of calcium channels in vertebrate cells. *Annu.Rev.Physiol* **51**, 367-384.
- Beblo, D. A. and Veenstra, R. D. (1997).** Monovalent cation permeation through the connexin40 gap junction channel. Cs, Rb, K, Na, Li, TEA, TMA, TBA, and effects of anions Br, Cl, F, acetate, aspartate, glutamate, and NO₃. *J.Gen.Physiol* **109**, 509-522.
- Beblo, D. A., Wang, H. Z., Beyer, E. C., Westphale, E. M., and Veenstra, R. D. (1995).** Unique conductance, gating, and selective permeability properties of gap junction channels formed by connexin40. *Circ.Res.* **77**, 813-822.
- Beck, E. J., Sorensen, R. G., Slater, S. J., and Covarrubias, M. (1998).** Interactions between multiple phosphorylation sites in the inactivation particle of a K⁺ channel. Insights into the molecular mechanism of protein kinase C action. *J.Gen.Physiol* **112**, 71-84.

- Beeler, G. W. and McGuigan, J. A. (1978).** Voltage clamping of multicellular myocardial preparations: capabilities and limitations of existing methods. *Prog.Biophys.Mol.Biol.* **34**, 219-254.
- Beeler, G. W. and Reuter, H. (1977).** Reconstruction of the action potential of ventricular myocardial fibres. *J.Physiol* **268**, 177-210.
- Belcher, S. M. and Howe, J. R. (1996).** Cloning of the cDNA encoding the sodium channel beta 1 subunit from rabbit. *Gene* **170**, 285-286.
- Benndorf, K., Boldt, W., and Nilius, B. (1985).** Sodium current in single myocardial mouse cells. *Pflugers Arch.* **404**, 190-196.
- Bennett, P., McKinney, L., Begenisich, T., and Kass, R. S. (1986).** Adrenergic modulation of the delayed rectifier potassium channel in calf cardiac Purkinje fibers. *Biophys.J.* **49**, 839-848.
- Bennett, P. B. and Begenisich, T. B. (1987).** Catecholamines modulate the delayed rectifying potassium current (IK) in guinea pig ventricular myocytes. *Pflugers Arch.* **410**, 217-219.
- Bennett, P. B., McKinney, L. C., Kass, R. S., and Begenisich, T. (1985).** Delayed rectification in the calf cardiac Purkinje fiber. Evidence for multiple state kinetics. *Biophys.J.* **48**, 553-567.
- Benz, I., Herzig, J. W., and Kohlhardt, M. (1992).** Opposite effects of angiotensin II and the protein kinase C activator OAG on cardiac Na⁺ channels. *J.Membr.Biol.* **130**, 183-190.
- Berglund, E., Grove, B. K., Thornell, L. E., and Stigbrand, T. (1991).** Brain-associated glycoproteins expressed in bovine heart Purkinje fibres. *Histochemistry* **95**, 435-440.
- Beuckelmann, D. J., Nabauer, M., and Erdmann, E. (1993).** Alterations of K⁺ currents in isolated human ventricular myocytes from patients with terminal heart failure. *Circ.Res.* **73**, 379-385.
- Bezzina, C., Veldkamp, M. W., van Den Berg, M. P., Postma, A. V., Rook, M. B., Viersma, J. W., van Langen, I. M., Tan-Sindhunata, G., Bink-Boelkens, M. T., Der Hout, A. H., Mannens, M. M., and Wilde, A. A. (1999).** A single Na⁽⁺⁾ channel mutation causing both long-QT and Brugada syndromes. *Circ.Res.* **85**, 1206-1213.
- Bianchi, L., Shen, Z., Dennis, A. T., Priori, S. G., Napolitano, C., Ronchetti, E., Bryskin, R., Schwartz, P. J., and Brown, A. M. (1999).** Cellular dysfunction of LQT5-minK mutants: abnormalities of IKs, IKr and trafficking in long QT syndrome. *Hum.Mol.Genet.* **8**, 1499-1507.
- Biel, M., Zong, X., Ludwig, A., Sautter, A., and Hofmann, F. (1999).** Structure and function of cyclic nucleotide-gated channels. *Rev.Physiol Biochem.Pharmacol.* **135**, 151-171.
- Blanck, Z. and Akhtar, M. (1993).** Ventricular tachycardia due to sustained bundle branch reentry: diagnostic and therapeutic considerations. *Clin.Cardiol.* **16**, 619-622.
- Blanco, G. and Mercer, R. W. (1998).** Isozymes of the Na-K-ATPase: heterogeneity in structure, diversity in function. *Am.J.Physiol* **275**, F633-F650.

- Blaustein, M. P., Fontana, G., and Rogowski, R. S. (1996).** The Na⁺-Ca²⁺ exchanger in rat brain synaptosomes. Kinetics and regulation. *Ann.N.Y.Acad.Sci.* **779**, 300-317.
- Blumenthal, E. M. and Kaczmarek, L. K. (1992).** Modulation by cAMP of a slowly activating potassium channel expressed in *Xenopus* oocytes. *J.Neurosci.* **12**, 290-296.
- Blumenthal, E. M. and Kaczmarek, L. K. (1994).** The minK potassium channel exists in functional and nonfunctional forms when expressed in the plasma membrane of *Xenopus* oocytes. *J.Neurosci.* **14**, 3097-3105.
- Bodewei, R., Hering, S., Lemke, B., Rosenshtraukh, L. V., Undrovinas, A. I., and Wollenberger, A. (1982).** Characterization of the fast sodium current in isolated rat myocardial cells: simulation of the clamped membrane potential. *J.Physiol* **325**, 301-315.
- Bonhaus, D. W., Herman, R. C., Brown, C. M., Cao, Z., Chang, L. F., Loury, D. N., Sze, P., Zhang, L., and Hunter, J. C. (1996).** The beta 1 sodium channel subunit modifies the interactions of neurotoxins and local anesthetics with the rat brain IIA alpha sodium channel in isolated membranes but not in intact cells. *Neuropharmacology* **35**, 605-613.
- Bonne, G., Carrier, L., Bercovici, J., Cruaud, C., Richard, P., Hainque, B., Gautel, M., Labeit, S., James, M., Beckmann, J., and . (1995).** Cardiac myosin binding protein-C gene splice acceptor site mutation is associated with familial hypertrophic cardiomyopathy. *Nat.Genet.* **11**, 438-440.
- Bosch, R. F., Gaspo, R., Busch, A. E., Lang, H. J., Li, G. R., and Nattel, S. (1998).** Effects of the chromanol 293B, a selective blocker of the slow, component of the delayed rectifier K⁺ current, on repolarization in human and guinea pig ventricular myocytes. *Cardiovasc.Res.* **38**, 441-450.
- Bou-Abboud, E. and Nerbonne, J. M. (1999).** Molecular correlates of the calcium-independent, depolarization- activated K⁺ currents in rat atrial myocytes. *J.Physiol* **517 (Pt 2)**, 407-420.
- Bouman, L. N. and Jongsma, H. J. (1986).** Structure and function of the sino-atrial node: a review. *Eur.Heart J.* **7**, 94-104.
- Boyett, M. R. (1981b).** A study of the effect of the rate of stimulation on the transient outward current in sheep cardiac Purkinje fibres. *J.Physiol* **319**, 1-22.
- Boyett, M. R. (1981a).** Effect of rate-dependent changes in the transient outward current on the action potential in sheep Purkinje fibres. *J.Physiol* **319**, 23-41.
- Boyle, W. A. and Nerbonne, J. M. (1991).** A novel type of depolarization-activated K⁺ current in isolated adult rat atrial myocytes. *Am.J.Physiol* **260**, H1236-H1247.
- Boyle, W. A. and Nerbonne, J. M. (1992).** Two functionally distinct 4-aminopyridine-sensitive outward K⁺ currents in rat atrial myocytes. *J.Gen.Physiol* **100**, 1041-1067.
- Brachmann, J., Scherlag, B. J., Rosenshtraukh, L. V., and Lazzara, R. (1983).** Bradycardia-dependent triggered activity: relevance to drug-induced multiform ventricular tachycardia. *Circulation* **68**, 846-856.

- Brahmajothi, M. V., Campbell, D. L., Rasmusson, R. L., Morales, M. J., Trimmer, J. S., Nerbonne, J. M., and Strauss, H. C.** (1999). Distinct transient outward potassium current (I_{to}) phenotypes and distribution of fast-inactivating potassium channel alpha subunits in ferret left ventricular myocytes. *J.Gen.Physiol* **113**, 581-600.
- Brahmajothi, M. V., Morales, M. J., Liu, S., Rasmusson, R. L., Campbell, D. L., and Strauss, H. C.** (1996). In situ hybridization reveals extensive diversity of K⁺ channel mRNA in isolated ferret cardiac myocytes. *Circ.Res.* **78**, 1083-1089.
- Braun, A. P., Fedida, D., Clark, R. B., and Giles, W. R.** (1990). Intracellular mechanisms for alpha 1-adrenergic regulation of the transient outward current in rabbit atrial myocytes. *J.Physiol* **431**, 689-712.
- Brown, A. M., Lee, K. S., and Powell, T.** (1981). Sodium current in single rat heart muscle cells. *J.Physiol* **318**, 479-500.
- Brown, H. and DiFrancesco, D.** (1980). Voltage-clamp investigations of membrane currents underlying pace-maker activity in rabbit sino-atrial node. *J.Physiol* **308**, 331-351.
- Brown, H., DiFrancesco, D., and Noble, S.** (1979a). Cardiac pacemaker oscillation and its modulation by autonomic transmitters. *J.Exp.Biol.* **81**, 175-204.
- Brown, H. F., DiFrancesco, D., and Noble, S. J.** (1979b). How does adrenaline accelerate the heart? *Nature* **280**, 235-236.
- Brown, H. F., Giles, W., and Noble, S. J.** (1977). Membrane currents underlying activity in frog sinus venosus. *J.Physiol* **271**, 783-816.
- Bryant, S. M., Wan, X., Shipsey, S. J., and Hart, G.** (1998). Regional differences in the delayed rectifier current (I_{Kr} and I_{Ks}) contribute to the differences in action potential duration in basal left ventricular myocytes in guinea-pig. *Cardiovasc.Res.* **40**, 322-331.
- Bukauskas, F. F., Elfgang, C., Willecke, K., and Weingart, R.** (1995). Biophysical properties of gap junction channels formed by mouse connexin40 in induced pairs of transfected human HeLa cells. *Biophys.J.* **68**, 2289-2298.
- Burgess, M. J.** (1979). Relation of ventricular repolarization to electrocardiographic T wave-form and arrhythmia vulnerability. *Am.J.Physiol* **236**, H391-H402.
- Burnashev, N. A. and Zilberter, Y.** (1986). Two types of single inward rectifying potassium channels in rat myocardial cells. *Gen.Physiol Biophys.* **5**, 495-504.
- Busch, A. E., Suessbrich, H., Waldegger, S., Sailer, E., Greger, R., Lang, H., Lang, F., Gibson, K. J., and Maylie, J. G.** (1996). Inhibition of I_{Ks} in guinea pig cardiac myocytes and guinea pig I_{sK} channels by the chromanol 293B. *Pflugers Arch.* **432**, 1094-1096.
- Bustamante, J. O. and McDonald, T. F.** (1983). Sodium currents in segments of human heart cells. *Science* **220**, 320-321.

- Callewaert, G., Carmeliet, E., and Vereecke, J.** (1984). Single cardiac Purkinje cells: general electrophysiology and voltage-clamp analysis of the pace-maker current. *J.Physiol* **349**, 643-661.
- Campbell, D. L., Qu, Y., Rasmusson, R. L., and Strauss, H. C.** (1993a). The calcium-independent transient outward potassium current in isolated ferret right ventricular myocytes. II. Closed state reverse use-dependent block by 4-aminopyridine. *J.Gen.Physiol* **101**, 603-626.
- Campbell, D. L., Rasmusson, R. L., Qu, Y., and Strauss, H. C.** (1993b). The calcium-independent transient outward potassium current in isolated ferret right ventricular myocytes. I. Basic characterization and kinetic analysis. *J.Gen.Physiol* **101**, 571-601.
- Campbell, D.L., Rasmusson, R.L., Comer, M.B., and Strauss, H.C.** (1995). The cardiac calcium-independent transient outward potassium current: kinetics, molecular properties, and role in ventricular repolarization. In Zipes, D. P., and J.J. Jalife, eds. *Cardiac electrophysiology: from cell to bedside*. Philadelphia, W.B. Saunders Co. 83-96.
- Carey, P. A., Turner, M., Fry, C. H., and Sheridan, D. J.** (2001). Reduced anisotropy of action potential conduction in left ventricular hypertrophy. *J.Cardiovasc. Electrophysiol.* **12**, 830-835.
- Carmeliet, E.** (1987). Slow inactivation of the sodium current in rabbit cardiac Purkinje fibres. *Pflugers Arch.* **408**, 18-26.
- Catterall, W. A.** (2000a). From ionic currents to molecular mechanisms: the structure and function of voltage-gated sodium channels. *Neuron* **26**, 13-25.
- Catterall, W. A.** (2000b). Structure and regulation of voltage-gated Ca²⁺ channels. *Annu.Rev.Cell Dev.Biol.* **16**, 521-555.
- Cerbai, E., Barbieri, M., and Mugelli, A.** (1996). Occurrence and properties of the hyperpolarization-activated current I_f in ventricular myocytes from normotensive and hypertensive rats during aging. *Circulation* **94**, 1674-1681.
- Cerbai, E., Crucitti, A., Sartiani, L., De Paoli, P., Pino, R., Rodriguez, M. L., Gensini, G., and Mugelli, A.** (2000). Long-term treatment of spontaneously hypertensive rats with losartan and electrophysiological remodeling of cardiac myocytes. *Cardiovasc.Res.* **45**, 388-396.
- Cerbai, E., Pino, R., Porciatti, F., Sani, G., Toscano, M., Maccherini, M., Giunti, G., and Mugelli, A.** (1997). Characterization of the hyperpolarization-activated current, I_f(f), in ventricular myocytes from human failing heart. *Circulation* **95**, 568-571.
- Cerbai, E., Pino, R., Sartiani, L., and Mugelli, A.** (1999). Influence of postnatal-development on I_f(f) occurrence and properties in neonatal rat ventricular myocytes. *Cardiovasc.Res.* **42**, 416-423.
- Chalvidan, T., Cellarier, G., Deharo, J. C., Colin, R., Savon, N., Barra, N., Peyre, J. P., and Djiane, P.** (2000). His-Purkinje system reentry as a proarrhythmic effect of flecainide. *Pacing Clin.Electrophysiol.* **23**, 530-533.
- Chen, Q., Kirsch, G. E., Zhang, D., Brugada, R., Brugada, J., Brugada, P., Potenza, D., Moya, A., Borggrefe, M., Breithardt, G., Ortiz-Lopez, R., Wang, Z., Antzelevitch, C.,**

- O'Brien, R. E., Schulze-Bahr, E., Keating, M. T., Towbin, J. A., and Wang, Q.** (1998). Genetic basis and molecular mechanism for idiopathic ventricular fibrillation. *Nature* **392**, 293-296.
- Chen, X. H., Bezprozvanny, I., and Tsien, R. W.** (1996). Molecular basis of proton block of L-type Ca²⁺ channels. *J.Gen.Physiol* **108**, 363-374.
- Cheng, G., Litchenberg, W. H., Cole, G. J., Mikawa, T., Thompson, R. P., and Gourdie, R. G.** (1999). Development of the cardiac conduction system involves recruitment within a multipotent cardiomyogenic lineage. *Development* **126**, 5041-5049.
- Cheon, J. and Reeves, J. P.** (1988). Site density of the sodium-calcium exchange carrier in reconstituted vesicles from bovine cardiac sarcolemma. *J.Biol.Chem.* **263**, 2309-2315.
- Choe, H., Sackin, H., and Palmer, L. G.** (2000). Permeation properties of inward-rectifier potassium channels and their molecular determinants. *J.Gen.Physiol* **115**, 391-404.
- Clapham, D. E.** (1998). Not so funny anymore: pacing channels are cloned. *Neuron* **21**, 5-7.
- Clark, R. B., Giles, W. R., and Imaizumi, Y.** (1988). Properties of the transient outward current in rabbit atrial cells. *J.Physiol* **405**, 147-168.
- Clay JR, Ogbaghebriel A, Paquette T, Sasyniuk BI, Shrier A.** (1995). A quantitative description of the E-4031-sensitive repolarization current in rabbit ventricular myocytes. *Biophys. J.* **69**(5), 1830-7.
- Coetzee, W. A. and Opie, L. H.** (1992). Effects of oxygen free radicals on isolated cardiac myocytes from guinea-pig ventricle: electrophysiological studies. *J.Mol.Cell Cardiol.* **24**, 651-663.
- Cohen, S. A.** (1996). Immunocytochemical localization of rH1 sodium channel in adult rat heart atria and ventricle. Presence in terminal intercalated disks. *Circulation* **94**, 3083-3086.
- Colatsky, J. J. and Tsien, R. W.** (1979). Sodium channels in rabbit cardiac Purkinje fibres. *Nature* **278**, 265-268.
- Collin, T., Wang, J. J., Nargeot, J., and Schwartz, A.** (1993). Molecular cloning of three isoforms of the L-type voltage-dependent calcium channel beta subunit from normal human heart. *Circ.Res.* **72**, 1337-1344.
- Compton, S. J., Lux, R. L., Ramsey, M. R., Strellich, K. R., Sanguinetti, M. C., Green, L. S., Keating, M. T., and Mason, J. W.** (1996). Genetically defined therapy of inherited long-QT syndrome. Correction of abnormal repolarization by potassium. *Circulation* **94**, 1018-1022.
- Cooper, C. L., Vandaele, S., Barhanin, J., Fosset, M., Lazdunski, M., and Hosey, M. M.** (1987). Purification and characterization of the dihydropyridine-sensitive voltage-dependent calcium channel from cardiac tissue. *J.Biol.Chem.* **262**, 509-512.
- Coppen, S. R., Severs, N. J., and Gourdie, R. G.** (1999). Connexin45 (alpha 6) expression delineates an extended conduction system in the embryonic and mature rodent heart. *Dev.Genet.* **24**, 82-90.

- Coraboeuf, E., Deroubaix, E., and Coulombe, A.** (1979). Effect of tetrodotoxin on action potentials of the conducting system in the dog heart. *Am.J.Physiol* **236**, H561-H567.
- Cordeiro, J. M., Spitzer, K. W., and Giles, W. R.** (1998). Repolarizing K⁺ currents in rabbit heart Purkinje cells. *J.Physiol* **508 (Pt 3)**, 811-823.
- Courtemanche, M., Ramirez, R. J., and Nattel, S.** (1998). Ionic mechanisms underlying human atrial action potential properties: insights from a mathematical model. *Am.J.Physiol* **275**, H301-H321.
- Cranefield, P. F.** (1983). Channels, cables, networks, and the conduction of the cardiac impulse. *Am.J.Physiol* **245**, H901-H910.
- Cribbs, L. L., Lee, J. H., Yang, J., Satin, J., Zhang, Y., Daud, A., Barclay, J., Williamson, M. P., Fox, M., Rees, M., and Perez-Reyes, E.** (1998). Cloning and characterization of alpha1H from human heart, a member of the T-type Ca²⁺ channel gene family. *Circ.Res.* **83**, 103-109.
- Cui, J., Kagan, A., Qin, D., Mathew, J., Melman, Y. F., and McDonald, T. V.** (2001). Analysis of the cyclic nucleotide binding domain of the HERG potassium channel and interactions with KCNE2. *J.Biol.Chem.* **276**, 17244-17251.
- Cui, J., Melman, Y., Palma, E., Fishman, G. I., and McDonald, T. V.** (2000). Cyclic AMP regulates the HERG K(+) channel by dual pathways. *Curr.Biol.* **10**, 671-674.
- Curran, E.J.** (1909). A constant bursa in relation with the bundle of His. *Anat. Rec.* **3**, 618-639.
- Curran, M. E., Splawski, I., Timothy, K. W., Vincent, G. M., Green, E. D., and Keating, M. T.** (1995). A molecular basis for cardiac arrhythmia: HERG mutations cause long QT syndrome. *Cell* **80**, 795-803.
- Damiano, B. P. and Rosen, M. R.** (1984). Effects of pacing on triggered activity induced by early afterdepolarizations. *Circulation* **69**, 1013-1025.
- Dascal, N., Lim, N. F., Schreibmayer, W., Wang, W., Davidson, N., and Lester, H. A.** (1993b). Expression of an atrial G-protein-activated potassium channel in *Xenopus* oocytes. *Proc.Natl.Acad.Sci.U.S.A* **90**, 6596-6600.
- Dascal, N., Schreibmayer, W., Lim, N. F., Wang, W., Chavkin, C., DiMagno, L., Labarca, C., Kieffer, B. L., Gaveriaux-Ruff, C., Trollinger, D., and .** (1993a). Atrial G protein-activated K⁺ channel: expression cloning and molecular properties. *Proc.Natl.Acad.Sci.U.S.A* **90**, 10235-10239.
- Davidenko, J. M., Cohen, L., Goodrow, R., and Antzelevitch, C.** (1989). Quinidine-induced action potential prolongation, early afterdepolarizations, and triggered activity in canine Purkinje fibers. Effects of stimulation rate, potassium, and magnesium. *Circulation* **79**, 674-686.
- Davis, L. M., Kanter, H. L., Beyer, E. C., and Saffitz, J. E.** (1994). Distinct gap junction protein phenotypes in cardiac tissues with disparate conduction properties. *J.Am.Coll.Cardiol.* **24**, 1124-1132.

- De Biasi, M., Hartmann, H. A., Drewe, J. A., Taglialatela, M., Brown, A. M., and Kirsch, G. E.** (1993). Inactivation determined by a single site in K⁺ pores. *Pflugers Arch.* **422**, 354-363.
- de Groot, I. J., Sanders, E., Visser, S. D., Lamers, W. H., de Jong, F., Los, J. A., and Moorman, A. F.** (1987). Isomyosin expression in developing chicken atria: a marker for the development of conductive tissue?. *Anat.Embryol.(Berl)* **176**, 515-523.
- De Jongh, K. S., Murphy, B. J., Colvin, A. A., Hell, J. W., Takahashi, M., and Catterall, W. A.** (1996). Specific phosphorylation of a site in the full-length form of the alpha 1 subunit of the cardiac L-type calcium channel by adenosine 3',5'- cyclic monophosphate-dependent protein kinase. *Biochemistry* **35**, 10392-10402.
- Deal, K. K., England, S. K., and Tamkun, M. M.** (1996). Molecular physiology of cardiac potassium channels. *Physiol Rev.* **76**, 49-67.
- Decher, N., Uyguner, O., Scherer, C. R., Karaman, B., Yuksel-Apak, M., Busch, A. E., Steinmeyer, K., and Wollnik, B.** (2001). hKChIP2 is a functional modifier of hKv4.3 potassium channels: cloning and expression of a short hKChIP2 splice variant. *Cardiovasc.Res.* **52**, 255-264.
- Deck, K., Nern, R., and Trautwein** (1964). Voltage clamp technique in mammalian cardiac fibers. *Pluegers Arch.* **280**, 50-62.
- Delorme, B., Dahl, E., Jarry-Guichard, T., Marics, I., Briand, J. P., Willecke, K., Gros, D., and Theveniau-Ruissy, M.** (1995). Developmental regulation of connexin40 gene expression in mouse heart correlates with the differentiation of the conduction system. *Dev.Dyn.* **204**, 358-371.
- Demolombe, S., Baro, I., Pereon, Y., Blied, J., Mohammad-Panah, R., Pollard, H., Morid, S., Mannens, M., Wilde, A., Barhanin, J., Charpentier, F., and Escande, D.** (1998). A dominant negative isoform of the long QT syndrome 1 gene product. *J.Biol.Chem.* **273**, 6837-6843.
- Dhar, M. J., Chen, C., Rivolta, I., Abriel, H., Malhotra, R., Mattei, L. N., Brosius, F. C., Kass, R. S., and Isom, L. L.** (2001). Characterization of sodium channel alpha- and beta-subunits in rat and mouse cardiac myocytes. *Circulation* **103**, 1303-1310.
- Di Diego, J. M., Sun, Z. Q., and Antzelevitch, C.** (1996). I_(to) and action potential notch are smaller in left vs. right canine ventricular epicardium. *Am.J.Physiol* **271**, H548-H561.
- DiFrancesco, D.** (1981). A new interpretation of the pace-maker current in calf Purkinje fibres. *J.Physiol* **314**, 359-376.
- DiFrancesco, D.** (1985). The cardiac hyperpolarizing-activated current, *if*. Origins and developments. *Prog.Biophys.Mol.Biol.* **46**, 163-183.
- DiFrancesco, D.** (1993). Pacemaker mechanisms in cardiac tissue. *Annu.Rev.Physiol* **55**, 455-472.
- DiFrancesco, D.** (1995). The onset and autonomic regulation of cardiac pacemaker activity: relevance of the *f* current. *Cardiovasc.Res.* **29**, 449-456.

- DiFrancesco, D., Ferroni, A., Mazzanti, M., and Tromba, C.** (1986). Properties of the hyperpolarizing-activated current (if) in cells isolated from the rabbit sino-atrial node. *J.Physiol* **377**, 61-88.
- DiFrancesco, D. and Noble, D.** (1985). A model of cardiac electrical activity incorporating ionic pumps and concentration changes. *Philos.Trans.R.Soc.Lond B Biol.Sci.* **307**, 353-398.
- DiFrancesco, D. and Ojeda, C.** (1980). Properties of the current if in the sino-atrial node of the rabbit compared with those of the current iK₁ in Purkinje fibres. *J.Physiol* **308**, 353-367.
- DiFrancesco, D. and Tortora, P.** (1991). Direct activation of cardiac pacemaker channels by intracellular cyclic AMP. *Nature* **351**, 145-147.
- DiFrancesco, D. and Tromba, C.** (1988a). Inhibition of the hyperpolarization-activated current (if) induced by acetylcholine in rabbit sino-atrial node myocytes. *J.Physiol* **405**, 477-491.
- DiFrancesco, D. and Tromba, C.** (1988b). Muscarinic control of the hyperpolarization-activated current (if) in rabbit sino-atrial node myocytes. *J.Physiol* **405**, 493-510.
- Dipla, K., Mattiello, J. A., Margulies, K. B., Jeevanandam, V., and Houser, S. R.** (1999). The sarcoplasmic reticulum and the Na⁺/Ca²⁺ exchanger both contribute to the Ca²⁺ transient of failing human ventricular myocytes. *Circ.Res.* **84**, 435-444.
- Dixon, J. E. and McKinnon, D.** (1994). Quantitative analysis of potassium channel mRNA expression in atrial and ventricular muscle of rats. *Circ.Res.* **75**, 252-260.
- Dixon, J. E., Shi, W., Wang, H. S., McDonald, C., Yu, H., Wymore, R. S., Cohen, I. S., and McKinnon, D.** (1996). Role of the Kv4.3 K⁺ channel in ventricular muscle. A molecular correlate for the transient outward current. *Circ.Res.* **79**, 659-668.
- Douplnik, C. A., Davidson, N., and Lester, H. A.** (1995). The inward rectifier potassium channel family. *Curr.Opin.Neurobiol.* **5**, 268-277.
- Doyle, D. A., Morais, C. J., Pfuetzner, R. A., Kuo, A., Gulbis, J. M., Cohen, S. L., Chait, B. T., and MacKinnon, R.** (1998). The structure of the potassium channel: molecular basis of K⁺ conduction and selectivity. *Science* **280**, 69-77.
- Dudel, J., Peper, K., Rudel, R., and Trautwein, W.** (1967). The dynamic chloride component of membrane current in Purkinje fibers. *Pflugers Arch.Gesamte Physiol Menschen.Tiere.* **295**, 197-212.
- Dyck, C., Omelchenko, A., Elias, C. L., Quednau, B. D., Philipson, K. D., Hnatowich, M., and Hryshko, L. V.** (1999). Ionic regulatory properties of brain and kidney splice variants of the NCX1 Na⁽⁺⁾-Ca⁽²⁺⁾ exchanger. *J.Gen.Physiol* **114**, 701-711.
- el Sherif, N., Caref, E. B., Yin, H., and Restivo, M.** (1996). The electrophysiological mechanism of ventricular arrhythmias in the long QT syndrome. Tridimensional mapping of activation and recovery patterns. *Circ.Res.* **79**, 474-492.

- Emdad, L., Uzzaman, M., Takagishi, Y., Honjo, H., Uchida, T., Severs, N. J., Kodama, I., and Murata, Y.** (2001). Gap junction remodeling in hypertrophied left ventricles of aortic- banded rats: prevention by angiotensin II type 1 receptor blockade. *J.Mol.Cell Cardiol.* **33**, 219-231.
- England, S. K., Uebele, V. N., Kodali, J., Bennett, P. B., and Tamkun, M. M.** (1995a). A novel K⁺ channel beta-subunit (hKv beta 1.3) is produced via alternative mRNA splicing. *J.Biol.Chem.* **270**, 28531-28534.
- England, S. K., Uebele, V. N., Shear, H., Kodali, J., Bennett, P. B., and Tamkun, M. M.** (1995b). Characterization of a voltage-gated K⁺ channel beta subunit expressed in human heart. *Proc.Natl.Acad.Sci.U.S.A* **92**, 6309-6313.
- Ertel, E. A., Campbell, K. P., Harpold, M. M., Hofmann, F., Mori, Y., Perez-Reyes, E., Schwartz, A., Snutch, T. P., Tanabe, T., Birnbaumer, L., Tsien, R. W., and Catterall, W. A.** (2000). Nomenclature of voltage-gated calcium channels. *Neuron* **25**, 533-535.
- Escande, D., Coulombe, A., Faivre, J. F., Deroubaix, E., and Coraboeuf, E.** (1987). Two types of transient outward currents in adult human atrial cells. *Am.J.Physiol* **252**, H142-H148.
- Eskinder, H., Supan, F. D., Turner, L. A., Kampine, J. P., and Bosnjak, Z. J.** (1993). The effects of halothane and isoflurane on slowly inactivating sodium current in canine cardiac Purkinje cells. *Anesth.Analg.* **77**, 32-37.
- Eubanks, J., Srinivasan, J., Dinulos, M. B., Disteché, C. M., and Catterall, W. A.** (1997). Structure and chromosomal localization of the beta2 subunit of the human brain sodium channel. *Neuroreport* **8**, 2775-2779.
- Fahmi, A. I., Patel, M., Stevens, E. B., Fowden, A. L., John, J. E., Lee, K., Pinnock, R., Morgan, K., Jackson, A. P., and Vandenberg, J. I.** (2001). The sodium channel beta-subunit SCN3b modulates the kinetics of SCN5a and is expressed heterogeneously in sheep heart. *J.Physiol* **537**, 693-700.
- Faivre, J. F. and Findlay, I.** (1990). Action potential duration and activation of ATP-sensitive potassium current in isolated guinea-pig ventricular myocytes. *Biochim.Biophys.Acta* **1029**, 167-172.
- Fakler, B., Brandle, U., Glowatzki, E., Zenner, H. P., and Ruppersberg, J. P.** (1994). Kir2.1 inward rectifier K⁺ channels are regulated independently by protein kinases and ATP hydrolysis. *Neuron* **13**, 1413-1420.
- Fan, J., Shuba, Y. M., and Morad, M.** (1996). Regulation of cardiac sodium-calcium exchanger by beta-adrenergic agonists. *Proc.Natl.Acad.Sci.U.S.A* **93**, 5527-5532.
- Fedida, D. and Bouchard, R. A.** (1992). Mechanisms for the positive inotropic effect of alpha 1-adrenoceptor stimulation in rat cardiac myocytes. *Circ.Res.* **71**, 673-688.
- Fedida, D., Braun, A. P., and Giles, W. R.** (1991). Alpha 1-adrenoceptors reduce background K⁺ current in rabbit ventricular myocytes. *J.Physiol* **441**, 673-684.

- Fedida, D., Noble, D., Rankin, A. C., and Spindler, A. J.** (1987). The arrhythmogenic transient inward current i_{TI} and related contraction in isolated guinea-pig ventricular myocytes. *J.Physiol* **392**, 523-542.
- Fedida, D., Shimoni, Y., and Giles, W. R.** (1989). A novel effect of norepinephrine on cardiac cells is mediated by alpha 1-adrenoceptors. *Am.J.Physiol* **256**, H1500-H1504.
- Fedida, D., Shimoni, Y., and Giles, W. R.** (1990). Alpha-adrenergic modulation of the transient outward current in rabbit atrial myocytes. *J.Physiol* **423**, 257-277.
- Fedida, D., Wible, B., Wang, Z., Fermini, B., Faust, F., Nattel, S., and Brown, A. M.** (1993). Identity of a novel delayed rectifier current from human heart with a cloned K^+ channel current. *Circ.Res.* **73**, 210-216.
- Felipe, A., Knittle, T. J., Doyle, K. L., and Tamkun, M. M.** (1994). Primary structure and differential expression during development and pregnancy of a novel voltage-gated sodium channel in the mouse. *J.Biol.Chem.* **269**, 30125-30131.
- Fermini, B., Wang, Z., Duan, D., and Nattel, S.** (1992). Differences in rate dependence of transient outward current in rabbit and human atrium. *Am.J.Physiol* **263**, H1747-H1754.
- Field, E.J.** (1951). The development of the conducting system in the heart of sheep. *Br.Heart J.* **13**, 129-147.
- Fink, M., Duprat, F., Lesage, F., Heurteaux, C., Romey, G., Barhanin, J., and Lazdunski, M.** (1996). A new K^+ channel beta subunit to specifically enhance $Kv2.2$ (CDRK) expression. *J.Biol.Chem.* **271**, 26341-26348.
- Firek, L. and Giles, W. R.** (1995). Outward currents underlying repolarization in human atrial myocytes. *Cardiovasc.Res.* **30**, 31-38.
- Fiset, C., Clark, R. B., Shimoni, Y., and Giles, W. R.** (1997). Shal-type channels contribute to the Ca^{2+} -independent transient outward K^+ current in rat ventricle. *J.Physiol* **500** (Pt 1), 51-64.
- Fleming, J. W., Wisler, P. L., and Watanabe, A. M.** (1992). Signal transduction by G proteins in cardiac tissues. *Circulation* **85**, 420-433.
- Folander, K., Smith, J. S., Antanavage, J., Bennett, C., Stein, R. B., and Swanson, R.** (1990). Cloning and expression of the delayed-rectifier IsK channel from neonatal rat heart and diethylstilbestrol-primed rat uterus. *Proc.Natl.Acad.Sci.U.S.A* **87**, 2975-2979.
- Follmer, C. H. and Colatsky, T. J.** (1990). Block of delayed rectifier potassium current, IK , by flecainide and E-4031 in cat ventricular myocytes. *Circulation* **82**, 289-293.
- Follmer, C. H., Ten Eick, R. E., and Yeh, J. Z.** (1987). Sodium current kinetics in cat atrial myocytes. *J.Physiol* **384**, 169-197.
- Fozzard, H.A.** (1993). Cardiac electrogenesis and the sodium channel. In Spooner PM, Brown AM, Catterall WA, Kaczorowski GJ, and Strauss HC, eds. *Ion channel in the cardiovascular system, Function and dysfunction*, New York, Future Publishing Company, Inc. 81-100.

- Fozzard, H.A. and Arhdsdorf, M.F.** (1992) Cardiac electrophysiology. In Fozzard HA and Arhdsdorf MF ed. *The Heart and Cardiovascular System*, Raven Press New York©.
- Fozzard, H. A.** (1977). Cardiac muscle: excitability and passive electrical properties. *Prog. Cardiovasc.Dis.* **19**, 343-359.
- Fozzard, H. A. and Beeler, G. W., Jr.** (1975). The voltage clamp and cardiac electrophysiology. *Circ.Res.* **37**, 403-413.
- Fozzard, H. A. and Hiraoka, M.** (1973). The positive dynamic current and its inactivation properties in cardiac Purkinje fibres. *J.Physiol* **234**, 569-586.
- Fozzard, H. A., January, C. T., and Makielski, J. C.** (1985). New studies of the excitatory sodium currents in heart muscle. *Circ.Res.* **56**, 475-485.
- Frank, J. S., Mottino, G., Reid, D., Molday, R. S., and Philipson, K. D.** (1992). Distribution of the Na(+)-Ca²⁺ exchange protein in mammalian cardiac myocytes: an immunofluorescence and immunocolloidal gold-labeling study. *J.Cell Biol.* **117**, 337-345.
- Frankenhaeuser, B.** (1963). Inactivation of the sodium-carrying mechanism in myelinated nerve fibres of *Xenopus laevis*. *J. Physiol*, **169**, 445-451.
- Fraser, I. D., Tavalin, S. J., Lester, L. B., Langeberg, L. K., Westphal, A. M., Dean, R. A., Marrion, N. V., and Scott, J. D.** (1998). A novel lipid-anchored A-kinase Anchoring Protein facilitates cAMP- responsive membrane events. *EMBO J.* **17**, 2261-2272.
- Freeman, L. C. and Kass, R. S.** (1993a). Delayed rectifier potassium channels in ventricle and sinoatrial node of the guinea pig: molecular and regulatory properties. *Cardiovasc.Drugs Ther.* **7 Suppl 3**, 627-635.
- Freeman, L. C. and Kass, R. S.** (1993b). Expression of a minimal K⁺ channel protein in mammalian cells and immunolocalization in guinea pig heart. *Circ.Res.* **73**, 968-973.
- Freeman, L. C., Pacioretty, L. M., Moise, N. S., Kass, R. S., and Gilmour, R. F., Jr.** (1997). Decreased density of Ito in left ventricular myocytes from German shepherd dogs with inherited arrhythmias. *J.Cardiovasc.Electrophysiol.* **8**, 872-883.
- Frelin, C., Cognard, C., Vigne, P., and Lazdunski, M.** (1986). Tetrodotoxin-sensitive and tetrodotoxin-resistant Na⁺ channels differ in their sensitivity to Cd²⁺ and Zn²⁺. *Eur.J. Pharmacol.* **122**, 245-250.
- Frohnwieser, B., Chen, L. Q., Schreiber, W., and Kallen, R. G.** (1997). Modulation of the human cardiac sodium channel alpha-subunit by cAMP- dependent protein kinase and the responsible sequence domain. *J.Physiol* **498 (Pt 2)**, 309-318.
- Fujioka, Y., Hiroe, K., and Matsuoka, S.** (2000a). Regulation kinetics of Na⁺-Ca²⁺ exchange current in guinea-pig ventricular myocytes. *J.Physiol* **529 Pt 3**, 611-623.
- Fujioka, Y., Komeda, M., and Matsuoka, S.** (2000b). Stoichiometry of Na⁺-Ca²⁺ exchange in inside-out patches excised from guinea-pig ventricular myocytes. *J.Physiol* **523 Pt 2**, 339-351.

- Fukushima, Y. and Hagiwara, S.** (1983). Voltage-gated Ca²⁺ channel in mouse myeloma cells. *Proc.Natl.Acad.Sci.U.S.A* **80**, 2240-2242.
- Furman, I., Cook, O., Kasir, J., and Rahamimoff, H.** (1993). Cloning of two isoforms of the rat brain Na(+)-Ca²⁺ exchanger gene and their functional expression in HeLa cells. *FEBS Lett.* **319**, 105-109.
- Furukawa, T., Ito, H., Nitta, J., Tsujino, M., Adachi, S., Hiroe, M., Marumo, F., Sawanobori, T., and Hiraoka, M.** (1992b). Endothelin-1 enhances calcium entry through T-type calcium channels in cultured neonatal rat ventricular myocytes. *Circ.Res.* **71**, 1242-1253.
- Furukawa, T., Kimura, S., Furukawa, N., Bassett, A. L., and Myerburg, R. J.** (1992a). Potassium rectifier currents differ in myocytes of endocardial and epicardial origin. *Circ.Res.* **70**, 91-103.
- Furukawa, T., Myerburg, R. J., Furukawa, N., Bassett, A. L., and Kimura, S.** (1990). Differences in transient outward currents of feline endocardial and epicardial myocytes. *Circ.Res.* **67**, 1287-1291.
- Furukawa, T., Myerburg, R. J., Furukawa, N., Kimura, S., and Bassett, A. L.** (1994). Metabolic inhibition of I_{Ca,L} and I_K differs in feline left ventricular hypertrophy. *Am.J.Physiol* **266**, H1121-H1131.
- Gao, T., Puri, T. S., Gerhardstein, B. L., Chien, A. J., Green, R. D., and Hosey, M. M.** (1997a). Identification and subcellular localization of the subunits of L-type calcium channels and adenylyl cyclase in cardiac myocytes. *J.Biol.Chem.* **272**, 19401-19407.
- Gao, T., Yatani, A., Dell'Acqua, M. L., Sako, H., Green, S. A., Dascal, N., Scott, J. D., and Hosey, M. M.** (1997b). cAMP-dependent regulation of cardiac L-type Ca²⁺ channels requires membrane targeting of PKA and phosphorylation of channel subunits. *Neuron* **19**, 185-196.
- Garlid, K. D., Paucek, P., Yarov-Yarovoy, V., Murray, H. N., Darbenzio, R. B., D'Alonzo, A. J., Lodge, N. J., Smith, M. A., and Grover, G. J.** (1997). Cardioprotective effect of diazoxide and its interaction with mitochondrial ATP-sensitive K⁺ channels. Possible mechanism of cardioprotection. *Circ.Res.* **81**, 1072-1082.
- Gasser, R. N. and Vaughan-Jones, R. D.** (1990). Mechanism of potassium efflux and action potential shortening during ischaemia in isolated mammalian cardiac muscle. *J.Physiol* **431**, 713-741.
- Gaughan, J. P., Hefner, C. A., and Houser, S. R.** (1998). Electrophysiological properties of neonatal rat ventricular myocytes with alpha1-adrenergic-induced hypertrophy. *Am.J.Physiol* **275**, H577-H590.
- Gellens, M. E., George, A. L., Jr., Chen, L. Q., Chahine, M., Horn, R., Barchi, R. L., and Kallen, R. G.** (1992). Primary structure and functional expression of the human cardiac tetrodotoxin-insensitive voltage-dependent sodium channel. *Proc.Natl.Acad. Sci.U.S.A* **89**, 554-558.

- George, A. L., Jr., Knittle, T. J., and Tamkun, M. M.** (1992). Molecular cloning of an atypical voltage-gated sodium channel expressed in human heart and uterus: evidence for a distinct gene family. *Proc.Natl.Acad.Sci.U.S.A* **89**, 4893-4897.
- Gershon, E., Weigl, L., Lotan, I., Schreibmayer, W., and Dascal, N.** (1992). Protein kinase A reduces voltage-dependent Na⁺ current in Xenopus oocytes. *J.Neurosci.* **12**, 3743-3752.
- Gerster, U., Neuhuber, B., Groschner, K., Striessnig, J., and Flucher, B. E.** (1999). Current modulation and membrane targeting of the calcium channel α_1C subunit are independent functions of the beta subunit. *J.Physiol* **517 (Pt 2)**, 353-368.
- Gidh-Jain, M., Huang, B., Jain, P., and el Sherif, N.** (1996). Differential expression of voltage-gated K⁺ channel genes in left ventricular remodeled myocardium after experimental myocardial infarction. *Circ.Res.* **79**, 669-675.
- Giles, W., Nakajima, T., Ono, K., and Shibata, E. F.** (1989). Modulation of the delayed rectifier K⁺ current by isoprenaline in bull- frog atrial myocytes. *J.Physiol* **415**, 233-249.
- Giles, W. R. and Imaizumi, Y.** (1988). Comparison of potassium currents in rabbit atrial and ventricular cells. *J.Physiol* **405**, 123-145.
- Gilmour, R. F., Jr. and Moise, N. S.** (1996). Triggered activity as a mechanism for inherited ventricular arrhythmias in German shepherd Dogs. *J.Am.Coll.Cardiol.* **27**, 1526-1533.
- Gintant, G. A., Datyner, N. B. and I. S. Cohen.** (1984). Slow inactivation of a tetrodotoxin-sensitive current in canine cardiac Purkinje fibers. *Biophys.J.* **45** (3), 509-512.
- Gintant, G. A.** (1996). Two components of delayed rectifier current in canine atrium and ventricle. Does IKs play a role in the reverse rate dependence of class III agents? *Circ.Res.* **78**, 26-37.
- Gintant, G. A., Datyner, N. B., and Cohen, I. S.** (1985). Gating of delayed rectification in acutely isolated canine cardiac Purkinje myocytes. Evidence for a single voltage-gated conductance. *Biophys.J.* **48**, 1059-1064.
- Gintant, G. A., Limberis, J. T., McDermott, J. S., Wegner, C. D., and Cox, B. F.** (2001). The canine Purkinje fiber: an in vitro model system for acquired long QT syndrome and drug-induced arrhythmogenesis. *J.Cardiovasc.Pharmacol.* **37**, 607-618.
- Gintant, G. A. and Liu, D. W.** (1992). Beta-adrenergic modulation of fast inward sodium current in canine myocardium. Syncytial preparations versus isolated myocytes. *Circ.Res.* **70**, 844-850.
- Glitsch, H. G.** (2001). Electrophysiology of the sodium-potassium-ATPase in cardiac cells. *Physiol Rev.* **81**, 1791-1826.
- Goldin, A. L.** (2001). Resurgence of sodium channel research. *Annu.Rev.Physiol* **63**, 871-894.
- Goldin, A. L., Barchi, R. L., Caldwell, J. H., Hofmann, F., Howe, J. R., Hunter, J. C., Kallen, R. G., Mandel, G., Meisler, M. H., Netter, Y. B., Noda, M., Tamkun, M. M., Waxman, S. G., Wood, J. N., and Catterall, W. A.** (2000). Nomenclature of voltage-gated sodium channels. *Neuron* **28**, 365-368.

- Goldstein, S. A. and Miller, C. (1991).** Site-specific mutations in a minimal voltage-dependent K⁺ channel alter ion selectivity and open-channel block. *Neuron* **7**, 403-408.
- Goldstein, S. A. and Miller, C. (1993).** Mechanism of charybdotoxin block of a voltage-gated K⁺ channel. *Biophys.J.* **65**, 1613-1619.
- Gonzalez-Sanchez, A. and Bader, D. (1985).** Characterization of a myosin heavy chain in the conductive system of the adult and developing chicken heart. *J.Cell Biol.* **100**, 270-275.
- Gordon, D., Merrick, D., Wollner, D. A., and Catterall, W. A. (1988).** Biochemical properties of sodium channels in a wide range of excitable tissues studied with site-directed antibodies. *Biochemistry* **27**, 7032-7038.
- Gorza, L., Schiaffino, S., and Vitadello, M. (1988).** Heart conduction system: a neural crest derivative?. *Brain Res.* **457**, 360-366.
- Gorza, L. and Vitadello, M. (1989).** Distribution of conduction system fibers in the developing and adult rabbit heart revealed by an antineurofilament antibody. *Circ.Res.* **65**, 360-369.
- Gourdie, R. G., Green, C. R., Severs, N. J., Anderson, R. H., and Thompson, R. P. (1993a).** Evidence for a distinct gap-junctional phenotype in ventricular conduction tissues of the developing and mature avian heart. *Circ.Res.* **72**, 278-289.
- Gourdie, R. G., Mima, T., Thompson, R. P., and Mikawa, T. (1995).** Terminal diversification of the myocyte lineage generates Purkinje fibers of the cardiac conduction system. *Development* **121**, 1423-1431.
- Gourdie, R. G., Severs, N. J., Green, C. R., Rothery, S., Germroth, P., and Thompson, R. P. (1993b).** The spatial distribution and relative abundance of gap-junctional connexin40 and connexin43 correlate to functional properties of components of the cardiac atrioventricular conduction system. *J.Cell Sci.* **105 (Pt 4)**, 985-991.
- Gourdie, R. G., Wei, Y., Kim, D., Klatt, S. C., and Mikawa, T. (1998).** Endothelin-induced conversion of embryonic heart muscle cells into impulse-conducting Purkinje fibers. *Proc.Natl.Acad.Sci.U.S.A* **95**, 6815-6818.
- Grant, A. O. and Starmer, C. F. (1987).** Mechanisms of closure of cardiac sodium channels in rabbit ventricular myocytes: single-channel analysis. *Circ.Res.* **60**, 897-913.
- Gray, P. C., Johnson, B. D., Westenbroek, R. E., Hays, L. G., Yates, J. R., III, Scheuer, T., Catterall, W. A., and Murphy, B. J. (1998).** Primary structure and function of an A kinase anchoring protein associated with calcium channels. *Neuron* **20**, 1017-1026.
- Greenstein, J. L., Wu, R., Po, S., Tomaselli, G. F., and Winslow, R. L. (2000).** Role of the calcium-independent transient outward current I_(to1) in shaping action potential morphology and duration. *Circ.Res.* **87**, 1026-1033.
- Gribble, F. M., Tucker, S. J., and Ashcroft, F. M. (1997).** The essential role of the Walker A motifs of SUR1 in K-ATP channel activation by Mg-ADP and diazoxide. *EMBO J.* **16**, 1145-1152.

- Gribble, F. M., Tucker, S. J., Seino, S., and Ashcroft, F. M. (1998). Tissue specificity of sulfonylureas: studies on cloned cardiac and beta- cell K(ATP) channels. *Diabetes* **47**, 1412-1418.
- Gros, D., Jarry-Guichard, T., Ten, V., I, de Maziere, A., van Kempen, M. J., Davoust, J., Briand, J. P., Moorman, A. F., and Jongsma, H. J. (1994). Restricted distribution of connexin40, a gap junctional protein, in mammalian heart. *Circ.Res.* **74**, 839-851.
- Gros, D. B. and Jongsma, H. J. (1996). Connexins in mammalian heart function. *Bioessays* **18**, 719-730.
- Grosson, C. L., Cannon, S. C., Corey, D. P., and Gusella, J. F. (1996). Sequence of the voltage-gated sodium channel beta1-subunit in wild-type and in quivering mice. *Brain Res.Mol.Brain Res.* **42**, 222-226.
- Gulch, R. W., Baumann, R., and Jacob, R. (1979). Analysis of myocardial action potential in left ventricular hypertrophy of Goldblatt rats. *Basic Res.Cardiol.* **74**, 69-82.
- Guo, W., Kamiya, K., Hojo, M., Kodama, I., and Toyama, J. (1998). Regulation of Kv4.2 and Kv1.4 K⁺ channel expression by myocardial hypertrophic factors in cultured newborn rat ventricular cells. *J.Mol.Cell Cardiol.* **30**, 1449-1455.
- Guo, W., Li, H., London, B., and Nerbonne, J. M. (2000). Functional consequences of elimination of i(to,f) and i(to,s): early afterdepolarizations, atrioventricular block, and ventricular arrhythmias in mice lacking Kv1.4 and expressing a dominant-negative Kv4 alpha subunit. *Circ.Res.* **87**, 73-79.
- Haase, H., Bartel, S., Karczewski, P., Morano, I., and Krause, E. G. (1996a). In-vivo phosphorylation of the cardiac L-type calcium channel beta- subunit in response to catecholamines. *Mol.Cell Biochem.* **163-164**, 99-106.
- Haase, H., Kresse, A., Hohaus, A., Schulte, H. D., Maier, M., Osterziel, K. J., Lange, P. E., and Morano, I. (1996b). Expression of calcium channel subunits in the normal and diseased human myocardium. *J.Mol.Med.* **74**, 99-104.
- Haase, H., Striessnig, J., Holtzhauer, M., Vetter, R., and Glossmann, H. (1991). A rapid procedure for the purification of cardiac 1,4-dihydropyridine receptors from porcine heart. *Eur.J.Pharmacol.* **207**, 51-59.
- Habbab, M. A. and el Sherif, N. (1990). Drug-induced torsades de pointes: role of early afterdepolarizations and dispersion of repolarization. *Am.J.Med.* **89**, 241-246.
- Haddock, P. S., Artman, M., and Coetzee, W. A. (1998). Influence of postnatal changes in action potential duration on Na-Ca exchange in rabbit ventricular myocytes. *Pflugers Arch.* **435**, 789-795.
- Hagendorff, A., Schumacher, B., Kirchhoff, S., Luderitz, B., and Willecke, K. (1999). Conduction disturbances and increased atrial vulnerability in Connexin40-deficient mice analyzed by transesophageal stimulation. *Circulation* **99**, 1508-1515.

- Hagiwara, N., Irisawa, H., and Kameyama, M. (1988). Contribution of two types of calcium currents to the pacemaker potentials of rabbit sino-atrial node cells. *J.Physiol* **395**, 233-253.
- Hagiwara, S., Kusano, K., and Saito, N. (1961). Membrane changes of Onchidium nerve cells in potassium rich media. *J. Physiol* **291**, 217-232.
- Hagiwara, S. and Ohmori, H. (1983). Studies of single calcium channel currents in rat clonal pituitary cells. *J Physiol* **336**, 649-661.
- Hagiwara, S., Ozawa, S., and Sand, O. (1975). Voltage clamp analysis of two inward current mechanisms in the egg cell membrane of a starfish. *J Gen.Physiol* **65**, 617-644.
- Han, W., Chartier, D., Li, D., and Nattel, S. (2001b). Ionic remodeling of cardiac Purkinje cells by congestive heart failure. *Circulation* **104**, 2095-2100.
- Han, W., Wang, Z., and Nattel, S. (2000). A comparison of transient outward currents in canine cardiac Purkinje cells and ventricular myocytes. *Am.J.Physiol Heart Circ.Physiol* **279**, H466-H474.
- Han, W., Wang, Z., and Nattel, S. (2001a). Slow delayed rectifier current and repolarization in canine cardiac Purkinje cells. *Am.J.Physiol Heart Circ.Physiol* **280** , H1075-H1080.
- Hanck, D. A., Makielski, J. C., and Sheets, M. F. (1994). Kinetic effects of quaternary lidocaine block of cardiac sodium channels: a gating current study. *J.Gen.Physiol* **103**, 19-43.
- Hanck, D. A. and Sheets, M. F. (1992). Time-dependent changes in kinetics of Na⁺ current in single canine cardiac Purkinje cells. *Am.J.Physiol* **262**, H1197-H1207.
- Hancox, J. C., Levi, A. J., and Witchel, H. J. (1998). Time course and voltage dependence of expressed HERG current compared with native "rapid" delayed rectifier K current during the cardiac ventricular action potential. *Pflugers Arch.* **436**, 843-853.
- Hart, G. (1994). Cellular electrophysiology in cardiac hypertrophy and failure. *Cardiovasc.Res.* **28**, 933-946.
- Hartmann, H. A., Kirsch, G. E., Drewe, J. A., Tagliatela, M., Joho, R. H., and Brown, A. M. (1991). Exchange of conduction pathways between two related K⁺ channels. *Science* **251**, 942-944.
- Hauswirth, O., Noble, D., and Tsien, R. W. (1968). Adrenaline: mechanism of action on the pacemaker potential in cardiac Purkinje fibers. *Science* **162**, 916-917.
- Heath, B. M. and Terrar, D. A. (1996). Separation of the components of the delayed rectifier potassium current using selective blockers of IKr and IKs in guinea-pig isolated ventricular myocytes. *Exp.Physiol* **81**, 587-603.
- Heath, B. M. and Terrar, D. A. (2000). Protein kinase C enhances the rapidly activating delayed rectifier potassium current, IKr, through a reduction in C-type inactivation in guinea-pig ventricular myocytes. *J.Physiol* **522 Pt 3**, 391-402.

- Hecht, H.H., Hutter, O.F., and Lywood, D.W.** (1964). Voltage-current relation of short Purkinje fibers in sodium- deficient solution. *J. Physiol* **116**, 497-506.
- Heginbotham, L., Lu, Z., Abramson, T., and MacKinnon, R.** (1994). Mutations in the K⁺ channel signature sequence. *Biophys.J.* **66**, 1061-1067.
- Heidbuchel, H., Vereecke, J., and Carmeliet, E.** (1990). Three different potassium channels in human atrium. Contribution to the basal potassium conductance. *Circ.Res.* **66**, 1277-1286.
- Heinemann, S. H., Terlau, H., Stuhmer, W., Imoto, K., and Numa, S.** (1992). Calcium channel characteristics conferred on the sodium channel by single mutations. *Nature* **356**, 441-443.
- Hellmann, P., Winterhager, E., and Spray, D. C.** (1996). Properties of connexin40 gap junction channels endogenously expressed and exogenously overexpressed in human choriocarcinoma cell lines. *Pflugers Arch.* **432**, 501-509.
- Hess, P., Lansman, J. B., Nilius, B., and Tsien, R. W.** (1986). Calcium channel types in cardiac myocytes: modulation by dihydropyridines and beta-adrenergic stimulation. *J.Cardiovasc. Pharmacol.* **8 Suppl 9**, S11-S21.
- Himmel, H. M., Wettwer, E., Li, Q., and Ravens, U.** (1999). Four different components contribute to outward current in rat ventricular myocytes. *Am.J. Physiol* **277**, H107-H118.
- Hirano, Y., Fozzard, H. A., and January, C. T.** (1989). Characteristics of L- and T-type Ca²⁺ currents in canine cardiac Purkinje cells. *Am.J.Physiol* **256**, H1478-H1492.
- Hiraoka, M. and Kawano, S.** (1987). Mechanism of increased amplitude and duration of the plateau with sudden shortening of diastolic intervals in rabbit ventricular cells. *Circ.Res.* **60**, 14-26.
- Hiraoka, M. and Kawano, S.** (1989). Calcium-sensitive and insensitive transient outward current in rabbit ventricular myocytes. *J.Physiol* **410**, 187-212.
- Hiraoka, M., Kawano, S., Hirano, Y., and Furukawa, T.** (1998). Role of cardiac chloride currents in changes in action potential characteristics and arrhythmias. *Cardiovasc.Res.* **40**, 23-33.
- Ho, K., Nichols, C. G., Lederer, W. J., Lytton, J., Vassilev, P. M., Kanazirska, M. V., and Hebert, S. C.** (1993). Cloning and expression of an inwardly rectifying ATP-regulated potassium channel. *Nature* **362**, 31-38.
- Ho, W. K., Brown, H. F., and Noble, D.** (1994). High selectivity of the i(f) channel to Na⁺ and K⁺ in rabbit isolated sinoatrial node cells. *Pflugers Arch.* **426**, 68-74.
- Hodgkin A.L.** (1952). A quantitative description of membrane current and its application to conduction and excitation in nerve. *J. Physiol* **117**, 500-544.
- Holmgren, M., Shin, K. S., and Yellen, G.** (1998). The activation gate of a voltage-gated K⁺ channel can be trapped in the open state by an intersubunit metal bridge. *Neuron* **21**, 617-621.

- Hondeghem, L. M. and Snyders, D. J.** (1990). Class III antiarrhythmic agents have a lot of potential but a long way to go. Reduced effectiveness and dangers of reverse use dependence. *Circulation* **81**, 686-690.
- Honore, E., Attali, B., Romey, G., Heurteaux, C., Ricard, P., Lesage, F., Lazdunski, M., and Barhanin, J.** (1991). Cloning, expression, pharmacology and regulation of a delayed rectifier K⁺ channel in mouse heart. *EMBO J.* **10**, 2805-2811.
- Hoppe, U. C., Marban, E., and Johns, D. C.** (2000). Molecular dissection of cardiac repolarization by in vivo Kv4.3 gene transfer. *J.Clin.Invest* **105**, 1077-1084.
- Horie, M., Irisawa, H., and Noma, A.** (1987). Voltage-dependent magnesium block of adenosine-triphosphate-sensitive potassium channel in guinea-pig ventricular cells. *J.Physiol* **387**, 251-272.
- Hoshi, T., Zagotta, W. N., and Aldrich, R. W.** (1990). Biophysical and molecular mechanisms of Shaker potassium channel inactivation. *Science* **250**, 533-538.
- Houser, S. R., Piacentino, V., III, Mattiello, J., Weisser, J., and Gaughan, J. P.** (2000). Functional properties of failing human ventricular myocytes. *Trends Cardiovasc.Med.* **10**, 101-107.
- Howarth, F. C., Levi, A. J., and Hancox, J. C.** (1996). Characteristics of the delayed rectifier K current compared in myocytes isolated from the atrioventricular node and ventricle of the rabbit heart. *Pflugers Arch.* **431**, 713-722.
- Huang, B., El Sherif, T., Gidh-Jain, M., Qin, D., and el Sherif, N.** (2001). Alterations of sodium channel kinetics and gene expression in the postinfarction remodeled myocardium. *J.Cardiovasc.Electrophysiol.* **12**, 218-225.
- Huang, B., Qin, D., Deng, L., Boutjdir, M., and Sherif, N.** (2000). Reexpression of T-type Ca²⁺ channel gene and current in post-infarction remodeled rat left ventricle. *Cardiovasc.Res.* **46**, 442-449.
- Hullin, R., Singer-Lahat, D., Freichel, M., Biel, M., Dascal, N., Hofmann, F., and Flockerzi, V.** (1992). Calcium channel beta subunit heterogeneity: functional expression of cloned cDNA from heart, aorta and brain. *EMBO J.* **11**, 885-890.
- Hume, J. R. and Uehara, A.** (1985). Ionic basis of the different action potential configurations of single guinea-pig atrial and ventricular myocytes. *J.Physiol* **368**, 525-544.
- Hyer, J., Johansen, M., Prasad, A., Wessels, A., Kirby, M. L., Gourdie, R. G., and Mikawa, T.** (1999). Induction of Purkinje fiber differentiation by coronary arterialization. *Proc.Natl. Acad.Sci.U.S.A* **96**, 13214-13218.
- Inagaki, N., Gono, T., Clement, J. P., Namba, N., Inazawa, J., Gonzalez, G., Aguilar-Bryan, L., Seino, S., and Bryan, J.** (1995a). Reconstitution of IKATP: an inward rectifier subunit plus the sulfonylurea receptor. *Science* **270**, 1166-1170.

- Inagaki, N., Gono, T., Clement, J. P., Wang, C. Z., Aguilar-Bryan, L., Bryan, J., and Seino, S. (1996).** A family of sulfonylurea receptors determines the pharmacological properties of ATP-sensitive K⁺ channels. *Neuron* **16**, 1011-1017.
- Inagaki, N., Tsuura, Y., Namba, N., Masuda, K., Gono, T., Horie, M., Seino, Y., Mizuta, M., and Seino, S. (1995b).** Cloning and functional characterization of a novel ATP-sensitive potassium channel ubiquitously expressed in rat tissues, including pancreatic islets, pituitary, skeletal muscle, and heart. *J.Biol.Chem.* **270**, 5691-5694.
- Inoue, M. and Imanaga, I. (1993).** Masking of A-type K⁺ channel in guinea pig cardiac cells by extracellular Ca²⁺. *Am.J.Physiol* **264**, C1434-C1438.
- Irisawa, H., Brown, H. F., and Giles, W. (1993).** Cardiac pacemaking in the sinoatrial node. *Physiol Rev.* **73**, 197-227.
- Isacoff, E. Y., Jan, Y. N., and Jan, L. Y. (1991).** Putative receptor for the cytoplasmic inactivation gate in the Shaker K⁺ channel. *Nature* **353**, 86-90.
- Isenberg, G. (1976).** Cardiac Purkinje fibers: cesium as a tool to block inward rectifying potassium currents. *Pflugers Arch.* **365**, 99-106.
- Isenberg, G. and Trautwein, W. (1974).** The effect of dihydro-ouabain and lithium-ions on the outward current in cardiac Purkinje fibers. Evidence for electrogenicity of active transport. *Pflugers Arch.* **350**, 41-54.
- Isenberg, G., Vereecke, J., van der, H. G., and Carmeliet, E. (1983).** The shortening of the action potential by DNP in guinea-pig ventricular myocytes is mediated by an increase of a time-independent K conductance. *Pflugers Arch.* **397**, 251-259.
- Ishihara, K., Mitsuiye, T., Noma, A., and Takano, M. (1989).** The Mg²⁺ block and intrinsic gating underlying inward rectification of the K⁺ current in guinea-pig cardiac myocytes. *J.Physiol* **419**, 297-320.
- Ishii, T. M., Takano, M., Xie, L. H., Noma, A., and Ohmori, H. (1999).** Molecular characterization of the hyperpolarization-activated cation channel in rabbit heart sinoatrial node. *J.Biol.Chem.* **274**, 12835-12839.
- Isom, L. L. (2001).** Sodium channel beta subunits: anything but auxiliary. *Neuroscientist.* **7**, 42-54.
- Isom, L. L., De Jongh, K. S., Patton, D. E., Reber, B. F., Offord, J., Charbonneau, H., Walsh, K., Goldin, A. L., and Catterall, W. A. (1992).** Primary structure and functional expression of the beta 1 subunit of the rat brain sodium channel. *Science* **256**, 839-842.
- Isom, L. L., Ragsdale, D. S., De Jongh, K. S., Westenbroek, R. E., Reber, B. F., Scheuer, T., and Catterall, W. A. (1995).** Structure and function of the beta 2 subunit of brain sodium channels, a transmembrane glycoprotein with a CAM motif. *Cell* **83**, 433-442.
- Isomoto, S., Kondo, C., Yamada, M., Matsumoto, S., Higashiguchi, O., Horio, Y., Matsuzawa, Y., and Kurachi, Y. (1996).** A novel sulfonylurea receptor forms with BIR (Kir6.2) a smooth muscle type ATP-sensitive K⁺ channel. *J.Biol.Chem.* **271**, 24321-24324.

- Ito, H., Tung, R. T., Sugimoto, T., Kobayashi, I., Takahashi, K., Katada, T., Ui, M., and Kurachi, Y.** (1992). On the mechanism of G protein beta gamma subunit activation of the muscarinic K⁺ channel in guinea pig atrial cell membrane. Comparison with the ATP-sensitive K⁺ channel. *J.Gen.Physiol* **99**, 961-983.
- Iwamoto, T., Pan, Y., Wakabayashi, S., Imagawa, T., Yamanaka, H. I., and Shigekawa, M.** (1996). Phosphorylation-dependent regulation of cardiac Na⁺/Ca²⁺ exchanger via protein kinase C. *J.Biol.Chem.* **271**, 13609-13615.
- Iwamoto, T. and Shigekawa, M.** (1998). Differential inhibition of Na⁺/Ca²⁺ exchanger isoforms by divalent cations and isothiourea derivative. *Am.J.Physiol* **275**, C423-C430.
- Iwamoto, T., Wakabayashi, S., and Shigekawa, M.** (1995). Growth factor-induced phosphorylation and activation of aortic smooth muscle Na⁺/Ca²⁺ exchanger. *J.Biol.Chem.* **270**, 8996-9001.
- James, T. N.** (2001). The internodal pathways of the human heart. *Prog.Cardiovasc.Dis.* **43**, 495-535.
- January, C. T. and Moscucci, A.** (1992). Cellular mechanisms of early afterdepolarizations. *Ann.N.Y.Acad.Sci.* **644**, 23-32.
- Jiang, M., Cabo, C., Yao, J., Boyden, P. A., and Tseng, G.** (2000). Delayed rectifier K currents have reduced amplitudes and altered kinetics in myocytes from infarcted canine ventricle. *Cardiovasc.Res.* **48**, 34-43.
- Jiang, M., Tseng-Crank, J., and Tseng, G. N.** (1997). Suppression of slow delayed rectifier current by a truncated isoform of KvLQT1 cloned from normal human heart. *J.Biol.Chem.* **272**, 24109-24112.
- Jongsma, H. J. and Wilders, R.** (2000). Gap junctions in cardiovascular disease. *Circ.Res.* **86**, 1193-1197.
- Josephson, I. R., Sanchez-Chapula, J., and Brown, A. M.** (1984). Early outward current in rat single ventricular cells. *Circ.Res.* **54**, 157-162.
- Ju, Y., Gage, P. W., and Saint, D. A.** (1996). Tetrodotoxin-sensitive inactivation-resistant sodium channels in pacemaker cells influence heart rate. *Pflugers Arch.* **431**, 868-875.
- Ju, Y. K., Saint, D. A., and Gage, P. W.** (1994). Inactivation-resistant channels underlying the persistent sodium current in rat ventricular myocytes. *Proc.R.Soc. Lond B Biol.Sci.* **256**, 163-168.
- Jurkiewicz, N. K. and Sanguinetti, M. C.** (1993). Rate-dependent prolongation of cardiac action potentials by a methanesulfonanilide class III antiarrhythmic agent. Specific block of rapidly activating delayed rectifier K⁺ current by dofetilide. *Circ.Res.* **72**, 75-83.
- Jurkiewicz, N. K., Wang, J., Fermini, B., Sanguinetti, M. C., and Salata, J. J.** (1996). Mechanism of action potential prolongation by RP 58866 and its active enantiomer, terikalant. Block of the rapidly activating delayed rectifier K⁺ current, IKr. *Circulation* **94**, 2938-2946.

- Kaab, S., Dixon, J., Duc, J., Ashen, D., Nabauer, M., Beuckelmann, D. J., Steinbeck, G., McKinnon, D., and Tomaselli, G. F.** (1998). Molecular basis of transient outward potassium current downregulation in human heart failure: a decrease in Kv4.3 mRNA correlates with a reduction in current density. *Circulation* **98**, 1383-1393.
- Kaab, S., Nuss, H. B., Chiamvimonvat, N., O'Rourke, B., Pak, P. H., Kass, D. A., Marban, E., and Tomaselli, G. F.** (1996). Ionic mechanism of action potential prolongation in ventricular myocytes from dogs with pacing-induced heart failure. *Circ.Res.* **78**, 262-273.
- Kaczmarek, L. K. and Blumenthal, E. M.** (1997). Properties and regulation of the minK potassium channel protein. *Physiol Rev.* **77**, 627-641.
- Takei, M. and Noma, A.** (1984). Adenosine-5'-triphosphate-sensitive single potassium channel in the atrioventricular node cell of the rabbit heart. *J.Physiol* **352**, 265-284.
- Kameyama, M., Hofmann, F., and Trautwein, W.** (1985). On the mechanism of beta-adrenergic regulation of the Ca channel in the guinea-pig heart. *Pflugers Arch.* **405**, 285-293.
- Kaprielian, R., Wickenden, A. D., Kassiri, Z., Parker, T. G., Liu, P. P., and Backx, P. H.** (1999). Relationship between K⁺ channel down-regulation and [Ca²⁺]_i in rat ventricular myocytes following myocardial infarction. *J.Physiol* **517 (Pt 1)**, 229-245.
- Kaupp, U. B. and Seifert, R.** (2001). Molecular diversity of pacemaker ion channels. *Annu.Rev.Physiol* **63**, 235-257.
- Kawano, S. and Hiraoka, M.** (1991). Transient outward currents and action potential alterations in rabbit ventricular myocytes. *J.Mol.Cell Cardiol.* **23**, 681-693.
- Kawano, S., Hirayama, Y., and Hiraoka, M.** (1995). Activation mechanism of Ca(2⁺)-sensitive transient outward current in rabbit ventricular myocytes. *J.Physiol* **486 (Pt 3)**, 593-604.
- Keef, K. D., Hume, J. R., and Zhong, J.** (2001). Regulation of cardiac and smooth muscle Ca(2⁺) channels (Ca(V)1.2a,b) by protein kinases. *Am.J.Physiol Cell Physiol* **281**, C1743-C1756.
- Kenyon, J. L. and Gibbons, W. R.** (1979b). 4-Aminopyridine and the early outward current of sheep cardiac Purkinje fibers. *J.Gen.Physiol* **73**, 139-157.
- Kenyon, J. L. and Gibbons, W. R.** (1979a). Influence of chloride, potassium, and tetraethylammonium on the early outward current of sheep cardiac Purkinje fibers. *J.Gen.Physiol* **73**, 117-138.
- Kiehn, J., Lacerda, A. E., Wible, B., and Brown, A. M.** (1996). Molecular physiology and pharmacology of HERG. Single-channel currents and block by dofetilide. *Circulation* **94**, 2572-2579.
- Kieval, R. S., Bloch, R. J., Lindenmayer, G. E., Ambesi, A., and Lederer, W. J.** (1992). Immunofluorescence localization of the Na-Ca exchanger in heart cells. *Am.J.Physiol* **263**, C545-C550.
- Kimura, J., Miyamae, S., and Noma, A.** (1987). Identification of sodium-calcium exchange current in single ventricular cells of guinea-pig. *J.Physiol* **384**, 199-222.

- Kimura, J., Noma, A., and Irisawa, H.** (1986). Na-Ca exchange current in mammalian heart cells. *Nature* **319**, 596-597.
- Kiyosue, T. and Arita, M.** (1989). Late sodium current and its contribution to action potential configuration in guinea pig ventricular myocytes. *Circ.Res.* **64**, 389-397.
- Kleber, A. G.** (1999). Discontinuous propagation of the cardiac impulse and arrhythmogenesis. *J.Cardiovasc.Electrophysiol.* **10**, 1025-1027.
- Kleiman, R. B. and Houser, S. R.** (1989). Outward currents in normal and hypertrophied feline ventricular myocytes. *Am.J.Physiol* **256**, H1450-H1461.
- Klockner, U. and Isenberg, G.** (1994). Intracellular pH modulates the availability of vascular L-type Ca²⁺ channels. *J.Gen.Physiol* **103**, 647-663.
- Klugbauer, N., Lacinova, L., Marais, E., Hobom, M., and Hofmann, F.** (1999). Molecular diversity of the calcium channel alpha2delta subunit. *J.Neurosci.* **19**, 684-691.
- Kofuji, P., Lederer, W. J., and Schulze, D. H.** (1994). Mutually exclusive and cassette exons underlie alternatively spliced isoforms of the Na/Ca exchanger. *J.Biol. Chem.* **269**, 5145-5149.
- Koller, M. L., Riccio, M. L., and Gilmour, R. F., Jr.** (1998). Dynamic restitution of action potential duration during electrical alternans and ventricular fibrillation. *Am.J.Physiol* **275**, H1635-H1642.
- Komuro, I., Wenninger, K. E., Philipson, K. D., and Izumo, S.** (1992). Molecular cloning and characterization of the human cardiac Na⁺/Ca²⁺ exchanger cDNA. *Proc.Natl.Acad.Sci.U.S.A* **89**, 4769-4773.
- Konarzewska, H., Peeters, G. A., and Sanguinetti, M. C.** (1995). Repolarizing K⁺ currents in nonfailing human hearts. Similarities between right septal subendocardial and left subepicardial ventricular myocytes. *Circulation* **92**, 1179-1187.
- Kontis, K. J. and Goldin, A. L.** (1997). Sodium channel inactivation is altered by substitution of voltage sensor positive charges. *J.Gen.Physiol* **110**, 403-413.
- Kontis, K. J., Rounaghi, A., and Goldin, A. L.** (1997). Sodium channel activation gating is affected by substitutions of voltage sensor positive charges in all four domains. *J.Gen.Physiol* **110**, 391-401.
- Koumi, S., Backer, C. L., Arentzen, C. E., and Sato, R.** (1995c). beta-Adrenergic modulation of the inwardly rectifying potassium channel in isolated human ventricular myocytes. Alteration in channel response to beta-adrenergic stimulation in failing human hearts. *J.Clin.Invest* **96**, 2870-2881.
- Koumi, S. and Wasserstrom, J. A.** (1994). Acetylcholine-sensitive muscarinic K⁺ channels in mammalian ventricular myocytes. *Am.J.Physiol* **266**, H1812-H1821.
- Koumi, S., Wasserstrom, J. A., and Ten Eick, R. E.** (1995a). Beta-adrenergic and cholinergic modulation of inward rectifier K⁺ channel function and phosphorylation in guinea-pig ventricle. *J.Physiol* **486 (Pt 3)**, 661-678.

- Koumi, S., Wasserstrom, J. A., and Ten Eick, R. E. (1995b).** beta-adrenergic and cholinergic modulation of the inwardly rectifying K⁺ current in guinea-pig ventricular myocytes. *J.Physiol* **486** (Pt 3), 647-659.
- Kraev, A., Chumakov, I., and Carafoli, E. (1996).** Molecular biological studies of the cardiac sodium-calcium exchanger. *Ann.N.Y.Acad.Sci.* **779**, 103-109.
- Kramer, J. W., Post, M. A., Brown, A. M., and Kirsch, G. E. (1998).** Modulation of potassium channel gating by coexpression of Kv2.1 with regulatory Kv5.1 or Kv6.1 alpha-subunits. *Am.J.Physiol* **274**, C1501-C1510.
- Krapivinsky, G., Gordon, E. A., Wickman, K., Velimirovic, B., Krapivinsky, L., and Clapham, D. E. (1995).** The G-protein-gated atrial K⁺ channel IKACH is a heteromultimer of two inwardly rectifying K(+)-channel proteins. *Nature* **374**, 135-141.
- Kubo, Y., Baldwin, T. J., Jan, Y. N., and Jan, L. Y. (1993b).** Primary structure and functional expression of a mouse inward rectifier potassium channel. *Nature* **362**, 127-133.
- Kubo, Y., Reuveny, E., Slesinger, P. A., Jan, Y. N., and Jan, L. Y. (1993a).** Primary structure and functional expression of a rat G-protein-coupled muscarinic potassium channel. *Nature* **364**, 802-806.
- Kuboki, K., Ohkawa, S., Chida, K., Watanabe, C., Ueda, K., and Sugiura, M. (1999).** Torsades de pointes in a case of hypertrophic cardiomyopathy with special reference to the pathologic findings of the heart including the conduction system. *Jpn.Heart J.* **40**, 233-238.
- Kumar, N. M. and Gilula, N. B. (1996).** The gap junction communication channel. *Cell* **84**, 381-388.
- Kunze, D. L., Lacerda, A. E., Wilson, D. L., and Brown, A. M. (1985).** Cardiac Na currents and the inactivating, reopening, and waiting properties of single cardiac Na channels. *J.Gen.Physiol* **86**, 691-719.
- Kuo, H. C., Cheng, C. F., Clark, R. B., Lin, J. J., Lin, J. L., Hoshijima, M., Nguyen-Tran, V. T., Gu, Y., Ikeda, Y., Chu, P. H., Ross, J., Giles, W. R., and Chien, K. R. (2001).** A defect in the Kv channel-interacting protein 2 (KChIP2) gene leads to a complete loss of I(to) and confers susceptibility to ventricular tachycardia. *Cell* **107**, 801-813.
- Kupersmidt, S., Yang, T., Anderson, M. E., Wessels, A., Niswender, K. D., Magnuson, M. A., and Roden, D. M. (1999).** Replacement by homologous recombination of the minK gene with lacZ reveals restriction of minK expression to the mouse cardiac conduction system. *Circ.Res.* **84**, 146-152.
- Kupersmidt, S., Yang, T., and Roden, D. M. (1998).** Modulation of cardiac Na⁺ current phenotype by beta1-subunit expression. *Circ.Res.* **83**, 441-447.
- Kurachi, Y. (1995).** G protein regulation of cardiac muscarinic potassium channel. *Am.J.Physiol* **269**, C821-C830.

- Kurachi, Y., Nakajima, T., and Sugimoto, T.** (1986). On the mechanism of activation of muscarinic K⁺ channels by adenosine in isolated atrial cells: involvement of GTP-binding proteins. *Pflugers Arch.* **407**, 264-274.
- Kurachi, Y., Tung, R. T., Ito, H., and Nakajima, T.** (1992). G protein activation of cardiac muscarinic K⁺ channels. *Prog. Neurobiol.* **39**, 229-246.
- Kuryshv, Y. A., Gudz, T. I., Brown, A. M., and Wible, B. A.** (2000). KChAP as a chaperone for specific K(+) channels. *Am.J.Physiol Cell Physiol* **278**, C931-C941.
- Kusuoka, H., Camilion de Hurtado, M. C., and Marban, E.** (1993). Role of sodium/calcium exchange in the mechanism of myocardial stunning: protective effect of reperfusion with high sodium solution. *J.Am.Coll.Cardiol.* **21**, 240-248.
- Kwan, Y. W. and Qi, A. D.** (1997). Inhibition by extracellular ATP of L-type calcium channel currents in guinea-pig single sinoatrial nodal cells: involvement of protein kinase C. *Can.J.Cardiol.* **13**, 1202-1211.
- Lacerda, A. E., Kim, H. S., Ruth, P., Perez-Reyes, E., Flockerzi, V., Hofmann, F., Birnbaumer, L., and Brown, A. M.** (1991). Normalization of current kinetics by interaction between the alpha 1 and beta subunits of the skeletal muscle dihydropyridine-sensitive Ca²⁺ channel. *Nature* **352**, 527-530.
- Lai, L. P., Lin, J. L., Hwang, J. J., and Huang, S. K.** (1998). Entrance site of the slow conduction zone of verapamil-sensitive idiopathic left ventricular tachycardia: evidence supporting macroreentry in the Purkinje system. *J.Cardiovasc. Electrophysiol.* **9**, 184-190.
- Lamers, W. H., Geerts, W. J., and Moorman, A. F.** (1990). Distribution pattern of acetylcholinesterase in early embryonic chicken hearts. *Anat.Rec.* **228**, 297-305.
- Lamers, W. H., te, K. A., Los, J. A., and Moorman, A. F.** (1987). Acetylcholinesterase in prenatal rat heart: a marker for the early development of the cardiac conductive tissue?. *Anat.Rec.* **217**, 361-370.
- Lee, J. H., Daud, A. N., Cribbs, L. L., Lacerda, A. E., Pereverzev, A., Klockner, U., Schneider, T., and Perez-Reyes, E.** (1999). Cloning and expression of a novel member of the low voltage-activated T-type calcium channel family. *J.Neurosci.* **19**, 1912-1921.
- Lee, J. H. and Rosen, M. R.** (1994). Alpha 1-adrenergic receptor modulation of repolarization in canine Purkinje fibers. *J.Cardiovasc. Electrophysiol.* **5**, 232-240.
- Lee, J. K., Kodama, I., Honjo, H., Anno, T., Kamiya, K., and Toyama, J.** (1997). Stage-dependent changes in membrane currents in rats with monocrotaline-induced right ventricular hypertrophy. *Am.J.Physiol* **272**, H2833-H2842.
- Lee, K. S., Weeks, T. A., Kao, R. L., Akaike, N., and Brown, A. M.** (1979). Sodium current in single heart muscle cells. *Nature* **278**, 269-271.
- Lees-Miller, J. P., Duan, Y., Teng, G. Q., and Duff, H. J.** (2000). Molecular determinant of high-affinity dofetilide binding to HERG1 expressed in *Xenopus* oocytes: involvement of S6 sites. *Mol.Pharmacol.* **57**, 367-374.

- Lees-Miller, J. P., Kondo, C., Wang, L., and Duff, H. J.** (1997). Electrophysiological characterization of an alternatively processed ERG K⁺ channel in mouse and human hearts. *Circ.Res.* **81**, 719-726.
- Lesage, F., Attali, B., Lazdunski, M., and Barhanin, J.** (1992). ISK, a slowly activating voltage-sensitive K⁺ channel. Characterization of multiple cDNAs and gene organization in the mouse. *FEBS Lett.* **301**, 168-172.
- Leuranguer, V., Monteil, A., Bourinet, E., Dayanithi, G., and Nargeot, J.** (2000). T-type calcium currents in rat cardiomyocytes during postnatal development: contribution to hormone secretion. *Am.J.Physiol Heart Circ.Physiol* **279**, H2540-H2548.
- Li, D., Melnyk, P., Feng, J., Wang, Z., Petrecca, K., Shrier, A., and Nattel, S.** (2000). Effects of experimental heart failure on atrial cellular and ionic electrophysiology. *Circulation* **101**, 2631-2638.
- Li, D., Zhang, L., Kneller, J., and Nattel, S.** (2001). Potential ionic mechanism for repolarization differences between canine right and left atrium. *Circ.Res.* **88**, 1168-1175.
- Li, G. R., Feng, J., Wang, Z., Fermini, B., and Nattel, S.** (1996b). Adrenergic modulation of ultrarapid delayed rectifier K⁺ current in human atrial myocytes. *Circ.Res.* **78**, 903-915.
- Li, G. R., Feng, J., Yue, L., and Carrier, M.** (1998). Transmural heterogeneity of action potentials and I_{to1} in myocytes isolated from the human right ventricle. *Am.J.Physiol* **275**, H369-H377.
- Li, G. R., Feng, J., Yue, L., Carrier, M., and Nattel, S.** (1996a). Evidence for two components of delayed rectifier K⁺ current in human ventricular myocytes. *Circ.Res.* **78**, 689-696.
- Li, Z., Matsuoka, S., Hryshko, L. V., Nicoll, D. A., Bersohn, M. M., Burke, E. P., Lifton, R. P., and Philipson, K. D.** (1994). Cloning of the NCX2 isoform of the plasma membrane Na⁽⁺⁾-Ca²⁺ exchanger. *J.Biol.Chem.* **269**, 17434-17439.
- Light, P. E., Cordeiro, J. M., and French, R. J.** (1999). Identification and properties of ATP-sensitive potassium channels in myocytes from rabbit Purkinje fibres. *Cardiovasc.Res.* **44**, 356-369.
- Linck, B., Qiu, Z., He, Z., Tong, Q., Hilgemann, D. W., and Philipson, K. D.** (1998). Functional comparison of the three isoforms of the Na⁺/Ca²⁺ exchanger (NCX1, NCX2, NCX3). *Am.J.Physiol* **274**, C415-C423.
- Litovsky, S. H. and Antzelevitch, C.** (1988). Transient outward current prominent in canine ventricular epicardium but not endocardium. *Circ.Res.* **62**, 116-126.
- Litwin, S. E. and Bridge, J. H.** (1997). Enhanced Na⁽⁺⁾-Ca²⁺ exchange in the infarcted heart. Implications for excitation-contraction coupling. *Circ.Res.* **81**, 1083-1093.
- Liu, D. W. and Antzelevitch, C.** (1995). Characteristics of the delayed rectifier current (I_{Kr} and I_{Ks}) in canine ventricular epicardial, midmyocardial, and endocardial myocytes. A weaker I_{Ks} contributes to the longer action potential of the M cell. *Circ.Res.* **76**, 351-365.

- Liu, D. W., Gintant, G. A., and Antzelevitch, C.** (1993). Ionic bases for electrophysiological distinctions among epicardial, midmyocardial, and endocardial myocytes from the free wall of the canine left ventricle. *Circ.Res.* **72**, 671-687.
- Liu, Y., Jurman, M. E., and Yellen, G.** (1996a). Dynamic rearrangement of the outer mouth of a K⁺ channel during gating. *Neuron* **16**, 859-867.
- Liu, Y., Sato, T., O'Rourke, B., and Marban, E.** (1998). Mitochondrial ATP-dependent potassium channels: novel effectors of cardioprotection? *Circulation* **97**, 2463-2469.
- Liu, Y. M., DeFelice, L. J., and Mazzanti, M.** (1992). Na channels that remain open throughout the cardiac action potential plateau. *Biophys.J.* **63**, 654-662.
- Liu, Z. W., Zou, A. R., Demir, S. S., Clark, J. W., and Nathan, R. D.** (1996b). Characterization of a hyperpolarization-activated inward current in cultured pacemaker cells from the sinoatrial node. *J.Mol.Cell Cardiol.* **28**, 2523-2535.
- Llinas, R., Sugimori, M., Hillman, D. E., and Cherksey, B.** (1992). Distribution and functional significance of the P-type, voltage-dependent Ca²⁺ channels in the mammalian central nervous system. *Trends Neurosci.* **15**, 351-355.
- Llinas, R. and Yarom, Y.** (1981). Electrophysiology of mammalian inferior olivary neurones in vitro. Different types of voltage-dependent ionic conductances. *J Physiol* **315**, 549-567.
- Logothetis, D. E., Kurachi, Y., Galper, J., Neer, E. J., and Clapham, D. E.** (1987). The beta gamma subunits of GTP-binding proteins activate the muscarinic K⁺ channel in heart. *Nature* **325**, 321-326.
- Lombet, A. and Lazdunski, M.** (1984). Characterization, solubilization, affinity labeling and purification of the cardiac Na⁺ channel using Tityus toxin gamma. *Eur.J. Biochem.* **141**, 651-660.
- London, B., Trudeau, M. C., Newton, K. P., Beyer, A. K., Copeland, N. G., Gilbert, D. J., Jenkins, N. A., Satler, C. A., and Robertson, G. A.** (1997). Two isoforms of the mouse ether-a-go-go-related gene coassemble to form channels with properties similar to the rapidly activating component of the cardiac delayed rectifier K⁺ current. *Circ.Res.* **81**, 870-878.
- London, B., Wang, D. W., Hill, J. A., and Bennett, P. B.** (1998). The transient outward current in mice lacking the potassium channel gene Kvl.4. *J.Physiol* **509 (Pt 1)**, 171-182.
- Lopatin, A. N., Makhina, E. N., and Nichols, C. G.** (1994). Potassium channel block by cytoplasmic polyamines as the mechanism of intrinsic rectification. *Nature* **372**, 366-369.
- Lopez-Barneo, J., Hoshi, T., Heinemann, S. H., and Aldrich, R. W.** (1993). Effects of external cations and mutations in the pore region on C-type inactivation of Shaker potassium channels. *Receptors.Channels* **1**, 61-71.
- Low, W., Kasir, J., and Rahamimoff, H.** (1993). Cloning of the rat heart Na⁽⁺⁾-Ca²⁺ exchanger and its functional expression in HeLa cells. *FEBS Lett.* **316**, 63-67.

- Lu, T., Lee, H. C., Kabat, J. A., and Shibata, E. F. (1999).** Modulation of rat cardiac sodium channel by the stimulatory G protein alpha subunit. *J.Physiol* **518 (Pt 2)**, 371-384.
- Lu, Z., Kamiya, K., Opthof, T., Yasui, K., and Kodama, I. (2001).** Density and kinetics of I(Kr) and I(Ks) in guinea pig and rabbit ventricular myocytes explain different efficacy of I(Ks) blockade at high heart rate in guinea pig and rabbit: implications for arrhythmogenesis in humans. *Circulation* **104**, 951-956.
- Ludwig, A., Zong, X., Jeglitsch, M., Hofmann, F., and Biel, M. (1998).** A family of hyperpolarization-activated mammalian cation channels. *Nature* **393**, 587-591.
- Ludwig, A., Zong, X., Stieber, J., Hullin, R., Hofmann, F., and Biel, M. (1999).** Two pacemaker channels from human heart with profoundly different activation kinetics. *EMBO J.* **18**, 2323-2329.
- Lue, W. M. and Boyden, P. A. (1992).** Abnormal electrical properties of myocytes from chronically infarcted canine heart. Alterations in Vmax and the transient outward current. *Circulation* **85**, 1175-1188.
- Lupoglazoff, J. M., Cheav, T., Baroudi, G., Berthet, M., Denjoy, I., Cauchemez, B., Extramiana, F., Chahine, M., and Guicheney, P. (2001).** Homozygous SCN5A mutation in long-QT syndrome with functional two-to-one atrioventricular block. *Circ.Res.* **89**, E16-E21.
- MacKinnon, R. (1991).** New insights into the structure and function of potassium channels. *Curr.Opin.Neurobiol.* **1**, 14-19.
- MacKinnon, R. (1995).** Pore loops: an emerging theme in ion channel structure. *Neuron* **14**, 889-892.
- MacKinnon, R. and Doyle, D. A. (1997).** Prokaryotes offer hope for potassium channel structural studies. *Nat.Struct.Biol.* **4**, 877-879.
- MacKinnon, R., Reinhart, P. H., and White, M. M. (1988).** Charybdotoxin block of Shaker K⁺ channels suggests that different types of K⁺ channels share common structural features. *Neuron* **1**, 997-1001.
- MacKinnon, R. and Yellen, G. (1990).** Mutations affecting TEA blockade and ion permeation in voltage- activated K⁺ channels. *Science* **250**, 276-279.
- Maier, S.K., Westenbroek, R.E., Schenkman, K.A., Feigl, E.O., Scheuer, T., and Catterall, W.A. (2002).** An unexpected role for brain-type sodium channels in coupling of cell surface depolarization to contraction in the heart. *Proc.Natl.Acad.Sci. U.S.A.* **19**, 99(6):4073-8.
- Majumder, K., De Biasi, M., Wang, Z., and Wible, B. A. (1995).** Molecular cloning and functional expression of a novel potassium channel beta-subunit from human atrium. *FEBS Lett.* **361**, 13-16.
- Makielski, J. C., Limberis, J. T., Chang, S. Y., Fan, Z., and Kyle, J. W. (1996).** Coexpression of beta 1 with cardiac sodium channel alpha subunits in oocytes decreases lidocaine block. *Mol.Pharmacol.* **49**, 30-39.

- Makielski, J. C., Sheets, M. F., Hanck, D. A., January, C. T., and Fozzard, H. A. (1987).** Sodium current in voltage clamped internally perfused canine cardiac Purkinje cells. *Biophys.J.* **52**, 1-11.
- Makita, N., Bennett, P. B., Jr., and George, A. L., Jr. (1994).** Voltage-gated Na⁺ channel beta 1 subunit mRNA expressed in adult human skeletal muscle, heart, and brain is encoded by a single gene. *J.Biol.Chem.* **269**, 7571-7578.
- Malhotra, J. D., Kazen-Gillespie, K., Hortsch, M., and Isom, L. L. (2000).** Sodium channel beta subunits mediate homophilic cell adhesion and recruit ankyrin to points of cell-cell contact. *J.Biol.Chem.* **275**, 11383-11388.
- Marban, E. (1999).** Heart failure: the electrophysiologic connection. *J.Cardiovasc. Electrophysiol.* **10**, 1425-1428.
- Marban, E. (2002).** Cardiac channelopathies. *Nature* **415**, 213-218.
- Marban, E., Yamagishi, T., and Tomaselli, G. F. (1998).** Structure and function of voltage-gated sodium channels. *J.Physiol* **508 (Pt 3)**, 647-657.
- Markowitz, S. M., Stein, K. M., Engelstein, E. D., and Lerman, B. B. (1995).** AV nodal-His-Purkinje reentry: a novel form of tachycardia. *J. Cardiovasc. Electrophysiol.* **6**, 400-409.
- Maruoka, F., Nakashima, Y., Takano, M., Ono, K., and Noma, A. (1994).** Cation-dependent gating of the hyperpolarization-activated cation current in the rabbit sino-atrial node cells. *J.Physiol* **477 (Pt 3)**, 423-435.
- Mathias, R.T., Eisenberg, B.R., Datyner, N.B., Gintant, G.A., and Cohen, I.S. (1985).** Impedance and morphology of isolated canine cardiac Purkinje myocytes: comparison with intact strand preparations. *Biophys J.* **47(2, Pt. 2)**:499a. (Abstr.).
- Matsuda, H. (1988).** Open-state substructure of inwardly rectifying potassium channels revealed by magnesium block in guinea-pig heart cells. *J.Physiol* **397**, 237-258.
- Matsuda, H. (1993).** Effects of internal and external Na⁺ ions on inwardly rectifying K⁺ channels in guinea-pig ventricular cells. *J.Physiol* **460**, 311-326.
- Matsuda, H. and Cruz, J. S. (1993).** Voltage-dependent block by internal Ca²⁺ ions of inwardly rectifying K⁺ channels in guinea-pig ventricular cells. *J.Physiol* **470**, 295-311.
- Matsuda, H., Saigusa, A., and Irisawa, H. (1987).** Ohmic conductance through the inwardly rectifying K channel and blocking by internal Mg²⁺. *Nature* **325**, 156-159.
- Matsuda, J. J., Lee, H., and Shibata, E. F. (1992).** Enhancement of rabbit cardiac sodium channels by beta-adrenergic stimulation. *Circ.Res.* **70**, 199-207.
- Mays, D. J., Foose, J. M., Philipson, L. H., and Tamkun, M. M. (1995).** Localization of the Kv1.5 K⁺ channel protein in explanted cardiac tissue. *J.Clin.Invest* **96**, 282-292.
- McAllister, R. E., Noble, D., and Tsien, R. W. (1975).** Reconstruction of the electrical activity of cardiac Purkinje fibres. *J.Physiol* **251**, 1-59.

- McCabe, C. F., Gourdie, R. G., Thompson, R. P., and Cole, G. J.** (1995). Developmentally regulated neural protein EAP-300 is expressed by myocardium and cardiac neural crest during chick embryogenesis. *Dev.Dyn.* **203**, 51-60.
- McClatchey, A. I., Cannon, S. C., Slaughter, S. A., and Gusella, J. F.** (1993). The cloning and expression of a sodium channel beta 1-subunit cDNA from human brain. *Hum.Mol.Genet.* **2**, 745-749.
- McDonald, R. L., Colyer, J., and Harrison, S. M.** (2000). Quantitative analysis of Na⁺-Ca²⁺ exchanger expression in guinea-pig heart. *Eur.J.Biochem.* **267**, 5142-5148.
- McDonald, T. V., Yu, Z., Ming, Z., Palma, E., Meyers, M. B., Wang, K. W., Goldstein, S. A., and Fishman, G. I.** (1997). A minK-HERG complex regulates the cardiac potassium current I(Kr). *Nature* **388**, 289-292.
- McHugh, D., Sharp, E. M., Scheuer, T., and Catterall, W. A.** (2000). Inhibition of cardiac L-type calcium channels by protein kinase C phosphorylation of two sites in the N-terminal domain. *Proc.Natl.Acad.Sci.U.S.A* **97**, 12334-12338.
- McKinnon, D.** (1999). Molecular identity of Ito: Kv1.4 redux. *Circ.Res.* **84**, 620-622.
- McRory, J. E., Santi, C. M., Hamming, K. S., Mezeyova, J., Sutton, K. G., Baillie, D. L., Stea, A., and Snutch, T. P.** (2001). Molecular and functional characterization of a family of rat brain T-type calcium channels. *J.Biol.Chem.* **276**, 3999-4011.
- Melnyk, P., Zhang, L., Shrier, A., and Nattel, S.** (2002). Differential distribution of Kir2.1 and Kir2.3 subunits in canine atrium and ventricle. *Am.J Physiol Heart Circ.Physiol* **283**, H1123-H1133.
- Mikami, A., Imoto, K., Tanabe, T., Niidome, T., Mori, Y., Takeshima, H., Narumiya, S., and Numa, S.** (1989). Primary structure and functional expression of the cardiac dihydropyridine-sensitive calcium channel. *Nature* **340**, 230-233.
- Mitcheson, J. S. and Hancox, J. C.** (1997). Modulation by mexiletine of action potentials, L-type Ca current and delayed rectifier K current recorded from isolated rabbit atrioventricular nodal myocytes. *Pflugers Arch.* **434**, 855-858.
- Mitcheson, J. S. and Sanguinetti, M. C.** (1999). Biophysical properties and molecular basis of cardiac rapid and slow delayed rectifier potassium channels. *Cell Physiol Biochem.* **9**, 201-216.
- Mitra, R. and Morad, M.** (1986). Two types of calcium channels in guinea pig ventricular myocytes. *Proc.Natl.Acad.Sci.U.S.A* **83**, 5340-5344.
- Mitrovic, N., George, A. L., Jr., and Horn, R.** (1998). Independent versus coupled inactivation in sodium channels. Role of the domain 2 S4 segment. *J.Gen.Physiol* **111**, 451-462.
- Mitsuiye, T. and Noma, A.** (1992). Exponential activation of the cardiac Na⁺ current in single guinea-pig ventricular cells. *J.Physiol* **453**, 261-277.

- Mitterdorfer, J., Froschmayr, M., Grabner, M., Moebius, F. F., Glossmann, H., and Striessnig, J. (1996). Identification of PK-A phosphorylation sites in the carboxyl terminus of L-type calcium channel alpha 1 subunits. *Biochemistry* **35**, 9400-9406.
- Moalic, J. M., Charlemagne, D., Mansier, P., Chevalier, B., and Swynghedauw, B. (1993). Cardiac hypertrophy and failure--a disease of adaptation. Modifications in membrane proteins provide a molecular basis for arrhythmogenicity. *Circulation* **87**, IV21-IV26.
- Molkentin, J. D. and Dorn II, G. W. (2001). Cytoplasmic signaling pathways that regulate cardiac hypertrophy. *Annu.Rev.Physiol* **63**, 391-426.
- Moorman, J. R., Kirsch, G. E., Lacerda, A. E., and Brown, A. M. (1989). Angiotensin II modulates cardiac Na⁺ channels in neonatal rat. *Circ.Res.* **65**, 1804-1809.
- Morales, M. J., Castellino, R. C., Crews, A. L., Rasmusson, R. L., and Strauss, H. C. (1995). A novel beta subunit increases rate of inactivation of specific voltage-gated potassium channel alpha subunits. *J.Biol.Chem.* **270**, 6272-6277.
- Moreno, A. P., Rook, M. B., Fishman, G. I., and Spray, D. C. (1994a). Gap junction channels: distinct voltage-sensitive and -insensitive conductance states. *Biophys.J.* **67**, 113-119.
- Moreno, A. P., Saez, J. C., Fishman, G. I., and Spray, D. C. (1994b). Human connexin43 gap junction channels. Regulation of unitary conductances by phosphorylation. *Circ.Res.* **74**, 1050-1057.
- Morgan, K., Stevens, E. B., Shah, B., Cox, P. J., Dixon, A. K., Lee, K., Pinnock, R. D., Hughes, J., Richardson, P. J., Mizuguchi, K., and Jackson, A. P. (2000). beta 3: an additional auxiliary subunit of the voltage-sensitive sodium channel that modulates channel gating with distinct kinetics. *Proc.Natl.Acad.Sci.U.S.A* **97**, 2308-2313.
- Morishige, K., Takahashi, N., Findlay, I., Koyama, H., Zanelli, J. S., Peterson, C., Jenkins, N. A., Copeland, N. G., Mori, N., and Kurachi, Y. (1993). Molecular cloning, functional expression and localization of an inward rectifier potassium channel in the mouse brain. *FEBS Lett.* **336**, 375-380.
- Moroni, A., Barbuti, A., Altomare, C., Viscomi, C., Morgan, J., Baruscotti, M., and DiFrancesco, D. (2000). Kinetic and ionic properties of the human HCN2 pacemaker channel. *Pflugers Arch.* **439**, 618-626.
- Mounsey, J. P. and DiMarco, J. P. (2000). Cardiovascular drugs. Dofetilide. *Circulation* **102**, 2665-2670.
- Mukherjee, R. and Spinale, F. G. (1998). L-type calcium channel abundance and function with cardiac hypertrophy and failure: a review. *J.Mol.Cell Cardiol.* **30**, 1899-1916.
- Murphy, B. J., Rogers, J., Perdichizzi, A. P., Colvin, A. A., and Catterall, W. A. (1996). cAMP-dependent phosphorylation of two sites in the alpha subunit of the cardiac sodium channel. *J.Biol.Chem.* **271**, 28837-28843.

- Murray, K. T., Fahrig, S. A., Deal, K. K., Po, S. S., Hu, N. N., Snyders, D. J., Tamkun, M. M., and Bennett, P. B.** (1994). Modulation of an inactivating human cardiac K⁺ channel by protein kinase C. *Circ.Res.* **75**, 999-1005.
- Murray, K. T., Hu, N. N., Daw, J. R., Shin, H. G., Watson, M. T., Mashburn, A. B., and George, A. L., Jr.** (1997). Functional effects of protein kinase C activation on the human cardiac Na⁺ channel. *Circ.Res.* **80**, 370-376.
- Musil, L. S. and Goodenough, D. A.** (1991). Biochemical analysis of connexin43 intracellular transport, phosphorylation, and assembly into gap junctional plaques. *J Cell Biol.* **115**, 1357-1374.
- Nabauer, M., Beuckelmann, D. J., and Erdmann, E.** (1993). Characteristics of transient outward current in human ventricular myocytes from patients with terminal heart failure. *Circ.Res.* **73**, 386-394.
- Nabauer, M., Beuckelmann, D. J., Uberfuhr, P., and Steinbeck, G.** (1996). Regional differences in current density and rate-dependent properties of the transient outward current in subepicardial and subendocardial myocytes of human left ventricle. *Circulation* **93**, 168-177.
- Nabauer, M. and Kaab, S.** (1998). Potassium channel down-regulation in heart failure. *Cardiovasc.Res.* **37**, 324-334.
- Nakagawa, M., Thompson, R. P., Terracio, L., and Borg, T. K.** (1993). Developmental anatomy of HNK-1 immunoreactivity in the embryonic rat heart: co-distribution with early conduction tissue. *Anat.Embryol.(Berl)* **187**, 445-460.
- Nakamura, T. Y., Artman, M., Rudy, B., and Coetzee, W. A.** (1998). Inhibition of rat ventricular IK1 with antisense oligonucleotides targeted to Kir2.1 mRNA. *Am.J.Physiol* **274**, H892-H900.
- Nakamura, T. Y., Coetzee, W. A., Vega-Saenz, D. M., Artman, M., and Rudy, B.** (1997). Modulation of Kv4 channels, key components of rat ventricular transient outward K⁺ current, by PKC. *Am.J.Physiol* **273**, H1775-H1786.
- Nakamura, T. Y., Pountney, D. J., Ozaita, A., Nandi, S., Ueda, S., Rudy, B., and Coetzee, W. A.** (2001). A role for frequenin, a Ca²⁺-binding protein, as a regulator of Kv4 K⁺- currents. *Proc.Natl.Acad.Sci.U.S.A* **98**, 12808-12813.
- Nakasaki, Y., Iwamoto, T., Hanada, H., Imagawa, T., and Shigekawa, M.** (1993). Cloning of the rat aortic smooth muscle Na⁺/Ca²⁺ exchanger and tissue- specific expression of isoforms. *J.Biochem.(Tokyo)* **114**, 528-534.
- Nakayama, T. and Fozzard, H. A.** (1988). Adrenergic modulation of the transient outward current in isolated canine Purkinje cells. *Circ.Res.* **62**, 162-172.
- Nakayama, T. and Irisawa, H.** (1985). Transient outward current carried by potassium and sodium in quiescent atrioventricular node cells of rabbits. *Circ.Res.* **57**, 65-73.
- Nakayama, T., Palfrey, C., and Fozzard, H. A.** (1989). Modulation of the cardiac transient outward current by catecholamines. *J.Mol.Cell Cardiol.* **21 Suppl 1**, 109-118.

- Nargeot, J., Lory, P., and Richard, S.** (1997). Molecular basis of the diversity of calcium channels in cardiovascular tissues. *Eur.Heart J.* **18 Suppl A**, A15-A26.
- Nattel, S. and Quantz, M. A.** (1988). Pharmacological response of quinidine induced early afterdepolarisations in canine cardiac Purkinje fibres: insights into underlying ionic mechanisms. *Cardiovasc.Res.* **22**, 808-817.
- Neher, E. and Sakmann, B.** (1976). Single-channel currents recorded from membrane of denervated frog muscle fibres. *Nature* **260**, 799-802.
- Nerbonne, J. M.** (2000). Molecular basis of functional voltage-gated K⁺ channel diversity in the mammalian myocardium. *J.Physiol* **525 Pt 2**, 285-298.
- Nichols, C. G. and Lederer, W. J.** (1991). The mechanism of KATP channel inhibition by ATP. *J.Gen.Physiol* **97**, 1095-1098.
- Nichols, C. G. and Lopatin, A. N.** (1997). Inward rectifier potassium channels. *Annu.Rev.Physiol* **59**, 171-191.
- Nichols, C. G., Ripoll, C., and Lederer, W. J.** (1991). ATP-sensitive potassium channel modulation of the guinea pig ventricular action potential and contraction. *Circ.Res.* **68**, 280-287.
- Nicoll, D. A., Longoni, S., and Philipson, K. D.** (1990). Molecular cloning and functional expression of the cardiac sarcolemmal Na⁽⁺⁾-Ca²⁺ exchanger. *Science* **250**, 562-565.
- Nicoll, D. A., Quednau, B. D., Qui, Z., Xia, Y. R., Lusic, A. J., and Philipson, K. D.** (1996). Cloning of a third mammalian Na⁺-Ca²⁺ exchanger, NCX3. *J.Biol.Chem.* **271**, 24914-24921.
- Nilius, B., Hess, P., Lansman, J. B., and Tsien, R. W.** (1985). A novel type of cardiac calcium channel in ventricular cells. *Nature* **316**, 443-446.
- Nitta, J., Furukawa, T., Marumo, F., Sawanobori, T., and Hiraoka, M.** (1994). Subcellular mechanism for Ca⁽²⁺⁾-dependent enhancement of delayed rectifier K⁺ current in isolated membrane patches of guinea pig ventricular myocytes. *Circ.Res.* **74**, 96-104.
- Noble, D., LeGuennec, J. Y., and Winslow, R.** (1996). Functional roles of sodium-calcium exchange in normal and abnormal cardiac rhythm. *Ann.N.Y.Acad.Sci.* **779**, 480-488.
- Noble, D. and Tsien, R. W.** (1968). The kinetics and rectifier properties of the slow potassium current in cardiac Purkinje fibres. *J.Physiol* **195**, 185-214.
- Noble, D. and Tsien, R. W.** (1969). Outward membrane currents activated in the plateau range of potentials in cardiac Purkinje fibres. *J.Physiol* **200**, 205-231.
- Noda, M., Ikeda, T., Suzuki, H., Takeshima, H., Takahashi, T., Kuno, M., and Numa, S.** (1986). Expression of functional sodium channels from cloned cDNA. *Nature* **322**, 826-828.
- Noda, M., Shimizu, S., Tanabe, T., Takai, T., Kayano, T., Ikeda, T., Takahashi, H., Nakayama, H., Kanaoka, Y., Minamino, N., and .** (1984). Primary structure of Electrophorus electricus sodium channel deduced from cDNA sequence. *Nature* **312**, 121-127.

- Noma, A.** (1983). ATP-regulated K⁺ channels in cardiac muscle. *Nature* **305**, 147-148.
- Noma, A. and Irisawa, H.** (1976a). A time- and voltage-dependent potassium current in the rabbit sinoatrial node cell. *Pflugers Arch.* **366**, 251-258.
- Noma, A. and Irisawa, H.** (1976b). Membrane currents in the rabbit sinoatrial node cell as studied by the double microelectrode method. *Pflugers Arch.* **364**, 45-52.
- Noma, A., Nakayama, T., Kurachi, Y., and Irisawa, H.** (1984). Resting K conductances in pacemaker and non-pacemaker heart cells of the rabbit. *Jpn.J.Physiol* **34**, 245-254.
- Noma, A., Peper, K., and Trautwein, W.** (1979). Acetylcholine-induced potassium current fluctuations in the rabbit sino-atrial node. *Pflugers Arch.* **381**, 255-262.
- Noma, A. and Trautwein, W.** (1978). Relaxation of the ACh-induced potassium current in the rabbit sinoatrial node cell. *Pflugers Arch.* **377**, 193-200.
- Nowycky, M. C., Fox, A. P., and Tsien, R. W.** (1985). Three types of neuronal calcium channel with different calcium agonist sensitivity. *Nature* **316**, 440-443.
- Nuss, H. B., Chiamvimonvat, N., Perez-Garcia, M. T., Tomaselli, G. F., and Marban, E.** (1995). Functional association of the beta 1 subunit with human cardiac (hH1) and rat skeletal muscle (mu 1) sodium channel alpha subunits expressed in *Xenopus* oocytes. *J.Gen.Physiol* **106**, 1171-1191.
- Nuss, H. B. and Houser, S. R.** (1993). T-type Ca²⁺ current is expressed in hypertrophied adult feline left ventricular myocytes. *Circ.Res.* **73**, 777-782.
- Nuss, H. B., Kambouris, N. G., Marban, E., Tomaselli, G. F., and Balsler, J. R.** (2000). Isoform-specific lidocaine block of sodium channels explained by differences in gating. *Biophys.J.* **78**, 200-210.
- O'Rourke, B., Kass, D. A., Tomaselli, G. F., Kaab, S., Tunin, R., and Marban, E.** (1999). Mechanisms of altered excitation-contraction coupling in canine tachycardia-induced heart failure, I: experimental studies. *Circ.Res.* **84**, 562-570.
- Ohya, S., Morohashi, Y., Muraki, K., Tomita, T., Watanabe, M., Iwatsubo, T., and Imaizumi, Y.** (2001). Molecular cloning and expression of the novel splice variants of K(+) channel-interacting protein 2. *Biochem.Biophys.Res.Comm.* **282**, 96-102.
- Ono, K., Fozzard, H. A., and Hanck, D. A.** (1993). Mechanism of cAMP-dependent modulation of cardiac sodium channel current kinetics. *Circ.Res.* **72**, 807-815.
- Ono, K. and Ito, H.** (1995). Role of rapidly activating delayed rectifier K⁺ current in sinoatrial node pacemaker activity. *Am.J.Physiol* **269**, H453-H462.
- Oosthoek, P. W., Viragh, S., Lamers, W. H., and Moorman, A. F.** (1993a). Immunohistochemical delineation of the conduction system. II: The atrioventricular node and Purkinje fibers. *Circ.Res.* **73**, 482-491.

- Oosthoek, P. W., Viragh, S., Mayen, A. E., van Kempen, M. J., Lamers, W. H., and Moorman, A. F.** (1993b). Immunohistochemical delineation of the conduction system. I: The sinoatrial node. *Circ.Res.* **73**, 473-481.
- Oshima, T., Ikeda, K., Furukawa, M., and Takasaka, T.** (1997). Alternatively spliced isoforms of the Na⁺/Ca²⁺ exchanger in the guinea pig cochlea. *Biochem.Biophys. Res.Commun.* **233**, 737-741.
- Osterrieder, W., Brum, G., Hescheler, J., Trautwein, W., Flockerzi, V., and Hofmann, F.** (1982). Injection of subunits of cyclic AMP-dependent protein kinase into cardiac myocytes modulates Ca²⁺ current. *Nature* **298**, 576-578.
- Oudit, G. Y., Kassiri, Z., Sah, R., Ramirez, R. J., Zobel, C., and Backx, P. H.** (2001). The molecular physiology of the cardiac transient outward potassium current (I_{to}) in normal and diseased myocardium. *J.Mol.Cell Cardiol.* **33**, 851-872.
- Panyi, G., Sheng, Z., and Deutsch, C.** (1995). C-type inactivation of a voltage-gated K⁺ channel occurs by a cooperative mechanism. *Biophys.J.* **69**, 896-903.
- Papazian, D. M., Schwarz, T. L., Tempel, B. L., Jan, Y. N., and Jan, L. Y.** (1987). Cloning of genomic and complementary DNA from Shaker, a putative potassium channel gene from *Drosophila*. *Science* **237**, 749-753.
- Parker, C., Li, Q., and Fedida, D.** (1999). Non-specific action of methoxamine on I_{to}, and the cloned channels hKv 1.5 and Kv 4.2. *Br.J.Pharmacol.* **126**, 595-606.
- Pascual, J. M., Shieh, C. C., Kirsch, G. E., and Brown, A. M.** (1995). Multiple residues specify external tetraethylammonium blockade in voltage-gated potassium channels. *Biophys.J.* **69**, 428-434.
- Patlak, J. B. and Ortiz, M.** (1985). Slow currents through single sodium channels of the adult rat heart. *J.Gen.Physiol* **86**, 89-104.
- Patten, B.M.** (1956). The development of the sinoventricular conduction system. *Uni. Mich. Med.Bull.* **22**, 1-21.
- Patterson, E., Scherlag, B. J., and Lazzara, R.** (1993). Rapid inward current in ischemically-injured subepicardial myocytes bordering myocardial infarction. *J.Cardiovasc.Electrophysiol.* **4**, 9-22.
- Patton, D. E., West, J. W., Catterall, W. A., and Goldin, A. L.** (1992). Amino acid residues required for fast Na⁽⁺⁾-channel inactivation: charge neutralizations and deletions in the III-IV linker. *Proc.Natl.Acad.Sci.U.S.A* **89**, 10905-10909.
- Peper, K. and Trautwein, W.** (1969). A note on the pacemaker current in Purkinje fibers. *Pflugers Arch.* **309**, 356-361.
- Perchenet, L., Hinde, A. K., Patel, K. C., Hancox, J. C., and Levi, A. J.** (2000). Stimulation of Na/Ca exchange by the beta-adrenergic/protein kinase A pathway in guinea-pig ventricular myocytes at 37 degrees C. *Pflugers Arch.* **439**, 822-828.

- Pereon, Y., Demolombe, S., Baro, I., Drouin, E., Charpentier, F., and Escande, D. (2000).** Differential expression of KvLQT1 isoforms across the human ventricular wall. *Am.J.Physiol Heart Circ.Physiol* **278**, H1908-H1915.
- Perets, T., Blumenstein, Y., Shistik, E., Lotan, I., and Dascal, N. (1996).** A potential site of functional modulation by protein kinase A in the cardiac Ca²⁺ channel alpha 1C subunit. *FEBS Lett.* **384**, 189-192.
- Perez-Reyes, E., Cribbs, L. L., Daud, A., Lacerda, A. E., Barclay, J., Williamson, M. P., Fox, M., Rees, M., and Lee, J. H. (1998).** Molecular characterization of a neuronal low-voltage-activated T-type calcium channel. *Nature* **391**, 896-900.
- Perez-Reyes, E., Yuan, W., Wei, X., and Bers, D. M. (1994).** Regulation of the cloned L-type cardiac calcium channel by cyclic-AMP- dependent protein kinase. *FEBS Lett.* **342**, 119-123.
- Peters, N. S., Coromilas, J., Severs, N. J., and Wit, A. L. (1997).** Disturbed connexin43 gap junction distribution correlates with the location of reentrant circuits in the epicardial border zone of healing canine infarcts that cause ventricular tachycardia. *Circulation* **95**, 988-996.
- Petersen, K. R. and Nerbonne, J. M. (1999).** Expression environment determines K⁺ current properties: Kv1 and Kv4 alpha-subunit-induced K⁺ currents in mammalian cell lines and cardiac myocytes. *Pflugers Arch.* **437**, 381-392.
- Petrecca, K., Amellal, F., Laird, D. W., Cohen, S. A., and Shrier, A. (1997).** Sodium channel distribution within the rabbit atrioventricular node as analysed by confocal microscopy. *J.Physiol* **501 (Pt 2)**, 263-274.
- Petrecca, K., Miller, D. M., and Shrier, A. (2000).** Localization and enhanced current density of the Kv4.2 potassium channel by interaction with the actin-binding protein filamin. *J.Neurosci.* **20**, 8736-8744.
- Pfaffinger, P. J., Martin, J. M., Hunter, D. D., Nathanson, N. M., and Hille, B. (1985).** GTP-binding proteins couple cardiac muscarinic receptors to a K channel. *Nature* **317**, 536-538.
- Philipson, K. D. and Nicoll, D. A. (2000).** Sodium-calcium exchange: a molecular perspective. *Annu.Rev.Physiol* **62**, 111-133.
- Pichler, M., Cassidy, T. N., Reimer, D., Haase, H., Kraus, R., Ostler, D., and Striessnig, J. (1997).** Beta subunit heterogeneity in neuronal L-type Ca²⁺ channels. *J.Biol.Chem.* **272**, 13877-13882.
- Pike, M. M., Kitakaze, M., and Marban, E. (1990).** ²³Na-NMR measurements of intracellular sodium in intact perfused ferret hearts during ischemia and reperfusion. *Am.J.Physiol* **259**, H1767-H1773.
- Pinto, J. M. and Boyden, P. A. (1998).** Reduced inward rectifying and increased E-4031-sensitive K⁺ current density in arrhythmogenic subendocardial purkinje myocytes from the infarcted heart. *J.Cardiovasc.Electrophysiol.* **9**, 299-311.

- Pogwizd, S. M., Schlotthauer, K., Li, L., Yuan, W., and Bers, D. M.** (2001). Arrhythmogenesis and contractile dysfunction in heart failure: Roles of sodium-calcium exchange, inward rectifier potassium current, and residual beta-adrenergic responsiveness. *Circ.Res.* **88**, 1159-1167.
- Pond, A. L., Scheve, B. K., Benedict, A. T., Petrecca, K., Van Wagoner, D. R., Shrier, A., and Nerbonne, J. M.** (2000). Expression of distinct ERG proteins in rat, mouse, and human heart. Relation to functional I(Kr) channels. *J.Biol.Chem.* **275**, 5997-6006.
- Powell, T. and Twist, V. W.** (1976). A rapid technique for the isolation and purification of adult cardiac muscle cells having respiratory control and a tolerance to calcium. *Biochem. Biophys.Res.Comm.* **72**, 327-333.
- Priori, S. G., Mantica, M., Napolitano, C., and Schwartz, P. J.** (1990). Early afterdepolarizations induced in vivo by reperfusion of ischemic myocardium. A possible mechanism for reperfusion arrhythmias. *Circulation* **81**, 1911-1920.
- Pu, J. and Boyden, P. A.** (1997). Alterations of Na⁺ currents in myocytes from epicardial border zone of the infarcted heart. A possible ionic mechanism for reduced excitability and postrepolarization refractoriness. *Circ.Res.* **81**, 110-119.
- Qin, D., Huang, B., Deng, L., El Adawi, H., Ganguly, K., Sowers, J. R., and el Sherif, N.** (2001). Downregulation of K(+) channel genes expression in type I diabetic cardiomyopathy. *Biochem.Biophys.Res.Comm.* **283**, 549-553.
- Qu, Y., Ghatpande, A., el Sherif, N., and Boutjdir, M.** (2000). Gene expression of Na⁺/Ca²⁺ exchanger during development in human heart. *Cardiovasc.Res.* **45**, 866-873.
- Qu, Y., Isom, L. L., Westenbroek, R. E., Rogers, J. C., Tanada, T. N., McCormick, K. A., Scheuer, T., and Catterall, W. A.** (1995). Modulation of cardiac Na⁺ channel expression in *Xenopus* oocytes by beta 1 subunits. *J.Biol.Chem.* **270**, 25696-25701.
- Qu, Y., Rogers, J., Tanada, T., Scheuer, T., and Catterall, W. A.** (1994). Modulation of cardiac Na⁺ channels expressed in a mammalian cell line and in ventricular myocytes by protein kinase C. *Proc.Natl.Acad.Sci.U.S.A* **91**, 3289-3293.
- Qu, Y., Rogers, J. C., Tanada, T. N., Catterall, W. A., and Scheuer, T.** (1996). Phosphorylation of S1505 in the cardiac Na⁺ channel inactivation gate is required for modulation by protein kinase C. *J.Gen.Physiol* **108**, 375-379.
- Quednau, B. D., Nicoll, D. A., and Philipson, K. D.** (1997). Tissue specificity and alternative splicing of the Na⁺/Ca²⁺ exchanger isoforms NCX1, NCX2, and NCX3 in rat. *Am.J.Physiol* **272**, C1250-C1261.
- Raab-Graham, K. F., Radeke, C. M., and Vandenberg, C. A.** (1994). Molecular cloning and expression of a human heart inward rectifier potassium channel. *Neuroreport* **5**, 2501-2505.
- Rakotonirina, A. and Soustre, H.** (1989). Effects of isoprenaline on tonic tension and Na-Ca exchange in frog atrial fibres. *Gen.Physiol Biophys.* **8**, 313-326.
- Reimann, F. and Ashcroft, F. M.** (1999). Inwardly rectifying potassium channels. *Curr.Opin.Cell Biol.* **11**, 503-508.

- Rentschler, S., Vaidya, D. M., Tamaddon, H., Degenhardt, K., Sassoon, D., Morley, G. E., Jalife, J., and Fishman, G. I.** (2001). Visualization and functional characterization of the developing murine cardiac conduction system. *Development* **128**, 1785-1792.
- Rettig, J., Heinemann, S. H., Wunder, F., Lorra, C., Parcej, D. N., Dolly, J. O., and Pongs, O.** (1994). Inactivation properties of voltage-gated K⁺ channels altered by presence of beta-subunit. *Nature* **369**, 289-294.
- Reuter, H.** (1967). The dependence of slow inward current in Purkinje fibres on the extracellular calcium-concentration. *J Physiol* **192**, 479-492.
- Reuter, H.** (1974). Localization of beta adrenergic receptors, and effects of noradrenaline and cyclic nucleotides on action potentials, ionic currents and tension in mammalian cardiac muscle. *J.Physiol* **242**, 429-451.
- Reuter, H. and Scholz, H.** (1977). The regulation of the calcium conductance of cardiac muscle by adrenaline. *J Physiol* **264**, 49-62.
- Reuter, H. and Seitz, N.** (1968). The dependence of calcium efflux from cardiac muscle on temperature and external ion composition. *J.Physiol* **195**, 451-470.
- Richmond, J. E., Featherstone, D. E., Hartmann, H. A., and Ruben, P. C.** (1998). Slow inactivation in human cardiac sodium channels. *Biophys.J.* **74**, 2945-2952.
- Roberds, S. L. and Tamkun, M. M.** (1991). Developmental expression of cloned cardiac potassium channels. *FEBS Lett.* **284**, 152-154.
- Robinson, R. B., Liu, Q. Y., and Rosen, M. R.** (2000). Ionic basis for action potential prolongation by phenylephrine in canine epicardial myocytes. *J.Cardiovasc. Electrophysiol.* **11**, 70-76.
- Roden, D. M., Bennett, P. B., Snyders, D. J., Balsler, J. R., and Hondeghem, L. M.** (1988). Quinidine delays IK activation in guinea pig ventricular myocytes. *Circ.Res.* **62**, 1055-1058.
- Roden, D. M. and Kupersmidt, S.** (1999). From genes to channels: normal mechanisms. *Cardiovasc.Res.* **42**, 318-326.
- Roden, D. M., Lazzara, R., Rosen, M., Schwartz, P. J., Towbin, J., and Vincent, G. M.** (1996). Multiple mechanisms in the long-QT syndrome. Current knowledge, gaps, and future directions. The SADS Foundation Task Force on LQTS. *Circulation* **94**, 1996-2012.
- Rogart, R.** (1981). Sodium channels in nerve and muscle membrane. *Annu.Rev.Physiol* **43**, 711-725.
- Rogart, R. B.** (1986). High-STX-affinity vs. low-STX-affinity Na⁺ channel subtypes in nerve, heart, and skeletal muscle. *Ann.N.Y.Acad.Sci.* **479**, 402-430.
- Rogart, R. B., Cribbs, L. L., Muglia, L. K., Kephart, D. D., and Kaiser, M. W.** (1989). Molecular cloning of a putative tetrodotoxin-resistant rat heart Na⁺ channel isoform. *Proc.Natl.Acad.Sci.U.S.A* **86**, 8170-8174.

- Rosati, B., Pan, Z., Lypen, S., Wang, H. S., Cohen, I., Dixon, J. E., and McKinnon, D. (2001).** Regulation of KChIP2 potassium channel beta subunit gene expression underlies the gradient of transient outward current in canine and human ventricle. *J.Physiol* **533**, 119-125.
- Rozanski, G. J., Xu, Z., Whitney, R. T., Murakami, H., and Zucker, I. H. (1997).** Electrophysiology of rabbit ventricular myocytes following sustained rapid ventricular pacing. *J.Mol.Cell Cardiol.* **29**, 721-732.
- Rozanski, G. J., Xu, Z., Zhang, K., and Patel, K. P. (1998).** Altered K⁺ current of ventricular myocytes in rats with chronic myocardial infarction. *Am.J.Physiol* **274**, H259-H265.
- Rubart, M., Pressler, M. L., Pride, H. P., and Zipes, D. P. (1993).** Electrophysiological mechanisms in a canine model of erythromycin-associated long QT syndrome. *Circulation* **88**, 1832-1844.
- Rudy, B. (1978).** Slow inactivation of the sodium conductance in squid giant axons. Pronase resistance. *J.Physiol* **283**, 1-21.
- Ruknudin, A., He, S., Lederer, W. J., and Schulze, D. H. (2000).** Functional differences between cardiac and renal isoforms of the rat Na⁺-Ca²⁺ exchanger NCX1 expressed in *Xenopus* oocytes. *J.Physiol* **529 Pt 3**, 599-610.
- Safayhi, H., Haase, H., Kramer, U., Bihlmayer, A., Roenfeldt, M., Ammon, H. P., Froschmayr, M., Cassidy, T. N., Morano, I., Ahlijanian, M. K., and Striessnig, J. (1997).** L-type calcium channels in insulin-secreting cells: biochemical characterization and phosphorylation in RINm5F cells. *Mol.Endocrinol.* **11**, 619-629.
- Saffitz, J. E., Green, K. G., and Schuessler, R. B. (1997).** Structural determinants of slow conduction in the canine sinus node. *J.Cardiovasc.Electrophysiol.* **8**, 738-744.
- Saffitz, J. E., Kanter, H. L., Green, K. G., Tolley, T. K., and Beyer, E. C. (1994).** Tissue-specific determinants of anisotropic conduction velocity in canine atrial and ventricular myocardium. *Circ.Res.* **74**, 1065-1070.
- Sah, R., Ramirez, R. J., Kaprielian, R., and Backx, P. H. (2001).** Alterations in action potential profile enhance excitation-contraction coupling in rat cardiac myocytes. *J.Physiol* **533**, 201-214.
- Saint, D. A., Ju, Y. K., and Gage, P. W. (1992).** A persistent sodium current in rat ventricular myocytes. *J.Physiol* **453**, 219-231.
- Sakakibara, Y., Wasserstrom, J. A., Furukawa, T., Jia, H., Arentzen, C. E., Hartz, R. S., and Singer, D. H. (1992).** Characterization of the sodium current in single human atrial myocytes. *Circ.Res.* **71**, 535-546.
- Sakmann, B., Noma, A., and Trautwein, W. (1983).** Acetylcholine activation of single muscarinic K⁺ channels in isolated pacemaker cells of the mammalian heart. *Nature* **303**, 250-253.
- Sakmann, B. and Trube, G. (1984b).** Conductance properties of single inwardly rectifying potassium channels in ventricular cells from guinea-pig heart. *J.Physiol* **347**, 641-657.

- Sakmann, B. and Trube, G.** (1984a). Voltage-dependent inactivation of inward-rectifying single-channel currents in the guinea-pig heart cell membrane. *J.Physiol* **347**, 659-683.
- Sakmann, B. F., Spindler, A. J., Bryant, S. M., Linz, K. W., and Noble, D.** (2000). Distribution of a persistent sodium current across the ventricular wall in guinea pigs. *Circ.Res.* **87**, 910-914.
- Salata, J. J., Jurkiewicz, N. K., Jow, B., Folander, K., Guinasso, P. J., Jr., Raynor, B., Swanson, R., and Fermini, B.** (1996). IK of rabbit ventricle is composed of two currents: evidence for IKs. *Am.J.Physiol* **271**, H2477-H2489.
- Salinas, M., Duprat, F., Heurteaux, C., Hugnot, J. P., and Lazdunski, M.** (1997). New modulatory alpha subunits for mammalian Shab K⁺ channels. *J.Biol.Chem.* **272**, 24371-24379.
- Sanguinetti, M. C.** (2002). When the KChIPs are down. *Nat.Med.* **8**, 18-19.
- Sanguinetti, M. C., Curran, M. E., Zou, A., Shen, J., Spector, P. S., Atkinson, D. L., and Keating, M. T.** (1996). Coassembly of K(V)LQT1 and minK (IsK) proteins to form cardiac I(Ks) potassium channel. *Nature* **384**, 80-83.
- Sanguinetti, M. C., Jiang, C., Curran, M. E., and Keating, M. T.** (1995). A mechanistic link between an inherited and an acquired cardiac arrhythmia: HERG encodes the IKr potassium channel. *Cell* **81**, 299-307.
- Sanguinetti, M. C. and Jurkiewicz, N. K.** (1990). Two components of cardiac delayed rectifier K⁺ current. Differential sensitivity to block by class III antiarrhythmic agents. *J.Gen.Physiol* **96**, 195-215.
- Sanguinetti, M. C. and Jurkiewicz, N. K.** (1991). Delayed rectifier outward K⁺ current is composed of two currents in guinea pig atrial cells. *Am.J.Physiol* **260**, H393-H399.
- Sanguinetti, M. C. and Jurkiewicz, N. K.** (1992). Role of external Ca²⁺ and K⁺ in gating of cardiac delayed rectifier K⁺ currents. *Pflugers Arch.* **420**, 180-186.
- Sanguinetti, M. C., Jurkiewicz, N. K., Scott, A., and Siegl, P. K.** (1991). Isoproterenol antagonizes prolongation of refractory period by the class III antiarrhythmic agent E-4031 in guinea pig myocytes. Mechanism of action. *Circ.Res.* **68**, 77-84.
- Sanguinetti, M. C. and Xu, Q. P.** (1999). Mutations of the S4-S5 linker alter activation properties of HERG potassium channels expressed in *Xenopus* oocytes. *J.Physiol* **514 (Pt 3)**, 667-675.
- Santoro, B., Chen, S., Luthi, A., Pavlidis, P., Shumyatsky, G. P., Tibbs, G. R., and Siegelbaum, S. A.** (2000). Molecular and functional heterogeneity of hyperpolarization-activated pacemaker channels in the mouse CNS. *J.Neurosci.* **20**, 5264-5275.
- Santoro, B., Grant, S. G., Bartsch, D., and Kandel, E. R.** (1997). Interactive cloning with the SH3 domain of N-src identifies a new brain specific ion channel protein, with homology to eag and cyclic nucleotide-gated channels. *Proc.Natl.Acad. Sci.U.S.A* **94**, 14815-14820.
- Santoro, B., Liu, D. T., Yao, H., Bartsch, D., Kandel, E. R., Siegelbaum, S. A., and Tibbs, G. R.** (1998). Identification of a gene encoding a hyperpolarization-activated pacemaker channel of brain. *Cell* **93**, 717-729.

- Sartore, S., Pierobon-Bormioli, S., and Schiaffino, S.** (1978). Immunohistochemical evidence for myosin polymorphism in the chicken heart. *Nature* **274**, 82-83.
- Satin, J., Kyle, J. W., Chen, M., Bell, P., Cribbs, L. L., Fozzard, H. A., and Rogart, R. B.** (1992). A mutant of TTX-resistant cardiac sodium channels with TTX-sensitive properties. *Science* **256**, 1202-1205.
- Sato, R. and Koumi, S.** (1995). Modulation of the inwardly rectifying K⁺ channel in isolated human atrial myocytes by alpha 1-adrenergic stimulation. *J.Membr.Biol.* **148**, 185-191.
- Satoh, H.** (1992). Inhibition in L-type Ca²⁺ channel by stimulation of protein kinase C in isolated guinea pig ventricular cardiomyocytes. *Gen.Pharmacol.* **23**, 1097-1102.
- Satoh, H. and Hashimoto, K.** (1988). Effect of alpha 1-adrenoceptor stimulation with methoxamine and phenylephrine on spontaneously beating rabbit sino-atrial node cells. *Naunyn Schmiedebergs Arch.Pharmacol.* **337**, 415-422.
- Scamps, F. and Carmeliet, E.** (1989). Delayed K⁺ current and external K⁺ in single cardiac Purkinje cells. *Am.J.Physiol* **257**, C1086-C1092.
- Schaller, K. L., Krzemien, D. M., McKenna, N. M., and Caldwell, J. H.** (1992). Alternatively spliced sodium channel transcripts in brain and muscle. *J.Neurosci.* **12**, 1370-1381.
- Schneider, M., Proebstle, T., Hombach, V., Hannekum, A., and Rudel, R.** (1994). Characterization of the sodium currents in isolated human cardiocytes. *Pflugers Arch.* **428**, 84-90.
- Schönherr, R. and Heinemann, S. H.** (1996). Molecular determinants for activation and inactivation of HERG, a human inward rectifier potassium channel. *J.Physiol* **493 (Pt 3)**, 635-642.
- Schreibmayer, W., Frohnwieser, B., Dascal, N., Platzer, D., Spreitzer, B., Zechner, R., Kallen, R. G., and Lester, H. A.** (1994). Beta-adrenergic modulation of currents produced by rat cardiac Na⁺ channels expressed in *Xenopus laevis* oocytes. *Receptors.Channels* **2**, 339-350.
- Schroder, F., Handrock, R., Beuckelmann, D. J., Hirt, S., Hullin, R., Priebe, L., Schwinger, R. H., Weil, J., and Herzig, S.** (1998). Increased availability and open probability of single L-type calcium channels from failing compared with nonfailing human ventricle. *Circulation* **98**, 969-976.
- Schroeder, B. C., Waldegger, S., Fehr, S., Bleich, M., Warth, R., Greger, R., and Jentsch, T. J.** (2000). A constitutively open potassium channel formed by KCNQ1 and KCNE3. *Nature* **403**, 196-199.
- Schubert, B., VanDongen, A. M., Kirsch, G. E., and Brown, A. M.** (1989). Beta-adrenergic inhibition of cardiac sodium channels by dual G-protein pathways. *Science* **245**, 516-519.
- Schultz, D., Mikala, G., Yatani, A., Engle, D. B., Iles, D. E., Segers, B., Sinke, R. J., Weghuis, D. O., Klockner, U., Wakamori, M., and .** (1993). Cloning, chromosomal localization, and functional expression of the alpha 1 subunit of the L-type voltage-dependent calcium channel from normal human heart. *Proc.Natl. Acad.Sci.U.S.A* **90**, 6228-6232.

- Schwanstecher, M., Sieverding, C., Dorschner, H., Gross, I., Aguilar-Bryan, L., Schwanstecher, C., and Bryan, J. (1998). Potassium channel openers require ATP to bind to and act through sulfonylurea receptors. *EMBO J.* **17**, 5529-5535.
- Seifert, R., Scholten, A., Gauss, R., Mincheva, A., Lichter, P., and Kaupp, U. B. (1999). Molecular characterization of a slowly gating human hyperpolarization-activated channel predominantly expressed in thalamus, heart, and testis. *Proc. Natl. Acad. Sci. U.S.A.* **96**, 9391-9396.
- Seoh, S. A., Sigg, D., Papazian, D. M., and Bezanilla, F. (1996). Voltage-sensing residues in the S2 and S4 segments of the Shaker K⁺ channel. *Neuron* **16**, 1159-1167.
- Sesti, F., Abbott, G. W., Wei, J., Murray, K. T., Saksena, S., Schwartz, P. J., Priori, S. G., Roden, D. M., George, A. L., Jr., and Goldstein, S. A. (2000). A common polymorphism associated with antibiotic-induced cardiac arrhythmia. *Proc. Natl. Acad. Sci. U.S.A.* **97**, 10613-10618.
- Sham, J. S., Hatem, S. N., and Morad, M. (1995). Species differences in the activity of the Na⁽⁺⁾-Ca²⁺ exchanger in mammalian cardiac myocytes. *J. Physiol* **488 (Pt 3)**, 623-631.
- Shamraj, O. I. and Lingrel, J. B. (1994). A putative fourth Na⁺,K⁽⁺⁾-ATPase alpha-subunit gene is expressed in testis. *Proc. Natl. Acad. Sci. U.S.A.* **91**, 12952-12956.
- Shi, W., Wymore, R., Yu, H., Wu, J., Wymore, R. T., Pan, Z., Robinson, R. B., Dixon, J. E., McKinnon, D., and Cohen, I. S. (1999). Distribution and prevalence of hyperpolarization-activated cation channel (HCN) mRNA expression in cardiac tissues. *Circ. Res.* **85**, e1-e6.
- Shibasaki, T. (1987). Conductance and kinetics of delayed rectifier potassium channels in nodal cells of the rabbit heart. *J. Physiol* **387**, 227-250.
- Shibata, E. F., Drury, T., Refsum, H., Aldrete, V., and Giles, W. (1989). Contributions of a transient outward current to repolarization in human atrium. *Am. J. Physiol* **257**, H1773-H1781.
- Shieh, C. C., Coghlan, M., Sullivan, J. P., and Gopalakrishnan, M. (2000). Potassium channels: molecular defects, diseases, and therapeutic opportunities. *Pharmacol. Rev.* **52**, 557-594.
- Shimizu, W., Ohe, T., Kurita, T., Takaki, H., Aihara, N., Kamakura, S., Matsuhisa, M., and Shimomura, K. (1991). Early afterdepolarizations induced by isoproterenol in patients with congenital long QT syndrome. *Circulation* **84**, 1915-1923.
- Shimoni, Y., Ewart, H. S., and Severson, D. (1998). Type I and II models of diabetes produce different modifications of K⁺ currents in rat heart: role of insulin. *J. Physiol* **507 (Pt 2)**, 485-496.
- Shimoni, Y., Fiset, C., Clark, R. B., Dixon, J. E., McKinnon, D., and Giles, W. R. (1997). Thyroid hormone regulates postnatal expression of transient K⁺ channel isoforms in rat ventricle. *J. Physiol* **500 (Pt 1)**, 65-73.
- Shimoni, Y. and Severson, D. L. (1995). Thyroid status and potassium currents in rat ventricular myocytes. *Am. J. Physiol* **268**, H576-H583.

- Shyng, S., Ferrigni, T., and Nichols, C. G. (1997b).** Control of rectification and gating of cloned KATP channels by the Kir6.2 subunit. *J.Gen.Physiol* **110**, 141-153.
- Shyng, S., Ferrigni, T., and Nichols, C. G. (1997a).** Regulation of KATP channel activity by diazoxide and MgADP. Distinct functions of the two nucleotide binding folds of the sulfonylurea receptor. *J.Gen.Physiol* **110**, 643-654.
- Shyng, S. and Nichols, C. G. (1997).** Octameric stoichiometry of the KATP channel complex. *J.Gen.Physiol* **110**, 655-664.
- Siegelbaum, S. A. and Tsien, R. W. (1980).** Calcium-activated transient outward current in calf cardiac Purkinje fibres. *J.Physiol* **299**, 485-506.
- Singer, D., Biel, M., Lotan, I., Flockerzi, V., Hofmann, F., and Dascal, N. (1991).** The roles of the subunits in the function of the calcium channel. *Science* **253**, 1553-1557.
- Sipido, K. R., Callewaert, G., and Carmeliet, E. (1993).** $[Ca^{2+}]_i$ transients and $[Ca^{2+}]_i$ -dependent chloride current in single Purkinje cells from rabbit heart. *J.Physiol* **468**, 641-667.
- Sipido, K. R., Volders, P. G., Vos, M. A., and Verdonck, F. (2002).** Altered Na/Ca exchange activity in cardiac hypertrophy and heart failure: a new target for therapy? *Cardiovasc.Res.* **53**, 782-805.
- Smith, L., Porzig, H., Lee, H. W., and Smith, J. B. (1995).** Phorbol esters downregulate expression of the sodium/calcium exchanger in renal epithelial cells. *Am.J.Physiol* **269**, C457-C463.
- Smith, P. L., Baukrowitz, T., and Yellen, G. (1996).** The inward rectification mechanism of the HERG cardiac potassium channel. *Nature* **379**, 833-836.
- Snutch, T. P., Tomlinson, W. J., Leonard, J. P., and Gilbert, M. M. (1991).** Distinct calcium channels are generated by alternative splicing and are differentially expressed in the mammalian CNS. *Neuron* **7**, 45-57.
- Snyders, D. J. (1999).** Structure and function of cardiac potassium channels. *Cardiovasc. Res.* **42**, 377-390.
- Soejima, M. and Noma, A. (1984).** Mode of regulation of the ACh-sensitive K-channel by the muscarinic receptor in rabbit atrial cells. *Pflugers Arch.* **400**, 424-431.
- Spach, M. S. (1999).** Anisotropy of cardiac tissue: a major determinant of conduction? *J.Cardiovasc.Electrophysiol.* **10**, 887-890.
- Spach, M. S. and Heidlage, J. F. (1995).** The stochastic nature of cardiac propagation at a microscopic level. Electrical description of myocardial architecture and its application to conduction. *Circ.Res.* **76**, 366-380.
- Spach, M. S., Heidlage, J. F., Dolber, P. C., and Barr, R. C. (2000).** Electrophysiological effects of remodeling cardiac gap junctions and cell size: experimental and model studies of normal cardiac growth. *Circ.Res.* **86**, 302-311.

- Spector, P. S., Curran, M. E., Keating, M. T., and Sanguinetti, M. C.** (1996a). Class III antiarrhythmic drugs block HERG, a human cardiac delayed rectifier K⁺ channel. Open-channel block by methanesulfonanilides. *Circ.Res.* **78**, 499-503.
- Spector, P. S., Curran, M. E., Zou, A., Keating, M. T., and Sanguinetti, M. C.** (1996b). Fast inactivation causes rectification of the IKr channel. *J.Gen.Physiol* **107**, 611-619.
- Splawski, I., Shen, J., Timothy, K. W., Lehmann, M. H., Priori, S., Robinson, J. L., Moss, A. J., Schwartz, P. J., Towbin, J. A., Vincent, G. M., and Keating, M. T.** (2000). Spectrum of mutations in long-QT syndrome genes. KVLQT1, HERG, SCN5A, KCNE1, and KCNE2. *Circulation* **102**, 1178-1185.
- Splawski, I., Tristani-Firouzi, M., Lehmann, M. H., Sanguinetti, M. C., and Keating, M. T.** (1997). Mutations in the hminK gene cause long QT syndrome and suppress IKs function. *Nat.Genet.* **17**, 338-340.
- Spruce, A. E., Standen, N. B., and Stanfield, P. R.** (1987). Studies of the unitary properties of adenosine-5'-triphosphate- regulated potassium channels of frog skeletal muscle. *J.Physiol* **382**, 213-236.
- Standen, N. B., Quayle, J. M., Davies, N. W., Brayden, J. E., Huang, Y., and Nelson, M. T.** (1989). Hyperpolarizing vasodilators activate ATP-sensitive K⁺ channels in arterial smooth muscle. *Science* **245**, 177-180.
- Steinberg, T. H., Civitelli, R., Geist, S. T., Robertson, A. J., Hick, E., Veenstra, R. D., Wang, H. Z., Warlow, P. M., Westphale, E. M., Laing, J. G., and .** (1994). Connexin43 and connexin45 form gap junctions with different molecular permeabilities in osteoblastic cells. *EMBO J.* **13**, 744-750.
- Stevens, E. B., Cox, P. J., Shah, B. S., Dixon, A. K., Richardson, P. J., Pinnock, R. D., and Lee, K.** (2001). Tissue distribution and functional expression of the human voltage-gated sodium channel beta3 subunit. *Pflugers Arch.* **441**, 481-488.
- Striessnig, J.** (1999). Pharmacology, structure and function of cardiac L-type Ca(2+) channels. *Cell Physiol Biochem.* **9**, 242-269.
- Stuhmer, W., Conti, F., Suzuki, H., Wang, X. D., Noda, M., Yahagi, N., Kubo, H., and Numa, S.** (1989). Structural parts involved in activation and inactivation of the sodium channel. *Nature* **339**, 597-603.
- Sweadner, K. J., Herrera, V. L., Amato, S., Moellmann, A., Gibbons, D. K., and Repke, K. R.** (1994). Immunologic identification of Na⁺,K⁽⁺⁾-ATPase isoforms in myocardium. Isoform change in deoxycorticosterone acetate-salt hypertension. *Circ.Res.* **74**, 669-678.
- Tai, K. K., Wang, K. W., and Goldstein, S. A.** (1997). MinK potassium channels are heteromultimeric complexes. *J.Biol.Chem.* **272**, 1654-1658.
- Takagishi, Y., Yasui, K., Severs, N. J., and Murata, Y.** (2000). Species-specific difference in distribution of voltage-gated L-type Ca(2+) channels of cardiac myocytes. *Am.J.Physiol Cell Physiol* **279**, C1963-C1969.

- Takebayashi-Suzuki, K., Yanagisawa, M., Gourdie, R. G., Kanzawa, N., and Mikawa, T.** (2000). In vivo induction of cardiac Purkinje fiber differentiation by coexpression of preproendothelin-1 and endothelin converting enzyme-1. *Development* **127**, 3523-3532.
- Takimoto, K., Li, D., Hershman, K. M., Li, P., Jackson, E. K., and Levitan, E. S.** (1997). Decreased expression of Kv4.2 and novel Kv4.3 K⁺ channel subunit mRNAs in ventricles of renovascular hypertensive rats. *Circ.Res.* **81**, 533-539.
- Takumi, T., Ohkubo, H., and Nakanishi, S.** (1988). Cloning of a membrane protein that induces a slow voltage-gated potassium current. *Science* **242**, 1042-1045.
- Tamkun, M. M., Knoth, K. M., Walbridge, J. A., Kroemer, H., Roden, D. M., and Glover, D. M.** (1991). Molecular cloning and characterization of two voltage-gated K⁺ channel cDNAs from human ventricle. *FASEB J.* **5**, 331-337.
- Tan, H. L., Bink-Boelkens, M. T., Bezzina, C. R., Viswanathan, P. C., Beaufort-Krol, G. C., van Tintelen, P. J., van Den Berg, M. P., Wilde, A. A., and Balsler, J. R.** (2001). A sodium-channel mutation causes isolated cardiac conduction disease. *Nature* **409**, 1043-1047.
- Tani, M. and Neely, J. R.** (1989). Role of intracellular Na⁺ in Ca²⁺ overload and depressed recovery of ventricular function of reperfused ischemic rat hearts. Possible involvement of H⁺-Na⁺ and Na⁺-Ca²⁺ exchange. *Circ.Res.* **65**, 1045-1056.
- Terzic, A., Jahangir, A., and Kurachi, Y.** (1995). Cardiac ATP-sensitive K⁺ channels: regulation by intracellular nucleotides and K⁺ channel-opening drugs. *Am.J. Physiol* **269**, C525-C545.
- Terzic, A., Tung, R. T., and Kurachi, Y.** (1994). Nucleotide regulation of ATP sensitive potassium channels. *Cardiovasc.Res.* **28**, 746-753.
- Tessier, S., Karczewski, P., Krause, E. G., Pansard, Y., Acar, C., Lang-Lazdunski, M., Mercadier, J. J., and Hatem, S. N.** (1999). Regulation of the transient outward K⁽⁺⁾ current by Ca⁽²⁺⁾/calmodulin- dependent protein kinases II in human atrial myocytes. *Circ.Res.* **85**, 810-819.
- Therien, A. G. and Blostein, R.** (2000). Mechanisms of sodium pump regulation. *Am.J.Physiol Cell Physiol* **279**, C541-C566.
- Thomas, D., Zhang, W., Karle, C. A., Kathofer, S., Schols, W., Kubler, W., and Kiehn, J.** (1999). Deletion of protein kinase A phosphorylation sites in the HERG potassium channel inhibits activation shift by protein kinase A. *J.Biol.Chem.* **274**, 27457-27462.
- Thomas, S. A., Schuessler, R. B., Berul, C. I., Beardslee, M. A., Beyer, E. C., Mendelsohn, M. E., and Saffitz, J. E.** (1998). Disparate effects of deficient expression of connexin43 on atrial and ventricular conduction: evidence for chamber-specific molecular determinants of conduction. *Circulation* **97**, 686-691.
- Tohse, N., Nakaya, H., Hattori, Y., Endou, M., and Kanno, M.** (1990). Inhibitory effect mediated by alpha 1-adrenoceptors on transient outward current in isolated rat ventricular cells. *Pflugers Arch.* **415**, 575-581.

- Tomaselli, G. F. and Marban, E.** (1999). Electrophysiological remodeling in hypertrophy and heart failure. *Cardiovasc.Res.* **42**, 270-283.
- Trudeau, M. C., Warmke, J. W., Ganetzky, B., and Robertson, G. A.** (1995). HERG, a human inward rectifier in the voltage-gated potassium channel family. *Science* **269**, 92-95.
- Tseng, G. N.** (2001). I(Kr): the hERG channel. *J.Mol.Cell Cardiol.* **33**, 835-849.
- Tseng, G. N. and Boyden, P. A.** (1989). Multiple types of Ca²⁺ currents in single canine Purkinje cells. *Circ.Res.* **65**, 1735-1750.
- Tseng, G. N. and Hoffman, B. F.** (1989). Two components of transient outward current in canine ventricular myocytes. *Circ.Res.* **64**, 633-647.
- Tsien, R. W.** (1973). Adrenaline-like effects of intracellular iontophoresis of cyclic AMP in cardiac Purkinje fibres. *Nat.New Biol.* **245**, 120-122.
- Tsien, R. W. and Carpenter, D. O.** (1978). Ionic mechanisms of pacemaker activity in cardiac Purkinje fibers. *Fed.Proc.* **37**, 2127-2131.
- Tsien, R. W., Fox, A. P., Hess, P., McCleskey, E. W., Nilius, B., Nowycky, M. C., and Rosenberg, R. L.** (1987b). Multiple types of calcium channel in excitable cells. *Soc.Gen. Physiol Ser.* **41**, 167-187.
- Tsien, R. W., Giles, W., and Greengard, P.** (1972). Cyclic AMP mediates the effects of adrenaline on cardiac purkinje fibres. *Nat.New Biol.* **240**, 181-183.
- Tsien, R. W., Hess, P., McCleskey, E. W., and Rosenberg, R. L.** (1987a). Calcium channels: mechanisms of selectivity, permeation, and block. *Annu.Rev.Biophys. Biophys.Chem.* **16**, 265-290.
- Tsuji, Y., Opthof, T., Kamiya, K., Yasui, K., Liu, W., Lu, Z., and Kodama, I.** (2000). Pacing-induced heart failure causes a reduction of delayed rectifier potassium currents along with decreases in calcium and transient outward currents in rabbit ventricle. *Cardiovasc.Res.* **48**, 300-309.
- Tucker, S. J., Gribble, F. M., Zhao, C., Trapp, S., and Ashcroft, F. M.** (1997). Truncation of Kir6.2 produces ATP-sensitive K⁺ channels in the absence of the sulphonylurea receptor. *Nature* **387**, 179-183.
- Turgeon, J., Daleau, P., Bennett, P. B., Wiggins, S. S., Selby, L., and Roden, D. M.** (1994). Block of IKs, the slow component of the delayed rectifier K⁺ current, by the diuretic agent indapamide in guinea pig myocytes. *Circ.Res.* **75**, 879-886.
- Uebele, V. N., England, S. K., Chaudhary, A., Tamkun, M. M., and Snyders, D. J.** (1996). Functional differences in Kv1.5 currents expressed in mammalian cell lines are due to the presence of endogenous Kv beta 2.1 subunits. *J.Biol.Chem.* **271**, 2406-2412.
- Ufret-Vincenty, C. A., Baro, D. J., Lederer, W. J., Rockman, H. A., Quinones, L. E., and Santana, L. F.** (2001). Role of sodium channel deglycosylation in the genesis of cardiac arrhythmias in heart failure. *J.Biol.Chem.* **276**, 28197-28203.

- Undrovinas, A. I., Maltsev, V. A., and Sabbah, H. N.** (1999). Repolarization abnormalities in cardiomyocytes of dogs with chronic heart failure: role of sustained inward current. *Cell Mol.Life Sci.* **55**, 494-505.
- Ursell, P. C., Gardner, P. I., Albala, A., Fenoglio, J. J., Jr., and Wit, A. L.** (1985). Structural and electrophysiological changes in the epicardial border zone of canine myocardial infarcts during infarct healing. *Circ.Res.* **56**, 436-451.
- Vaccari, T., Moroni, A., Rocchi, M., Gorza, L., Bianchi, M. E., Beltrame, M., and DiFrancesco, D.** (1999). The human gene coding for HCN2, a pacemaker channel of the heart. *Biochim.Biophys.Acta* **1446**, 419-425.
- Valiunas, V., Bukauskas, F. F., and Weingart, R.** (1997). Conductances and selective permeability of connexin43 gap junction channels examined in neonatal rat heart cells. *Circ.Res.* **80**, 708-719.
- van der Velden, H. M., van Kempen, M. J., Wijffels, M. C., van Zijverden, M., Groenewegen, W. A., Allessie, M. A., and Jongsma, H. J.** (1998). Altered pattern of connexin40 distribution in persistent atrial fibrillation in the goat. *J.Cardiovasc .Electrophysiol.* **9**, 596-607.
- Van Wagoner, D. R., Kirian, M., and Lamorgese, M.** (1996). Phenylephrine suppresses outward K⁺ currents in rat atrial myocytes. *Am.J.Physiol* **271**, H937-H946.
- Varnum, M. D., Busch, A. E., Bond, C. T., Maylie, J., and Adelman, J. P.** (1993). The min K channel underlies the cardiac potassium current IKs and mediates species-specific responses to protein kinase C. *Proc.Natl.Acad.Sci.U.S.A* **90**, 11528-11532.
- Varro, A., Balati, B., Iost, N., Takacs, J., Virag, L., Lathrop, D. A., Csaba, L., Talosi, L., and Papp, J. G.** (2000). The role of the delayed rectifier component IKs in dog ventricular muscle and Purkinje fibre repolarization. *J.Physiol* **523 Pt 1**, 67-81.
- Varro, A., Nanasi, P. P., and Lathrop, D. A.** (1993). Potassium currents in isolated human atrial and ventricular cardiocytes. *Acta Physiol Scand.* **149**, 133-142.
- Vassalle, M.** (1966). Analysis of cardiac pacemaker potential using a "voltage clamp" technique. *Am.J.Physiol* **210**, 1335-1341.
- Veenstra, R. D., Wang, H. Z., Beyer, E. C., and Brink, P. R.** (1994). Selective dye and ionic permeability of gap junction channels formed by connexin45. *Circ.Res.* **75**, 483-490.
- Veldkamp, M. W., van Ginneken, A. C., and Bouman, L. N.** (1993). Single delayed rectifier channels in the membrane of rabbit ventricular myocytes. *Circ.Res.* **72**, 865-878.
- Veldkamp, M. W., Viswanathan, P. C., Bezzina, C., Baartscheer, A., Wilde, A. A., and Balsler, J. R.** (2000). Two distinct congenital arrhythmias evoked by a multidysfunctional Na⁽⁺⁾ channel. *Circ.Res.* **86**, E91-E97.
- Verkerk, A. O., Veldkamp, M. W., Bouman, L. N., and van Ginneken, A. C.** (2000). Calcium-activated Cl⁽⁻⁾ current contributes to delayed afterdepolarizations in single Purkinje and ventricular myocytes. *Circulation* **101**, 2639-2644.

- Viragh, S. and Challice, C. E.** (1981). The origin of the epicardium and the embryonic myocardial circulation in the mouse. *Anat.Rec.* **201**, 157-168.
- Vitadello, M., Matteoli, M., and Gorza, L.** (1990). Neurofilament proteins are co-expressed with desmin in heart conduction system myocytes. *J.Cell Sci.* **97 (Pt 1)**, 11-21.
- Volders, P. G., Sipido, K. R., Carmeliet, E., Spatjens, R. L., Wellens, H. J., and Vos, M. A.** (1999a). Repolarizing K⁺ currents ITO1 and IKs are larger in right than left canine ventricular midmyocardium. *Circulation* **99**, 206-210.
- Volders, P. G., Sipido, K. R., Vos, M. A., Spatjens, R. L., Leunissen, J. D., Carmeliet, E., and Wellens, H. J.** (1999b). Downregulation of delayed rectifier K(+) currents in dogs with chronic complete atrioventricular block and acquired torsades de pointes. *Circulation* **100**, 2455-2461.
- Volk, T., Nguyen, T. H., Schultz, J. H., and Ehmke, H.** (1999). Relationship between transient outward K⁺ current and Ca²⁺ influx in rat cardiac myocytes of endo- and epicardial origin. *J.Physiol* **519 Pt 3**, 841-850.
- Wagner, J. A., Sax, F. L., Weisman, H. F., Porterfield, J., McIntosh, C., Weisfeldt, M. L., Snyder, S. H., and Epstein, S. E.** (1989). Calcium-antagonist receptors in the atrial tissue of patients with hypertrophic cardiomyopathy. *N.Engl.J.Med.* **320**, 755-761.
- Walsh, K. B., Arena, J. P., Kwok, W. M., Freeman, L., and Kass, R. S.** (1991). Delayed-rectifier potassium channel activity in isolated membrane patches of guinea pig ventricular myocytes. *Am.J.Physiol* **260**, H1390-H1393.
- Walsh, K. B. and Kass, R. S.** (1988). Regulation of a heart potassium channel by protein kinase A and C. *Science* **242**, 67-69.
- Wang, D. W., Kiyosue, T., Shigematsu, S., and Arita, M.** (1995c). Abnormalities of K⁺ and Ca²⁺ currents in ventricular myocytes from rats with chronic diabetes. *Am.J.Physiol* **269**, H1288-H1296.
- Wang, H., Yang, B., Zhang, Y., Han, H., Wang, J., Shi, H., and Wang, Z.** (2001). Different subtypes of alpha1-adrenoceptor modulate different K⁺ currents via different signaling pathways in canine ventricular myocytes. *J.Biol.Chem.* **276**, 40811-40816.
- Wang, J., Trudeau, M. C., Zappia, A. M., and Robertson, G. A.** (1998a). Regulation of deactivation by an amino terminal domain in human ether-a-go-go-related gene potassium channels. *J.Gen.Physiol* **112**, 637-647.
- Wang, Q., Shen, J., Splawski, I., Atkinson, D., Li, Z., Robinson, J. L., Moss, A. J., Towbin, J. A., and Keating, M. T.** (1995b). SCN5A mutations associated with an inherited cardiac arrhythmia, long QT syndrome. *Cell* **80**, 805-811.
- Wang, S., Morales, M. J., Liu, S., Strauss, H. C., and Rasmusson, R. L.** (1996). Time, voltage and ionic concentration dependence of rectification of h-erg expressed in *Xenopus* oocytes. *FEBS Lett.* **389**, 167-173.

- Wang, Z., Feng, J., Shi, H., Pond, A., Nerbonne, J. M., and Nattel, S. (1999).** Potential molecular basis of different physiological properties of the transient outward K⁺ current in rabbit and human atrial myocytes. *Circ.Res.* **84**, 551-561.
- Wang, Z., Fermini, B., Feng, J., and Nattel, S. (1995a).** Role of chloride currents in repolarizing rabbit atrial myocytes. *Am.J.Physiol* **268**, H1992-H2002.
- Wang, Z., Fermini, B., and Nattel, S. (1993).** Sustained depolarization-induced outward current in human atrial myocytes. Evidence for a novel delayed rectifier K⁺ current similar to Kv1.5 cloned channel currents. *Circ.Res.* **73**, 1061-1076.
- Wang, Z., Fermini, B., and Nattel, S. (1994).** Rapid and slow components of delayed rectifier current in human atrial myocytes. *Cardiovasc.Res.* **28**, 1540-1546.
- Wang, Z., Yue, L., White, M., Pelletier, G., and Nattel, S. (1998b).** Differential distribution of inward rectifier potassium channel transcripts in human atrium versus ventricle. *Circulation* **98**, 2422-2428.
- Warmke, J. W. and Ganetzky, B. (1994).** A family of potassium channel genes related to eag in *Drosophila* and mammals. *Proc.Natl.Acad.Sci.U.S.A* **91**, 3438-3442.
- Wasserstrom, J. A. and Salata, J. J. (1988).** Basis for tetrodotoxin and lidocaine effects on action potentials in dog ventricular myocytes. *Am.J.Physiol* **254**, H1157-H1166.
- Watkins, H., Conner, D., Thierfelder, L., Jarcho, J. A., MacRae, C., McKenna, W. J., Maron, B. J., Seidman, J. G., and Seidman, C. E. (1995).** Mutations in the cardiac myosin binding protein-C gene on chromosome 11 cause familial hypertrophic cardiomyopathy. *Nat.Genet.* **11**, 434-437.
- Watson, C. L. and Gold, M. R. (1997).** Modulation of Na⁺ current inactivation by stimulation of protein kinase C in cardiac cells. *Circ.Res.* **81**, 380-386.
- Weerapura, M., Nattel, S., Chartier, D., Caballero, R., and Hebert, T. E. (2002).** A comparison of currents carried by HERG, with and without coexpression of MiRP1, and the native rapid delayed rectifier current. Is MiRP1 the missing link? *J Physiol* **540**, 15-27.
- Weidmann, S. (1951).** Effect of current flow on membrane potential of cardiac muscle. *J. Physiol*, **115**, 227-236.
- Weidmann, S. (1955a).** The effect of the cardiac membrane potential on the rapid availability of the sodium carrying system. *J. Physiol*, **127**, 213-24.
- Weidmann, S. (1955 b).** Rectifier properties of Purkinje fibers. *Am. J. Physiol*, **183**, 671.
- West, J. W., Patton, D. E., Scheuer, T., Wang, Y., Goldin, A. L., and Catterall, W. A. (1992).** A cluster of hydrophobic amino acid residues required for fast Na⁽⁺⁾- channel inactivation. *Proc.Natl.Acad.Sci.U.S.A* **89**, 10910-10914.
- Wettwer, E., Amos, G., Gath, J., Zerkowski, H. R., Reidemeister, J. C., and Ravens, U. (1993).** Transient outward current in human and rat ventricular myocytes. *Cardiovasc.Res.* **27**, 1662-1669.

- Wettwer, E., Amos, G. J., Posival, H., and Ravens, U.** (1994). Transient outward current in human ventricular myocytes of subepicardial and subendocardial origin. *Circ.Res.* **75**, 473-482.
- Wetzel, G. T., Chen, F., and Klitzner, T. S.** (1993). Ca²⁺ channel kinetics in acutely isolated fetal, neonatal, and adult rabbit cardiac myocytes. *Circ.Res.* **72**, 1065-1074.
- White, T. W. and Paul, D. L.** (1999). Genetic diseases and gene knockouts reveal diverse connexin functions. *Annu.Rev.Physiol* **61**, 283-310.
- Wible, B. A., Yang, Q., Kuryshv, Y. A., Accili, E. A., and Brown, A. M.** (1998). Cloning and expression of a novel K⁺ channel regulatory protein, KChAP. *J.Biol.Chem.* **273**, 11745-11751.
- Wickenden, A. D., Jegla, T. J., Kaprielian, R., and Backx, P. H.** (1999b). Regional contributions of Kv1.4, Kv4.2, and Kv4.3 to transient outward K⁺ current in rat ventricle. *Am.J.Physiol* **276**, H1599-H1607.
- Wickenden, A. D., Lee, P., Sah, R., Huang, Q., Fishman, G. I., and Backx, P. H.** (1999c). Targeted expression of a dominant-negative K(v)4.2 K(+) channel subunit in the mouse heart. *Circ.Res.* **85**, 1067-1076.
- Wickenden, A. D., Tsushima, R. G., Losito, V. A., Kaprielian, R., and Backx, P. H.** (1999a). Effect of Cd²⁺ on Kv4.2 and Kv1.4 expressed in *Xenopus* oocytes and on the transient outward currents in rat and rabbit ventricular myocytes. *Cell Physiol Biochem.* **9**, 11-28.
- Wickman, K. D., Iniguez-Lluhl, J. A., Davenport, P. A., Taussig, R., Krapivinsky, G. B., Linder, M. E., Gilman, A. G., and Clapham, D. E.** (1994). Recombinant G-protein beta gamma-subunits activate the muscarinic-gated atrial potassium channel. *Nature* **368**, 255-257.
- Wilde, A. A.** (1993). Role of ATP-sensitive K⁺ channel current in ischemic arrhythmias. *Cardiovasc.Drugs Ther.* **7 Suppl 3**, 521-526.
- Wilde, A. A. and Janse, M. J.** (1994). Electrophysiological effects of ATP sensitive potassium channel modulation: implications for arrhythmogenesis. *Cardiovasc.Res.* **28**, 16-24.
- Winslow, R. L., Rice, J., and Jafri, S.** (1998). Modeling the cellular basis of altered excitation-contraction coupling in heart failure. *Prog.Biophys.Mol.Biol.* **69**, 497-514.
- Wischmeyer, E. and Karschin, A.** (1996). Receptor stimulation causes slow inhibition of IRK1 inwardly rectifying K⁺ channels by direct protein kinase A-mediated phosphorylation. *Proc.Natl.Acad.Sci.U.S.A* **93**, 5819-5823.
- Wollmuth, L. P. and Hille, B.** (1992). Ionic selectivity of I_h channels of rod photoreceptors in tiger salamanders. *J.Gen.Physiol* **100**, 749-765.
- Wollner, D. A., Scheinman, R., and Catterall, W. A.** (1988). Sodium channel expression and assembly during development of retinal ganglion cells. *Neuron* **1**, 727-737.
- Woo, S. H. and Lee, C. O.** (1999). Role of PKC in the effects of alpha1-adrenergic stimulation on Ca²⁺ transients, contraction and Ca²⁺ current in guinea-pig ventricular myocytes. *Pflugers Arch.* **437**, 335-344.

- Wright, S. N., Wang, S. Y., Kallen, R. G., and Wang, G. K.** (1997). Differences in steady-state inactivation between Na channel isoforms affect local anesthetic binding affinity. *Biophys.J.* **73**, 779-788.
- Wu, J. Y. and Lipsius, S. L.** (1990). Effects of extracellular Mg²⁺ on T- and L-type Ca²⁺ currents in single atrial myocytes. *Am.J.Physiol* **259**, H1842-H1850.
- Xu, H., Guo, W., and Nerbonne, J. M.** (1999a). Four kinetically distinct depolarization-activated K⁺ currents in adult mouse ventricular myocytes. *J.Gen.Physiol* **113**, 661-678.
- Xu, H., Li, H., and Nerbonne, J. M.** (1999b). Elimination of the transient outward current and action potential prolongation in mouse atrial myocytes expressing a dominant negative Kv4 alpha subunit. *J.Physiol* **519 Pt 1**, 11-21.
- Xu, X. P. and Best, P. M.** (1990). Increase in T-type calcium current in atrial myocytes from adult rats with growth hormone-secreting tumors. *Proc.Natl.Acad.Sci. U.S.A* **87**, 4655-4659.
- Xu, Z. and Rozanski, G. J.** (1998). K⁺ current inhibition by amphiphilic fatty acid metabolites in rat ventricular myocytes. *Am.J.Physiol* **275**, C1660-C1667.
- Yamada, M., Inanobe, A., and Kurachi, Y.** (1998). G protein regulation of potassium ion channels. *Pharmacol.Rev.* **50**, 723-760.
- Yanagihara, K. and Irisawa, H.** (1980). Inward current activated during hyperpolarization in the rabbit sinoatrial node cell. *Pflugers Arch.* **385**, 11-19.
- Yang, E. K., Alvira, M. R., Levitan, E. S., and Takimoto, K.** (2001). Kvbeta subunits increase expression of Kv4.3 channels by interacting with their C termini. *J.Biol.Chem.* **276**, 4839-4844.
- Yang, N. and Horn, R.** (1995). Evidence for voltage-dependent S4 movement in sodium channels. *Neuron* **15**, 213-218.
- Yang, T., Kupersmidt, S., and Roden, D. M.** (1995). Anti-minK antisense decreases the amplitude of the rapidly activating cardiac delayed rectifier K⁺ current. *Circ.Res.* **77**, 1246-1253.
- Yellen, G., Jurman, M. E., Abramson, T., and MacKinnon, R.** (1991). Mutations affecting internal TEA blockade identify the probable pore-forming region of a K⁺ channel. *Science* **251**, 939-942.
- Yellen, G., Sodickson, D., Chen, T. Y., and Jurman, M. E.** (1994). An engineered cysteine in the external mouth of a K⁺ channel allows inactivation to be modulated by metal binding. *Biophys.J.* **66**, 1068-1075.
- Yokoshiki, H., Kohya, T., Tomita, F., Tohse, N., Nakaya, H., Kanno, M., and Kitabatake, A.** (1997). Restoration of action potential duration and transient outward current by regression of left ventricular hypertrophy. *J.Mol.Cell Cardiol.* **29**, 1331-1339.
- Yu, H., Chang, F., and Cohen, I. S.** (1995). Pacemaker current i(f) in adult canine cardiac ventricular myocytes. *J.Physiol* **485 (Pt 2)**, 469-483.

- Yu, H., Gao, J., Wang, H., Wymore, R., Steinberg, S., McKinnon, D., Rosen, M. R., and Cohen, I. S.** (2000). Effects of the renin-angiotensin system on the current $I_{(to)}$ in epicardial and endocardial ventricular myocytes from the canine heart. *Circ.Res.* **86**, 1062-1068.
- Yu, H., Wu, J., Potapova, I., Wymore, R. T., Holmes, B., Zuckerman, J., Pan, Z., Wang, H., Shi, W., Robinson, R. B., El Maghrabi, M. R., Benjamin, W., Dixon, J., McKinnon, D., Cohen, I. S., and Wymore, R.** (2001). MinK-related peptide 1: A beta subunit for the HCN ion channel subunit family enhances expression and speeds activation. *Circ.Res.* **88**, E84-E87.
- Yuan, W., Ginsburg, K. S., and Bers, D. M.** (1996). Comparison of sarcolemmal calcium channel current in rabbit and rat ventricular myocytes. *J.Physiol* **493 (Pt 3)**, 733-746.
- Yue, D. T. and Marban, E.** (1988). A novel cardiac potassium channel that is active and conductive at depolarized potentials. *Pflugers Arch.* **413**, 127-133.
- Yue, L., Feng, J., Gaspo, R., Li, G. R., Wang, Z., and Nattel, S.** (1997). Ionic remodeling underlying action potential changes in a canine model of atrial fibrillation. *Circ.Res.* **81**, 512-525.
- Yue, L., Feng, J., Li, G. R., and Nattel, S.** (1996b). Characterization of an ultrarapid delayed rectifier potassium channel involved in canine atrial repolarization. *J.Physiol* **496 (Pt 3)**, 647-662.
- Yue, L., Feng, J., Li, G. R., and Nattel, S.** (1996a). Transient outward and delayed rectifier currents in canine atrium: properties and role of isolation methods. *Am.J.Physiol* **270**, H2157-H2168.
- Yue, L., Feng, J., Wang, Z., and Nattel, S.** (1999). Adrenergic control of the ultrarapid delayed rectifier current in canine atrial myocytes. *J.Physiol* **516 (Pt 2)**, 385-398.
- Zagotta, W. N. and Siegelbaum, S. A.** (1996). Structure and function of cyclic nucleotide-gated channels. *Annu.Rev.Neurosci.* **19**, 235-263.
- Zaritsky, J. J., Redell, J. B., Tempel, B. L., and Schwarz, T. L.** (2001). The consequences of disrupting cardiac inwardly rectifying $K^{(+)}$ current ($I_{(K1)}$) as revealed by the targeted deletion of the murine Kir2.1 and Kir2.2 genes. *J.Physiol.* **533**, 697-710.
- Zhang, K. and Ten Eick, R.E.** (1993). Transient outward currents inhibited by activation of protein kinase C but not A in feline ventricular myocytes. *Biophys. J.* **64**, A394.
- Zhang, L., Ina, K., Kitamura, H., Campbell, G. R., and Shimada, T.** (1996). The intercalated disc of monkey myocardial cells and Purkinje fibers as revealed by scanning electron microscopy. *Arch.Histol.Cytol.* **59**, 453-465.
- Zhang, M., Jiang, M., and Tseng, G. N.** (2001). minK-related peptide 1 associates with Kv4.2 and modulates its gating function: potential role as beta subunit of cardiac transient outward channel? *Circ.Res.* **88**, 1012-1019.
- Zhang, Z. J., Jurkiewicz, N. K., Folander, K., Lazarides, E., Salata, J. J., and Swanson, R.** (1994). K^{+} currents expressed from the guinea pig cardiac IsK protein are enhanced by activators of protein kinase C. *Proc.Natl.Acad.Sci.U.S.A.* **91**, 1766-1770.

- Zhong, Y. and Wu, C. F.** (1991). Alteration of four identified K⁺ currents in *Drosophila* muscle by mutations in *eag*. *Science* **252**, 1562-1564.
- Zhong, Y. and Wu, C. F.** (1993). Modulation of different K⁺ currents in *Drosophila*: a hypothetical role for the *Eag* subunit in multimeric K⁺ channels. *J.Neurosci.* **13**, 4669-4679.
- Zhou, J., Yi, J., Hu, N., George, A. L., Jr., and Murray, K. T.** (2000). Activation of protein kinase A modulates trafficking of the human cardiac sodium channel in *Xenopus* oocytes. *Circ.Res.* **87**, 33-38.
- Zhou, Z., Gong, Q., Ye, B., Fan, Z., Makielski, J. C., Robertson, G. A., and January, C. T.** (1998). Properties of HERG channels stably expressed in HEK 293 cells studied at physiological temperature. *Biophys.J.* **74**, 230-241.
- Zhou, Z. and Lipsius, S. L.** (1992). Properties of the pacemaker current (I_f) in latent pacemaker cells isolated from cat right atrium. *J.Physiol* **453**, 503-523.
- Zong, X., Schrieck, J., Mehrke, G., Welling, A., Schuster, A., Bosse, E., Flockerzi, V., and Hofmann, F.** (1995). On the regulation of the expressed L-type calcium channel by cAMP-dependent phosphorylation. *Pflugers Arch.* **430**, 340-347.
- Zou, A., Curran, M. E., Keating, M. T., and Sanguinetti, M. C.** (1997). Single HERG delayed rectifier K⁺ channels expressed in *Xenopus* oocytes. *Am.J.Physiol* **272**, H1309-H1314.
- Zygmunt, A. C.** (1994). Intracellular calcium activates a chloride current in canine ventricular myocytes. *Am.J.Physiol* **267**, H1984-H1995.
- Zygmunt, A. C., Eddlestone, G. T., Thomas, G. P., Nesterenko, V. V., and Antzelevitch, C.** (2001). Larger late sodium conductance in M cells contributes to electrical heterogeneity in canine ventricle. *Am.J.Physiol Heart Circ.Physiol* **281**, H689-H697.
- Zygmunt, A. C. and Gibbons, W. R.** (1991). Calcium-activated chloride current in rabbit ventricular myocytes. *Circ.Res.* **68**, 424-437.
- Zygmunt, A. C. and Gibbons, W. R.** (1992). Properties of the calcium-activated chloride current in heart. *J.Gen.Physiol* **99**, 391-414.
- Zygmunt, A. C., Goodrow, R. J., and Antzelevitch, C.** (2000). I(NaCa) contributes to electrical heterogeneity within the canine ventricle. *Am.J.Physiol Heart Circ.Physiol* **278**, H1671-H1678.

**CHAPTER 2. CHARACTERIZATION OF POTASSIUM CURRENTS
IN CANINE AND HUMAN CARDIAC PURKINJE CELLS**

There is little information available about repolarizing currents in cardiac Purkinje cells (PCs) from whole-cell patch clamp studies in isolated single cells; moreover, there is no information available about these currents in human PCs. The work described in Chapter 2 attempted to characterize specifically the repolarizing K^+ currents in PCs in comparison to those in ventricular myocytes (VM). The dog was used for initial study because of its similarity in atrial and ventricular ionic current properties and mechanisms of disease-induced remodeling to man. We first optimized a PC isolation technique. This allowed us to characterize repolarizing currents in single PCs in detail. We first characterized the properties of the transient outward current I_{to} in canine PCs and then extended the study of I_{to} and other K^+ repolarizing currents to human PCs.

A comparison of transient outward currents in canine cardiac Purkinje cells and ventricular myocytes

WEI HAN,^{1,3} ZHIGUO WANG,^{1,2} AND STANLEY NATTEL^{1,2,3}

¹Department of Medicine and Research Center, Montreal Heart Institute, Montreal, Quebec H1T 1C8; ²Department of Medicine, University of Montreal, Montreal, Quebec H3C 3J7; and ³Department of Pharmacology and Therapeutics, McGill University, Montreal, Quebec, Canada H3G 1Y6

Received 5 November 1999; accepted in final form 3 February 2000

Han, Wei, Zhiguo Wang, and Stanley Nattel. A comparison of transient outward currents in canine cardiac Purkinje cells and ventricular myocytes. *Am J Physiol Heart Circ Physiol* 279: H466–H474, 2000.—Although abnormalities in Purkinje cell (PC) repolarization are important causes of cardiac arrhythmias, the detailed properties of repolarizing currents in PCs are incompletely understood. We compared transient outward K⁺ current (*I*_{to}) in single PCs from canine false tendons with midmyocardial ventricular myocytes (VMs). *I*_{to} reactivation was biexponential, with a similar rapid-phase time constant (30 ± 5 and 35 ± 4 ms for VM and PC, respectively) but a large, slow component in PCs with a much greater time constant than VM (1,427 ± 70 vs. 181 ± 24 ms, *P* < 0.001). Tetraethylammonium had no effect on VM *I*_{to} but reversibly inhibited PC *I*_{to} (IC₅₀ = 2.4 ± 0.4 mM). PC *I*_{to} was also more sensitive to 4-aminopyridine (IC₅₀ = 50 ± 7 vs. 526 ± 49 μM in VM, *P* < 0.0001). H₂O₂ slowed *I*_{to} inactivation in PCs but did not affect VM *I*_{to}. We conclude that PC *I*_{to} shows significant differences from VM *I*_{to}, with some features, such as tetraethylammonium sensitivity, that have been reported in neither cardiac *I*_{to} of atrial or ventricular myocytes nor cloned K⁺ channel subunits (Kv1.4, Kv4.2, or Kv4.3) known to participate in cardiac *I*_{to}.

potassium channels; molecular biology of cardiac ion channels; cardiac arrhythmias; action potentials; potassium channel blockers; antiarrhythmic drugs

PURKINJE FIBERS are responsible for the rapid propagation of the cardiac impulse to the ventricles, provide life-saving ventricular escape rhythms if atrioventricular block occurs, and generate the arrhythmogenic early afterdepolarizations that cause the potentially lethal ventricular arrhythmias associated with the long Q-T syndrome (25, 31). The acquired long Q-T syndrome is the most serious complication limiting treatment with action potential (AP)-prolonging drugs (class IA and III) that are otherwise quite effective for reentrant cardiac arrhythmias. In contrast to atrial and ventricular myocytes, where the ion channel electrophysiology has been well characterized with patch-clamp methods, much less work has been done to study repolarizing currents in single Purkinje cells. Although

many voltage-clamp studies of cardiac Purkinje fibers were performed with classical two-electrode voltage-clamp methods, the inherent limitations of this methodology leave important questions about the ionic determinants of repolarization in Purkinje fibers unanswered. The present study was designed to characterize Ca²⁺-independent transient outward K⁺ current (*I*_{to}) in single canine Purkinje cells and compare it with *I*_{to} of canine ventricular myocytes. Because of the known variations in transient outward current of cells from different regions within the ventricular wall (23), midmyocardial cells were used, since these cells exhibit some properties intermediate between those of myocardial and Purkinje cells (34).

MATERIALS AND METHODS

Cell preparation. Adult mongrel dogs (20–30 kg) were anesthetized with pentobarbital sodium (30 mg/kg iv), and their hearts were removed and immersed in Tyrode solution equilibrated with 100% O₂. Purkinje fiber false tendons were excised from both ventricles into modified MEM (GIBCO-BRL) with 100 μM CaCl₂-containing collagenase (1,000 U/ml, Worthington type II) and 1% BSA (Sigma Chemical). The fibers were bubbled with 100% O₂ in a 37°C shaker bath for 50–100 min. After the endothelial sheath had been digested, revealing columns of Purkinje cells under light microscopy, the fibers were washed twice with a high-K⁺ salt solution and incubated for an additional 10 min. Individual cells were dispersed by hand pipetting, concentrated by centrifugation for 1 min, and kept in a high-K⁺ storage solution. Ventricular myocytes were isolated from the left ventricular free wall as previously described in detail (22) and kept in a high-K⁺ storage solution.

Solutions. The standard Tyrode solution for cell isolation and patch-clamp studies contained (mM) 136 NaCl, 5.4 KCl, 1.0 MgCl₂, 1.0 CaCl₂, 0.33 NaH₂PO₄, 5.0 HEPES, and 10 dextrose; pH was adjusted to 7.4 with NaOH. The high-K⁺ storage solution contained (mM) 20 KCl, 10 KH₂PO₄, 10 dextrose, 70 glutamic acid, 10 β-hydroxybutyric acid, 10 taurine, 10 EGTA, and 0.1% albumin; pH was adjusted to 7.4 with KOH. The pipette solution contained (mM) 110 potassium aspartate, 20 KCl, 1 MgCl₂, 5 Mg₂ATP, 10 HEPES, 5 phosphocreatine, 0.1 GTP, and 5 EGTA for current record-

Address for reprint requests and other correspondence: S. Nattel, Research Center, Montreal Heart Institute, 5000 Belanger St. E., Montreal, QC, Canada H1T 1C8 (E-mail: nattel@icm.umontreal.ca).

The costs of publication of this article were defrayed in part by the payment of page charges. The article must therefore be hereby marked "advertisement" in accordance with 18 U.S.C. Section 1734 solely to indicate this fact.

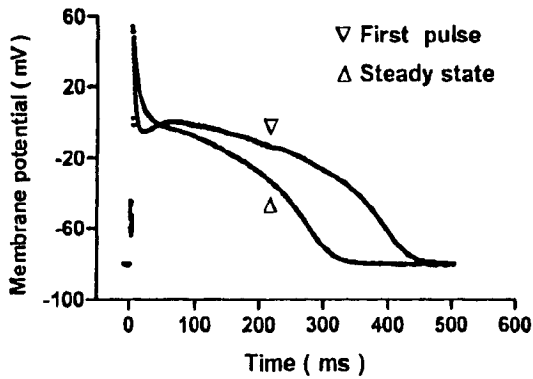


Fig. 1. Purkinje cell action potential (AP) on the onset of stimulation at 2 Hz. First AP after a 60-s pause and steady-state AP after 5 s of stimulation are shown.

ings or 0.05 EGTA for AP recordings; pH was adjusted to 7.2 with KOH. The high- K^+ salt solution contained (mM) 160 potassium glutamate, 5.7 $MgCl_2$, and 5 HEPES; pH was adjusted to 7.0 with KOH. For voltage-clamp studies, atropine (1 μM) was included in the extracellular solution to eliminate basal ACh-dependent K^+ current and $CdCl_2$ (200 μM) was included to block Ca^{2+} current (I_{Ca}).

Contamination by Na^+ current (I_{Na}) was prevented with a holding potential (HP) of -50 mV or by isomolar substitution with choline or Tris when more-negative HPs were necessary.

Data acquisition and analysis. General voltage-clamp techniques were carried out as previously described in detail (22, 41, 42), with recordings performed at $37^\circ C$. I_{to} amplitude was measured from the peak current level to the steady-state level at the end of a depolarizing pulse. Junction potential offsets averaged 10.0 ± 0.4 mV and were corrected for APs only. Smaller Purkinje cells were selected to ensure adequate voltage control. Mean capacitance averaged 125 ± 6 pF ($n = 40$) for Purkinje cells and 113 ± 6 pF ($n = 22$) for ventricular

myocytes. Compensated series resistance averaged 2.2 ± 0.5 and 2.1 ± 0.6 M Ω , respectively.

A nonlinear least-square curve-fitting program (CLAMP-FIT in pCLAMP 6) was used to perform exponential curve fitting. ANOVA with Bonferroni's t -test was used for multiple group comparisons and t -tests for single comparisons. $P < 0.05$ was considered to indicate statistical significance. Values are means \pm SE.

RESULTS

Purkinje cell APs. Figure 1 shows the behavior of a typical Purkinje cell AP after the onset of stimulation at 2 Hz. For clarity, only the response to the first pulse and the steady-state AP are shown. The first AP shows a clear notch, but as stimulation continues and the AP shortens, the notch is much reduced. The AP morphology and response to a pause are very similar to the well-recognized behavior of Purkinje fibers studied with classical microelectrode techniques (e.g., compared with Fig. 12 in Ref. 24).

Voltage dependence of I_{to} . Figure 2A shows representative recordings of I_{to} from a Purkinje cell, and Fig. 2B shows the mean I_{to} density-voltage relation for 36 cells. Figure 2C shows original recordings illustrating voltage-dependent inactivation in one cell. Mean results for experiments analyzing voltage dependence of inactivation (obtained from data of the type shown in Fig. 2C) and activation (obtained with the type of data shown in Fig. 2B, with correction for driving force by dividing by $TP - E_{rev}$, where TP is test potential and E_{rev} is the reversal potential of tail currents) are shown in Fig. 2D. The mean values of half-maximal voltage ($V_{1/2}$) and slope factor for activation (Boltzmann fits) were 8.6 ± 1.4 and 9.8 ± 0.6 mV ($n = 7$), whereas $V_{1/2}$ and slope factor for inactivation averaged -29.9 ± 1.9 and -10.7 ± 1.1 mV ($n = 13$). Corresponding $V_{1/2}$ and

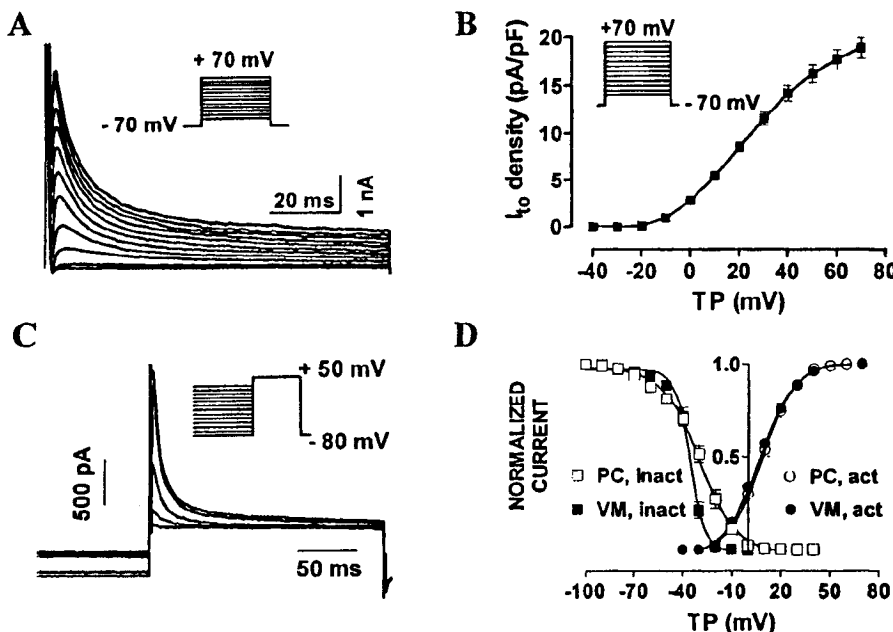
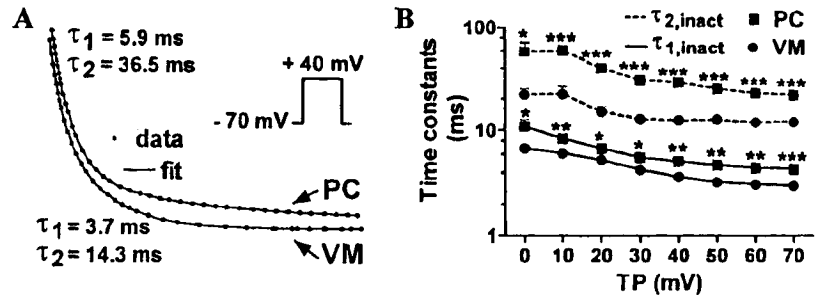


Fig. 2. A: representative recordings of transient outward K^+ current (I_{to}) in a Purkinje cell obtained during 100-ms voltage steps at 0.1 Hz from a holding potential (HP) of -70 mV. B: I_{to} density-voltage relations for 36 Purkinje cells. TP, test potential. Values are means \pm SE. C: recordings from an experiment assessing the voltage dependence of Purkinje I_{to} inactivation. A 200-ms test pulse to $+50$ mV was preceded by 1-s conditioning pulses to voltages between -120 and $+40$ mV (HP -80 mV, protocol applied at 0.1 Hz). For clarity, only recordings obtained with prepulse potentials of -120 , -70 , -30 , -20 and -10 mV are shown. D: data (means \pm SE) from experiments assessing the voltage dependence of Purkinje cell (PC) and ventricular myocyte (VM) inactivation (inact) and activation (act). Inactivation was studied as illustrated in C, and activation was assessed from the current-voltage relation with a correction for the driving force ($TP - E_{rev}$, where E_{rev} is the reversal potential determined from the reversal of I_{to} tail currents, which averaged -75 mV for Purkinje cells and -72 mV for ventricular myocytes). Curves are best-fit Boltzmann relations.

Fig. 3. Time-dependent inactivation of I_{to} in Purkinje cells and ventricular myocytes. *A*: representative data (points prepared with data reduction so curve fits can be seen) during 100-ms depolarizations to +40 mV, with best-fit biexponentials shown. τ , Time constant. *B*: voltage dependence of inactivation time constants. Values are means \pm SE for 12 Purkinje cells and 10 ventricular myocytes. * $P < 0.05$, ** $P < 0.01$, and *** $P < 0.001$ vs. ventricular myocytes.



slope factor values for ventricular myocytes (data also shown in Fig. 2D) were 7.1 ± 0.8 and 10.6 ± 0.2 mV for activation ($n = 9$) and -35.9 ± 1.1 and -4.9 ± 0.5 mV ($n = 9$) for inactivation. The slope factor for inactivation in Purkinje cells was significantly larger ($P < 0.001$) than the value for ventricular muscle cells, and the $V_{1/2}$ was slightly but significantly ($P < 0.05$) less negative. Activation parameters were not significantly different between ventricular and Purkinje cells.

Time-dependent inactivation and recovery. Examples of curve fits to I_{to} decay in illustrative Purkinje and ventricular myocytes are shown in Fig. 3A. Whereas current inactivation was biexponential for both, the time constants were larger in Purkinje cells. This is demonstrated by the mean data shown in Fig. 3B,

which indicate that time constants were significantly greater in Purkinje cells than in ventricular myocytes.

Figure 4 illustrates the time dependence of recovery from inactivation. Original recordings of currents elicited by depolarizing pulses with varying coupling intervals at an HP of -80 mV are shown for a ventricular myocyte in Fig. 4A and for a Purkinje cell in Fig. 4B. Whereas recovery was almost complete within 100 ms in the ventricular myocyte, it required >4 s in the Purkinje cell. Mean recovery data for ventricular and Purkinje cells are provided in Fig. 4, C and D, respectively. At -80 mV, Purkinje I_{to} recovered with time constants of 35 ± 4 and $1,427 \pm 70$ ms ($n = 7$) compared with 30 ± 5 and 181 ± 24 ms, respectively, for ventricular muscle cells ($n = 8$, $P =$ not significant (NS))

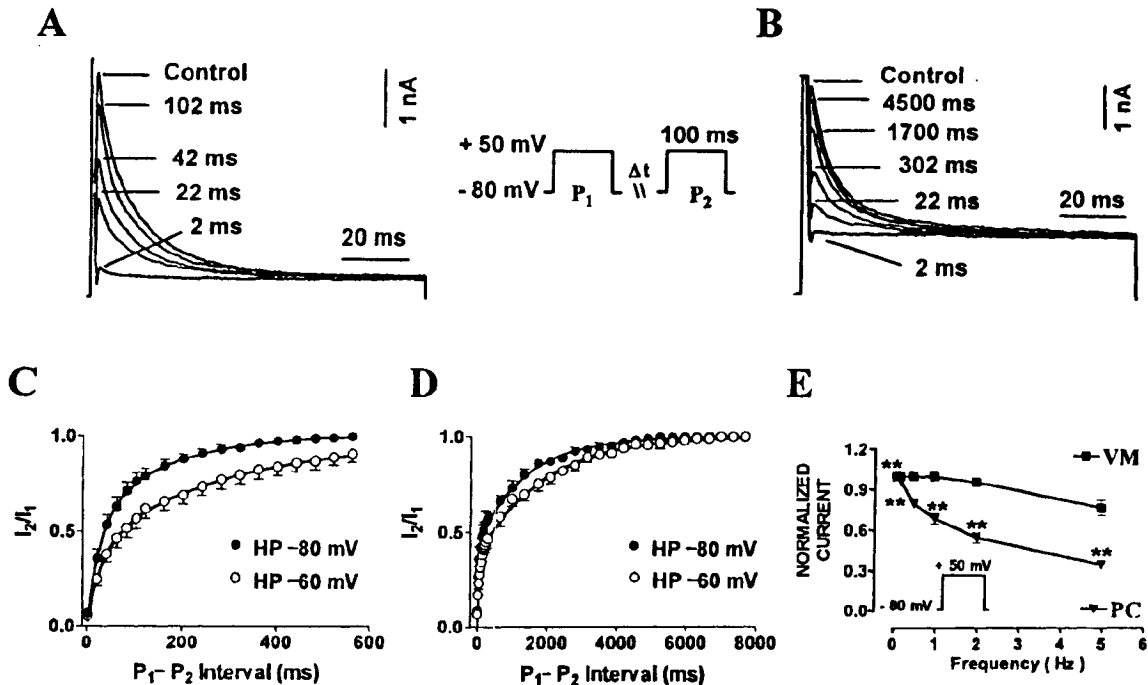


Fig. 4. Time-dependent reactivation of I_{to} , as determined with paired 100-ms pulses (P_1 and P_2) delivered at 0.1 Hz from -80 to $+50$ mV with various P_1 - P_2 intervals. *A* and *B*: recordings at P_1 - P_2 intervals from a representative ventricular myocyte and a Purkinje cell, respectively. *C* and *D*: ratios of current during P_2 (I_2) to current during P_1 (I_1) as a function of P_1 - P_2 interval at HPs of -80 and -60 mV. Values are means \pm SE for 8 ventricular myocytes (*C*) and 7 Purkinje cells (*D*). Best-fit biexponential functions are shown. *E*: frequency dependence of I_{to} as determined by the ratio of the current during the 15th pulse to the current during the 1st pulse of a train of 100-ms pulses from -80 to $+50$ mV. Trains were separated by 60 s at the HP. Values are means \pm SE for 8 Purkinje cells and 6 ventricular myocytes. ** $P < 0.01$ vs. ventricular myocytes.

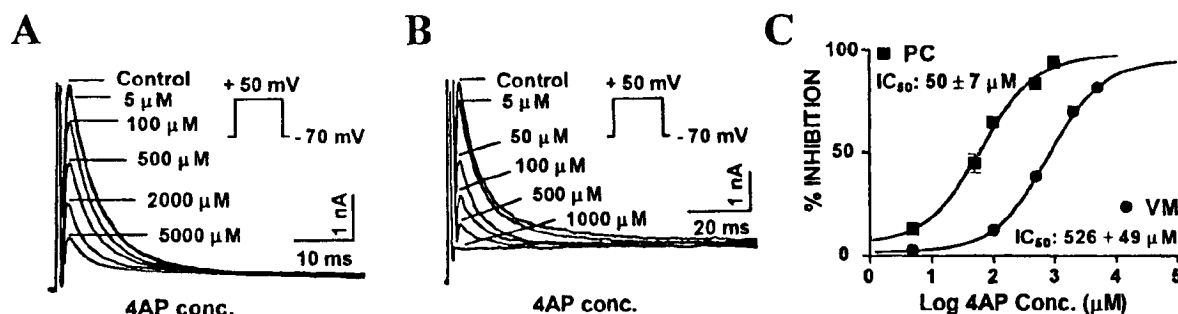


Fig. 5. Inhibition of Purkinje cell and ventricular myocyte I_{to} by 4-aminopyridine (4-AP). *A* and *B*: original recordings of ventricular myocyte and Purkinje cell I_{to} , respectively, obtained during 100-ms pulses from -70 to $+50$ mV before and after exposure to 4-AP. *C*: concentration-response data (means \pm SE) for 4-AP inhibition of I_{to} in 6 ventricular myocytes and 9 Purkinje cells. Curves represent best fit to the equation in RESULTS.

for fast phase, $P < 0.0001$ vs. Purkinje cells for slow-phase time constant]. The slower kinetic component comprised $62 \pm 4\%$ of Purkinje I_{to} reactivation vs. $34 \pm 3\%$ of ventricular muscle reactivation ($P < 0.001$). At -60 mV in the same cells, reactivation time constants were 56 ± 5 and $1,900 \pm 138$ ms for Purkinje cells compared with 29 ± 6 and 307 ± 43 ms for muscle cells ($P < 0.01$ and $P < 0.0001$, respectively). The slower component accounted for $62 \pm 2\%$ of reactivation at -60 mV in Purkinje cells vs. $51 \pm 8\%$ in muscle cells ($P = \text{NS}$).

The frequency dependence of I_{to} in Purkinje cells and ventricular myocytes is compared in Fig. 4*E*, with steady-state I_{to} at each frequency plotted as a function of I_{to} of the first pulse after 60 s at the HP. Purkinje I_{to} showed substantially greater frequency dependence. For example, at 2 Hz, steady-state I_{to} in Purkinje cells was $55 \pm 4\%$ of the value during the first pulse, whereas in ventricular myocytes I_{to} at 2 Hz was $96 \pm 3\%$ of the first-pulse value ($P < 0.001$).

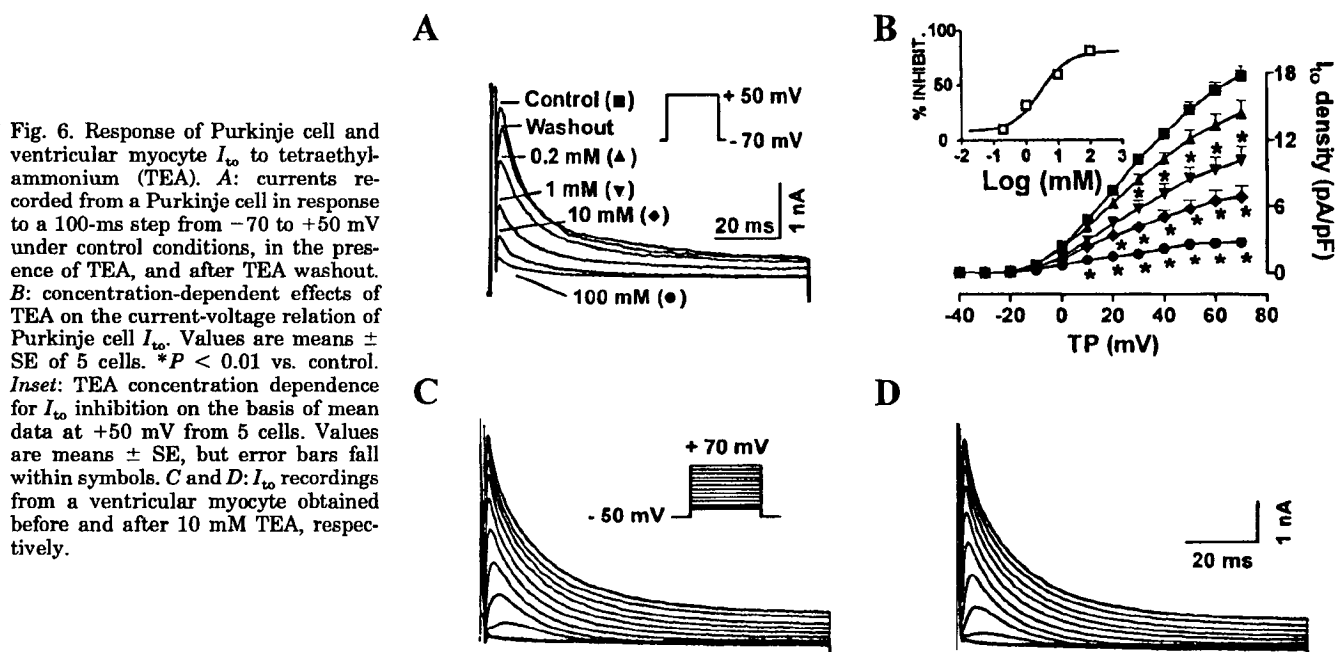
Pharmacological properties of Purkinje I_{to} . 4-Aminopyridine (4-AP) is commonly used to block I_{to} in mammalian cardiac cells (33). Figure 5 illustrates the 4-AP sensitivity of ventricular and Purkinje cell I_{to} . Concentration-response curves were obtained for the inhibition of I_{to} elicited by pulses to $+50$ mV at 0.1 Hz, as illustrated by the original recordings from a ventricular myocyte (Fig. 5*A*) and a Purkinje cell (Fig. 5*B*). Whereas $500 \mu\text{M}$ 4-AP produced $<50\%$ I_{to} inhibition in the ventricular cell, $100 \mu\text{M}$ 4-AP reduced Purkinje I_{to} by $>50\%$. Figure 5*C* shows mean concentration-response data, along with best-fit curves according to the following equation: $B = 100/[1 + (IC_{50}/D)^n]$, where B is the percentage of maximal current block at a concentration D , IC_{50} is the 50% blocking concentration, and n is the Hill coefficient. The 4-AP IC_{50} in Purkinje cells averaged $50 \pm 7 \mu\text{M}$, significantly less than the IC_{50} ($526 \pm 49 \mu\text{M}$) for ventricular myocytes ($P < 0.0001$). The Hill coefficients averaged 1.0 ± 0.1 for Purkinje cells and 1.3 ± 0.1 for ventricular myocytes, suggesting 1:1 stoichiometry for the 4-AP- I_{to} interaction in both cases.

Tetraethylammonium (TEA) is a classical K^+ channel blocker that does not affect canine atrial I_{to} (41). Figure 6*A* shows original recordings of Purkinje I_{to}

before and after exposure to a series of TEA concentrations (TEA was substituted for choline in the extracellular solution for >1 mM TEA to prevent changes in osmolarity). Inhibition appeared rapidly, was clearly observed at 0.2 mM, increased with increasing concentration, and reversed substantially after drug washout. The I_{to} density-voltage relation is shown for different TEA concentrations in Fig. 6*B*. Significant inhibition was seen at all voltages. Maximum inhibition at 100 mM was on the order of 82%. Figure 6, *inset*, shows the concentration-response relation for TEA inhibition, which had an IC_{50} of 2.4 ± 0.4 mM. Figure 6, *C* and *D*, shows I_{to} from a ventricular myocyte before and after exposure to 10 mM TEA. In this and six other cells studied in the same way, 10 mM TEA had no effect on ventricular muscle I_{to} .

The antiarrhythmic drug flecainide has been used to obtain information about the potential molecular basis of I_{to} , because the cloned K^+ channel subunit Kv4 is more sensitive to the drug than the cloned K^+ channel subunit Kv1.4 (40). Figure 7 shows the concentration-dependent effects of flecainide on ventricular cell and Purkinje I_{to} . As shown by the results of representative cells in Fig. 7, *A* and *B*, flecainide produced concentration-dependent inhibition in both cell types. The IC_{50} averaged $29 \pm 13 \mu\text{M}$ ($n = 6$) in ventricular myocytes and $42 \pm 13 \mu\text{M}$ in Purkinje cells ($n = 5$, $P = \text{NS}$). Flecainide accelerated current decay, as previously reported in human atrial myocytes (38), in ventricular and Purkinje cells, decreasing the rapid-phase time constant to a significant and similar extent in each (Fig. 7, *C* and *D*).

Oxidative stress is known to produce significant slowing of I_{to} carried by the Kv1.4 subunit and to have little effect on Kv4 channels (10). Figure 8*A* shows the effects of 0.01% H_2O_2 on I_{to} in a Purkinje cell and a ventricular myocyte. H_2O_2 did not alter I_{to} in the ventricular myocyte but clearly slowed I_{to} inactivation in the Purkinje cell. Mean inactivation time constants in seven Purkinje cells and eight ventricular myocytes before and after H_2O_2 are shown in Fig. 8*B*. A significant increase in the slow-phase time constant was seen in Purkinje cells, with no changes in ventricular myocytes. In addition to slowing the slow-phase time constant, H_2O_2 increased the proportion of inactivation

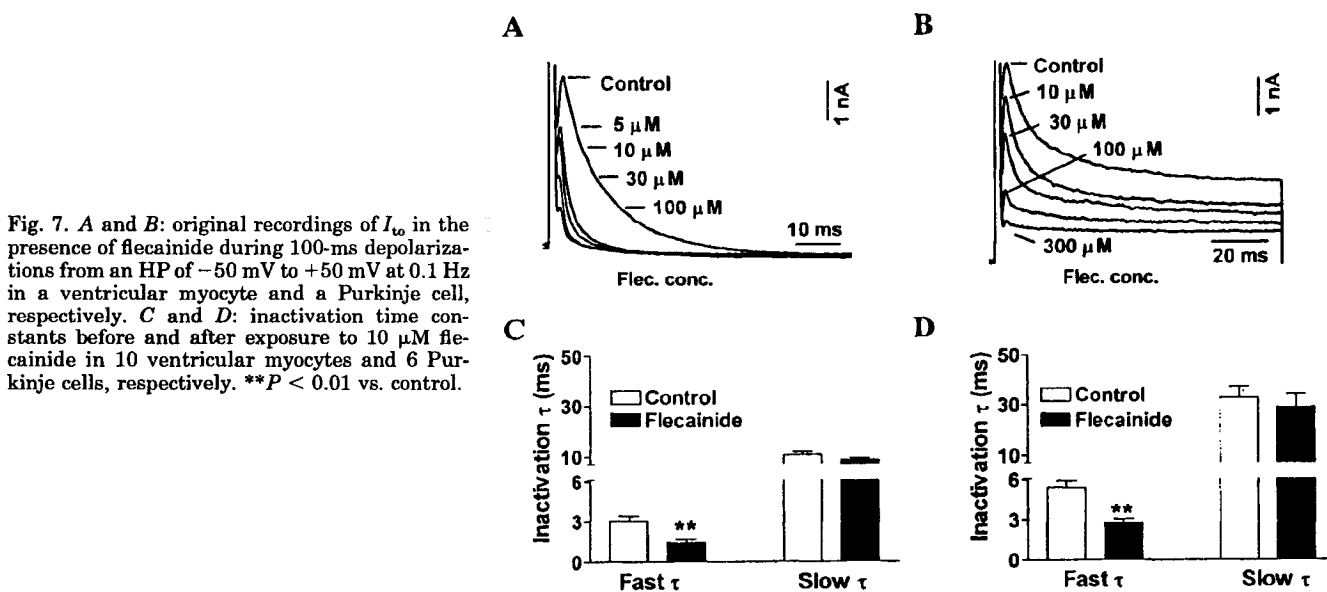


comprised by the slow phase from 41 ± 4 to $54 \pm 6\%$ ($P < 0.05$).

Finally, we evaluated the effects of two toxins known to affect cloned K^+ channels. Blood-depressing substance (BDS) is a sea anemone toxin that specifically and potently ($IC_{50} \sim 50$ nM) inhibits I_{to} carried by the expression of Kv3.4 channels (9). Figure 9A shows the lack of effect of 100 nM BDS on Purkinje cell I_{to} , as seen in this and three other cells studied at the same concentration. At the highest concentration evaluated, i.e., 1 μ M, Purkinje cell I_{to} density before and after BDS averaged 16 ± 2 and 15 ± 3 pA/pF ($P = NS$) on stepping from -50 to $+50$ mV in four cells.

Some members of the *Shaker* subfamily of voltage-gated K^+ channel subunit proteins, including Kv1.1, Kv1.2, and Kv1.3, can be inhibited by TEA as well as dendrotoxin (DTX) (15, 35). As shown in Fig. 9B, relatively high concentrations of DTX (100 nM) slightly reduced I_{to} in Purkinje cells. In eight Purkinje cells exposed to 100 nM DTX, the drug reduced current density by $27 \pm 6\%$ ($P < 0.001$ vs. control). DTX was not found to significantly affect ventricular I_{to} .

Effects of blocking I_{to} on the Purkinje cell AP. To obtain an indication of the potential functional role of 4-AP- and TEA-sensitive I_{to} in the Purkinje cell AP, we exposed Purkinje cells to concentrations of



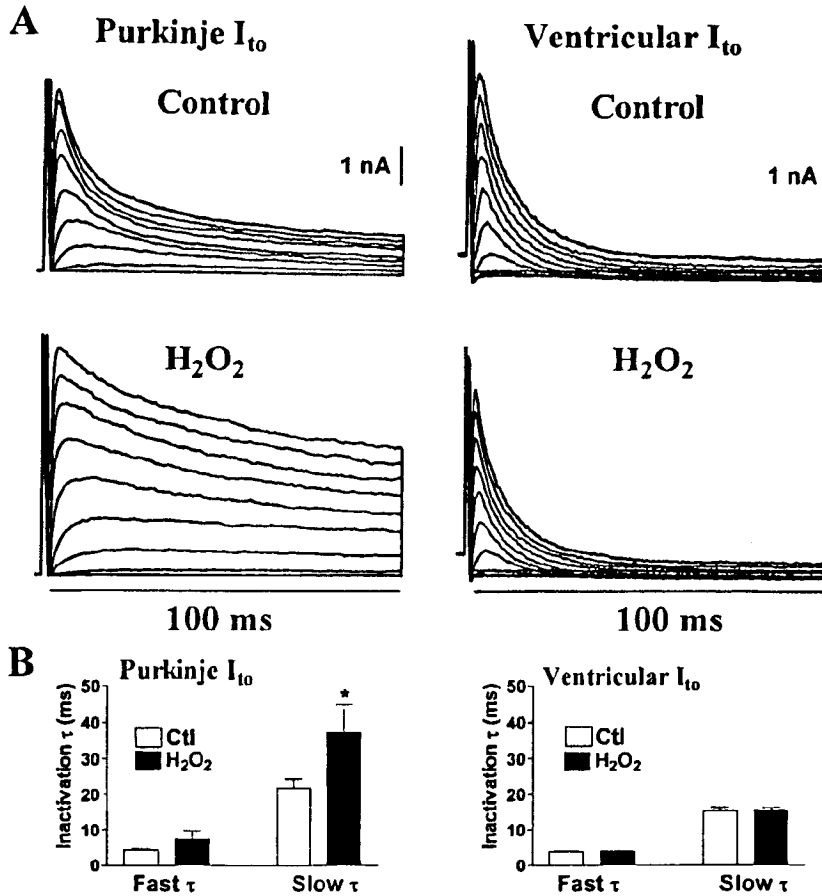


Fig. 8. Effects of H_2O_2 on I_{to} inactivation in Purkinje cells and ventricular myocytes. **A**: original recordings of I_{to} during 100-ms depolarizations from an HP of -50 mV to voltages between -30 and $+50\text{ mV}$ in 10-mV increments before and after 0.01% H_2O_2 . **B**: inactivation time constants before and after exposure to 0.01% H_2O_2 in 7 Purkinje cells and 8 ventricular myocytes. * $P < 0.01$ vs. control (Ctl).

these agents that would be expected to have a selective effect on I_{to} . To confirm the effects of the drugs on ionic currents, we performed voltage clamp with an HP of -50 mV (to inactivate I_{Na}) on each cell from which APs were recorded. Figure 10 shows APs and ionic currents (on depolarization to $+50\text{ mV}$) recorded at 0.1 Hz from representative cells exposed to $50\text{ }\mu\text{M}$ 4-AP (Fig. 10A) and 5 mM TEA (Fig. 10B). The AP changes are consistent with the strong I_{to} inhibition shown by the voltage-clamp recordings, with a marked slowing in repolarization (particularly the earlier phases to 50% repolarization) and elevation of the plateau. AP duration to 20, 50, 70, and 90% repolarization were increased by 86 ± 44 , 119 ± 77 , 12 ± 9 , and $2 \pm 4\%$, respectively ($n = 4$), by 4-AP and

by 53 ± 7 , 84 ± 27 , 30 ± 11 , and $12 \pm 5\%$, respectively, ($n = 6$) by TEA.

DISCUSSION

We have studied the properties of Purkinje cell I_{to} in detail and compared them with those of I_{to} in ventricular cells in the midmyocardium. We found several important differences between Purkinje cell and muscle cell I_{to} , notably in terms of the kinetics of inactivation and recovery from inactivation, frequency dependence, and sensitivity to block by 4-AP and TEA.

Comparison with previous single-cell voltage-clamp studies of I_{to} in cardiac myocytes and putative cloned cardiac I_{to} subunits in heterologous expression systems.

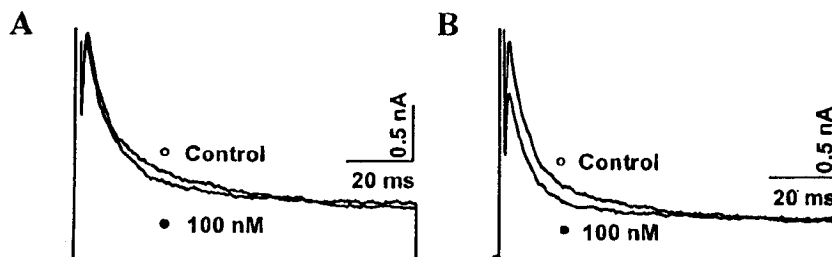


Fig. 9. Effects of blood-depressing substance and dendrotoxin on Purkinje cell I_{to} . Original recordings of I_{to} during 100-ms depolarizations from an HP of -50 mV to $+50\text{ mV}$ are shown before and after blood-depressing substance (A) and dendrotoxin (B).

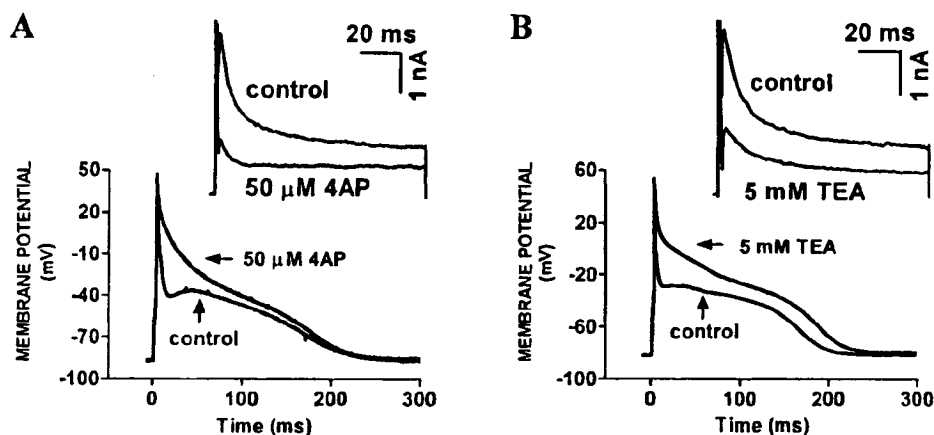


Fig. 10. Effects of 50 μ M 4-AP (A) and 5 mM TEA (B) on APs of Purkinje cells. *Insets*: currents in each cell elicited by a 100-ms pulse from -50 to $+50$ mV. As expected, 4-AP and TEA strongly inhibited I_{to} and delayed repolarization, particularly the earlier phases.

Whereas the properties of canine ventricular I_{to} that we observed are quite consistent with previous observations regarding cardiac I_{to} in a variety of tissues and species (1), those we noted for Purkinje cell I_{to} were quite different in several important respects. Most noteworthy is the sensitivity of Purkinje cell I_{to} to TEA. Similar to canine ventricular I_{to} , canine atrial I_{to} is not affected by TEA at up to 100 mM (41). Similarly, I_{to} in atrial, ventricular, and nodal cells from a variety of species are insensitive to TEA (1). The molecular species recognized to participate in cardiac I_{to} include Kv4.2 (1, 12, 17, 37), Kv4.3 (10, 12, 17, 37), and Kv1.4 (37). None of these are inhibited by TEA, even at relatively large concentrations (10, 29, 35). In addition, the 4-AP sensitivity of Purkinje cell I_{to} is greater than that reported for native atrial (41) or ventricular I_{to} , as well as for Kv1.4 (27) and Kv4.2 (29).

Comparison with previous reports regarding cardiac Purkinje cell I_{to} . The presence of I_{to} in cardiac Purkinje fibers was recognized in early dual-microelectrode voltage-clamp studies of multicellular preparations (8). The ionic specificity of Purkinje cell I_{to} was the subject of some controversy until Kenyon and Gibbons (19, 20) showed in 1979 that $\sim 20\%$ of the current was sensitive to Cl^- substitution, whereas the vast majority could be suppressed by the K^+ channel blockers 4-AP and TEA (19, 20). Formal concentration-response studies were not performed, but 500 μ M 4-AP caused full inhibition of the Cl^- -insensitive component (19). TEA was effective at much higher concentrations (20–40 mM) and required prolonged perfusion (in the range of hours) to act (20). I_{to} recovery in Purkinje fibers has also been shown to be relatively slow, with a reactivation time constant in the range of 500 ms at -80 mV (13). These dual-microelectrode voltage-clamp studies of multicellular preparations were limited by great technical difficulty, potential problems of voltage control, and issues of slow and uneven distribution of drugs requiring diffusion across superfused multicellular preparations. Furthermore, we were unable to find in the previous literature detailed concentration-response analyses for TEA or 4-AP effects on Purkinje fibers or direct comparisons between I_{to} properties in Purkinje and muscle tissue with similar methods. Furthermore, we are not

aware of previous observations regarding the effects of flecainide, oxidative stress, BDS, or DTX on Purkinje cell I_{to} . Cordeiro et al. (7) recently performed voltage-clamp studies of rabbit Purkinje cells from free-running false tendons. They noted a substantial I_{to} , with a current density at $+60$ mV of ~ 15 pA/pF, similar to I_{to} density in canine Purkinje cells in the present study. Rabbit Purkinje cell I_{to} was strongly inhibited by 2 mM 4-AP, but concentration-response analyses were not performed.

Potential mechanisms and significance. The present study is the first of which we are aware to characterize in detail the pharmacological response of canine Purkinje cell I_{to} and to compare directly the biophysical and pharmacological properties of Purkinje cell I_{to} with those of ventricular myocytes from the same species. It is now clear that the *Shal* (Kv4) family of genes play a prominent role in encoding pore-forming K^+ channel subunits of I_{to} in mammalian atrial and ventricular myocytes (2, 12, 37). Recent evidence suggests that Kv1.4 subunits, the first I_{to} -like channel subunits to be cloned from cardiac tissue (30, 36), are also likely to contribute to a slowly recovering I_{to} component in rabbit atrial myocytes (37), rat ventricular septum (39), and ferret ventricular subendocardium (5).

The properties of Purkinje cell I_{to} do not match those of I_{to} carried by any single cloned subunit. The response to oxidative stress and the slowly recovering component resemble the behavior of Kv1.4 channels but are not compatible with the rapidly recovering component and the response to flecainide. The latter responses are compatible with Kv4.x channels, but the former are not. Moreover, the TEA sensitivity of Purkinje cell I_{to} is not compatible with currents carried by any of the subunits (Kv1.4, Kv4.2, or Kv4.3) implicated in atrial and ventricular I_{to} , which are insensitive to TEA at up to 100 mM (10, 29, 35). Furthermore, a large proportion of Purkinje cell I_{to} is TEA sensitive (Fig. 6), indicating that a TEA-sensitive subunit must participate in the formation of most Purkinje cell I_{to} channels. K^+ currents resulting from the expression of the Kv3 (*Shaw* Kv3) family of genes are typically sensitive to TEA, and two Kv3 genes, Kv3.3 and Kv3.4, carry an I_{to} -like current on heterologous expression (14, 28, 32).

Although Kv3 genes have yet to be cloned from cardiac tissue, Brahmajothi et al. (6) showed the presence of Kv3 transcripts with *in situ* hybridization in the ferret heart, and we have described a TEA-sensitive ultra-rapid delayed rectifier in dog atrial cells with functional properties that most closely resemble those of currents carried by Kv3.1 subunit expression (41). On the other hand, the TEA sensitivity of Kv3 channels is about an order of magnitude greater than that of Purkinje cell I_{to}, and the Kv3.4 blocker BDS had no effect on Purkinje cell I_{to}. It thus remains to be determined whether the TEA sensitivity of Purkinje cell I_{to} is due to the presence of a novel K⁺ channel subunit, to coassembly of different α -subunits, or possibly to associated accessory subunits.

I_{to} clearly plays a significant role in Purkinje fiber repolarization. This role is evidenced by the effect of 4-AP and TEA to raise the plateau and prolong AP duration (Fig. 10). The major limitation to antiarrhythmic drug therapy today is the risk of proarrhythmic responses, of which a prime type is torsade de pointes in association with excess Q-T prolongation. The origin of drug-induced torsade appears to be early afterdepolarizations from the Purkinje fiber network (11, 25). Patients with congestive heart failure have a high incidence of sudden death (3) and are particularly predisposed to drug-induced torsade (21). Experimental congestive heart failure causes downregulation of ventricular myocyte I_{to} (18) and is associated with ventricular repolarization abnormalities and a high incidence of sudden death (26). Furthermore, coronary artery disease is also a risk factor for drug-induced torsade (21), and I_{to} is reduced in the subendocardial Purkinje network overlying a myocardial infarction (16). Given the importance of I_{to} in Purkinje fiber repolarization, changes in Purkinje I_{to} may be involved in the genesis of spontaneous and drug-induced ventricular tachyarrhythmias caused by arrhythmogenic afterdepolarizations arising from cardiac Purkinje fibers. The present studies indicate that Purkinje cell I_{to} clearly has important properties that distinguish it from ventricular or atrial myocyte I_{to} and point to a potentially different molecular basis.

Potential limitations. The isolation of cells from free-running Purkinje fiber false tendons is a difficult technique, requiring enzymatic digestion of the surrounding sheath and with enzyme access to cells occurring via diffusion rather than coronary perfusion as for ventricular myocytes. The method of cell isolation can influence cell properties, although I_{to} appears to be relatively resistant to damage by isolation (42). The generally high quality of isolated cells is indicated by our ability to record APs of relatively normal appearance (Fig. 1), preserving the characteristic rate-dependent behavior of the Purkinje cell notch (24), which is due to the slow recovery kinetics of I_{to} (4). On the other hand, there was clear variability in Purkinje cell APs (cf. Figs. 1 and 10), likely because of the greater susceptibility of some currents (e.g., I_{Ca}) to damage by the isolation technique, leading to a more-negative plateau and shorter APs in some cells.

Conclusions. Canine Purkinje cell I_{to} properties show important differences from canine ventricular muscle I_{to}. Furthermore, some of the properties of Purkinje cell I_{to} (notably its TEA sensitivity) differ from those reported for ventricular, atrial, and nodal myocyte I_{to} in a variety of species and from the cloned channel subunits (Kv1.4, Kv4.2, and Kv4.3) presently recognized to underlie cardiac I_{to}. These findings suggest that Purkinje cell I_{to} may have a molecular composition different from that of atrial and ventricular muscle. Given the importance of Purkinje fibers in cardiac electrophysiology and, in particular, in the genesis of ventricular tachyarrhythmias associated with delayed repolarization, these findings are of great potential importance.

The authors thank Chantal St-Cyr for expert technical assistance, Luce Bégin and Annie Laprade for typing the manuscript, and Sylvie Diochot and Michel Lazdunski for providing BDS toxin.

This work was supported by operating grants from the Medical Research Council of Canada and the Quebec Heart Foundation and by the Fonds de Recherche de l'Institut de Cardiologie de Montréal. Z. Wang is a Canadian Heart Foundation research scholar.

REFERENCES

1. Barry DM and Nerbonne JM. Myocardial potassium channels: electrophysiological and molecular diversity. *Annu Rev Physiol* 58: 363–394, 1996.
2. Barry DM, Xu H, Schuessler RB, and Nerbonne JM. Functional knockout of the transient outward current, long-QT syndrome, and cardiac remodeling in mice expressing a dominant-negative Kv4 α -subunit. *Circ Res* 83: 560–567, 1998.
3. Bigger JT Jr. Why patients with congestive heart failure die: arrhythmias and sudden cardiac death. *Circulation* 75 Suppl IV: IV28–IV35, 1987.
4. Boyett MR. Effect of rate-dependent changes in the transient outward current on the action potential in sheep Purkinje fibers. *J Physiol (Lond)* 319: 23–41, 1981.
5. Brahmajothi MV, Campbell DL, Rasmusson RL, Morales MJ, Trimmer JS, Nerbonne JM, and Strauss HC. Distinct transient outward potassium current (I_{to}) phenotypes and distribution of fast-inactivating potassium channel α -subunits in ferret left ventricular myocytes. *J Gen Physiol* 113: 581–600, 1999.
6. Brahmajothi MV, Morales MJ, Liu S, Rasmusson RL, Campbell DL, and Strauss HC. *In situ* hybridization reveals extensive diversity of K⁺ channel mRNA in isolated ferret cardiac myocytes. *Circ Res* 78: 1083–1089, 1996.
7. Cordeiro JM, Spitzer KW, and Giles WR. Repolarizing K⁺ currents in rabbit heart Purkinje cells. *J Physiol (Lond)* 508: 811–823, 1998.
8. Deck KA and Trautwein W. Ionic currents in cardiac excitation. *Pflügers Arch* 280: 63–80, 1964.
9. Diochot S, Schweitz H, Beress L, and Lazdunski M. Sea anemone peptides with a specific blocking activity against the fast inactivation potassium channel Kv3.4. *J Biol Chem* 273: 6744–6749, 1998.
10. Dixon JE, Shi W, Wang HS, McDonald C, Yu H, Wymore RS, Cohen IS, and McKinnon D. Role of the Kv4.3 K⁺ channel in ventricular muscle: a molecular correlate for the transient outward current. *Circ Res* 79: 659–668, 1996.
11. El-Sherif N, Caref EB, Yin H, and Restivo M. The electrophysiological mechanism of ventricular arrhythmias in the long QT syndrome. Tridimensional mapping of activation and recovery patterns. *Circ Res* 79: 474–492, 1996.
12. Fiset C, Clark RB, Shimoni Y, and Giles WR. *Shal*-type channels contribute to the Ca²⁺-independent transient outward K⁺ current in rat ventricle. *J Physiol (Lond)* 500: 51–64, 1997.

13. Fozzard HA and Hiraoka M. The positive dynamic current and its inactivation properties in cardiac Purkinje fibres. *J Physiol (Lond)* 234: 569–586, 1973.
14. Goldman-Wohl DS, Chan E, Baird D, and Heintz N. Kv3.3b: a novel *Shaw*-type potassium channel expressed in terminally differentiated cerebellar Purkinje cells and deep cerebellar nuclei. *J Neurosci* 14: 511–522, 1994.
15. Grissmer S, Nguyen AN, Aiyar J, Hanson DC, Mather RJ, Gutman GA, Karmilowicz MJ, Auperin DD, and Chandy KG. Pharmacological characterization of five cloned voltage-gated K⁺ channels, types of Kv1.1, 1.2, 1.3, 1.5, and 3.1, stably expressed in mammalian cell lines. *Mol Pharmacol* 45: 1227–1234, 1994.
16. Jeck C, Pinto J, and Boyden P. Transient outward currents in subendocardial Purkinje myocytes surviving in the infarcted heart. *Circulation* 92: 465–473, 1995.
17. Johns DC, Nuss HB, and Marban E. Suppression of neuronal and cardiac transient outward currents by viral gene transfer of dominant-negative Kv4.2 constructs. *J Biol Chem* 272: 31598–31603, 1997.
18. Kaab S, Nuss HB, Chiamvimonvat N, O'Rourke B, Pak PH, Kass DA, Marban E, and Tomaselli GF. Ionic mechanisms of action potential prolongation in ventricular myocytes from dogs with pacing-induced heart failure. *Circ Res* 78: 262–273, 1996.
19. Kenyon JL and Gibbons WR. Influence of chloride, potassium, and tetraethylammonium on the early outward current of sheep cardiac Purkinje fibers. *J Gen Physiol* 73: 117–138, 1979.
20. Kenyon JL and Gibbons WR. 4-Aminopyridine and the early outward current of sheep cardiac Purkinje fibers. *J Gen Physiol* 73: 139–157, 1979.
21. Lehmann MH, Hardy S, Archibald D, Quart B, and MacNeil D. Sex difference in risk of torsade de pointes with *dl*-sotalol. *Circulation* 94: 2535–2541, 1996.
22. Li GR, Feng JL, Yue L, Carrier M, and Nattel S. Evidence for two components of delayed rectifier K⁺ current in human ventricular myocytes. *Circ Res* 78: 689–696, 1996.
23. Liu DW, Gintant GA, and Antzelevitch C. Ionic bases for electrophysiological distinctions among epicardial, midmyocardial, and endocardial myocytes from the free wall of the canine left ventricle. *Circ Res* 72: 671–687, 1993.
24. Miller JP, Wallace AG, and Feezor MD. A quantitative comparison of the relation between the shape of the action potential and the pattern of stimulation in canine ventricular muscle and Purkinje fibers. *J Mol Cell Cardiol* 2: 3–19, 1971.
25. Nattel S and Quantz MA. Pharmacological response of quinidine-induced early afterdepolarizations in canine cardiac Purkinje fibres: insights into underlying ionic mechanisms. *Cardiovasc Res* 22: 808–817, 1988.
26. Pak PH, Nuss HB, Tunin RS, Kööb S, Tomaselli GF, Marban E, and Kass D. Repolarization abnormalities, arrhythmia and sudden death in canine tachycardia-induced cardiomyopathy. *J Am Coll Cardiol* 30: 576–584, 1997.
27. Po S, Snyders DJ, Baker R, Tamkun MM, and Bennett PB. Functional expression of an inactivating potassium channel cloned from human heart. *Circ Res* 71: 732–736, 1992.
28. Rettig J, Wunder F, Stocker M, Lichtinghagen R, Mastiaux F, Beckh S, Kues W, Pedarzani P, Schröter KH, Ruppertsberg JP, Veh R, and Pongs O. Characterization of a *Shaw*-related potassium channel family in rat brain. *EMBO J* 11: 2473–2486, 1992.
29. Roberds SL, Knoth KM, Po S, Blair TA, Bennett PB, Hartshorne RP, Snyders DJ, and Tamkun MM. Molecular biology of the voltage-gated potassium channels of the cardiovascular system. *J Cardiovasc Electrophysiol* 4: 68–80, 1993.
30. Roberds SL and Tamkun MM. Cloning and tissue-specific expression of five voltage-gated potassium channel cDNAs expressed in rat heart. *Proc Natl Acad Sci USA* 88: 1798–1802, 1991.
31. Roden DM and Hoffman BF. Action potential prolongation and induction of abnormal automaticity by low quinidine concentrations in canine Purkinje fibers: relationship to potassium and cycle length. *Circ Res* 56: 857–867, 1985.
32. Schroter KH, Ruppertsberg JP, Wunder F, Rettig J, Stocker M, and Pong O. Cloning and functional expression of a TEA-sensitive A-type potassium channel from rat brain. *FEBS Lett* 278: 211–216, 1991.
33. Shibata EF, Drury T, Refsum H, Aldrete V, and Giles W. Contributions of a transient outward current to repolarization in human atrium. *Am J Physiol Heart Circ Physiol* 257: H1773–H1781, 1989.
34. Sicouri S and Antzelevitch C. A subpopulation of cells with unique electrophysiological properties in the deep subepicardium of the canine ventricle: the M cell. *Circ Res* 68: 1729–1741, 1991.
35. Stuhmer W, Ruppertsberg JP, Schroter KH, Sakmann B, Stocker M, Giese KP, Perschke A, Baumann A, and Pongs O. Molecular basis of functional diversity of voltage-gated potassium channels in mammalian brain. *EMBO J* 8: 3235–3244, 1989.
36. Tseng-Crank JC, Tseng GN, Schwartz A, and Tanouye MA. Molecular cloning and functional expression of a potassium channel cDNA isolated from a rat cardiac library. *FEBS Lett* 268: 63–68, 1990.
37. Wang Z, Feng J, Shi H, Pond A, Nerbonne JM, and Nattel S. Potential molecular basis of different physiological properties of the transient outward K⁺ current in rabbit and human atrial myocytes. *Circ Res* 84: 1–11, 1999.
38. Wang Z, Fermini B, and Nattel S. Effects of flecainide, quinidine, and 4-aminopyridine on transient outward and ultrarapid delayed rectifier currents in human atrial myocytes. *J Pharmacol Exp Ther* 272: 184–196, 1995.
39. Xu H, Guo W, and Nerbonne JM. Four kinetically distinct depolarization-activated K⁺ currents in adult mouse ventricular myocytes. *J Gen Physiol* 113: 661–678, 1999.
40. Yeola SW and Snyders DJ. Electrophysiological and pharmacological correspondence between Kv4.2 current and rat cardiac transient outward current. *Cardiovasc Res* 33: 540–547, 1997.
41. Yue L, Feng J, Li GR, and Nattel S. Characterization of an ultrarapid delayed rectifier potassium channel involved in canine atrial repolarization. *J Physiol (Lond)* 496: 647–662, 1996.
42. Yue L, Feng JL, Li GR, and Nattel S. Transient outward and delayed rectifier currents in canine atrium: properties and role of isolation methods. *Am J Physiol Heart Circ Physiol* 270: H2157–H2168, 1996.

Properties of potassium currents in Purkinje cells of failing human hearts

WEI HAN,^{1,3} LIMING ZHANG,¹ GERNOT SCHRAM,^{1,2} AND STANLEY
NATTEL,^{1,2,3}

¹Research Center, Montreal Heart Institute, Montreal, Quebec H1T 1C8; ²Department of Medicine, University of Montreal, Montreal, Quebec H3C 3J7; and ³Department of Pharmacology and Therapeutics, McGill University, Montreal, Quebec H3G 1Y6, Canada

Running Head: Potassium currents in human Purkinje fibers

Address reprint requests to S. Nattel, MD, Research Center, Montreal Heart Institute, 5000 Belanger Street East, Montreal, Quebec H1T 1C8, Canada. Tel.: 514-376-3330 ext. 3990; Fax: 514-376-1355; E-mail: nattel@icm.umontreal.ca

ABSTRACT

Cardiac Purkinje fibers play an important role in cardiac arrhythmias, but no information is available about ionic currents in human cardiac Purkinje cells (PCs). PCs and midmyocardial ventricular myocytes (VMs) were isolated from explanted human hearts. K^+ -currents were evaluated at 37°C with whole-cell patch-clamp. PCs had clear inward-rectifier current (I_{K1}), with a density not significantly different from VMs between -110 and -20 mV. A Cs^+ -sensitive time-dependent hyperpolarization-activated current was measurable negative to -60 mV. Transient outward current (I_{to}) density was smaller, but end-pulse sustained current (I_{sus}) was larger, in PCs vs. VMs. I_{to} recovery was substantially slower in PCs, leading to strong frequency-dependence. Unlike VM I_{to} , which was unaffected by 10-mM tetraethylammonium, Purkinje I_{to} was strongly inhibited by tetraethylammonium, and Purkinje I_{to} was 10-fold more sensitive to 4-aminopyridine than VM. PC I_{sus} was also reduced strongly by 10 mM tetraethylammonium. In conclusion, human PCs demonstrate a prominent I_{K1} , a time-dependent hyperpolarization-activated current, and an I_{to} with pharmacological sensitivity and recovery kinetics different from those in atrium or ventricle and compatible with a different molecular basis.

Key words: ion currents; cardiac Purkinje cells; potassium channel blockers

INTRODUCTION

Cardiac Purkinje fibers play a key role in conduction and arrhythmogenesis. As the prime cellular component of the cardiac conducting system, they are critical for assuring appropriate timing and sequence of ventricular contraction. They appear to play a particularly important role as a generator of early afterdepolarizations and initiator of transmural reentry in Torsades de Pointes arrhythmias associated with long QT syndromes (2, 3, 10, 23). In addition, there is evidence for significant participation of Purkinje cells (PCs) in ventricular tachyarrhythmias due to delayed afterdepolarizations (35), intraventricular reentry (26) and ventricular fibrillation (7).

K^+ -currents are a key determinant of cellular repolarization and consequently of the occurrence of cardiac arrhythmias. Recent work has shown that the properties of K^+ -currents in canine PCs differ from those in ventricular myocytes (13). Furthermore, the properties and molecular basis of specific K^+ -currents in human cardiac cells may be chamber-specific and distinct from those of corresponding regions in hearts of other animals (11, 19, 41, 43). We were unable to identify any voltage-clamp studies of human cardiac PCs in the literature. The objectives of the present study were to isolate PCs from free-running false tendons of human hearts explanted at the time of cardiac transplantation and to characterize a variety of ionic currents by voltage-clamp recording.

MATERIALS AND METHODS

Cell isolation. Free-running false tendons and left ventricular free-wall midmyocardium were obtained from nine explanted failing human hearts removed at the time of cardiac transplantation. Midmyocardial myocytes were used because they share some repolarization and phase-0 upstroke properties with Purkinje tissue (32). Table 1

lists the clinical characteristics of the patient population. The procedures for obtaining the tissues were approved by the Research Ethics Committee of the Montreal Heart Institute.

Free-running endocardial false tendons were excised quickly from both ventricles into modified Eagle's minimum essential medium (Gibco-BRL, pH 7.0 with HEPES-NaOH), followed by incubation with the same solution containing collagenase (1500 U/ml, Worthington type II) and 1% bovine serum albumin (Sigma Chemicals). False tendons were distinguished from trabeculae in that they were pale in color and thinner, and were removed from either ventricle by cutting with fine scissors. The fibers were agitated by continuous bubbling with 100% O₂ in a 37°C shaker bath for 4-6 h. After the endothelial sheath had been digested, revealing single cells and/or cell columns under light microscope, the digested fibers were washed twice with the high-K⁺ storage solution and were incubated for an additional 10 min. Individual cells were dispersed by gentle hand-pipetting, harvested by centrifugation, and kept in a high-K⁺ storage solution. Human ventricular myocytes were isolated with the use of coronary-artery perfusion methods described previously in detail (19). Both PCs and ventricular myocytes were Ca²⁺-tolerant and were studied concurrently within 18 h of isolation. PCs were characterized by a typical spindle-shaped, narrower and longer morphology with much less prominent cross-striations (Fig. 1) compared to VMs, from which they looked clearly different under light microscopy.

Solutions. The standard Tyrode solution for cell isolation and patch-clamp studies contained (mM): 136 NaCl, 5.4 KCl, 1.0 MgCl₂, 1.0 CaCl₂, 0.33 NaH₂PO₄, 5.0 HEPES, 10 dextrose, pH 7.4 (adjusted with NaOH). The high-K⁺ storage solution contained (mM): 20 KCl, 10 KH₂PO₄, 10 dextrose, 70 glutamic acid, 10 β-hydroxybutyric acid, 10 taurine, 10

EGTA, and 0.1% albumin, pH 7.4 (adjusted with KOH). The pipette solution contained (mM): 110 K⁺-aspartate, 20 KCl, 1 MgCl₂, 5 Mg₂ATP, 10 HEPES, 5 phosphocreatine, 0.1 GTP, 5 EGTA, pH 7.2 (adjusted with KOH).

Atropine (1 μM) was included in the extracellular solution to eliminate any basal activity of acetylcholine-activated current (16) and 4-aminopyridine-dependent K⁺ currents (30). CdCl₂ (200 μM) was added to block L-type Ca²⁺ current (I_{CaL}) and Ca²⁺-activated Cl⁻ current. T-type Ca²⁺-current was suppressed by holding at -50 mV and, in one protocol in which a more negative holding potential (-80 mV) was used, by pulsing to a voltage (+50 mV) at which T-type I_{Ca} in PCs is minimal (30). Contamination by Na⁺-current was prevented with a holding potential (HP) of -50 mV or, when a more negative HP was necessary, with Tris-Cl substitution for extracellular NaCl.

Data acquisition and analysis. The whole cell-patch clamp technique was used to record currents at 37°C as previously described in detail (11, 41). The capacitance of PCs averaged 199 ± 17 pF (*n* = 20) and the capacitance of midmyocardial myocytes was 237 ± 23 pF (*n* = 18). Compensated series resistances and capacitive time-constants averaged 2.7 ± 0.2 MΩ and 0.40 ± 0.02 ms for PCs and 1.7 ± 0.4 MΩ and 0.40 ± 0.05 ms for ventricular myocytes respectively. The maximum mean voltage drop across the series resistance was 6 mV. Junction potentials between bath and pipette solutions averaged 10 mV and were not corrected. Drug effects were studied at steady-state, after 5 minutes of exposure at each concentration.

Group data are presented as mean ± SEM. Nonlinear curve fitting was performed with Clampfit in pClamp 6. Student's *t*-tests were used for statistical comparisons. A two-tailed *P* < 0.05 indicated statistical significance.

RESULTS

Inward rectifier current. The inward rectifier K^+ -current (I_{K1}) was recorded as current sensitive to 1-mM Ba^{2+} . Figures 2A and B show typical recordings obtained from a PC and a ventricular myocyte respectively upon voltage steps from -40 mV before (left) and after (middle) the addition of 1-mM Ba^{2+} to the extracellular solution. In these cells, virtually all the current elicited upon voltage steps from -40 mV was suppressed by 1-mM Ba^{2+} . Ba^{2+} -sensitive currents were obtained by digital subtraction of recordings before and after Ba^{2+} , as illustrated in the right panels of Fig. 2A and B. Figure 2C shows mean (\pm SEM) I_{K1} density in five PCs and nine ventricular myocytes as a function of test potential. Currents in both cell types reversed at \sim -70 mV, which when corrected for the junction potential provides an estimated reversal potential of \sim -80 mV. I_{K1} in both cell types showed strong inward rectification, with a small but distinct outward component between about -70 and -20 mV, as shown on an expanded scale in Fig. 2D. No statistically-significant differences in I_{K1} density were observed over the voltage range between -110 and -20 mV; however, I_{K1} density was significantly greater in ventricular myocytes than in PCs at -120 mV.

Hyperpolarization-activated current. In 5/11 PCs subjected to hyperpolarizing steps, clear time-dependent currents were seen on hyperpolarization. Figure 3A shows time-dependent hyperpolarization-activated current (I_H) elicited upon 3910-ms voltage steps from a HP of -50 mV. Such currents were strongly suppressed by 2-mM Cs^+ , as shown in Fig. 3B. Figure 3C shows Cs^+ -sensitive current obtained by digital subtraction. Figure 3D shows mean I_H density-voltage relations in 5 PCs. I_H was relatively large (e.g., mean density -4.5 ± 1.0 pA/pF at -120 mV). Measurable time-dependent inward currents were

detectable at voltages as positive as -60 mV. Current activation kinetics were biexponential, with mean time-constants (τ s) in 5 PCs as shown in Fig. 3E. The proportion of activation in the faster phase decreased progressively at more positive voltages (Fig. 3F). Current activation became slower at more positive potentials, both because of significant voltage-dependent slowing of the rapid-phase time-constant (τ_{fast}) and a decreasing proportion of fast-phase activation at more positive voltages. No time-dependent activating current was observed upon hyperpolarization of ventricular myocytes (12 cells from 4 hearts).

Transient outward current. Voltage and time-dependent properties. Figures 4A and B show typical recordings of transient outward current (I_{to}) from a PC and a ventricular myocyte. Because of slower inactivation in PCs, longer pulses (300 ms) were used for PCs to permit steady-state inactivation (note the difference in time scale for Fig. 4A vs. 4B). I_{to} activated and inactivated rapidly in both cell types, but the sustained “pedestal” component was larger in PCs. Inactivation was best-fitted by biexponential functions. Figure 4C shows mean inactivation time constants in eight PCs and seven ventricular myocytes. Both kinetic components were slower in PCs than in ventricular muscle. Figure 4D shows current density-voltage relations for I_{to} in eight PCs and seven ventricular myocytes. I_{to} density (measured from peak current to end-pulse steady-state) was significant smaller in PCs between $+20$ and $+60$ mV. However, sustained current (I_{sus} , measured from the end-pulse level to the zero current level) density in the same cells was significantly larger between -10 and $+60$ mV in PCs (Fig. 4E). Figure 4F shows mean data for I_{to} activation and inactivation voltage-dependence, based on recordings in five PCs and five ventricular myocytes. Inactivation voltage-dependence was determined with the use of 1000-ms conditioning pulses followed by 200-ms test pulses to $+50$ mV. Activation

voltage-dependence was determined from the relation $I_V = I_{\max}(G_V/G_{\max})(V-V_{\text{rev}})$, where I_V and I_{\max} are current at voltage (V) and maximum current (at the most positive test potential) respectively; G_V and G_{\max} are conductance at voltage V and maximum conductance; and V_{rev} is reversal potential. Data were fitted by Boltzmann relations, as illustrated in the figure. The half-maximal inactivation voltage averaged -27 ± 2 mV in PCs and -21 ± 2 mV in ventricular myocytes ($P = \text{NS}$). The inactivation slope factor in PCs was -13 ± 2 mV, significantly larger than in ventricular myocytes (-5 ± 1 mV, $P < 0.01$). Half-maximal activation occurred at $+20 \pm 9$ and $+17 \pm 6$ mV in PCs and ventricular myocytes respectively ($P = \text{NS}$), and the activation slope-factor averaged 13 ± 5 and 14 ± 5 mV in Purkinje cells and ventricular myocytes ($P = \text{NS}$) respectively.

An analysis of I_{to} recovery kinetics is shown in Fig. 5. Figure 5A shows I_{to} recordings during paired pulses from a PC (left) and a ventricular myocyte (right) during 100-ms conditioning pulses (P_1) from a holding potential of -80 mV to $+50$ mV, followed by currents during test (P_2) pulses with the same duration and voltage at varying P_1P_2 intervals (paired-pulse protocol delivered at 0.1 Hz in ventricular myocytes and 0.066 Hz in PCs). PC I_{to} recovery was extremely slow, whereas I_{to} recovery was much faster in the ventricular myocyte. Figures 5B and C show mean (\pm SEM) data for the time-dependence of I_{to} reactivation in PCs ($n = 4$) and ventricular myocytes ($n = 6$) respectively. The ratio of I_{to} during P_2 to that in P_1 (I_2/I_1 ratio) was plotted as a function of P_1 - P_2 interval and fit with a biexponential function. Ventricular muscle I_{to} had a larger portion ($69 \pm 5\%$) of reactivation in the rapid phase, with a time-constant (τ_1) of 12 ± 1 ms, whereas PC I_{to} had a smaller rapid phase ($38 \pm 2\%$ of total, $P < 0.01$), with a time-constant of 31 ± 7 ms. The majority of Purkinje I_{to} recovery ($62 \pm 1\%$) proceeded very slowly, with a slow-phase

time-constant (τ_2) of 1575 ± 189 ms ($n = 4$). Ventricular I_{to} slow-phase τ_2 averaged 217 ± 55 ms ($n = 6$, $P < 0.001$ vs. PC). Correspondingly, Purkinje I_{to} was much more frequency-dependent than ventricular I_{to} (Fig. 5D).

Sensitivity to K^+ -channel blockers. The sensitivities to the K^+ -channel blockers tetraethylammonium (TEA) and 4-aminopyridine (4AP) are characteristic properties of K^+ -currents (24, 25). Figures 6A and 6B show recordings of I_{to} from a representative PC and a ventricular myocyte obtained upon depolarization to +50 mV before and after exposure to a series of 4AP concentrations. Whereas 500 μ M 4AP almost completely suppressed I_{to} in the PC, it caused less than 50% I_{to} inhibition in the ventricular myocyte. Figure 6C shows mean concentration-response data, along with best-fit Hill equations. The 50% blocking concentration (IC_{50}) for 4AP at +50 mV was 56 ± 7 μ M for Purkinje I_{to} ($n = 4$), significantly less than the IC_{50} of 511 ± 110 μ M ($n = 5$, $P < 0.01$) for ventricular I_{to} . The Hill coefficients averaged 1.9 ± 0.6 and 1.8 ± 0.6 ($P = NS$) respectively.

Figure 6 D and E illustrate the response of a ventricular myocyte (left) and a PC (right) to 10 mM TEA. I_{to} in the ventricular myocyte was not appreciably different before compared to after TEA exposure (Fig. 6D). In four ventricular myocytes, TEA did not significantly affect I_{to} , with a density averaging 9.3 ± 1.3 and 9.1 ± 1.4 pA/pF ($P = NS$) at +50 mV respectively before and after TEA. In contrast, the same concentration of TEA strongly inhibited Purkinje I_{to} , as illustrated by currents from one PC recorded before and after TEA (Fig. 6E). The inset in Fig. 6E shows mean I_{to} in five PCs before and after TEA, which caused a $67 \pm 9\%$ ($P < 0.05$) current reduction.

Sustained component. As mentioned under “Transient outward current” above, we found a larger sustained end-pulse current after I_{to} inactivation in human PCs than in VMs.

The end-pulse current in PCs was inhibited by 4AP, with an IC_{50} of $54 \pm 15 \mu\text{M}$ at +50 mV. For ventricular myocytes, 4AP had no significant effect on the end-pulse current, with a mean $4.6 \pm 2.1\%$ reduction at 1 mM. The end-pulse sustained component in PCs was also sensitive to TEA, which decreased I_{sus} by $46 \pm 5\%$ ($n = 5$, $P < 0.01$) at 10 mM, in contrast to a $4.3 \pm 1.7\%$ decrease ($P = \text{NS}$) in ventricular myocytes at the same concentration. In an attempt to dissociate I_{sus} from I_{to} , we recorded I_{sus} in additional cells with the use of 100-ms prepulses from -50 to $+50$ mV 10 ms before test depolarizations in order to suppress I_{to} , as previously used to study ultra-rapid delayed rectifier current I_{Kur} , in human atrial myocytes (11, 19, 37), followed by a repolarizing step to -40 mV to observe tail currents. I_{sus} either activated very rapidly or was instantaneous (activation kinetics could not be resolved) and showed slow inactivation (Fig. 7A, C), with no tail currents. 4AP ($50 \mu\text{M}$) decreased the current modestly by $33 \pm 8\%$ ($P = \text{NS}$) in five cells (Fig. 7B). TEA (10 mM) reduced the current (Fig. 7D) by $42 \pm 9\%$ ($P < 0.05$, $n = 5$).

DISCUSSION

We have succeeded in isolating human cardiac PCs, in which we have characterized a variety of ionic currents, including I_{K1} , I_{H} , I_{to} and I_{sus} . These currents were compared to corresponding currents in human ventricular myocytes, with some potentially-important differences observed, particularly for I_{to} and I_{sus} .

Comparison with previous studies of corresponding currents in PCs. Although the free-running Purkinje fiber false tendon preparation was widely used for classical voltage-clamp studies in multicellular preparations, much less work has been done in isolated PCs, largely because of the difficulty of isolating single PCs. Cordeiro et al. found I_{K1} to be

much smaller in rabbit PCs than in ventricular myocytes (6). In the present study, we found human PC I_{K1} to be substantial. PC I_{K1} density in our study was significantly smaller than that in ventricular myocytes at -120 mV, but was not significantly different from ventricular muscle I_{K1} density between -110 and 0 mV. Cordeiro et al. found I_{to} to be inhibited by 4AP, but the concentration-dependence of inhibition was not characterized (6). We have previously evaluated in detail the properties of canine PC I_{to} (13). Like human PC I_{to} in the present study, canine PC I_{to} recovered more slowly than ventricular I_{to} , with a large slowly-recovering component. Canine PC I_{to} had time constants averaging 35 and $1,427$ ms, quite similar to the values of 31 and $1,575$ ms for human PC I_{to} in the present study. The 4AP sensitivities of canine PC and ventricular I_{to} were also quite similar to those of human PC and ventricular I_{to} in the present study (13). Additional findings in canine hearts similar to those in the present study were the TEA sensitivity of canine PC I_{to} and the TEA insensitivity of canine ventricular I_{to} (13).

Callewaert et al. studied pacemaker current in single sheep PCs, and found that activation accelerated at more negative potentials (4). The properties of the I_H that we recorded in human PCs are similar to those described by Callewaert et al. Human PC I_H had a rapid kinetic component that activated more rapidly and constituted a larger proportion of current activation at more negative potentials. We found human PC I_H activation kinetics to be biexponential whereas Callewaert used a single time constant to characterize pacemaker current activation (4). The voltage- and time-dependence of I_H in human PCs would be consistent with a role in pacemaker function, although any such inferences must be very cautious in view of our inability to record action potentials from human PCs.

Comparison with other studies of K^+ -currents in the human heart. We were unable to identify previous studies of ionic currents in human cardiac PCs with which to compare our results. Several studies have evaluated human ventricular myocyte I_{to} . Wettwer et al. found I_{to} activation and inactivation voltage-dependence in human ventricular muscle cells (40) that was similar to what we observed. They obtained only a single recovery time constant (~ 20 ms), similar to the rapid-phase time constant in our ventricular myocytes. Nábauer et al. observed regional differences in human ventricular I_{to} , with I_{to} being smaller and recovering more slowly in subendocardial compared to subepicardial tissue (22). The time constants of I_{to} recovery were of the order of 10 and 900 ms for both tissue types, with the fast phase constituting 89% of recovery in subepicardium vs. 4% of subendocardium. Li et al. characterized I_{to} in epicardial, midmyocardial and endocardial regions of the human heart, reporting biexponential recovery with time constants averaging 12, 20 and 34 ms for fast-phase recovery in epicardium, midmyocardium and endocardium respectively, and slow-phase time constants of 229, 254 and 490 ms (18). Recovery was significantly slower in endocardium than in epicardium or midmyocardium and midmyocardial values were of the same order as our observations for midmyocardial ventricular myocytes. Amos et al. studied I_{to} in human atrial and ventricular subepicardial cells (1). They noted a recovery time constant of 24 ms for ventricular I_{to} . Neither atrial nor ventricular I_{to} were affected by 20 mM TEA (1). Cerbai et al. recorded I_f in ventricular myocytes from failing human hearts (5). They noted a density of ~ 2 pA/pF at -120 mV, about half of the value for I_H in human PCs in the present study. I_f activation was found to be monoexponential, with a time constant that increased at more positive voltages, consistent with the voltage-dependence of I_H activation kinetics that we observed.

In the present study, we noted a larger I_{sus} in human PCs compared to ventricular myocytes. Human atrial myocytes also have a larger I_{sus} compared to ventricular (11). Several observations suggest that PC I_{sus} has a different basis compared to atrial. Human atrial I_{sus} shows tail currents, even at 37°C (12): we did not observe I_{sus} tail currents in human PCs at either room temperature or 37°C. Human atrial I_{sus} is insensitive to TEA (37), whereas Purkinje I_{sus} was substantially inhibited by TEA. In fact, the response of PC end-pulse current to 4AP (IC_{50} $54 \pm 15 \mu\text{M}$) and 10 mM TEA ($46 \pm 5\%$ reduction) was quite similar to the effects on PC I_{to} of 4AP (IC_{50} $56 \pm 7 \mu\text{M}$) and 10 mM TEA ($67 \pm 9\%$), suggesting that PC I_{sus} is a non- or slowly-inactivating component of PC I_{to} , rather than a distinct TEA-insensitive current like the I_{Kur} that underlies most of human atrial I_{sus} (11,19).

Potential significance. PCs play an important role in a variety of cardiac arrhythmia mechanisms (2, 3, 7, 10, 23, 26, 35). They seem to be particularly significant in the generation of Torsades de Pointes arrhythmias associated with the long QT syndrome (2, 3, 10, 23), in which abnormalities in repolarization are central. It is therefore important to understand the properties of K^+ -currents that govern PC repolarization. The present study is, to our knowledge, the first voltage-clamp study of K^+ -currents in human cardiac PCs. We previously showed that canine cardiac PCs have I_{to} properties different from those of ventricular and atrial I_{to} (13). In the present study, we found that human PC I_{to} has very similar voltage-dependent, kinetic and pharmacological sensitivity patterns to canine PC I_{to} , with clear differences from human ventricular I_{to} . Furthermore, the sensitivity of human PC I_{to} to TEA contrasts with the TEA insensitivity to concentrations as high as 100 mM (9, 29, 33) of the α -subunits (Kv1.4, Kv4.2 and Kv4.3) believed to underlie

mammalian atrial and ventricular I_{to} (25, 33, 38). These results are compatible with a role for α -subunits other than Kv1.4 and Kv4.x in human PC I_{to} , such as TEA-sensitive Kv3-related subunits (13), which have been found to be expressed at the mRNA (15) and protein (unpublished data) levels in canine PCs.

The hyperpolarization-activated current I_f is believed to play an important role in pacemaker function of automatic cardiac tissues, like Purkinje fibers (8, 31). We found a robust current compatible with I_f in human cardiac PCs, consistent with PC function as cardiac escape pacemakers. We have referred to the current as I_H rather than I_f , because due to the limited number of cells available we could not characterize the current in biophysical detail. Substantial I_H was present at -70 mV and measurable current was still present at -60 mV, compatible with the voltage range of pacemaker activity in PCs of other species. Shi et al. have shown that rabbit Purkinje fibers are rich in mRNA corresponding to HCN1 and HCN4 (31), which encode cyclic nucleotide-sensitive cation channels with distinctive properties that strongly resemble I_f (21). Because expression studies of HCN channels have generally been performed at room temperature (21), it is difficult to compare directly the kinetics and voltage-dependence of human PC I_H components with those of cloned channels- further work in this area is of potentially great interest.

Potential limitations. The isolation of PCs from human cardiac false tendons was very difficult, with a very small number of Ca^{2+} -tolerant PCs available from each isolation. Action potentials could be recorded only rarely and had an abnormal, triangularized morphology. We were unable to record delayed-rectifier K^+ -currents, known to be particularly sensitive to isolation technique (42). Of note, PCs are notoriously difficult to isolate even from normal animal hearts, and several studies have been unable to record

significant I_K from PCs (6, 27) isolated from the hearts of animals in which I_K blockers are known to prolong Purkinje fiber action potential duration (20, 34). The currents we selected for study were large and had reproducible properties across cells. I_{to} in particular is known to be resistant to cell isolation (42).

The hearts from which PCs were isolated were clearly diseased and patients were taking a variety of medications that could have affected the results. These are well-recognized limitations of virtually all voltage-clamp studies of human ventricular myocytes in the literature, which have almost invariably been obtained from explanted recipient heart tissue obtained at the time of heart transplantation. The only exceptions are studies from countries in which explanted donor hearts are used for valve transplantation and cardiac tissue may be available for electrophysiological study (36), and studies of small (~5 mg) tissue cores obtained by myocardial biopsy (17, 39). Myocardial biopsy specimens are not useful for PC isolation. Despite the fact that the PCs we obtained were from diseased hearts, we were able to record large currents with analyzable properties compatible with those of corresponding currents previously studied in animal models. PC ionic currents are remodelled by CHF (14), with down-regulation of both I_{K1} and I_{to} densities but no change in their other properties. We were careful to compare currents in PCs with those of ventricular myocytes from the same hearts; because comparable down-regulation occurs in ventricular myocytes (28) and PCs (14) the comparisons should have at least qualitative validity. Nevertheless, our results must be considered in the context of the potential role of cardiac disease and cell isolation effects.

We identified PCs on the basis of their characteristic appearance and the fact that they were isolated from free-running false tendons. Previous studies have used similar approaches (4, 6, 27). Unfortunately, there is no independent marker that typifies PCs

with absolute certainty, requiring us (as well as previous investigators) to rely on these criteria. The characteristic features of human PC I_{to} that we observed, which are different from those of human ventricular I_{to} in the present study and from mammalian atrial or ventricular I_{to} in numerous previous studies, make it unlikely that our PC population was contaminated by ventricular myocytes.

Unlike Cerbai et al (5), we were unable to record I_f from ventricular cardiomyocytes of failing hearts. We are unable to account for this discrepancy in a direct way, although it may be related to differences in patient population and/or recording methods. We used Cd^{2+} to inhibit I_{Ca} in studies of I_{to} and I_{sus} . Divalent cations like Cd^{2+} can produce shifts in current voltage-dependence by neutralizing fixed negative surface charges, a phenomenon that must be kept in mind when considering our results.

ACKNOWLEDGEMENTS

The authors thank the Canadian Institutes of Health Research (CIHR) and the Quebec Heart Foundation for research funding, Evelyn Landry for expert technical assistance and France Thériault and Annie Laprade for secretary help with the manuscript. Wei Han was supported by a Heart and Stroke Foundation of Canada studentship and Gernot Schram is the recipient of a CIHR/Aventis fellowship.

REFERENCES

1. **Amos, G. J., E. Wettwer, F. Metzger, Q. Li, H. M. Himmel, and U. Ravens.** Differences between outward currents of human atrial and subepicardial ventricular myocytes. *J. Physiol.* 491: 31-50, 1996.
2. **Asano, Y., J. M. Davidenko, W. T. Baxter, R. A. Gray, and J. Jalife.** Optical mapping of drug-induced polymorphic arrhythmias and torsade de pointes in the isolated rabbit heart. *J. Am. Coll. Cardiol.* 29: 831-842, 1997.
3. **Berenfeld, O., and J. Jalife.** Purkinje-muscle reentry as a mechanism of polymorphic ventricular arrhythmias in a 3-dimensional model of the ventricles. *Circ. Res.* 82: 1063-1077, 1998.
4. **Callewaert, G., E. Carmeliet, and J. Vereecke.** Single cardiac Purkinje cells: general electrophysiology and voltage-clamp analysis of the pace-maker current. *J. Physiol.* 349: 643-661, 1984.
5. **Cerbai, E., R. Pino, F. Porciatti, G. Sani, M. Toscano, M. Maccherini, G. Giunti, and A. Mugelli.** Characterization of the hyperpolarization-activated current, I_f , in ventricular myocytes from human failing heart. *Circulation* 95: 568-571, 1997.
6. **Cordeiro, J. M., K. W. Spitzer, and W. R. Giles.** Repolarizing K^+ currents in rabbit heart Purkinje cells. *J. Physiol.* 508: 811-823, 1998.
7. **Damiano, R. J., Jr, P. K. Smith, H. F. Tripp, Jr, T. Assano, K. W. Small, J. E. Lowe, R. E. Ideker, and J. L. Cox.** The effect of chemical ablation of the endocardium on ventricular fibrillation threshold. *Circulation* 74: 645-652, 1986.

8. **Di Francesco, D.** A study of the ionic nature of the pace-maker current in calf Purkinje fibres. *J. Physiol.* 314: 377-393, 1981.
9. **Dixon, J. E., W. Shi, H. S. Wang, C. McDonald, H. Yu, R. S. Wymore, I. S. Cohen, and D. McKinnon.** Role of the Kv4.3 K⁺ channel in ventricular muscle. A molecular correlate for the transient outward current. *Circ. Res.* 79: 659-668, 1996.
10. **El-Sherif, N., E. B. Caref, H. Yin, and M. Restivo.** The electrophysiological mechanism of ventricular arrhythmias in the long QT syndrome. Tridimensional mapping of activation and recovery patterns. *Circ. Res.* 79: 474-492, 1996.
11. **Feng, J., B. Wible, G. R. Li, Z. Wang, and S. Nattel.** Antisense oligodeoxynucleotides directed against Kv1.5 mRNA specifically inhibit ultrarapid delayed rectifier K⁺ current in cultured adult human atrial myocytes. *Circ. Res.* 80: 572-579, 1997.
12. **Feng, J., D. Xu, Z. Wang, and S. Nattel.** Ultrarapid delayed rectifier current inactivation in human atrial myocytes: properties and consequences. *Am. J. Physiol.* 275: H1717-H1725, 1998.
13. **Han, W., Z. Wang, and S. Nattel.** A comparison of transient outward currents in canine cardiac Purkinje cells and ventricular myocytes. *Am. J. Physiol.* 279 (Heart Circ Physiol): H466-H474, 2000.
14. **Han, W., D. Chartier, D. Li, and S. Nattel.** Ionic remodeling of cardiac Purkinje cells by congestive heart failure. *Circulation* 104: 2095-2100, 2001.
15. **Han, W., Z. Wang, and S. Nattel.** Expression profile of ion channel mRNA in canine cardiac Purkinje fibers – A basis for electrophysiological specificity? (Abstract) *Circulation* 104(Suppl II): II-133, 2001.

16. **Heidbuchel, H., G. Callewaert, J. Vereecke, and E. Carmeliet.** Membrane-bound nucleoside diphosphate kinase activity in atrial cells of frog, guinea pig, and human. *Circ. Res.* 71: 808-820, 1992.
17. **Konarzewska, H., G. A. Peeters, and M. C. Sanguinetti.** Repolarizing K⁺ currents in nonfailing human hearts. Similarities between right septal subendocardial and left subepicardial ventricular myocytes. *Circulation* 92: 1179-1187, 1995.
18. **Li, G. R., J. Feng, L. Yue, and M. Carrier.** Transmural heterogeneity of action potentials and I_{to1} in myocytes isolated from the human right ventricle. *Am. J. Physiol.* 275 (Heart Circ Physiol): H369-H377, 1998.
19. **Li, G. R., J. Feng, L. Yue, M. Carrier, and S. Nattel.** Evidence for two components of delayed rectifier K⁺ current in human ventricular myocytes. *Circ. Res.* 78: 689-696, 1996.
20. **Lu, H. R., R. Marien, A. Saels, and F. De Clerck.** Species plays an important role in drug-induced prolongation of action potential duration and early afterdepolarizations in isolated Purkinje fibers. *J. Cardiovasc. Electrophysiol.* 12: 93-102, 2001.
21. **Moroni, A., L. Gorza, M. Beltrame, B. Gravante, T. Vaccari, M. E. Bianchi, C. Altomare, R. Longhi, C. Heurteaux, M. Vitadello, A. Malgaroli, and D. DiFrancesco.** Hyperpolarization-activated cyclic nucleotide-gated channel 1 is a molecular determinant of the cardiac pacemaker current I_f . *J. Biol. Chem.* 276: 29233-29241, 2001.
22. **Näbauer, M., D. J. Beuckelmann, P. Überfuhr, and G. Steinbeck.** Regional differences in current density and rate-dependent properties of the transient outward

- current in subepicardial and subendocardial myocytes of human left ventricle. *Circulation* 93: 168-177, 1996.
23. **Nattel, S., and M. A. Quantz.** Pharmacological response of quinidine induced early afterdepolarisations in canine cardiac Purkinje fibres: insights into underlying ionic mechanisms. *Cardiovasc. Res.* 22: 808-817, 1988.
 24. **Nattel, S., L. Yue, and Z. Wang.** Cardiac ultrarapid delayed rectifiers: a novel potassium current family of functional similarity and molecular diversity. *Cell. Physiol. Biochem.* 9: 217-226, 1999.
 25. **Nerbonne, J. M.** Molecular basis of functional voltage-gated K⁺ channel diversity in the mammalian myocardium. *J. Physiol.* 525: 285-298, 2000.
 26. **Nibley, C., and J. M. Wharton.** Ventricular tachycardias with left bundle branch block morphology. *Pacing Clin. Electrophysiol.* 18: 334-356, 1995.
 27. **Pinto, J. M., and P. A. Boyden.** Reduced inward rectifying and increased E-4031-sensitive K⁺ current density in arrhythmogenic subendocardial purkinje myocytes from the infarcted heart. *J. Cardiovasc. Electrophysiol.* 9: 299-311, 1998.
 28. **Priebe, L., and D. J. Beuckelmann.** Simulation study of cellular electric properties in heart failure. *Circ. Res.* 82: 1206-1223, 1998.
 29. **Roberds, S. L., K. M. Knoth, S. Po, T. A. Blair, P. B. Bennett, R. P. Hartshorne, D. J. Snyders, and M. M. Tamkun.** Molecular biology of the voltage-gated potassium channels of the cardiovascular system. *J. Cardiovasc. Electrophysiol.* 4: 68-80, 1993.
 30. **Shi, H., H. Wang, and Z. Wang.** Identification and characterization of multiple subtypes of muscarinic acetylcholine receptors and their physiological functions in canine hearts. *Mol. Pharmacol.* 55: 497-507, 1999.

31. **Shi, W., R. Wymore, H. Yu, J. Wu, R. T. Wymore, Z. Pan, R. B. Robinson, J. E. Dixon, D. McKinnon, and I. S. Cohen.** Distribution and prevalence of hyperpolarization-activated cation channel (HCN) mRNA expression in cardiac tissues. *Circ. Res.* 85: 1-6, 1999.
32. **Sicouri, S., and C. Antzelevitch.** A subpopulation of cells with unique electrophysiological properties in the deep subepicardium of the canine ventricle. The M cell. *Circ. Res.* 68: 1729-1741, 1991.
33. **Stuhmer, W., J. P. Ruppersberg, K. H. Schroter, B. Sakmann, M. Stocker, K. P. Giese, A. Perschke, A. Baumann, and O. Pongs.** Molecular basis of functional diversity of voltage-gated potassium channels in mammalian brain. *EMBO J.* 8: 3235-3244, 1989.
34. **Varro, A., B. Balati, N. Iost, J. Takacs, L. Virag, D. A. Lathrop, L. Csaba, L. Talosi, and J. G. Papp.** The role of the delayed rectifier component IKs in dog ventricular muscle and Purkinje fibre repolarization. *J. Physiol.* 523: 67-81, 2000.
35. **Verkerk, A. O., M. W. Veldkamp, L. N. Bouman, and A. C. van Ginneken.** Calcium-activated Cl(-) current contributes to delayed afterdepolarizations in single Purkinje and ventricular myocytes. *Circulation* 101: 2639-2644, 2000.
36. **Virag, L., N. Iost, M. Opincariu, J. Szolnoky, J. Szecsi, G. Bogats, P. Szenohradszky, A. Varro, and J. G. Papp.** The slow component of the delayed rectifier potassium current in undiseased human ventricular myocytes. *Cardiovasc. Res.* 49: 790-797, 2001.
37. **Wang, Z., B. Fermini, and S. Nattel.** Sustained depolarization - induced outward current in human atrial myocytes: evidence for a novel delayed rectifier K⁺ current similar to Kv1.5 cloned channel currents. *Circ. Res.* 73: 1061-1076, 1993.

38. **Wang, Z., J. Feng, H. Shi, A. Pond, J. M. Nerbonne, and S. Nattel.** Potential molecular basis of different physiological properties of the transient outward K^+ current in rabbit and human atrial myocytes. *Circ. Res.* 84: 551-561, 1999.
39. **Wang, Z., L. Yue, M. White, G. Pelletier, and S. Nattel.** Differential distribution of inward rectifier potassium channel transcripts in human atrium versus ventricle. *Circulation* 98: 2422-2428, 1998.
40. **Wettwer, E., G. Amos, J. Gath, H. R. Zerkowski, J. C. Reidemeister, and U. Ravens.** Transient outward current in human and rat ventricular myocytes. *Cardiovasc. Res.* 27: 1662-1669, 1993.
41. **Yue, L., J. Feng, G. R. Li, and S. Nattel.** Characterization of an ultrarapid delayed rectifier potassium channel involved in canine atrial repolarization. *J. Physiol.* 496: 647-662, 1996.
42. **Yue, L., J. Feng, G. R. Li, and S. Nattel.** Transient outward and delayed rectifier currents in canine atrium: properties and role of isolation methods. *Am. J. Physiol.* 270 (Heart Circ Physiol): H2157-H2168, 1996.
43. **Yue, L., Z. Wang, H. Rindt, and S. Nattel.** Molecular evidence for a role of Shaw (Kv3) potassium channel subunits in potassium currents of dog atrium. *J. Physiol.* (Lond) 527: 467-478, 2000.

Table. *Patient characteristics*

No.	Age/sex	Heart disease	Medications
1	51/M	CAD	D, F, K, ASA, W, Bd
2	48/M	CAD	D, F, Sp, AT ₁ -I, BB, Statin, Amio
3	32/M	IHSS	F, Sp, K, AT ₁ -I, BB, LAN
4	58/M	DCM	D, F, CEI, BB, LAN, ASA, Amio, Bd
5	62/F	DCM	D, F, Sp, CEI, BB, ASA, Clo, T4, Amio, Bd
6	42/M	DCM	D, F, CEI, BB, W, Mil
7	29/M	DCM	D, F, Sp, CEI, BB, Amio
8	61/M	CAD	D, F, CEI, LAN, W, Statin, Amio
9	51/M	CAD	F, CCB, LAN, ASA, Amio, Bd

CAD, coronary artery disease; IHSS, hypertrophic cardiomyopathy; DCM, dilated cardiomyopathy; D, digoxin; F, furosemide; K, potassium supplement; ASA, aspirin; W, warfarin; Bd, benzodiazepine; Sp, spironolactone; AT₁-I, angiotensin₁-receptor antagonist; BB, beta-blocker; Amio, amiodarone; W, warfarin; LAN, long-acting nitrate; CEI, converting-enzyme inhibitor; Mil, milrinone; Clo, clopidogrel; T4, thyroxin; CCB, calcium-channel blocker.

FIGURE LEGENDS

Figure 1. Photomicrographs of two human cardiac PCs (left) and ventricular myocytes (right) at comparable magnifications. The horizontal scales in each panel indicate 20 μm . PCs were typically longer and thinner than PCs and had less prominent cross-striations.

Figure 2. *A* and *B*: I_{K1} before and after exposure to 1 mM Ba^{2+} , and Ba^{2+} -sensitive I_{K1} obtained by digital subtraction of Ba^{2+} resistant (middle) from pre- Ba^{2+} current (left) in a PC (*A*) and a ventricular myocyte (VM, *B*). *C*, mean \pm SEM I_{K1} density-voltage relation in PCs and VMs. $*P < 0.05$, PC versus VM. *D*, I_{K1} over the range -80 to -20 mV on an enlarged scale. Note that junction potentials were not corrected, so true voltages are ~ 10 mV negative to those shown.

Figure 3. *A* and *B*, representative I_H recordings in the absence (*A*) and presence (*B*) of 2 mM Cs^+ in a PC, obtained with the protocol shown in the inset of *B*. *C*, Cs^+ -sensitive current obtained by digital subtraction of currents in *B* from those in *A*. *D*, mean \pm SEM density-voltage relation of time-dependent current activated by hyperpolarizing steps from -50 mV to various test potential (TP) values. *E*, voltage-dependent I_H activation fast (τ_{fast}) and slow (τ_{slow}) time constants obtained from bi-exponential fits of time-dependent current. *F*, portion of activation in fast component as a function of TP.

Figure 4. *A* and *B*, I_{to} recorded with the voltage protocol in inset of *B* at 0.1 Hz in a PC and a ventricular myocyte respectively. *C*, time constants of I_{to} inactivation. *D*, mean \pm SEM I_{to} density (measured from peak to end-pulse steady-state current) as function of test potential. *E*, I_{sus} (measured from end-pulse to zero current

level) as a function of test potential in PCs and ventricular myocytes. *F*, voltage-dependence of inactivation and activation in PCs and VMs. Curves are best-fit Boltzmann relations. **P* < 0.05, ***P* < 0.01, ****P* < 0.001, PCs versus ventricular myocytes in panels *C-E*.

Figure 5. *A*, I_{to} recorded during a 100-ms pulse to +50 mV (P_1) and during an identical subsequent P_2 pulse at varying P_1 - P_2 intervals in a PC (left) and a ventricular myocyte (right). *B*, mean \pm SEM I_{to} recorded during P_2 pulses (I_2) normalized to current during the P_1 pulse (I_1) as a function of the P_1 - P_2 interval in PCs. The recovery time course was fitted by a biexponential function as shown. Values provided for τ_1 and τ_2 are means for biexponential fits in four cells. *C*, data obtained from six ventricular myocytes with the protocol illustrated in *A*, and analyzed as shown in *B*. *D*, I_{to} frequency-dependence as determined by % decrease of current during the 10th pulse relative to current during the first pulse of a train of 100-ms depolarizations to +50 mV at the frequencies shown. ***P* < 0.01, ****P* < 0.001 for value in PCs versus ventricular myocytes at same frequency.

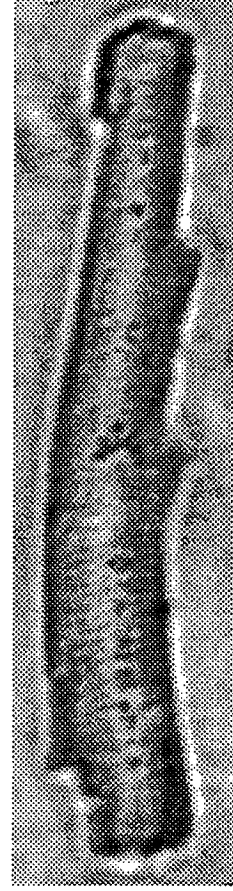
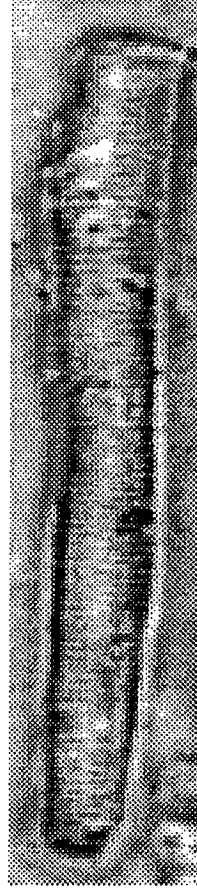
Figure 6. *A* and *B*, recordings of PC (*A*) and ventricular muscle (*B*) I_{to} upon depolarization to +50 mV before (CTL) and during exposure to a series of 4AP concentrations. *C*, Concentration- response curves for I_{to} inhibition by 4AP, along with Hill-equation fits ($n = 4$ PCs, 5 VMs). *D* and *E*, I_{to} recordings from a ventricular myocyte before and after exposure to 10 mM TEA respectively. *F* and *G*, I_{to} in the absence and presence of 10 mM TEA in a PC. *G* inset: PC I_{to} density ($n = 5$) in the absence and presence of 10 mM TEA. **P* < 0.05 versus

control. All drug effects were evaluated after 5 minutes of exposure at each concentration.

Figure 7. *A* and *B*, Purkinje I_{sus} elicited by the protocol shown in the inset of *A*, before and 5 minutes after exposure to 50 μ M 4AP. *C* and *D*, Purkinje I_{sus} before and 5 minutes after 10 mM TEA. Mean \pm SEM of current density before and after 4AP and TEA is shown in the inset of *B* and *D*, respectively. * $P < 0.05$ versus control.

Figure 1

VMs



20 μm

PCs

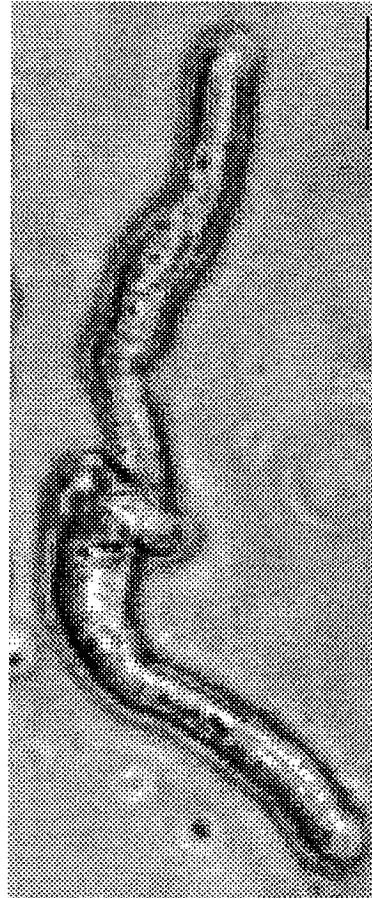
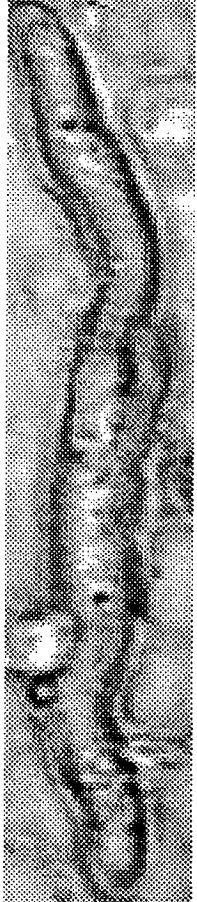


Figure 2

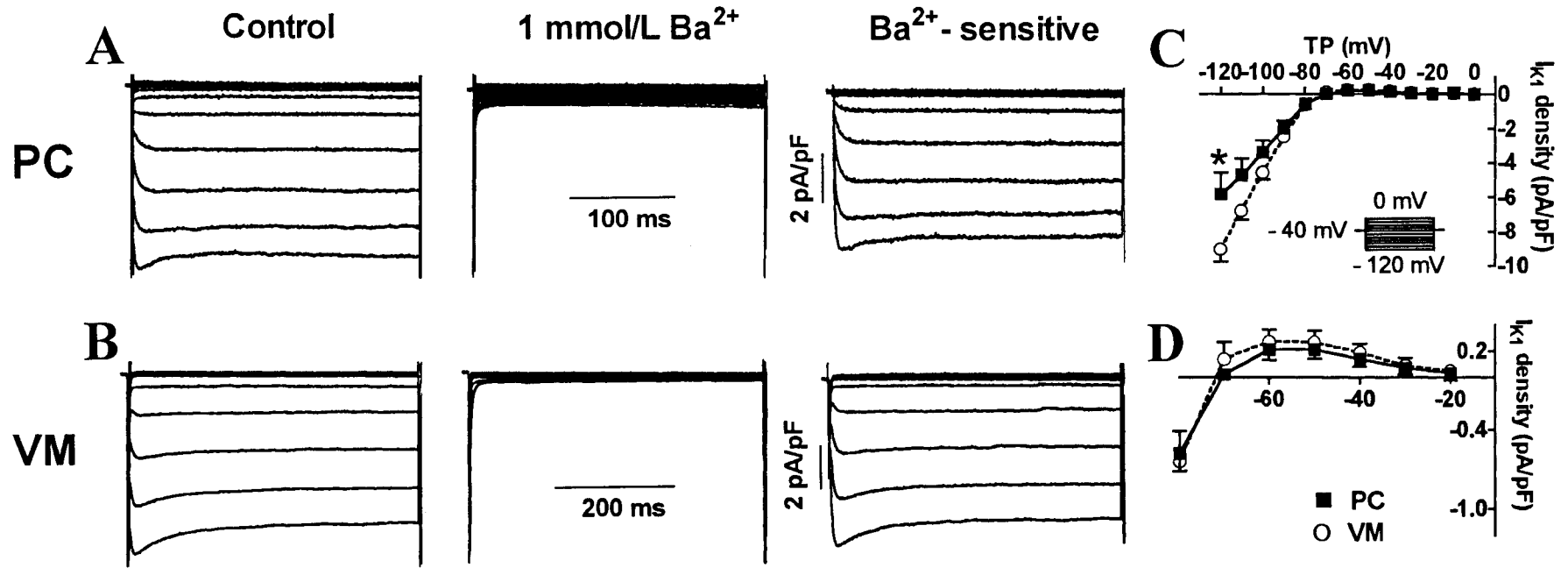


Figure 3

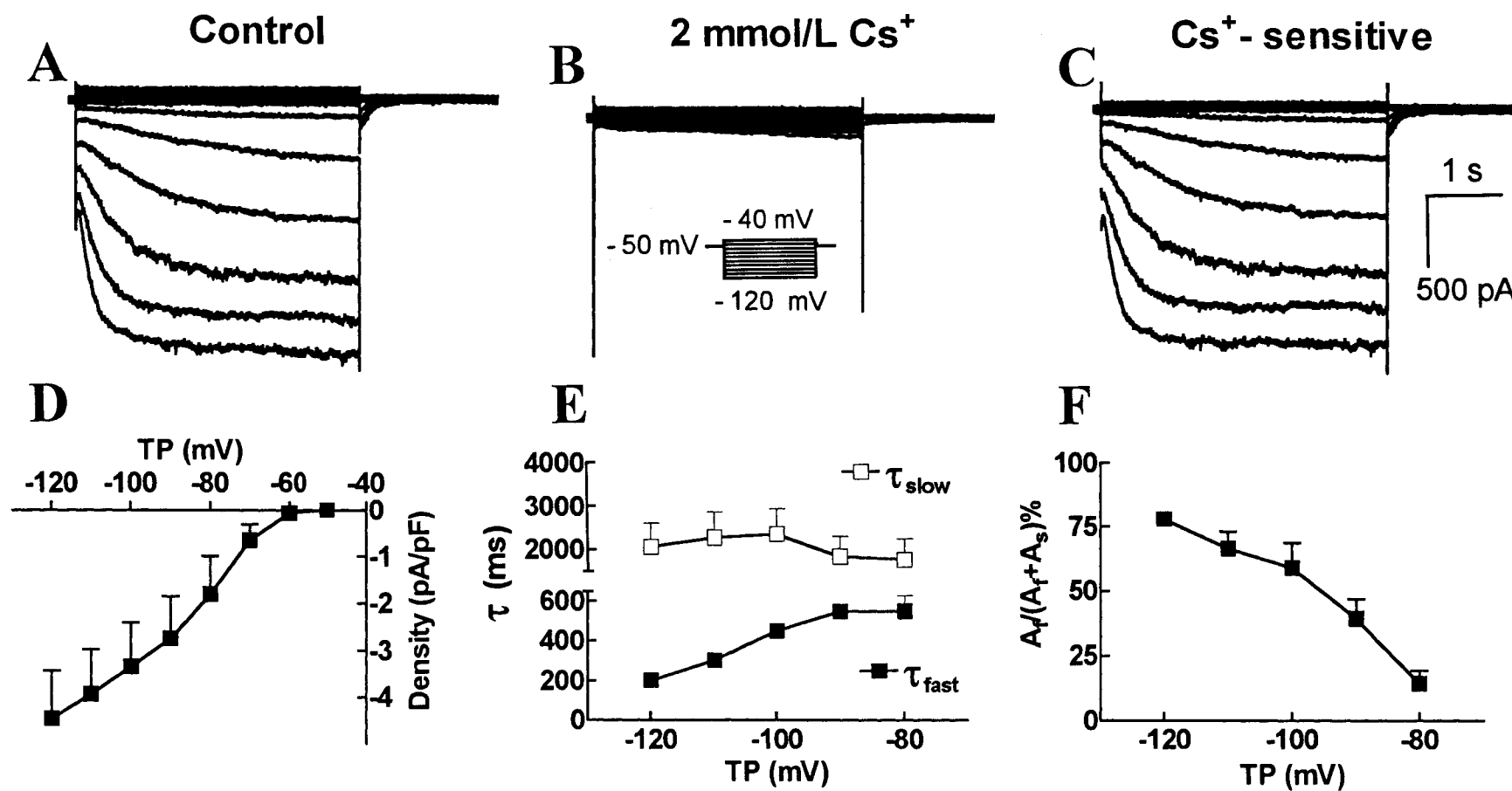


Figure 4

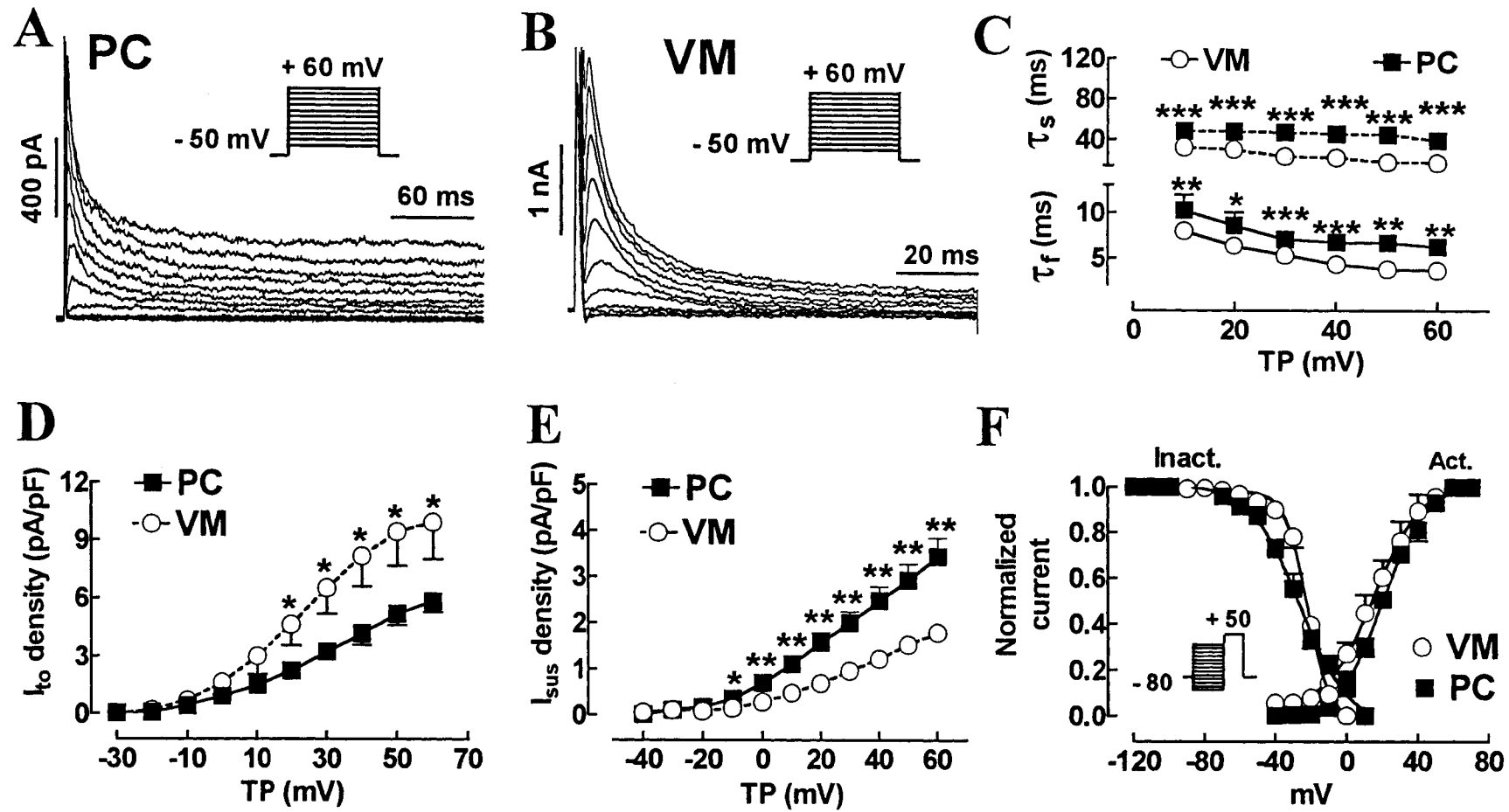


Figure 5

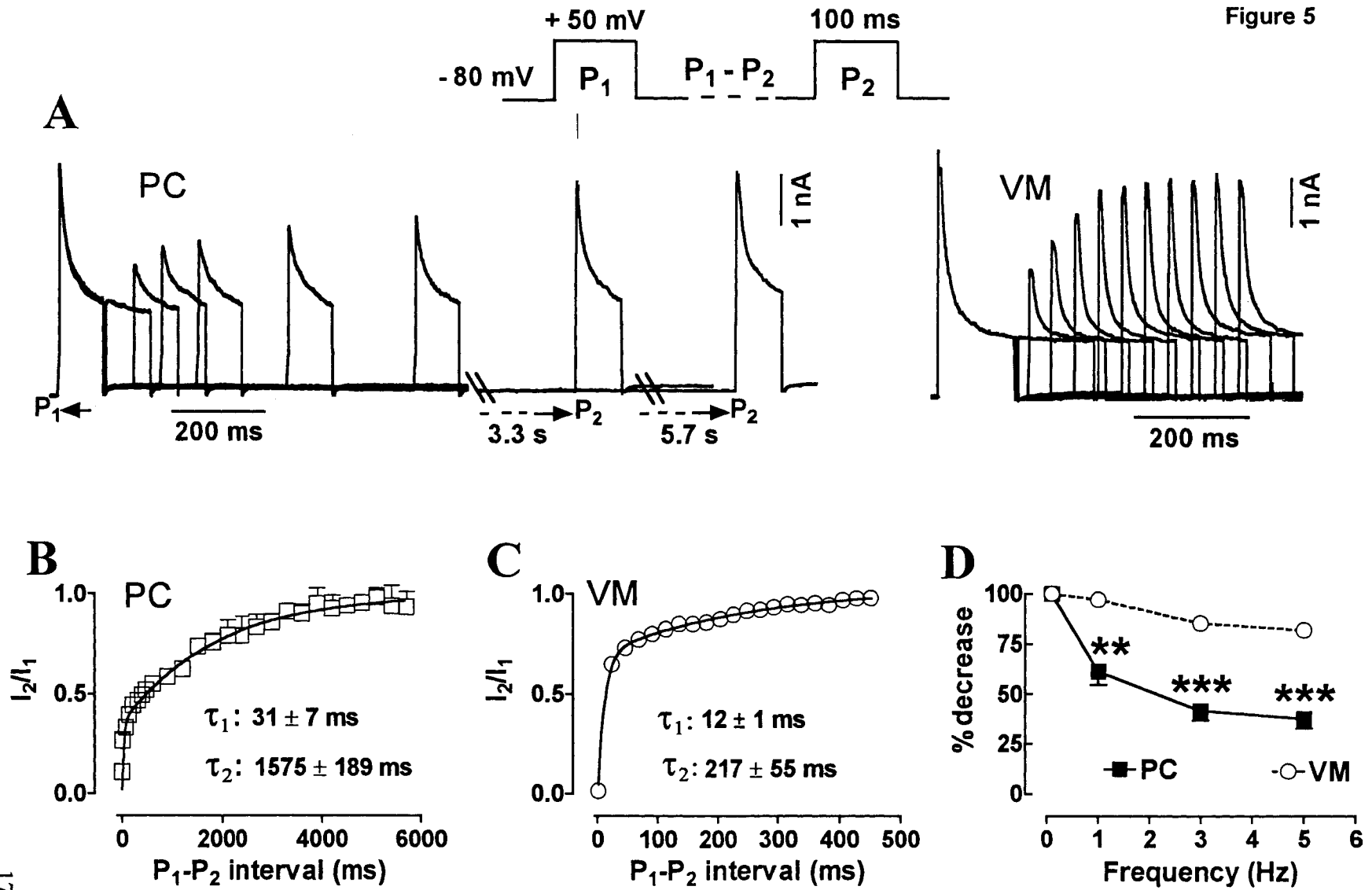


Figure 6

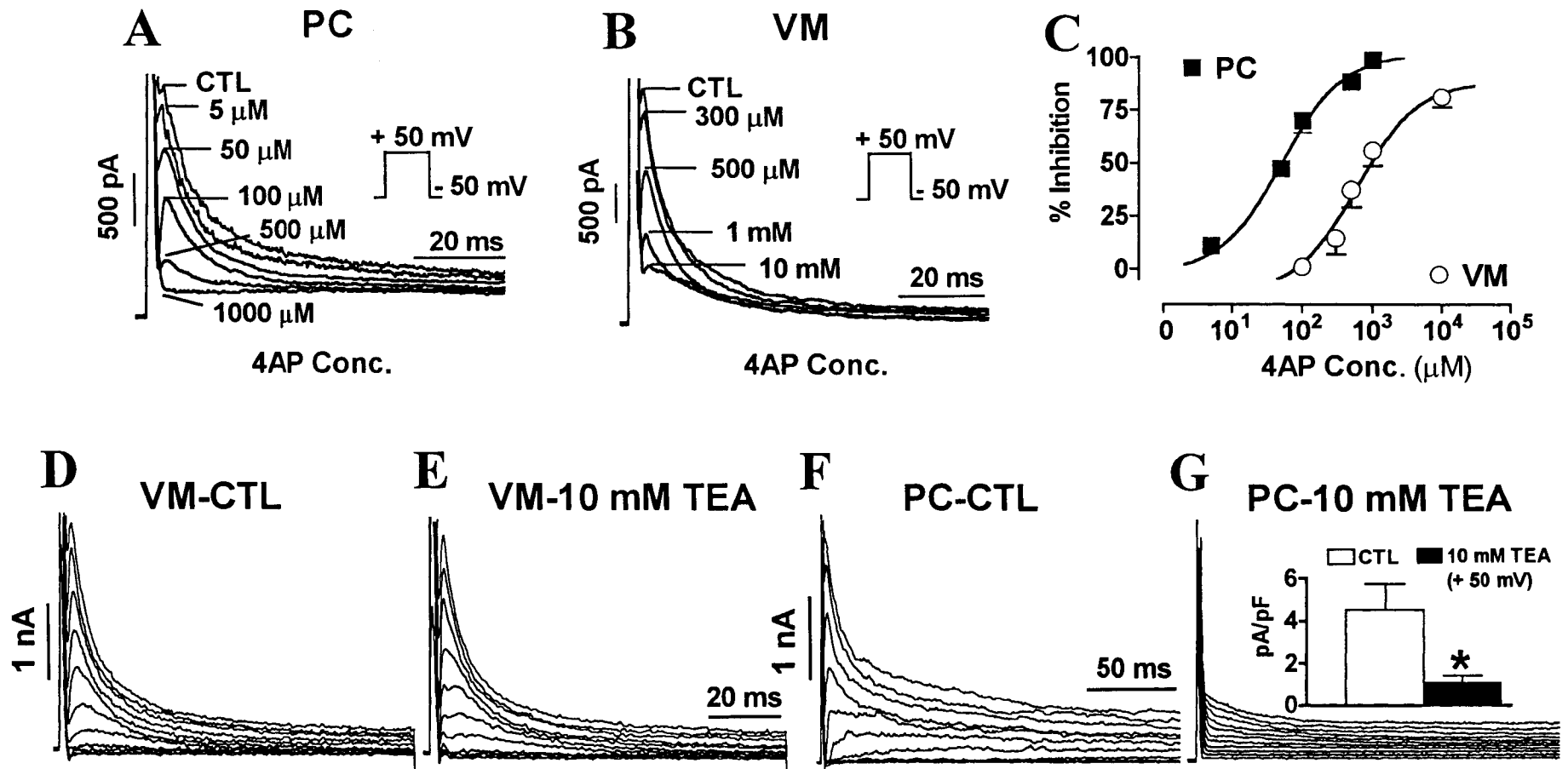
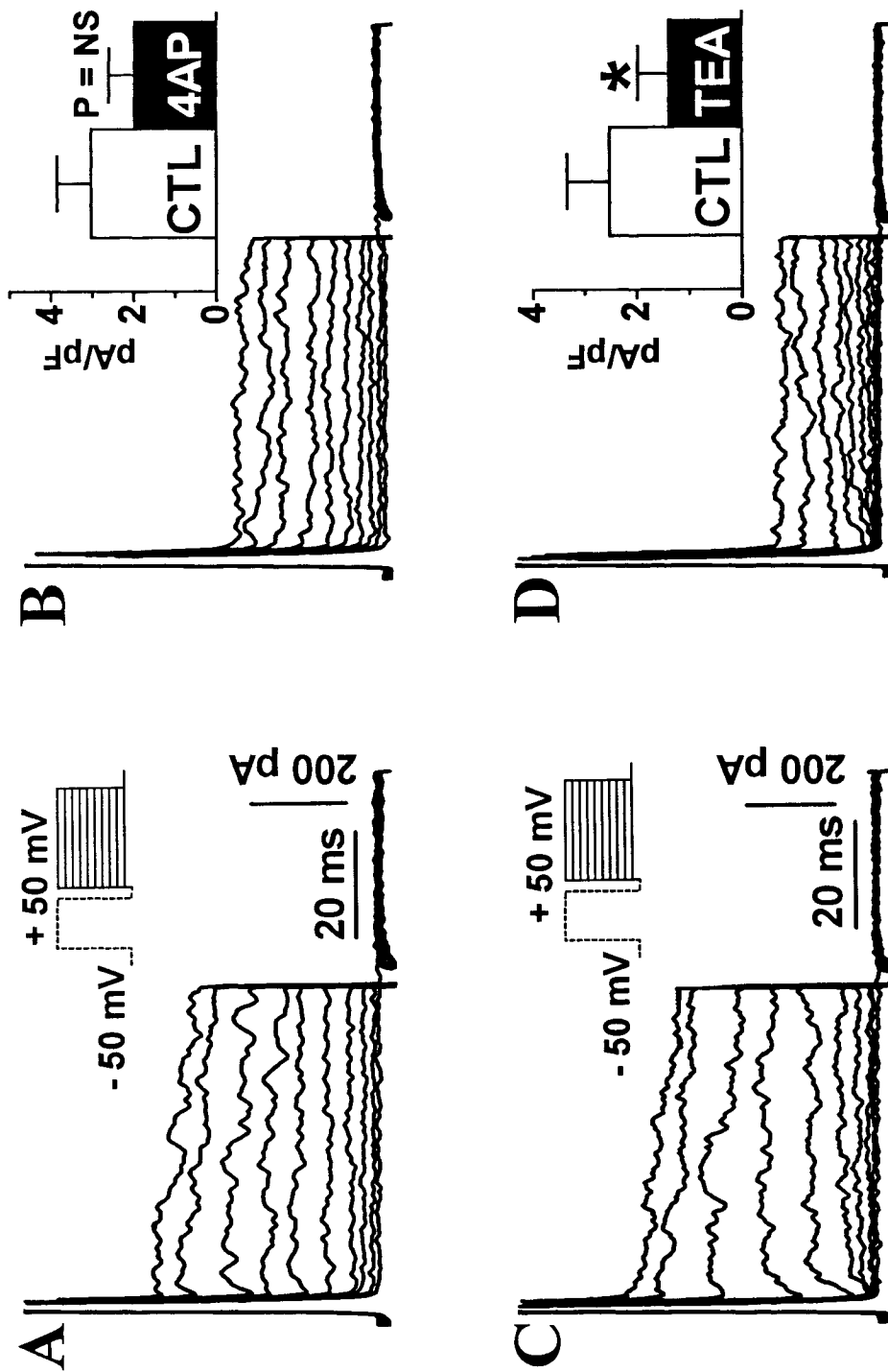


Figure 7



In comparison to dog atrial and ventricular myocytes I_{to} , the major features of PC I_{to} include:

- 1) PC I_{to} has a slower time course of inactivation.
- 2) PC I_{to} has a large, very slowly recovering component, leading to strong frequency dependence.
- 3) PC I_{to} is more sensitive to 4AP, and is sensitive to TEA, whereas working myocyte I_{to} is not.
- 4) H_2O_2 slows Purkinje I_{to} inactivation, whereas H_2O_2 has no effects on ventricular myocyte I_{to} .

These differences strongly suggest a different molecular composition of Purkinje I_{to} from working myocyte I_{to} . Similar findings in the kinetics and major pharmacological profiles such as TEA and 4AP sensitivity of canine Purkinje I_{to} are observed in human PCs, indicating a similar molecular mechanism operating in both canine and human PCs.

Purkinje cells have also some other important differences from working myocytes. For example, longer APD is seen in PCs compared to VM, which may subject PCs to early afterdepolarizations (EADs) that are important in specific ventricular arrhythmias, such as Torsade de Pointes. The presence of large I_f , as found in human PCs, is important for PC pacemaking activity. All of these important differences imply differences in ion channel subunit expression. We therefore designed the next study to characterize the expression profiles of ion channels underlying repolarization in PCs. Canine Purkinje fibers (PFs) were used, because of difficulties in obtaining enough human PF tissue for molecular analysis. Canine left midmyocardium (VM) was used as the comparator tissue.

**CHAPTER 3. MOLECULAR CHARACTERIZATION OF ION
CHANNELS UNDERLYING REPOLARIZATION IN
CANINE CARDIAC PURKINJE FIBERS**

Comparison of Ion-Channel Subunit Expression in Canine Cardiac Purkinje Fibers and Ventricular Muscle

Wei Han, Weisheng Bao, Zhiguo Wang, Stanley Nattel

Short Title: Ion-Channel Subunit Expression in Purkinje Fibers

Subject Codes: [5] Arrhythmias, clinical electrophysiology, drugs;

[106] Electrophysiology;

[132] Arrhythmias-basic studies

Word Count: 5,977

From Department of Medicine and Research Center, Montreal Heart Institute and University of Montreal (W.H., W.B., Z.W., S.N.), Montreal, Québec, Canada, and Department of Pharmacology, McGill University (W.H., S.N.), Montreal, Québec, Canada.

Correspondence to Stanley Nattel, MD, Montreal Heart Institute, Research Center, 5000 Belanger Street East, Montreal, Quebec, H1T 1C8, Canada. Tel.: (514) 376-3330; Fax: (514) 376-1355; E-mail nattel@icm.umontreal.ca

Abstract—Although Purkinje fibers (PFs) play an important role in cardiac electrophysiology, almost nothing is known about the expression of ion-channel subunits in PFs. We applied competitive reverse-transcription/polymerase-chain reaction (RT-PCR), Western blotting and immunocytochemistry to compare the expression of ion-channel subunit mRNA and protein in canine PFs versus ventricular muscle (VM). For transient outward current-related subunits, Kv4.2 was not detected and Kv1.4 expression was extremely low. Kv4.3 expression was of the same order for VM and PFs. The TEA-sensitive subunit Kv3.4 was expressed much more strongly in PFs than in VM, and Kv channel-interacting protein (KChIP2) transcript expression was 25-fold stronger in VM than in PFs. For delayed-rectifiers, ERG and KvLQT1 expression was lower in PFs at both mRNA and protein levels. While minK transcripts were more numerous in PFs, minK protein was significantly more strongly expressed in VM. L-type Ca^{2+} -current (I_{Ca}) α -subunit ($\text{Ca}_v1.2$) and Na^+ , Ca^{2+} -exchanger proteins were more strongly expressed in VM than in PFs. For T-type I_{Ca} , $\text{Ca}_v3.1$, 3.2 and 3.3 transcripts were all more strongly expressed in PFs. For I_f , HCN1 expression was sub-quantifiable, HCN2 transcript expression was comparable in PF and VM and HCN4 mRNA expression was strong in PFs but below detection threshold in VM. Both HCN2 and HCN4 protein expression was much stronger in PFs than VM. We conclude that ion-channel subunit expression in PFs differs from that in VM in ways that are consistent with, and shed light on the molecular basis of, well-recognized fundamental PF ionic properties.

Key Words: Molecular biology ■ cardiac arrhythmias ■ ion-currents

Introduction

Cardiac Purkinje fibers (PFs) play an important role in cardiac conduction and arrhythmogenesis. They are particularly significant in generating early afterdepolarizations (EADs) and triggering transmural reentry in Torsades des Pointes arrhythmias associated with long QT syndromes.¹⁻⁴ PFs also appear important in ventricular tachyarrhythmias due to delayed afterdepolarizations,⁵ intraventricular reentry⁶ and ventricular fibrillation.^{7,8}

PF action potentials (APs) have a number of properties that differentiate them from VM. They show prominent spontaneous phase 4 depolarization and automaticity,⁹ their AP durations increase much more than those of VM at slow rates,^{10,11} leading to preferential PF generation of EADs,¹ they show prominent rate-dependence of phase-1 repolarization¹² and they have a more negative plateau voltage. These AP differences likely reflect differences in the density and/or composition of ion channels in PFs compared to VM. Although much is known about the expression of ion-channel subunits in mammalian atrium and VM, the published literature contains very limited data regarding ion-channel subunit expression in PFs.¹³ The present study was designed to compare the expression of transcripts and (to the extent possible) proteins corresponding to ion-channel subunits and transporters in PFs with those in VM.

Materials and Methods

Hearts were removed from mongrel dogs (20-30 kg) euthanized with overdoses of pentobarbital. Mid-left ventricular myocardium and PFs in free-running false tendons were removed and fast-frozen in liquid-N₂. For all analyses, comparisons were based on

at least 4 hearts, with separate measurements in VM and PF (~100 mg tissue/heart) samples from each heart included.

Competitive RT-PCR

Competitive RT-PCR was used to quantify mRNA expression as previously described in detail.^{14,15} RNA was isolated,¹⁴ quantified spectrophotometrically at a 260-nm wavelength and integrity confirmed on a denaturing agarose gel. Total RNA was dissolved in RNA Storage Solution (Ambion) and stored at -80°C.

To synthesize RNA mimics (internal standards), gene-specific primers for RT-PCR (Table) were designed according to previously-described or cloned sequences with specificity confirmed by BLAST and FASTA. A 392-bp β -actin fragment was synthesized with the primers shown in the Table and used to construct mimics for the α_{1C} -subunit of the L-type Ca^{2+} -channel ($\text{Ca}_v1.2$), ERG, KvLQT1, minK, HCN1, HCN2, HCN4, and α_{1G} and α_{1H} -subunits of the T-type Ca^{2+} -channel ($\text{Ca}_v3.1$ and $\text{Ca}_v3.2$). A 460-bp α -actin fragment was used to construct mimics for Kv4.3, Kv3.4 and Kv1.4 subunits, Na^+ , Ca^{2+} /exchanger isoform-1 (NCX1), and the α_{1I} -subunit of T-type Ca^{2+} channel ($\text{Ca}_v3.3$).

First-strand cDNA was synthesized by reverse transcription with canine cardiac RNA and random primers. Chimeric primer-pairs were constructed by appending gene-specific primers at the 5'- and 3'- ends of actin primers, and an 8-nucleotide (GGCCGCGG) linker homologous to the 3'- end of the T7-promoter sequence was conjugated to the 5'-end of each gene-specific sense primer. The chimeric primers were used in a PCR reaction (*Taq* polymerase; annealing temperature, 55°C) with the first-strand DNA to generate an actin cDNA sequence flanked by gene-specific primers, with the short T7-promoter sequence at

the 5'- end. The product of this PCR was diluted 10-100 fold, and 1 μ L used as a template in a second PCR. Primers in the second PCR (annealing temperature, 60°C) included a T7-promoter primer (sense) and a gene-specific antisense primer. The resulting product (T7-promoter, gene-specific primers, and an internal α - or β -actin fragment) was gel-purified (QIAquick Gel Extraction Kit, Qiagen) and used as a template for in vitro transcription. In vitro transcription was conducted with *mMESSAGE mMACHINE* (Ambion) at 37°C for 3 hours. RNase-free DNase I (2 U) was added to a 20- μ L reaction mixture and incubated at 37°C for 30 minutes. Mimic RNA was purified with phenol chloroform extraction and RNA inactivation reagent (Ambion). The mimic RNA pellet was dried and dissolved in RNA Storage Solution (Ambion). The quantity of RNA was determined by spectrophotometry and denaturing gel analysis.

Serial dilutions of RNA mimics were added to 1- μ g samples of RNA in a series of reaction mixtures. RNA was denatured at 70°C for 10 minutes and ice-chilled for 5 minutes before addition to the reaction mixture. RT was conducted at 25°C for 10 minutes and 42°C for 60 minutes with a 20- μ L first-strand cDNA synthesis mixture (3.2 μ g random hexamers, 1 mmol/L deoxynucleotide mixture [dNTP], 50 U RNase inhibitor, 20 U MMLV reverse-transcriptase). Aliquots of first-strand cDNA (5 μ L) were amplified by PCR in a 25- μ L solution containing (mmol/L): Tris-HCl 10 (pH 8.3), KCl 50, MgCl₂ 1.5, dNTP 0.8; 2.6 U *Taq* polymerase (PCR High Fidelity Kit, Boehringer-Ingelheim) and 0.2 μ mol/L gene-specific primers. The reaction mixture was denatured (94°C, 3 minutes) and subjected to 30 PCR cycles (denaturing [94°C, 30 seconds], annealing [temperatures given in Table, 30 seconds], elongation [72°C, 40 seconds]), followed by a final 10-minute extension period at 72°C.

Final PCR products (10- μ L aliquot) were subjected to electrophoresis on 1.5%-2% agarose gels containing Tris-acetate (40 mmol/L), EDTA (1 mmol/L) and ethidium bromide. Ethidium bromide fluorescence images were captured with a Nighthawk camera under ultraviolet light, and band density determined with Quantity-One software. As mimic concentration in the initial reaction mixture decreases, the mimic-band intensity decreases and target-gene bands increase (Figure 1A). The bands should be of equal intensity when mimic and target mRNA concentrations in the reaction mixture are the same. A DNA mass ladder was used to construct a standard curve for quantification. The logarithm of mimic-to-target intensity-ratio was plotted as a function of the logarithm of RNA-mimic concentration. Linear regression was used to determine the point of identity.

The absence of genomic contamination in the RNA samples and of DNA contamination in RNA mimics was confirmed with reverse transcriptase–negative controls for each experiment. Known quantities of target and mimic RNA were co-amplified for each construct to confirm that target sequences and corresponding mimics amplified with similar efficiencies.

Western Blot

To extract membrane protein, tissues were pulverized in liquid-N₂ and suspended in 500 μ L of ice-cold TE buffer (Tris 20 mmol/L, EDTA 1 mmol/L, benzamidine 0.1 mg/mL, phenylmethylsulfonyl fluoride 10 mg/mL, leupeptin 5 μ g/mL, pepstatin A 5 μ g/mL, aprotinin 5 μ g/mL and Na-orthovanadate 100 μ mol/L). The suspension was homogenized, 2% Triton X-100 added, put on ice (2 hours) and then centrifuged (14000 g, 10 minutes, 4°C). The soluble fraction was retained and stored at -80°C. Protein concentration was

determined with the Bradford method. Samples (200- μ g protein) were denatured in Laemmli sample buffer, separated on 5-10% regular or 4-15% pre-cast gradient SDS-polyacrylamide gels (Biorad) and transferred to Immobilon-P polyvinylidene difluoride membranes. Membranes were blocked (2 hours, room temperature) with 5%-nonfat milk in 0.1%-Tween 80 Tris-buffered saline solution (TTBS) and incubated overnight at 4°C with rabbit polyclonal antibodies against Kv4.3, Kv3.4, minK, Cav1.2, HCN1, 2 and 4 (Alomone Labs), KvLQT1 (Chemicon) and ERG (Santa Cruz) or mouse monoclonal antibody against NCX1 (Bioreagents) and the internal control, GAPDH (Research Diagnostics). We were unable to obtain antibodies against KChiP2 and Cav3.1-3.3; therefore, analysis of these constructs was limited to mRNA expression. After 3 washes in TTBS, membranes were incubated in 1:5000-20000 dilutions of horseradish peroxidase-conjugated goat antirabbit IgG (Santa Cruz Biochemicals), donkey antigoat IgG (Santa Cruz) or goat antimouse IgM (Santa Cruz) in 5%-nonfat milk in TTBS (60 minutes, room temperature), followed by 3 additional washes in TTBS. Antibody was detected with Chemiluminescence Reagent Plus (New England Nuclear Life Sciences). Band density was quantified by laser densitometry with Quantity-One software. Densitometric comparison of PF and VM bands was performed on blots processed equally and exposed on the same X-ray film. Samples probed with primary antibody pre-incubated with antigenic peptides were used as negative controls. For KvLQT1 and NCX1, antigenic peptide was unavailable and negative controls were performed by omitting primary antibodies.

Immunocytochemistry

Ventricular myocytes and Purkinje cells freshly-isolated from canine left-midmyocardium and PFs of each dog were plated on laminin (15 $\mu\text{g}/\text{mL}$)-coated coverslips at 37°C and incubated (humidified 95%-O₂/5%-CO₂) for 1 hour. Cells were fixed with 2% pre-cooled paraformaldehyde containing 0.2% Triton X-100 for 30 minutes, followed by 3 additional washes with PBS, and blocked (2 hours, room temperature) with 10% donkey serum and 5% bovine serum albumin (BSA) in phosphate-buffered saline (PBS). Cells were incubated overnight with primary antibody in PBS containing 1%-BSA and 2% donkey serum. Negative controls consisted of cells exposed to primary antibody pre-incubated with the antigen (Kv3.4 and Kv4.3) or cells exposed to secondary antibody without primary antibody (NCX1). After 3 washes, cells were incubated (1 hour) with 1:200 fluorescence-conjugated goat antirabbit IgG (Jackson ImmunoResearch Laboratories) or goat antimouse IgM (Santa Cruz) and then thrice-rinsed with PBS. Coverslips containing cell aliquots were mounted on slides with 1-mg/mL p-phenylenediamine in 75% glycerol and examined under a Zeiss Axiovert 100-M microscope coupled to a Zeiss LSM-510 laser-scanning confocal system. Identical settings were used for PFs and VMs from each heart to obtain a qualitative comparison of relative expression.

Data Analysis

All comparisons were with paired PF and VM data from each dog, with *t*-tests used for statistical comparison. Average data are presented as mean \pm SEM.

Results

I_{to}-Subunit Expression

Figure 1B shows the mRNA expression levels of a variety of subunits related to cardiac I_{to}. Kv4.3 was richly expressed, with similar quantities in PFs and VM. Kv1.4 expression was low and similar in both tissues and Kv4.2 was not detected. A large quantity of mRNA encoding the tetraethylammonium-sensitive subunit Kv3.4¹⁶ was present in PFs, with significantly lower quantities in VM. In addition, KChIP2, a recently-reported β subunit with important interactions with cardiac Kv4-subunits,¹⁷ was expressed at 25-fold greater levels in VM than in PFs.

To pursue possible expression differences in I_{to}-encoding α -subunits, we used commercially-available antibodies to study protein expression. Figure 2A shows Western blots of Kv4.3 from 2 PF and 2 VM samples, with a 70-kDa band corresponding to the expected size of Kv4.3 (horizontal arrow at the right) and a ~60 kDa band detected. Both bands were absent upon probing with antibody pre-absorbed with antigenic peptide and were more intense in VM than in PFs. Mean intensity of the 70 kDa-band was about twice as great in VM compared to PFs (right panel). The 60 kDa band, which may represent a proteolytic product, was also significantly weaker in PFs, averaging 0.69 ± 0.05 of the intensity in VM ($P < 0.05$ versus VM). Figure 2B shows Kv4.3 immunocytochemistry. Upon probing with anti-Kv4.3 (top micrographs), signals were clearly present in both PF and VM myocytes, with a transverse striation pattern consistent with transverse-tubular localization. The middle panels show fluorescent images of cells probed with antibody pre-incubated with antigenic peptide, with corresponding phase-contrast micrographs of the same cells shown in the bottom panels. Antigen pre-absorption clearly eliminated the

Kv4.3 signal. Similar immunocytochemical results were seen for 6 PF and VM cell samples from 3 hearts exposed to Kv4.3 antibody alone and for 2 PF and VM cell samples from 2 hearts exposed to Kv4.3 antibody after antigen pre-incubation.

Figure 3A shows Western blots for Kv3.4. A 110-kDa band corresponding to Kv3.4 (horizontal arrow at the right) was stronger in PF samples and was suppressed by pre-incubation with the antigenic peptide. A second, lower-molecular weight band was present in VM, but was also present upon probing with antibody pre-incubated with antigenic peptide. Mean 110-kDa band intensities in 6 hearts were ~3-fold greater in PFs (right panel). On confocal imaging, clear and strong staining was seen in PF cells, with concentration both at cell-ends and transverse tubules (Figure 3B, left). VM myocyte staining was weak and with less clear subcellular localization. No signal was present in cells exposed to Kv3.4 antibody after pre-incubation with the antigenic peptide (middle panels), with phase contrast images for the cells exposed to antibody pre-incubated with antigen shown in right panels. Similar immunocytochemical results were seen for 8 PF and VM cell samples from 3 hearts exposed to Kv3.4 antibody alone and for 2 PF and VM cell samples from 2 hearts exposed to Kv3.4 antibody after antigen pre-incubation.

I_K -Subunit Expression

Figure 4A shows the mean mRNA concentrations of I_K subunits- ERG, KvLQT1 and minK. The α -subunits ERG and KvLQT1 were significantly less strongly expressed at the mRNA level in PF than in VM. MinK mRNA was significantly more concentrated in PFs. Typical Western blots for ERG, KvLQT1 and minK are shown in Figure 4B. A single clear ERG band was reproducibly detected at ~165 kDa in PF and VM samples. and

disappeared upon pre-incubation with antigen. KvLQT1 bands at ~78 kDa were strong in VM and much weaker in PFs. Antigenic peptide was not available for KvLQT1, but the ~78 kDa bands were absent upon Western blotting with omission of the primary antibody. A single 16-kDa band detected by the minK antibody was less intense in PFs than in VM, and was eliminated by pre-incubation with antigen. The GAPDH signals obtained on the same gels are shown at the bottom. A comparison of mean protein band intensities relative to GAPDH for ERG, KvLQT1 and minK in PFs versus VM is shown in Figure 4C. ERG and KvLQT1 bands were significantly less strong in PFs than in VM (ERG: 0.28 ± 0.08 versus 0.70 ± 0.09 , $P < 0.01$; KvLQT1: 0.26 ± 0.04 versus 0.62 ± 0.03 , $P < 0.01$). In contrast to its mRNA expression profile, the minK protein signal was also significantly weaker in PFs than in VM (0.38 ± 0.04 versus 2.50 ± 0.25 ; $P < 0.001$). Overall, GAPDH signal intensity was similar in PFs and VM, averaging 3.74 ± 0.22 and 3.71 ± 0.20 for each respectively ($P = \text{NS}$).

Expression of Ca_v1.2 and NCX1

Figure 5A shows mean mRNA concentrations of Ca_v1.2 and NCX1 genes. Ca_v1.2 mRNA was significantly more concentrated (~2-fold greater) in VM than PFs. NCX1 mRNA was present in very high concentrations, that were similar in both VM and PFs. Typical Western blots for Ca_v1.2 and NCX1 are shown in Figure 5B. A signal at the expected molecular weight for Ca_v1.2 (just over 200 kDa) was present in VM and was eliminated by pre-incubation with antigenic peptide (NC, negative control, lane at right) but was very faint in PFs. NCX1 antibody detected a strong signal at ~160 and ~125 kDa in both tissues, along with very faint bands at ~70 kDa. The 160 and 125 kDa-band levels were

consistently stronger in VM. The 70 kDa band was difficult to quantify because of its faintness and no consistent differences were seen. No NCX1 bands were seen upon omission of primary antibody (NC). Mean intensities for the ventricular Ca_v1.2 and the NCX1 bands are shown in Figure 5C. NCX1 signal was substantially stronger in VM compared to PF. The Ca_v1.2 band was below the limit for quantification in PFs. Immunocytochemical studies (Figure 5D) showed NCX1 to be localized at cell membranes in both VM and PF, but VM also showed a clear transverse-striation pattern, consistent with transverse-tubular localization, that was absent in PFs. Similar immunocytochemical results were obtained with NCX1 antibody in 6 VM and PF cell samples from 2 hearts. Negative control experiments performed by omitting the primary antibody showed no staining for 2 VM and PF samples from 2 hearts.

HCN-Isoform Expression

A very faint band corresponding to HCN1 was seen following RT-PCR in PFs but not in VM, and the HCN1 mRNA concentration in PFs was too low to be quantified. HCN4 mRNA was found at a quantifiable level in PFs but not in VM (Figure 6A). HCN2 mRNA was also quantifiable and at similar concentration in both VM and PFs, but was significantly less strongly expressed than HCN4 in PFs. Western blot analysis of HCN2 (Figure 6B) revealed two bands, of ~55 and ~90 kDa, in rat brain. A corresponding 55 kDa band was detected in PF and VM and was strongly suppressed by antigen pre-incubation. VM and PF bands at ~80 and ~50 kDa did not correspond to the rat-brain bands and were largely unaffected by antigen pre-exposure. HCN1 antibody did not detect a signal in PF or VM, but HCN4 antibody detected a strong ~160 kDa signal in PF

corresponding to the rat brain signal. HCN4 signals were suppressed by antigen pre-incubation. The mean intensities of the 55-kDa HCN2 and the 160-kDa HCN4 bands are provided in the lower-right panel. HCN2 was significantly stronger in PF than VM and HCN4 was below the threshold for quantification in VM.

Ca_v3-Subunit Expression

Figure 7A shows representative gels of competitive RT-PCRs to analyze the mRNA concentrations of Ca_v3.1, Ca_v3.2 and Ca_v3.3. Results for VM are at the left and PF at the right. The point at which target gene signals were equivalent to those for mimics were in each case further to the left for PFs than VM (ie, occurred at larger mimic concentrations). Figure 7B shows mean±SEM mRNA concentrations from 6 hearts for each construct. All isoforms were significantly more strongly expressed in PFs.

Discussion

We have completed a detailed study of the expression of subunits contributing to I_{to}, I_K, L- and T-type I_{Ca}, NCX, and I_f in canine cardiac PFs, in comparison with matched VM samples from the same animals. We found significant differences in subunit expression patterns that may contribute importantly to the functional electrophysiological specificity of PFs.

Relationship of our Findings to Specific Aspects of PF Electrophysiology

I_{to}

I_{to} was first noted to be a prominent feature of the ionic current profile of PFs in the early 1960s.¹⁸ Initial studies of PF I_{to} suggested it to be a Cl^- current,^{19,20} but subsequent work by Kenyon and Gibbons demonstrated that the vast majority of PF I_{to} is carried by a 4-aminopyridine and tetraethylammonium-sensitive K^+ -conductance.^{21,22} PF APs show rapid phase-1 repolarization and a subsequent notch at low frequencies, with the notch disappearing upon repetitive activation at higher rates.¹² This behaviour was demonstrated by Hauswirth et al to be due to slow time-dependent reactivation of PF I_{to} at diastolic potentials.¹² I_{to} inhibition can prolong PF APD^{21,23} and downregulation of PF I_{to} by CHF sensitizes PFs to the APD-prolonging effects of I_{Kr} -blocking class 3 drugs, adding to the proarrhythmic risk of class 3 agents.²⁴

Recent work has pointed out a variety of biophysical and pharmacological properties of PF I_{to} which differentiate it from I_{to} in atrium and VM.²³ Like VM I_{to} , PF I_{to} displays biexponential recovery from inactivation; however, the slow component in PF recovers an order of magnitude more slowly (time-constant, τ , 1.4 s) than in VM (τ 180 ms).²³ In addition, the slow component constitutes about 2/3 of overall recovery in PFs vs 1/3 in VM. PF I_{to} is an order of magnitude more sensitive to 4-aminopyridine compared to VM, and whereas ~80% of PF I_{to} is sensitive to tetraethylammonium, VM I_{to} is unaffected by tetraethylammonium.²³

The present study demonstrates differences between PFs and VM in the expression of I_{to} -encoding subunits that may help to understand the molecular basis for the functional discrepancies between PF and VM I_{to} . Kv1.4 subunits form slowly-reactivating I_{to} channels upon heterologous expression.²⁵ Kv1.4 subunit composition appears to underlie slowly-recovering I_{to} in the rabbit heart¹⁵ and is thus a potential candidate to explain the

slow recovery of PF I_{to} . However, we found Kv1.4 mRNA expression to be sparse and equivalent in PF and VM. On the other hand, we noted a marked difference in expression of the accessory subunit KChIP2 between VM and PF, with KChIP2 mRNA abundance in PFs being $\sim 1/25$ that in VM. KChIP2 co-expression substantially accelerates the reactivation of I_{to} carried by Kv4 subunits,²⁶ and its scarcity likely contributes to the characteristic slow reactivation of PF I_{to} .^{23,24} We also observed important differences in the expression of the Kv3.4 subunit. Kv3.4 was much more abundant at the mRNA and protein level in PFs than in VM. Moreover, immunocytochemical results point to specific subcellular localization in PFs, compared to a more diffuse pattern in VM. Since Kv3.4 subunits carry a tetraethylammonium-sensitive I_{to} ,¹⁶ our results point to Kv3.4 as a candidate for the large tetraethylammonium-sensitive component of PF I_{to} .

I_K

The first detailed description of I_K and its 2 kinetic components was obtained in multicellular PF preparations in 1969.²⁷ Although numerous subsequent publications dealt with I_K in multicellular PF preparations, the current has proven much more difficult to demonstrate in single Purkinje cells.^{28,29} This difficulty is likely due to the great sensitivity of I_K to cell isolation,³⁰ and the need for prolonged exposure to cell-isolating enzymes by the “chunk” method to isolate Purkinje cells. The biophysical properties of I_{Kf} and I_{Ks} in Purkinje cells are generally similar to those reported for ventricular myocytes;^{24,31} but valid quantitative comparisons between PF and VM I_K densities cannot be made because of difference in cell isolation techniques. Our results suggest potentially significant differences in I_K -subunit expression in PFs versus VM. The expression of all

3 constituent subunit proteins, ERG, KvLQT1 and minK, was significantly less in PF than in VM. This would be expected to result in smaller I_{Kr} and I_{Ks} densities in PF, and could contribute to the long-recognized discrepancy between PF and VM APD, with PF APD exceeding that in VM, particularly at slow activation rates.^{10,11} The smaller ERG and KvLQT1 expression in PFs may be due to transcriptional regulation, since ERG and KvLQT1 mRNA is sparser in PFs versus VM. Transcriptional regulation cannot explain the lesser abundance of minK protein in PFs, since minK transcript concentrations are greater in PF than VM.

Ca²⁺ Handling

We found a number of expression differences in Ca²⁺ handling elements that may be important for PF properties. PFs are known to have a less positive plateau voltage than VM,¹² which may be due to a smaller I_{CaL} .³² Our finding of substantially weaker expression of the α_{1c} -subunit in PF suggests a potential molecular basis for this difference. In contrast to I_{CaL} , T-type I_{Ca} (I_{CaT}) is prominently expressed in PFs, where it is almost as large as I_{CaL} ^{33,34} and is very small or absent in normal VM.³⁵ We observed much more limited expression of I_{CaT} -encoding transcripts in VM compared to PF. The NCX functions to remove from the cell Ca²⁺ that enters upon depolarization of voltage-dependent Ca²⁺-channels. We found that PFs had weaker expression of NCX, and lacked the t-tubular NCX distribution of VM. Lower-level NCX expression might limit the ability of PFs to extrude Ca²⁺ under conditions of Ca²⁺-loading, potentially contributing to the enhanced susceptibility of PFs to digitalis toxicity.³⁶ The lack of t-tubular NCX distribution in PFs (Figure 5), in contrast to the t-tubular distribution of ion channels like

Kv4.3 and 3.4 in PFs (Figures 2 and 3), may relate to the specialization of PFs for electrical activity in contrast to the crucial contractile function of VM.

Pacemaker Currents

The predominant contributor to spontaneous phase-4 depolarization of Purkinje fibers is the non-selective cation current, I_f .³⁷ HCN subunits are believed to underlie I_f .³⁸ In the rabbit, HCN1 and HCN4 constitute the most strongly-expressed mRNA forms in PFs, with some HCN2 present, whereas HCN2 is the only isoform in VM.³⁹ We found HCN1 mRNA expression to be very low in dog PFs, whereas HCN4 expression was high and HCN2 intermediate. Our Western blot studies confirmed the presence of HCN2 and HCN4 protein and their greater expression in PFs compared to VM, consistent with the more important pacemaker function of PFs. To our knowledge, this is the first such demonstration at the protein level.

Potential Significance

This is the first paper of which we are aware to study in detail the expression of a wide range of ion-channel subunit genes in PFs. Previous data regarding ion-channel subunit expression in PFs have been limited to studies of mRNA expression of HCN³⁹ and a number of detailed studies of connexin expression (reviewed in reference 13). Given the importance of PFs in a wide range of ventricular tachyarrhythmias,¹⁻⁸ highlighted by a recent report of malignant arrhythmia prevention in man by ablation of Purkinje tissue,⁸ a better understanding of the molecular basis of PF electrophysiology would seem to be of great significance. Our results indicate that PFs have a distinct ion-channel subunit

expression profile, consistent with electrophysiological evidence of the distinct nature of PF ionic and cellular electrophysiology.

Potential Limitations

We were unable to obtain antibodies against several ion-channel subunits of interest, limiting our evaluation of the expression of Ca_v3 and KChIP2 to assessments of transcript abundance. In addition, the antigenic peptide was unavailable for several antibodies (notably KvLQT1 and NCX1). Our results were performed in the dog, and cannot necessarily be extrapolated to other species. We compared PF tissue from free-running false tendons to left-ventricular mid-myocardium. Ion-channel expression is known to be regionally-determined,¹³ which must be considered in interpreting our findings.

Acknowledgments

The authors thank the Canadian Institutes of Health Research, the Quebec Heart and Stroke Foundation and the Mathematics of Information Technology and Complex Systems (MITACS) Network for research funding, Evelyn Landry and Chantal St-Cyr for technical assistance, France Thériault for secretarial help with the manuscript, and Drs Robert Dumaine and Charles Antzelevitch for providing KvLQT1 antibody for preliminary studies.

H:\THERFR\PUBL\Circ Res\Comparisonft_sn.doc

References

1. Nattel S, Quantz MA. Pharmacological response of quinidine induced early afterdepolarisations in canine cardiac Purkinje fibres: insights into underlying ionic mechanisms. *Cardiovasc Res.* 1988;22:808-817.
2. El-Sherif N, Caref EB, Yin H, Restivo M. The electrophysiological mechanism of ventricular arrhythmias in the long QT syndrome. Tridimensional mapping of activation and recovery patterns. *Circ Res.* 1996;79:474-492.
3. Asano Y, Davidenko JM, Baster WT, Gray RA, Jalife J. Optical mapping of drug-induced polymorphic arrhythmias and torsade de pointes in the isolated rabbit heart. *J Am Coll Cardiol.* 1997;29:831-842.
4. Berenfeld O, Jalife J. Purkinje-muscle reentry as a mechanism of polymorphic ventricular arrhythmias in a 3-dimensional model of the ventricles. *Circ Res.* 1998;82:1063-1077.
5. Verkerk AO, Veldkamp MW, Bouman LN, van Ginneken AC. Calcium-activated Cl(-) current contributes to delayed afterdepolarizations in single Purkinje and ventricular myocytes. *Circulation.* 2000;101:2639-2644.
6. Nibley C, Wharton JM. Ventricular tachycardias with left bundle branch block morphology. *Pacing Clin Electrophysiol.* 1995;18:334-356.
7. Damiano RJ Jr, Smith PK, Tripp HF Jr, Asano T, Small KW, Lowe JE, Ideker RE, Cox JL. The effect of chemical ablation of the endocardium on ventricular fibrillation threshold. *Circulation.* 1986;74:645-652.

8. Haissaguerre M, Shah DC, Jais P, Shoda M, Kautzner J, Arentz T, Kalushe D, Kadish A, Griffith M, Gaita F, Yamane T, Garrigue S, Hocini M, Clementy J. Role of Purkinje conducting system in triggering of idiopathic ventricular fibrillation. *Lancet*. 2002;359:677-678.
9. Hauswirth O, Noble D, Tsien RW. Adrenaline: mechanism of action on the pacemaker potential in cardiac Purkinje fibers. *Science*. 1968;162:916-917.
10. Carmeliet E. Repolarisation and frequency in cardiac cells. *J Physiol. (Paris)* 1977;73:903-923.
11. Moore EN, Preston JB, Moe GK. Durations of transmembrane action potentials and functional refractory periods of canine false tendons and ventricular myocardium: comparisons in single fibers. *Circ Res*. 1965;17:259-273.
12. Hauswirth O, Noble D, Tsien RW. The dependence of plateau currents in cardiac Purkinje fibres on the interval between action potentials. *J Physiol*. 1972;222:27-49.
13. Schram G, Pourrier M, Melnyk P, Nattel S. Differential distribution of cardiac ion-channel expression as a basis for regional specialization in electrical function. *Circ Res*. 2002;90:939-950.
14. Yue L, Melnyk P, Gaspo R, Wang Z, Nattel S. Molecular mechanisms underlying ionic remodeling in a dog model of atrial fibrillation. *Circ Res*. 1999;84:776-784.
15. Wang Z, Feng J, Shi H, Pond A, Nerbonne JM, Nattel S. Potential molecular basis of different physiological properties of the transient outward K⁺ current in rabbit and human atrial myocytes. *Circ Res*. 1999;84:551-561.
16. Vega-Saenz de Miera E, Moreno H, Fruhling D, Kentros C, Rudy B. Cloning of ShIII (Shaw-like) cDNAs encoding a novel high-voltage-activating, TEA-sensitive, type-A K⁺ channel. *Proc R Soc Lond*. 1992;248:9-18.

17. Rosati B, Pan Z, Lypen S, Wang HS, Cohen I, Dixon JE, McKinnon D. Regulation of KChIP2 potassium channel beta subunit gene expression underlies the gradient of transient outward current in canine and human ventricle. *J Physiol.* 2001;533:119-125.
18. Deck KA, Trautwein W. Ionic currents in cardiac excitation. *Pflugers Arch Eur J Physiol.* 1964;280:63-80.
19. Dudel J, Peper K, Rudel R, Trautwein W. The dynamic chloride component of membrane current in Purkinje fibers. *Pflugers Arch Gesamte Physiol Menschen Tiere.* 1967;295:197-212.
20. Fozzard HA, Hiraoka M. The positive dynamic current and its inactivation properties in cardiac Purkinje fibres. *J Physiol.* 1973;234:569-586.
21. Kenyon JL, Gibbons WR. Influence of chloride, potassium, and tetraethylammonium on the early outward current of sheep cardiac Purkinje fibers. *J Gen Physiol.* 1979;73:117-138.
22. Kenyon JL, Gibbons WR. 4-aminopyridine and the early outward current of sheep cardiac Purkinje fibers. *J Gen Physiol.* 1979;73:139-157.
23. Han W, Wang Z, Nattel S. A comparison of transient outward currents in canine cardiac Purkinje cells and ventricular myocytes. *Am J Physiol. (Heart Circ Physiol)* 2000;279:H466-H474.
24. Han W, Chartier D, Li D, Nattel S. Ionic remodeling of cardiac Purkinje cells by congestive heart failure. *Circulation.* 2001;104:2095-2100.
25. Po S, Roberds S, Snyders DJ, Tamkun MM, Bennett PB. Heteromultimeric assembly of human potassium channels. Molecular basis of a transient outward current? *Circ Res.* 1993;72:1326-1336.

26. An WF, Bowlby MR, Betty M, Cao J, Ling HP, Mendoza G, Hinson JW, Mattsson KI, Strassle BW, Trimmer JS, Rhodes KJ. Modulation of A-type potassium channels by a family of calcium sensors. *Nature*. 2000;403:553-556.
27. Noble D, Tsien RW. Outward membrane currents activated in the plateau range of potentials in cardiac Purkinje fibres. *J Physiol*. 1969;200:205-231.
28. Cordeiro JM, Spitzer KW, Giles WR. Repolarizing K⁺ currents in rabbit heart Purkinje cells. *J Physiol*. 1998;508:811-823.
29. Pinto JM, Boyden PA. Reduced inward rectifying and increased E-4031-sensitive K⁺ current density in arrhythmogenic subendocardial Purkinje myocytes from the infarcted heart. *J Cardiovasc Electrophysiol*. 1998;9:299-311.
30. Yue L, Feng J, Li G-R, Nattel S. Transient outward and delayed rectifier currents in canine atrium: properties and role of isolation methods. *Am J Physiol. (Heart Circ Physiol)* 1996;270:H2157-H2168.
31. Sanguinetti MC, Jurkiewicz NK. Two components of cardiac delayed rectifier K⁺ current. Differential sensitivity to block by class III antiarrhythmic agents. *J Gen Physiol*. 1990;96:195-215.
32. Verkerk AO, Veldkamp MW, Abbate F, Antoons G, Bouman LN, Ravestloot JH, van Ginneken AC. Two types of action potential configuration in single cardiac Purkinje cells of sheep. *Am J Physiol*. 1999;277:H1299-H1310.
33. Hirano Y, Fozzard HA, January CT. Characteristics of L- and T-type Ca²⁺ currents in canine cardiac Purkinje cells. *Am J Physiol*. 1989;256:H1478-H1492.
34. Tseng GN, Boyden PA. Multiple types of Ca²⁺ currents in single canine Purkinje cells. *Circ Res*. 1989;65:1735-1750.

35. Nuss HB, Houser SR. T-type Ca^{2+} current is expressed in hypertrophied adult feline left ventricular myocytes. *Circ Res.* 1993;73:777-782.
36. Palfi FJ, Besch HR Jr, Watanabe AM. Ouabain sensitivity of the Na^+ , K^+ -ATPase activity from single bovine cardiac Purkinje fiber and adjacent papillary muscle. *J Mol Cell Cardiol.* 1978;10:1149-1155.
37. DiFrancesco D. A new interpretation of the pace-maker current in calf Purkinje fibres. *J Physiol.* 1981;314:359-376.
38. Ludwig A, Zong X, Hofmann F, Biel M. Structure and function of cardiac pacemaker channels. *Cell Physiol Biochem.* 1999;9:179-186.
39. Shi W, Wymore R, Yu H, Wu J, Wymore RT, Pan Z, Robinson RB, Dixon JE, McKinnon D, Cohen IS. Distribution and prevalence of hyperpolarization-activated cation channel (HCN) mRNA expression in cardiac tissues. *Circ Res.* 1999;85:E1-E6.

Figure Legends

- Figure 1.** *I*_{to} subunit mRNA-expression. **A.** Representative agarose gels for competitive RT-PCR of Kv3.4 subunit in VM (left) and PF (right). M=mass ladder; lanes 1-6, results obtained with serial dilutions of RNA mimic in the initial reaction mixture (lane 1, 20000 pg; lane 2, 2000 pg; lane 3, 200 pg; lane 4, 20 pg; lane 5, 2 pg; lane 6, 0.2 pg); lane 7, RT-negative control. **B.** Mean±SEM Kv4.3, Kv1.4, Kv3.4 and KChIP2 mRNA concentrations. In all figures, numbers of analyses per construct (each with tissue from a separate heart) are provided in brackets; ***P*<0.01, ****P*<0.001 VM versus PF.
- Figure 2.** Protein expression and immunolocalization of Kv4.3. **A.** Left, representative Western blot. M=mass-marker. P1 and V1: lanes run with identical quantities of protein (200 µg) from PFs and VM of 1 heart, P2 and V2: corresponding samples from a different heart. Right, Kv 4.3 protein-band intensity in PF and VM. **P*<0.05, VM versus PF. **B.** Kv4.3 immunolocalization in cells from a PF and VM. Green fluorescent staining indicates the presence of Kv4.3 in PF (**a**) and VM (**c**). **b** and **d**, negative controls obtained with primary antibody pre-incubated with antigenic peptide. **b'** and **d'**, phase contrast images of same cells as in **b** and **d** respectively. Horizontal scales=20 µm.
- Figure 3.** Protein expression and immunolocalization of Kv3.4. **A.** Left, representative Western blot. M=mass-marker. P1 and V1: lanes run with 200 µg of protein each from PFs and VM of one heart; P2 and V2: corresponding samples from another heart. Right, Kv3.4 protein-band intensity in PF and VM. **P*<0.05, VM versus PF. **B.** Kv3.4 immunolocalization in cells from a PF (**a**) and VM

(c). *b* and *d*, negative controls obtained with primary antibody pre-incubated with antigenic peptide. *b'* and *d'*, phase-contrast images of same cells as in *b* and *d* respectively. Horizontal scales=20 μ m.

Figure 4. mRNA and protein expression of I_K subunits. *A.* Mean \pm SEM ERG, KvLQT1 and minK mRNA concentrations in PF and VM. *B.* Typical Western blots for ERG, KvLQT1 and minK, with corresponding GAPDH bands at bottom. *C.* Mean \pm SEM ERG, KvLQT1 and minK protein-band intensities. ** P <0.01, *** P <0.001, VM versus PF.

Figure 5. mRNA and protein expression of $Ca_v1.2$ -subunit and NCX1. *A.* Mean \pm SEM mRNA concentrations. * P <0.05, VM versus PF. *B.* Western blots for $Ca_v1.2$ and NCX1. NC=negative control. *C.* Mean \pm SEM protein-band intensities. *** P <0.001, VM versus PF. *D.* Comparison of NCX1 immunolocalization in Purkinje cells (PC) and ventricular myocytes (VM). Horizontal scales=20 μ m.

Figure 6. mRNA and protein expression of HCN isoforms. *A.* Mean \pm SEM HCN2 and HCN4 mRNA concentrations. *** P <0.001, HCN2 versus HCN4 in PF. *B.* Western blots for HCN2, HCN1 and HCN4. RB1 represents protein from one rat brain (protein-quantity loaded 12.5%, 25% and 50% of that from heart for HCN1, HCN4 and HCN2 respectively). Corresponding GAPDH bands are at bottom. Mean HCN-band intensity is at lower-right. * P <0.05, VM versus PF.

Figure 7. mRNA expression of Ca_v3 subunits. *A.* Representative agarose gels for competitive RT-PCR. M=mass ladder. Lanes 1-5: serial dilutions of RNA mimics (5-fold for $Ca_v3.1$, 10-fold for $Ca_v3.2$ and 3.3). RT-: negative control

without reverse transcriptase. *B.* Mean \pm SEM mRNA concentrations of Ca_v3 subunits. **P*<0.05, VM versus PF.

Fig. 1

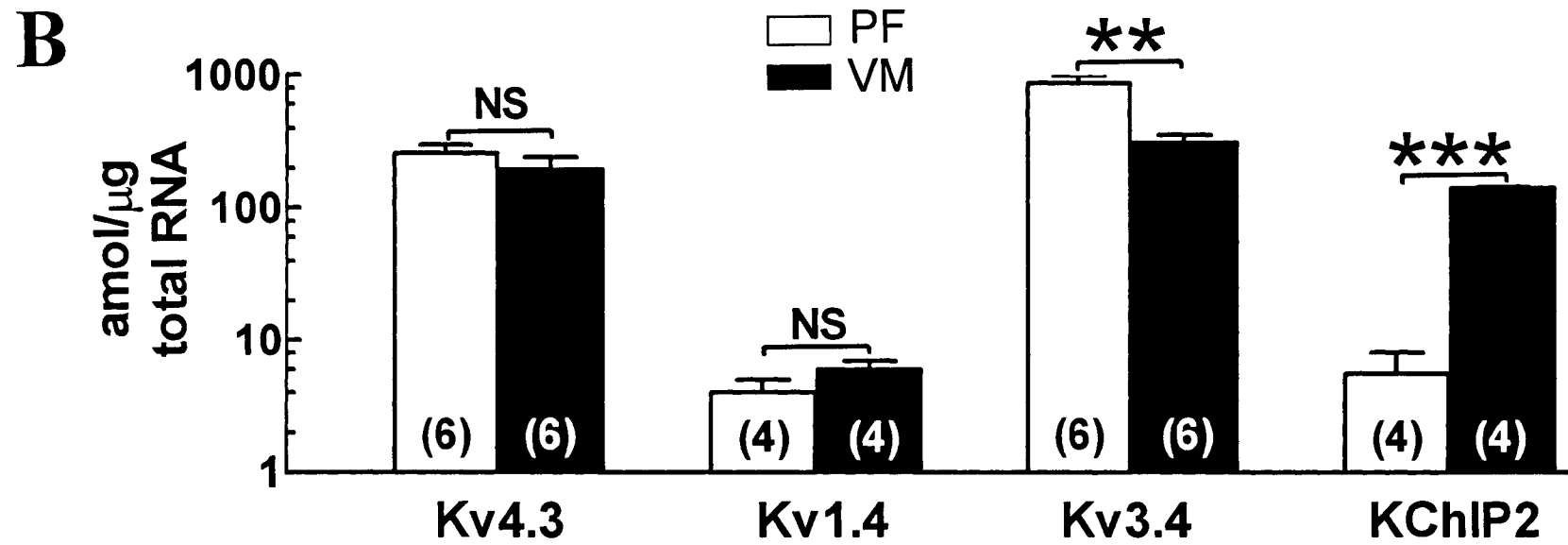
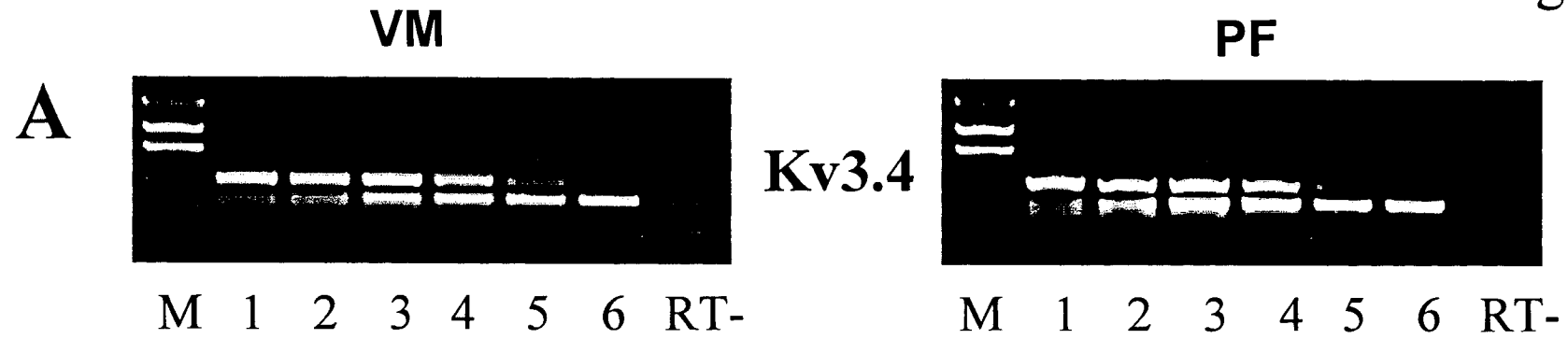


Fig 2

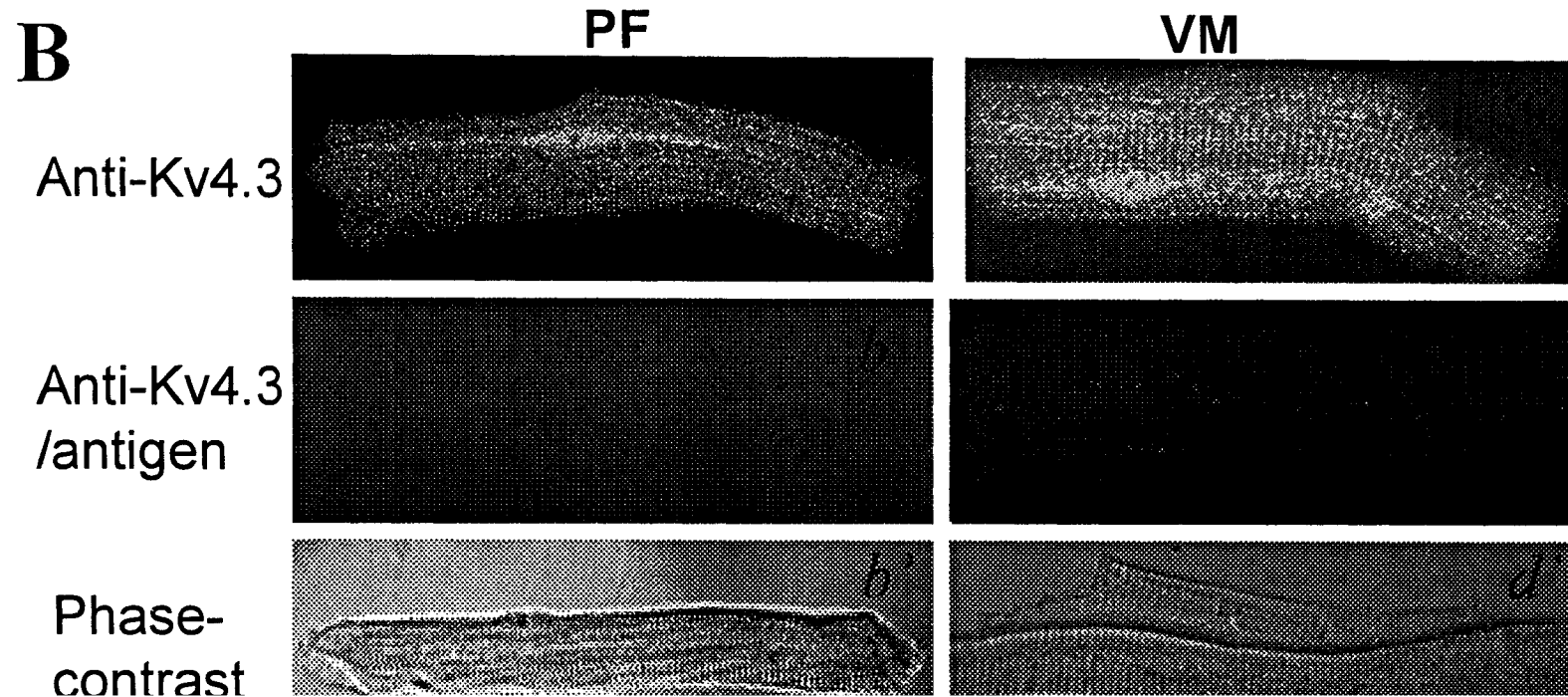
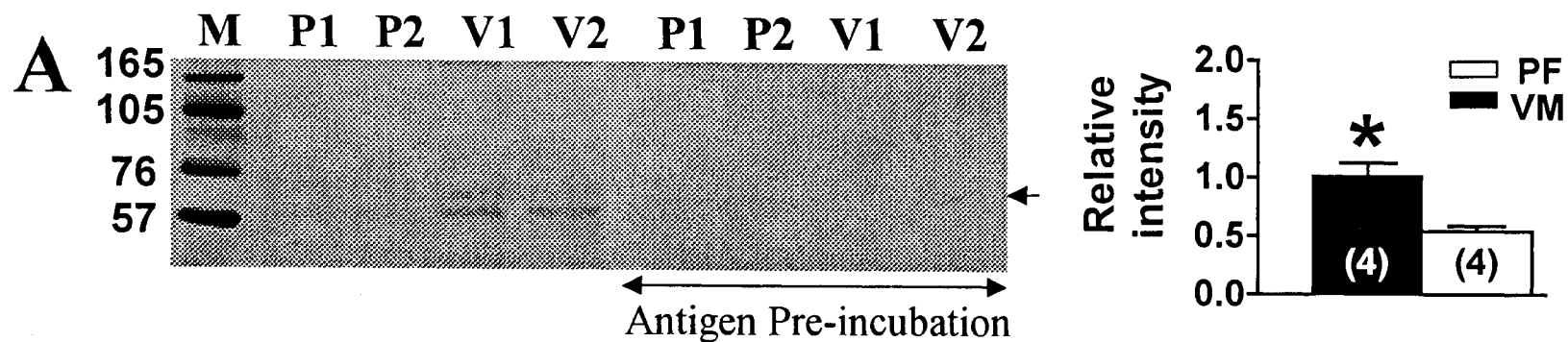


Fig 3

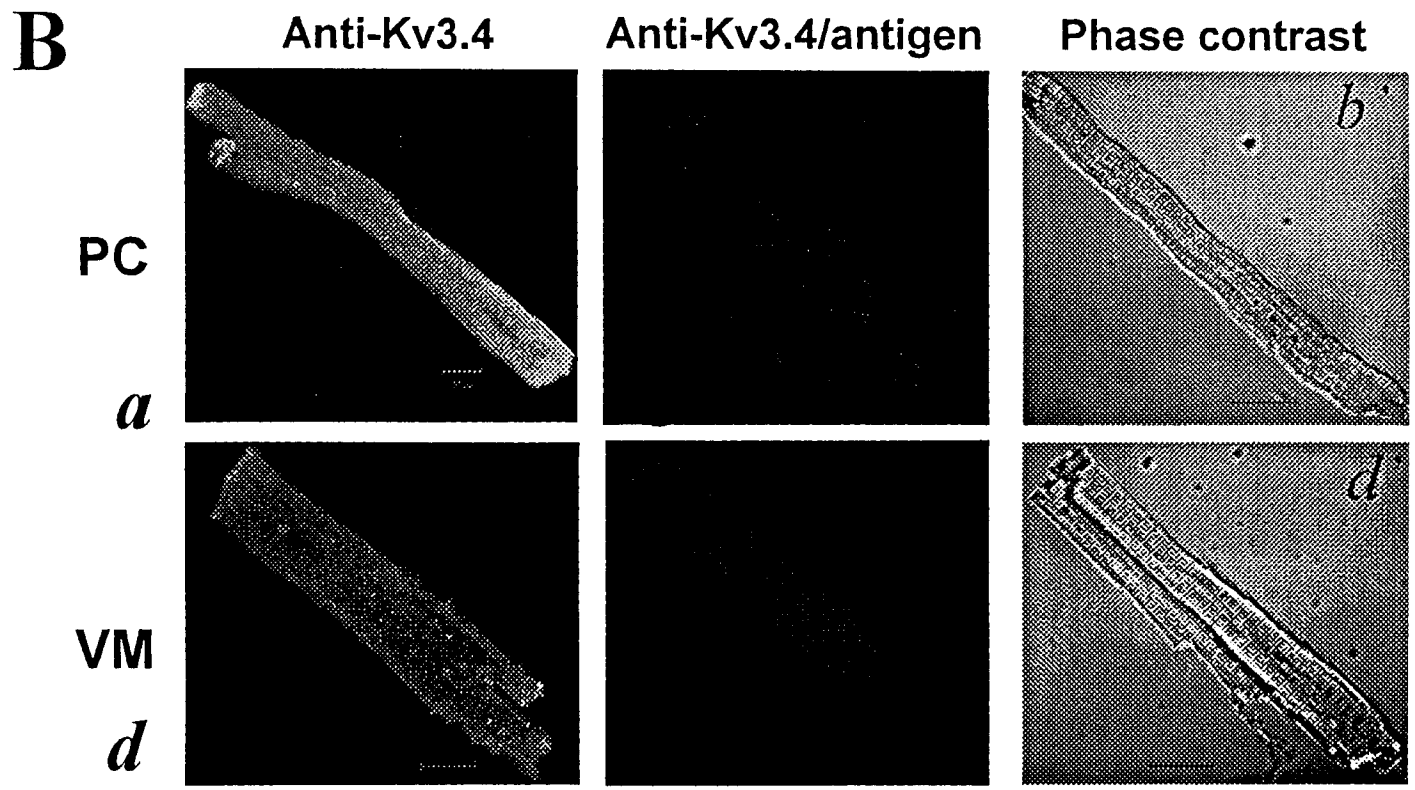
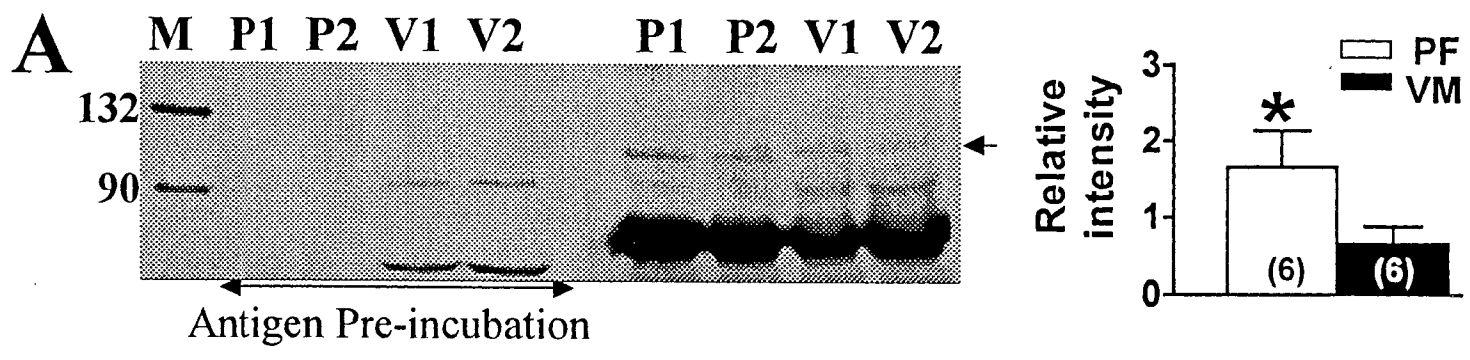


Fig 4

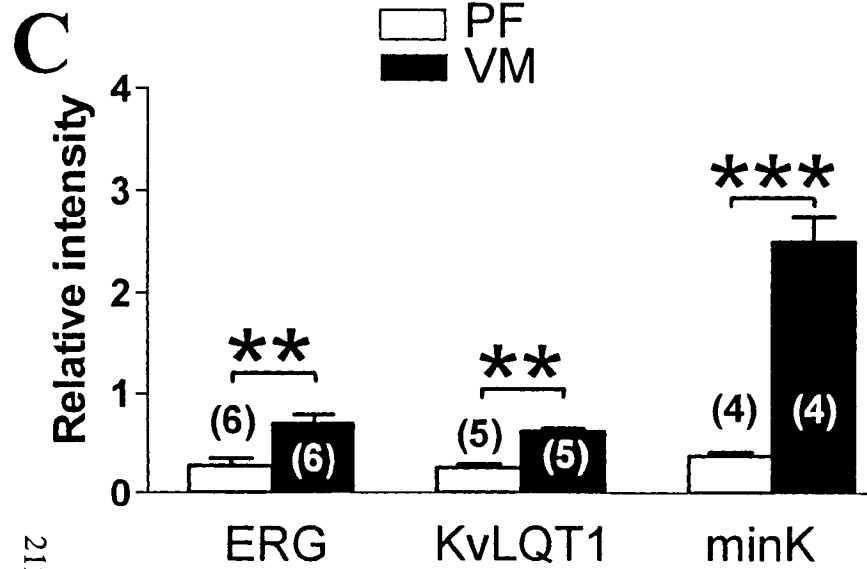
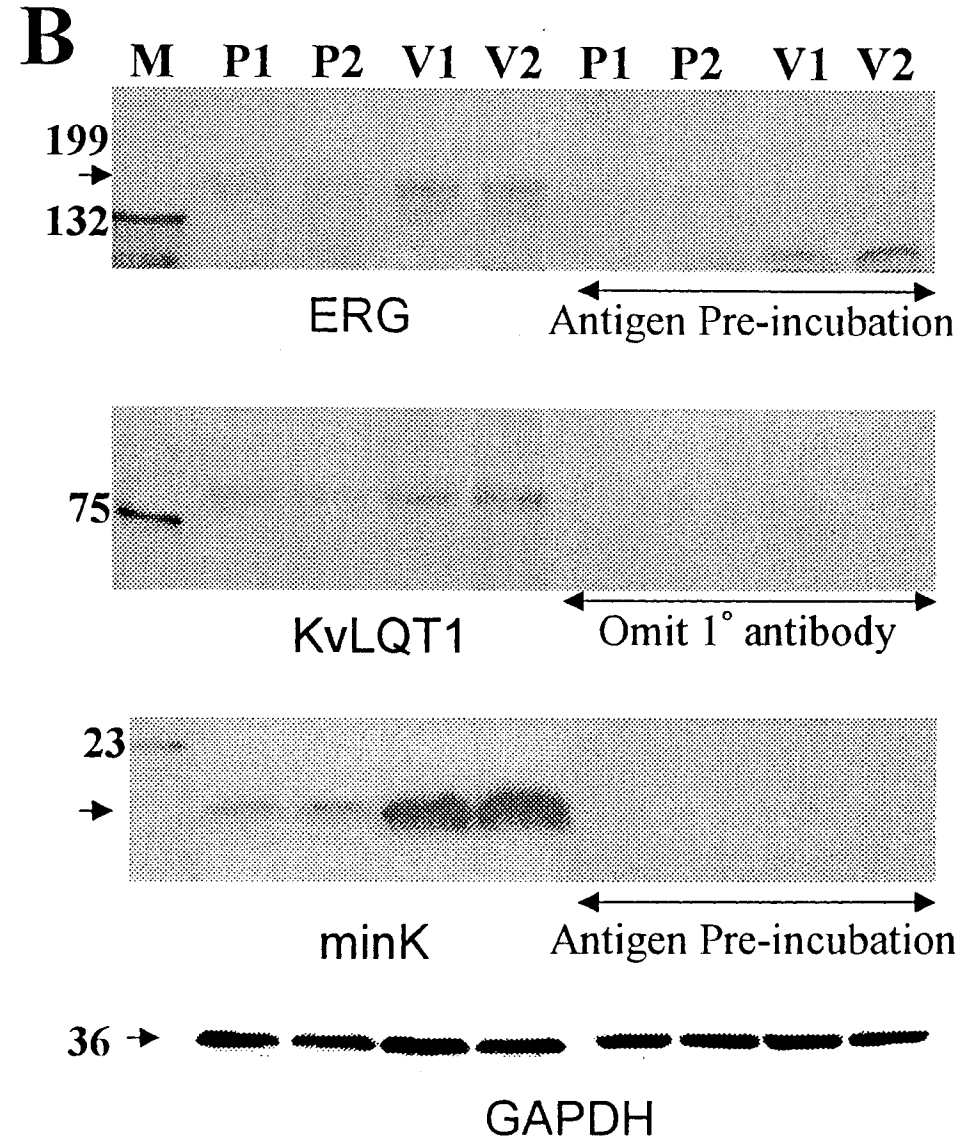
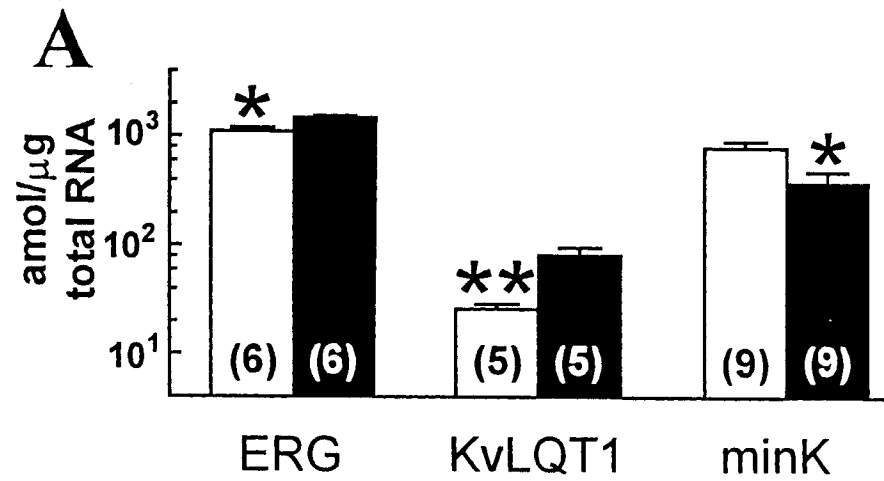


Fig 5

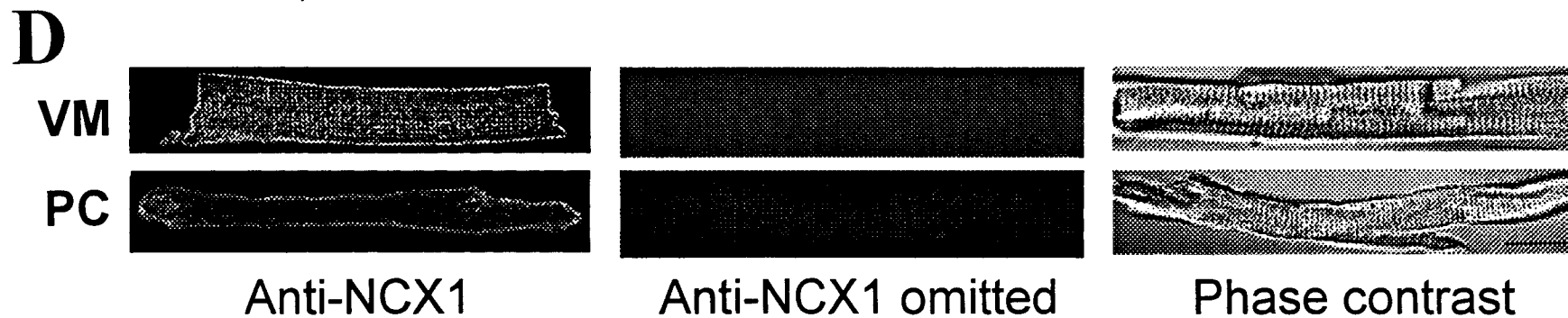
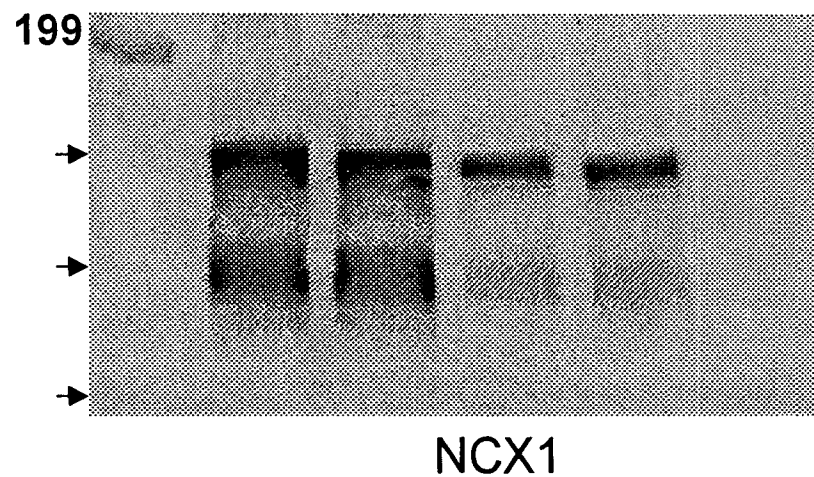
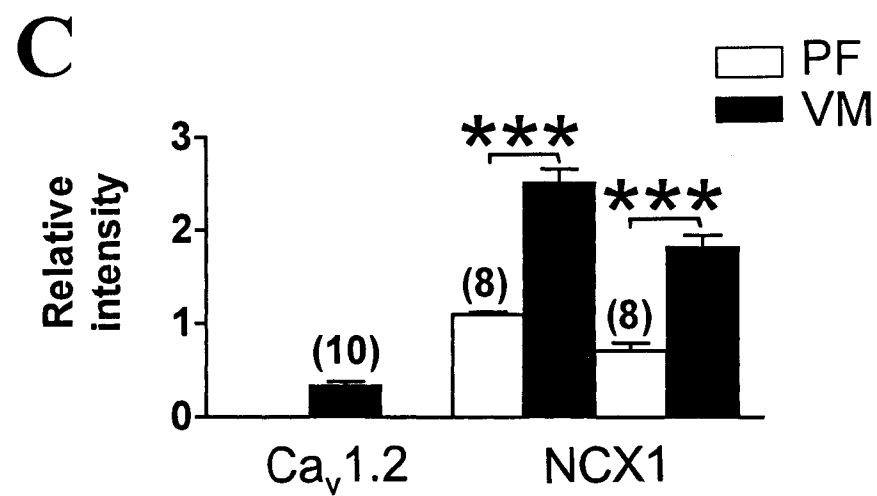
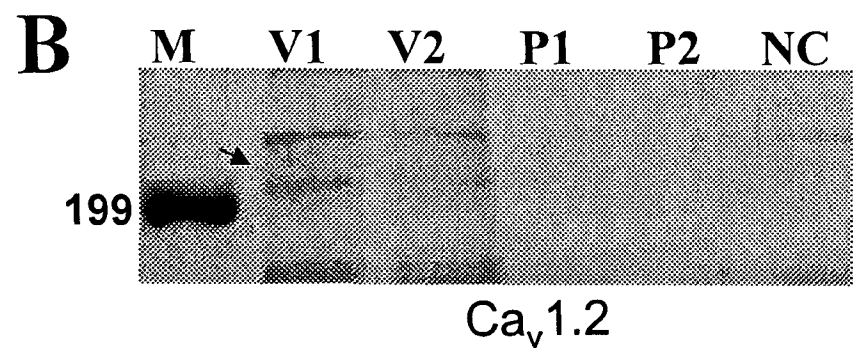
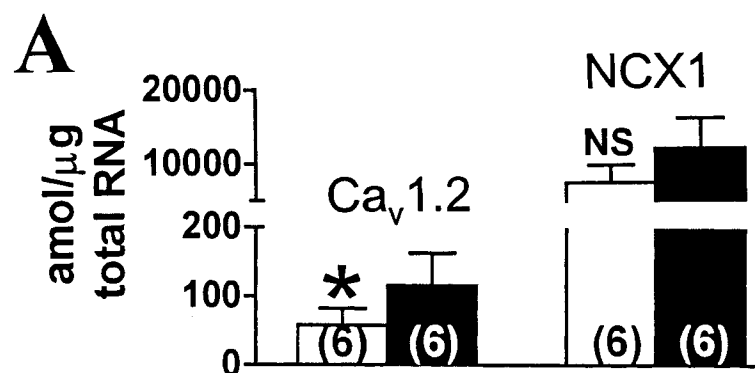


Fig 6

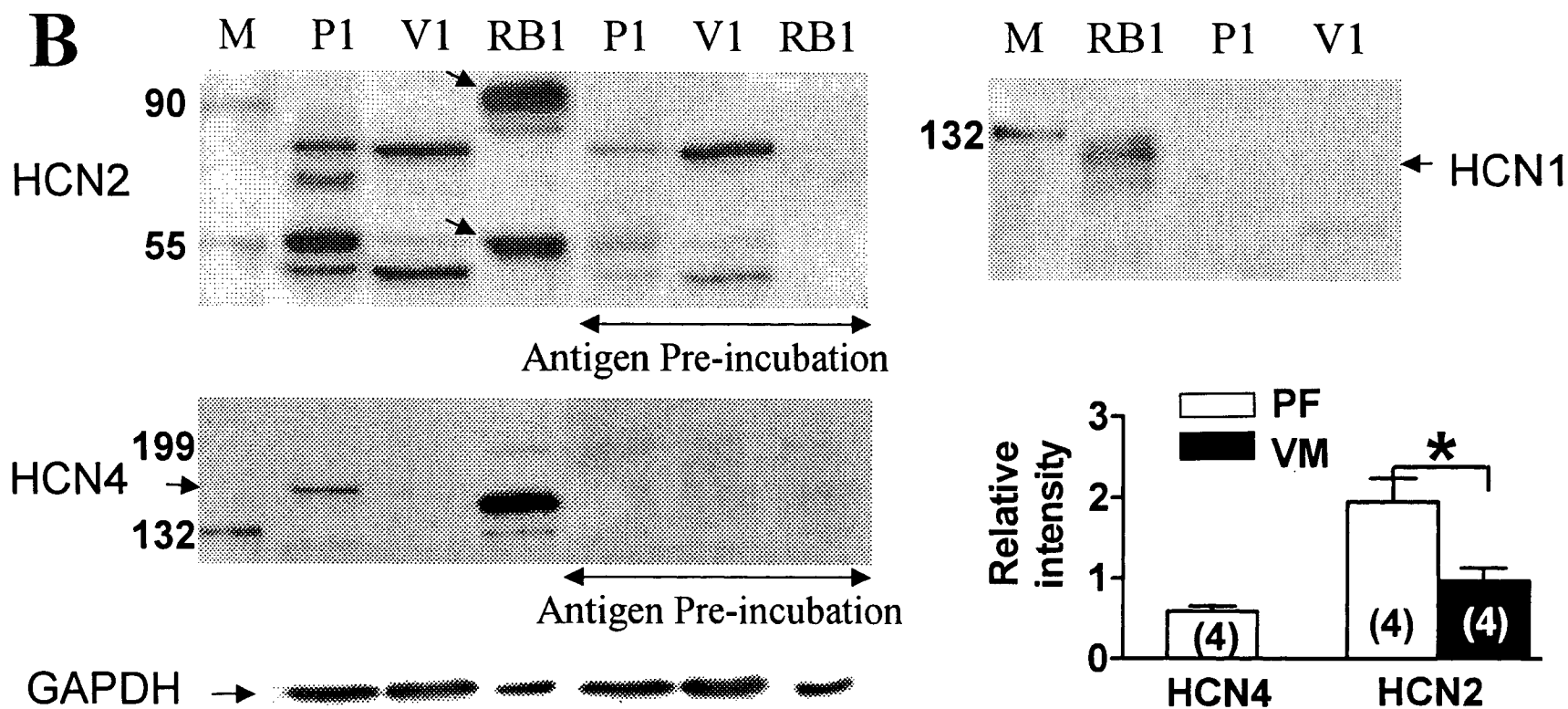
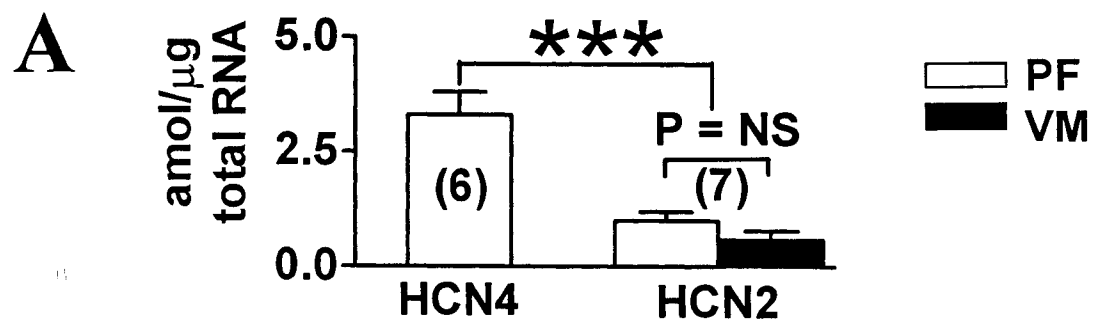


Fig 7

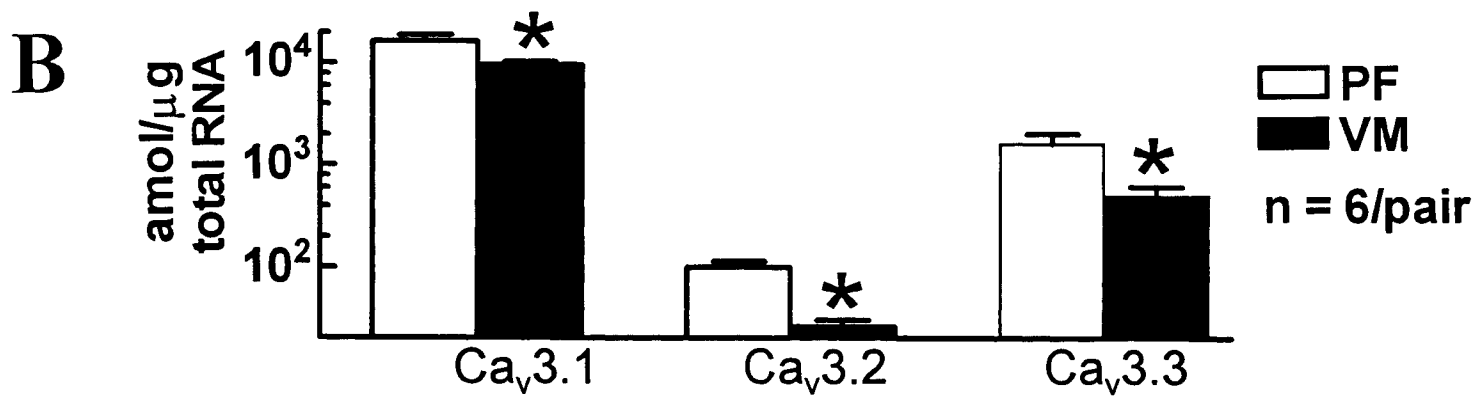
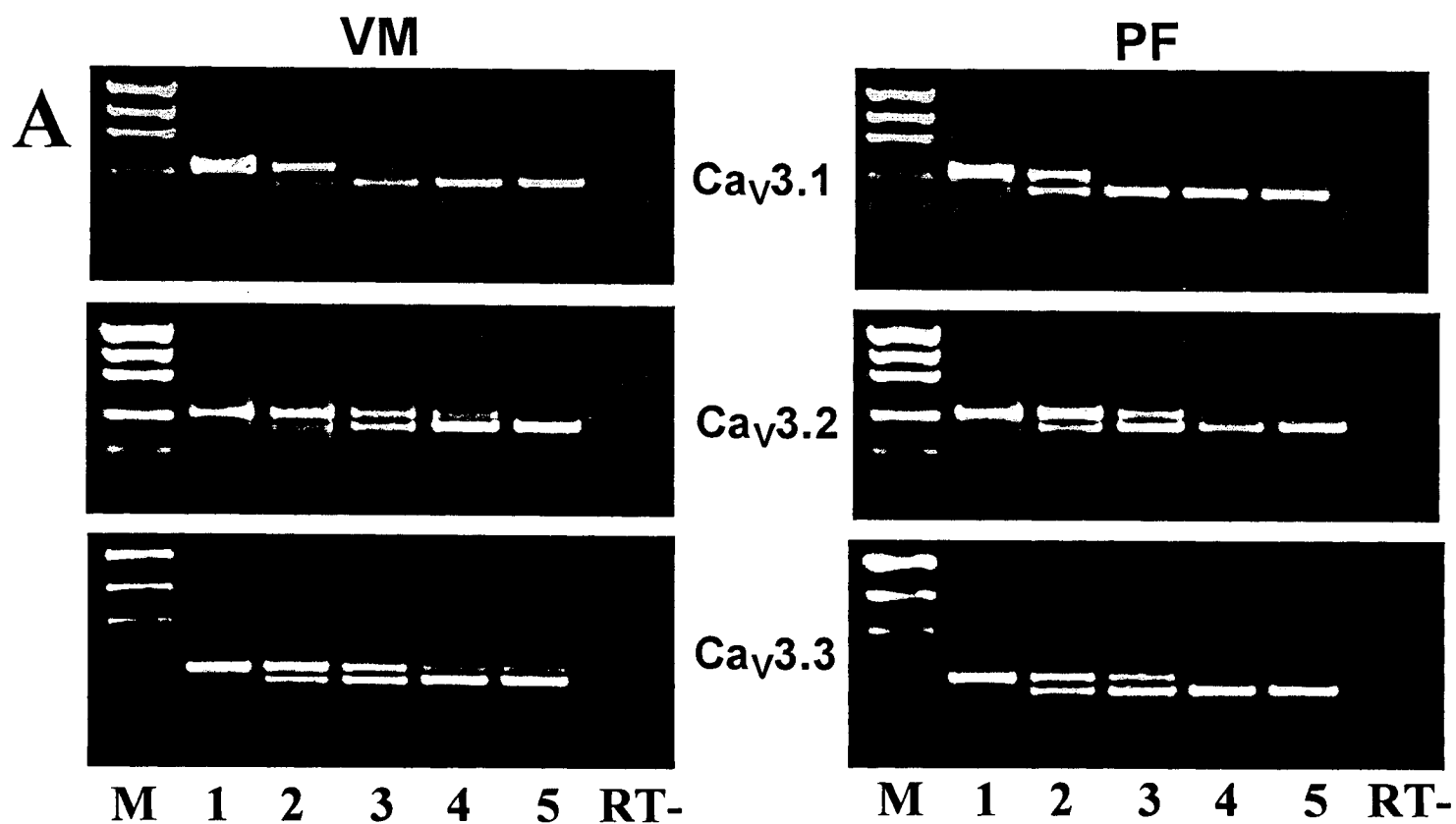


Table 1. Conditions Used for Competitive PCR

		Bases	Product	Tm	GeneBank
	Sense/Antisense Primer	spanned, bp	size, bp	°C	accession #
Kv4.3	TAGATGAGCAGATGTTTGAGC/ACTGCCCTGGATGTGGATG	1533–1744	212	54	AF049887
Kv1.4	ATCATTTCGTCTGGTCCGAGTATTC/AACTCCTTCTTCCATCTCTAG	2484–3005	522	54	XM006314
Kv3.4	CACCGACTTCAAGAACATCCC/GTAAATGGGTGACTCAAGCTGG	1653–1923	271	54	X62841
KChIP₂	GAGGACTTTGTGGCTGG/CCATCCTTGTTTCTGTCC	358–596	239	52	AF295530
ERG	GCTGCTGGTCATCTACAC/CCAGAGCCAAAGATGAG	1578–1880	303	54	NM013569
KvLQT1	GTCTACAACCTCCTCGAGCGTCCC/TTCCGGGCAAAGCGCAGC	130–389	260	52	U89364
minK	CTACATCCGCTCCAAGAAG/CAGGAAGGTGTGTGTTGG	210–388	179	52	NM000219
Ca_v1.2	CAATGACACGATCTTACC/GGATGCCAAAGGAGATG	4015–4283	269	52	NM000719
NCX1	TTGAGATTGGAGAGCCCC/CTCCTCCTCTTTGCTGGTC	1889–2100	212	52	M57523
HCN1	GAAATCATCCTGGACCC/CCAGAGGTCAGACATGC	250–756	507	52	AF064876
HCN2	GGTTCTACTGGGACTTCAC/GGGTCCAGGATGATCTC	667–871	205	52	XM042027
HCN4	CAAGGATGAGAACCAC/GAAGATGTAGTCCACGGG	1427–1634	208	55	NM005477
Ca_v3.1	GACAGTGAAGGTGGTGG/GATGAAGAAGGCACAGC	3975–4272	298	52	NM018896
Ca_v3.2	CTCCTTCCTGCTCATCG/GTTGCAGTACTTGAGGGC	4673–5006	334	52	AF290213
Ca_v3.3	CATCGTGGACAGCAAGTAC/CCAAGGATGCTGAAGATG	1906–2340	435	52	XM010005
β-actin	CAGAGCAAGAGGGGCATC/AGGTAGTCGGTCAGGTCC	111–502	392	55	Z70044
α-actin	ACCGGGAGAAGATGACTCAG/AATGAAGGAGGGCTGGAAG	329–1583@	460	55	J00070
T7- promoter	AGAATTCTAATACGACTCACTATAGGGCCGCGC				

**CHAPTER 4. PRESENCE OF DELAYED RECTIFIER CURRENT
AND POTENTIAL ROLE OF SLOW DELAYED RECTIFIER
CURRENT IN ABNORMAL REPOLARIZATION-RELATED
ARRHYTHMOGENESIS**

In Chapter 3, we showed that PCs have a discrete molecular composition of ion-channels determining pacemaker activity and repolarization compared to VM. Delayed rectifier subunits were clearly detected, albeit at lower concentrations than in VM. Previous patch-clamp studies had failed to detect significant delayed-rectifier current in isolated PCs (Cordeiro et al. 1998; Pinto and Boyden 1998). Delayed rectifier K^+ current (I_K) plays an important role in phase 3 repolarization and is thus a key determinant of APD. Abnormalities of I_K are believed to underlie 4 of 7 genetically-defined congenital long QT syndromes (LQTSs), including defects in genes encoding the slow component of I_K (I_{Ks}), KvLQT1 (LQT1) and minK (LQT5), and genes encoding fast component of I_K (I_{Kr}), HERG (LQT2) and MiRP1 (LQT6).

We were able to demonstrate a clear but very small I_{Kr} and robust I_{Ks} were present in isolated single PCs, with similar characteristic properties to those of I_K reported in most regions and species, as shown in the figure below. The ability of recording I_K allowed us to investigate the fundamental significance of abnormal repolarization in arrhythmogenesis.

This chapter and the next will deal with what the potential role of I_{Ks} in abnormal repolarization-related arrhythmogenesis is and how Purkinje repolarizing ion currents to be remodeled by congestive heart failure (CHF).

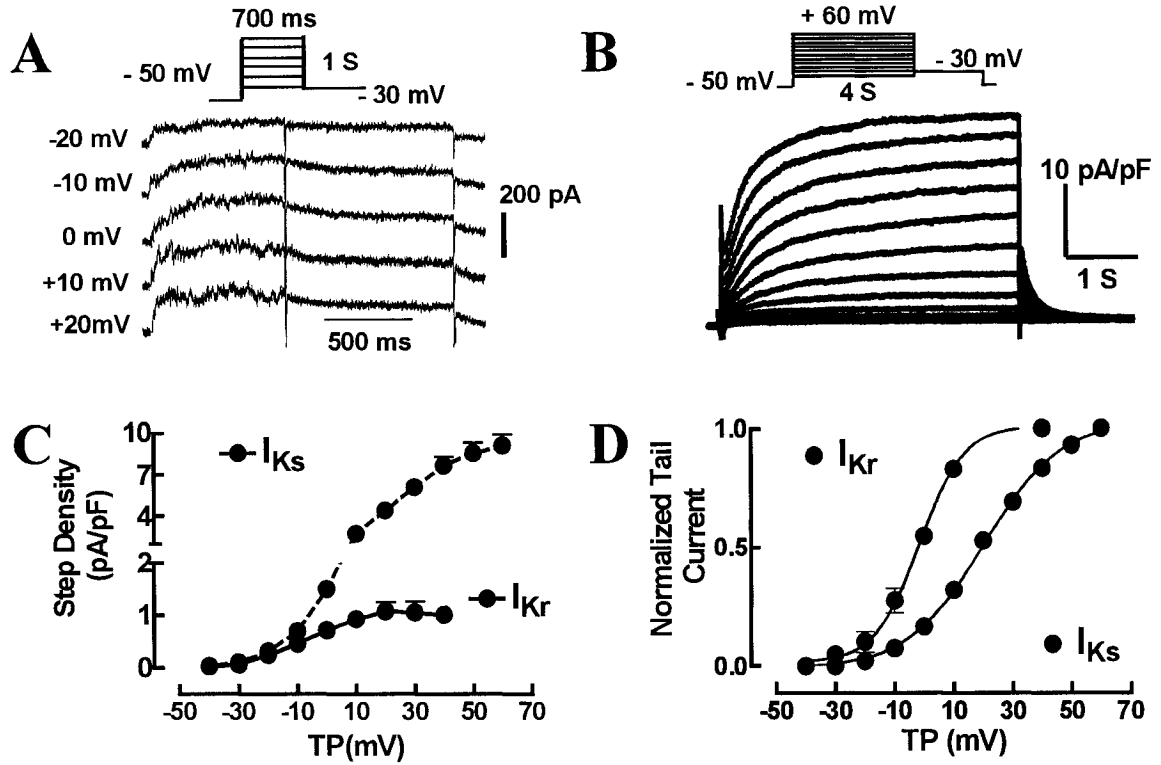


Figure 1. Delayed rectifier current (I_K) in isolated single canine Purkinje cells (PCs). *A* and *B*, Representative recordings of I_{Kr} and I_{Ks} . I_{Kr} was obtained with 5 μ M E4031-sensitive current. I_{Ks} was recorded in the presence of I_{Kr} blocker. *C*, Current densities of I_{Kr} and I_{Ks} in PCs. *D*, I-V relations of I_{Kr} and I_{Ks} in PCs.

Slow delayed rectifier current and repolarization in canine cardiac Purkinje cells

WEI HAN,¹ ZHIGUO WANG,² AND STANLEY NATTEL^{1,2}

¹Department of Pharmacology and Therapeutics, McGill University, Montreal, Quebec H3G 1Y6; and ²Research Center and Department of Medicine, Montreal Heart Institute, Montreal, Quebec H1T 1C8 and University of Montreal, Montreal, Quebec, Canada H3C 3J7

Received 25 April 2000; accepted in final form 12 October 2000

Han, Wei, Zhiguo Wang, and Stanley Nattel. Slow delayed rectifier current and repolarization in canine cardiac Purkinje cells. *Am J Physiol Heart Circ Physiol* 280: H1075–H1080, 2001.—Although cardiac Purkinje cells (PCs) are believed to be the source of early afterdepolarizations generating ventricular tachyarrhythmias in long Q-T syndromes (LQTS), the ionic determinants of PC repolarization are incompletely known. To evaluate the role of the slow delayed rectifier current (I_{Ks}) in PC repolarization, we studied PCs from canine ventricular false tendons with whole cell patch clamp (37°C). Typical I_{Ks} voltage- and time-dependent properties were noted. Isoproterenol enhanced I_{Ks} in a concentration-dependent fashion ($EC_{50} \sim 30$ nM), negatively shifted I_{Ks} activation voltage dependence, and accelerated I_{Ks} activation. Block of I_{Ks} with 293B did not alter PC action potential duration (APD) in the absence of isoproterenol; however, in the presence of isoproterenol, 293B significantly prolonged APD. We conclude that, without β -adrenergic stimulation, I_{Ks} contributes little to PC repolarization; however, β -adrenergic stimulation increases the contribution of I_{Ks} by increasing current amplitude, accelerating I_{Ks} activation, and shifting activation voltage toward the PC plateau voltage range. I_{Ks} may therefore provide an important “braking” function to limit PC APD prolongation in the presence of β -adrenergic stimulation.

ventricular arrhythmias; action potential; long Q-T syndrome

ADRENERGIC STIMULATION MODULATES Purkinje fiber delayed rectifier K^+ current (I_K) (4, 5, 11), selectively activating the slow component (I_{Ks}) in ventricular myocytes (21). Deficiency of either subunit of I_{Ks} , KvLQT1 or minK, causes congenital long Q-T syndrome (LQTS) (3, 19). KvLQT1 abnormalities cause LQTS1 (1), in which the occurrence of torsades de pointes (TdP) ventricular tachyarrhythmia is particularly adrenergically dependent (2, 28). Shimizu and Antzelevitch (25) showed that β -adrenergic stimulation causes a substrate for TdP in the presence of I_{Ks} inhibition with chromanol 293B. Repolarization abnormalities in the Purkinje system are believed to be important in TdP initiation (10, 16). It is conceivable that I_{Ks} deficiency in Purkinje cells (PCs) might lead to repolarization

abnormalities that play an important role in TdP. Despite the evidence in multicellular Purkinje fiber preparations (5, 17), recent publications have suggested that I_K may be small or absent in single cardiac PCs (9, 18). The present study was designed to evaluate I_{Ks} in PCs from free-running false tendons in the dog heart, determine the response of PC I_{Ks} to β -adrenergic stimulation, and establish the potential role of I_{Ks} in PC repolarization.

MATERIALS AND METHODS

Cell isolation. Mongrel dogs (20–30 kg) were anesthetized (pentobarbital sodium, 30 mg/kg iv), and their hearts were removed and immersed in Tyrode solution. False tendons were excised into modified MEM (GIBCO-BRL; pH 6.8, HEPES-NaOH) containing collagenase (800–900 U/ml, type II; Worthington) and 1% BSA. The fibers were agitated with 100% O_2 in a 37°C shaker bath (50–100 min). After the endothelial sheath had been digested, the fibers were washed twice with high- K^+ storage solution and incubated for 10 min at 37°C. Individual PCs were dispersed by trituration, harvested by centrifugation for 1 min, and kept in high- K^+ storage solution.

Solutions. The solutions contained (mM) 136 NaCl, 5.4 KCl, 1.0 $MgCl_2$, 1.0 $CaCl_2$, 0.33 NaH_2PO_4 , 5.0 HEPES, and 10 dextrose, with pH adjusted to 7.4 with NaOH (Tyrode solution); 20 KCl, 10 KH_2PO_4 , 10 dextrose, 70 glutamic acid, 10 β -hydroxybutyric acid, 10 taurine, 10 EGTA, and 0.1% albumin, with pH adjusted to 7.4 with KOH (storage solution); and 110 potassium aspartate, 20 KCl, 1 $MgCl_2$, 5 Mg_2ATP , 10 HEPES, 5 phosphocreatine, 0.1 GTP, and 5 EGTA (current recording) or 0.05 EGTA [action potential (AP) recording], with pH adjusted to 7.2 with KOH (pipette solution). All solutions were equilibrated with 100% O_2 .

Atropine (1 μM) was included in the extracellular solution to eliminate 4-aminopyridine (4-AP)-dependent K^+ currents (24) and nimodipine (1 μM) to block Ca^{2+} current (I_{Ca}). Na^+ current (I_{Na}) was suppressed by using a holding potential of -50 mV. Chromanol 293B (50 μM) was employed to inhibit I_{Ks} and dofetilide (1 μM) to block the slow component of I_K (I_{Kr}). Chromanol 293B fails to alter I_{Kr} , I_{K1} , I_{Ca} , or I_{Na} but inhibits transient outward current (I_{to}) by $\sim 65\%$ at a concentration of 50 μM (7). 4-AP (1 mM) was added to the bath to suppress I_{to} for voltage-clamp experiments. Isoproterenol (Iso) was freshly prepared as stock solutions of 100 μM and 1

Address for reprint requests and other correspondence: S. Nattel, Montreal Heart Institute, Research Center, 5000 Belanger St. East, Montreal, PQ, Canada H1T 1C8 (E-mail: nattel@icm.umontreal.ca).

The costs of publication of this article were defrayed in part by the payment of page charges. The article must therefore be hereby marked “advertisement” in accordance with 18 U.S.C. Section 1734 solely to indicate this fact.

mM and stabilized with 100 μ M ascorbic acid. L-768673 was kindly supplied by Merck Pharmaceuticals.

Data acquisition and analysis. General voltage-clamp techniques were as previously described (13, 30), with voltage-clamp and AP recordings performed at 0.1 Hz and 37°C. I_{Ks} step current was measured from the onset of activation to the level at the end of a depolarizing pulse and tail current from initial current on repolarization to the level at the end of the repolarizing pulse. Junction potential offsets averaged 10.0 ± 0.4 mV and were corrected only for APs. Small cells were selected to ensure spatial clamp (capacitance 127 ± 7 pF). Compensated series resistances and capacitive time constants averaged 2.5 ± 0.1 M Ω and 290 ± 10 μ s. For AP clamp, APs were recorded with current clamp at 0.1 Hz. The acquired AP waveform was then used as a voltage command signal to measure current flow during the AP, before and after Iso and/or 293B, with the difference current indicating the current inhibited by the drug during the AP in a given cell.

Nonlinear least-square curve fitting was used to fit experimental data. ANOVA and Bonferroni-adjusted *t*-tests were used for multiple group comparisons and *t*-tests for single comparisons. Values are means \pm SE.

RESULTS

Effects of β -adrenergic stimulation on I_{Ks} . Figure 1A shows representative I_{Ks} recordings from a PC in the absence of Iso (control) and in the presence of progressively increasing Iso concentrations. Iso effects were suppressed by propranolol; for example, in five cells, 500 nM Iso increased I_{Ks} step current at +40 mV from 8.4 ± 1.3 to 18.1 ± 2.2 pA/pF ($P < 0.001$), and addition of 1 μ M propranolol reduced step current in the continued presence of Iso to 9.5 ± 1.1 pA/pF ($P < 0.01$ vs. Iso alone). Average step and tail current density-voltage relations ($n = 7$ cells) are shown in Fig. 1, B and C. Both were significantly increased in a concentration-dependent manner. Concentration-response relations

are illustrated in Fig. 1D. The EC_{50} was in the range of 30 nM. To exclude effects mediated by the vehicle for Iso (ascorbic acid in Tyrode solution), we studied I_{Ks} before and after the highest ascorbic acid concentration used. In five cells, I_{Ks} step current at +40 mV averaged 7.0 ± 1.5 pA/pF before and 7.2 ± 1.5 pA/pF [$P =$ not significant (NS)] after 15 min of exposure to the vehicle.

Figure 2A shows I_{Ks} at 0.1 Hz before and after two concentrations of Iso, along with best biexponential fits to activation and deactivation data. Iso significantly decreased activation time constants (Fig. 2B) without altering the time course of deactivation. Figure 2C shows activation voltage dependence based on tail currents after steps to various voltages ($n = 5$ cells). Half-activation voltage was shifted from 23 ± 1 mV (control) to 16 ± 1 mV by 10 nM Iso and to 12 ± 1 mV by 500 nM Iso. Maximum decreases occurred at 50 nM Iso (Fig. 2B).

Effects of β -adrenergic stimulation and I_{Ks} inhibition on the AP. No clear effect of 293B on the AP is seen in the absence of Iso (Fig. 3A). Iso alone raised the plateau and accelerated phase 3, decreasing AP duration (APD; Fig. 3B) in the cell shown. In the presence of 293B, Iso increased APD (Fig. 3C). Mean APD changes are shown in Fig. 3D. 293B did not significantly alter APD in the absence of Iso; however, APD in the presence of Iso + 293B was significantly greater than with 293B or Iso alone, indicating that, in the absence of I_{Ks} , β -adrenergic stimulation delays PC repolarization. Iso alone increased APD slightly in some cells and decreased it in others, with no significant effect overall.

The AP-clamp technique was applied to evaluate the mechanisms of the effects of 293B and Iso. Figure 4, A–C, shows APs from one PC under control conditions, in the presence of Iso, and in the presence of Iso +

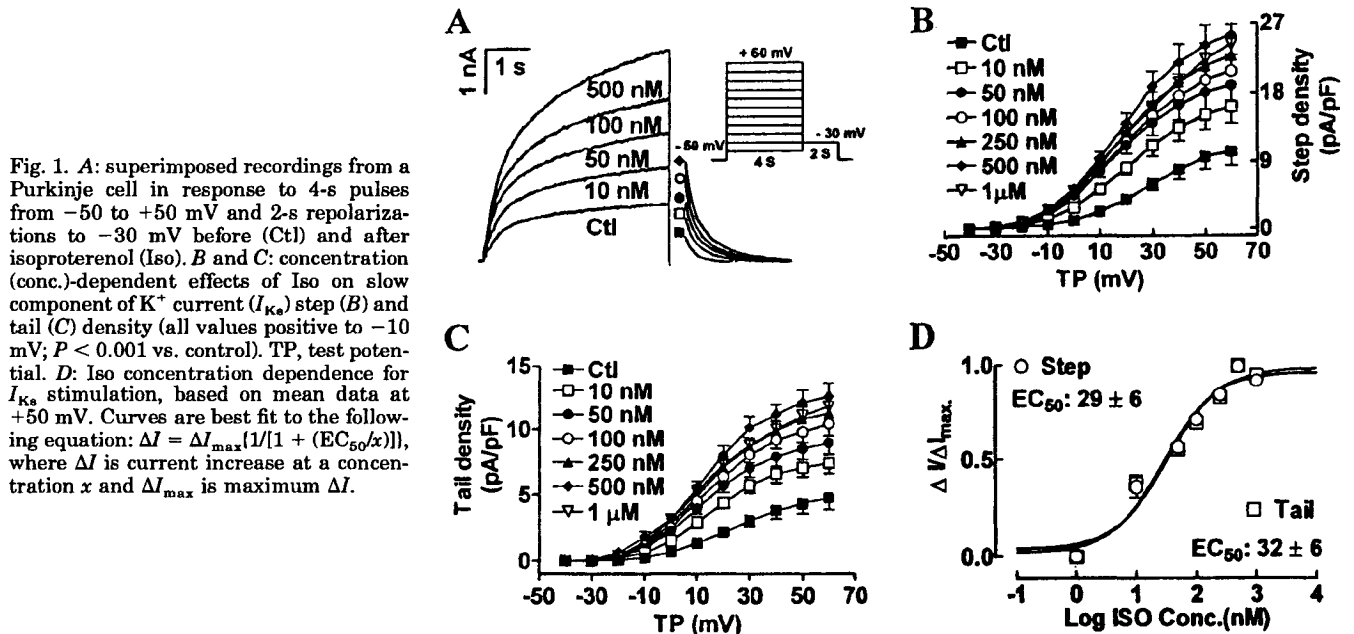


Fig. 1. A: superimposed recordings from a Purkinje cell in response to 4-s pulses from -50 to +50 mV and 2-s repolarizations to -30 mV before (Ctl) and after isoproterenol (Iso). B and C: concentration (conc.)-dependent effects of Iso on slow component of K^+ current (I_{Ks}) step (B) and tail (C) density (all values positive to -10 mV; $P < 0.001$ vs. control). TP, test potential. D: Iso concentration dependence for I_{Ks} stimulation, based on mean data at +50 mV. Curves are best fit to the following equation: $\Delta I = \Delta I_{max} / [1 + (EC_{50}/x)^n]$, where ΔI is current increase at a concentration x and ΔI_{max} is maximum ΔI .

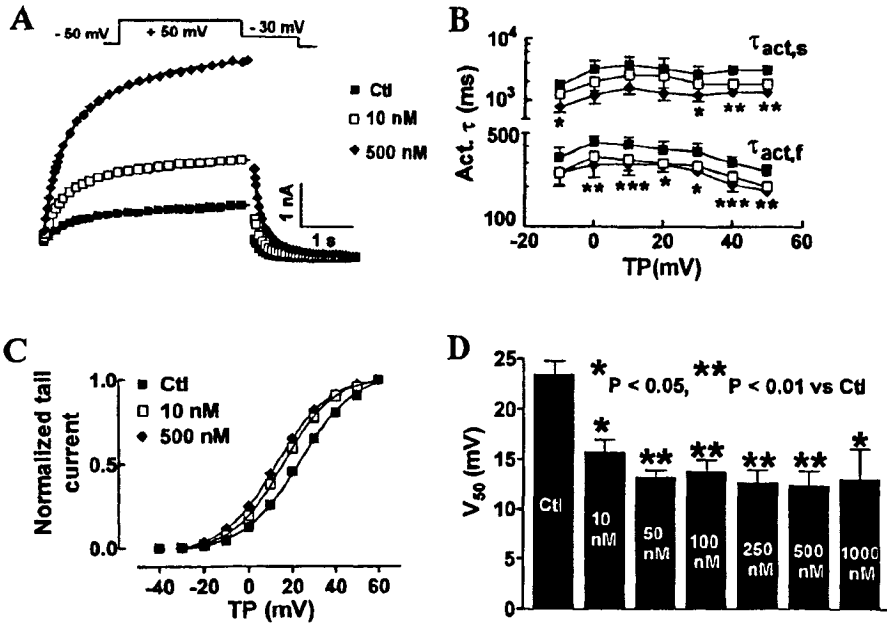


Fig. 2. *A*: representative data (data reduction applied so that curve fits can be seen) during 4-s depolarizations to +50 mV and 2-s repolarizations to -30 mV in the absence and presence of 10 and 500 nM Iso. Biexponential fits of activation and deactivation are shown. *B*: activation time constants (Act τ) for 6 cells (means \pm SE) before and after exposure to Iso. $\tau_{act,s}$ and $\tau_{act,f}$ slow and fast activation time constants, respectively. *C*: current-voltage (*I-V*) relations of tail currents normalized to current at most positive step potential under control conditions and in the presence of 10 and 500 nM Iso. Tail currents were fit by Boltzmann relations to obtain the half-activation voltage (V_{50}). *D*: activation V_{50} in 6 cells studied under control conditions and all Iso concentrations. * $P < 0.05$; ** $P < 0.01$; *** $P < 0.001$ vs. control.

293B. The control AP waveform was used to voltage clamp the cell before (Fig. 4*D*) and after (Fig. 4*E*) Iso. The Iso-sensitive current (Fig. 4*F*) included inward and outward components, compatible with I_{Ca} and I_{Ks} . The AP waveform recorded in the presence of Iso was then used to AP clamp the cell in the presence of Iso before (Fig. 4*G*) and after (Fig. 4*H*) 293B. The 293B-sensitive waveform (Fig. 4*I*) indicates that 293B suppressed early transient and more delayed plateau outward components, compatible with inhibition of I_{to} and I_{Ks} (7). These results indicate that 293B prolongation of the AP in the presence of Iso likely resulted from

outward current inhibition but that I_{to} and I_{Ks} could have been involved. Similar AP-clamp results were obtained in three other cells.

Because of the effects of 293B on I_{to} and I_{Ks} , we studied the effects of L-768673, reported to be a potent and selective inhibitor of I_{Ks} ($EC_{50} = 6$ nM) in guinea pig ventricular myocytes (23), on PC I_{Ks} . Unfortunately, L-768673 did not affect PC I_{Ks} . In five PCs, the density of I_{Ks} time-dependent activating current at the end of a 4-s pulse to +40 mV averaged 4.9 ± 0.7 and 5.1 ± 0.9 pA/pF ($P = NS$) before and after L-768673, respectively.

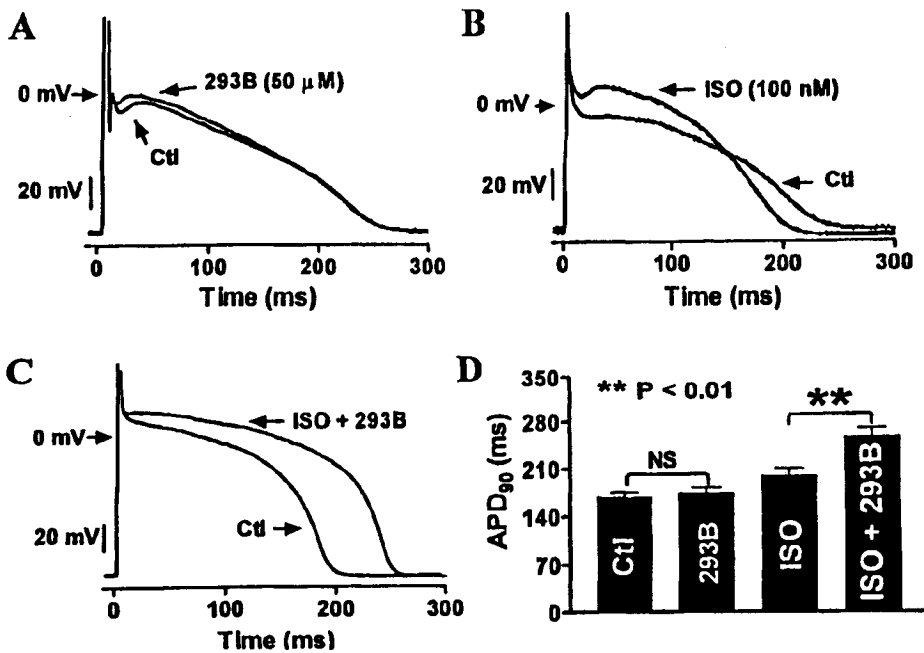
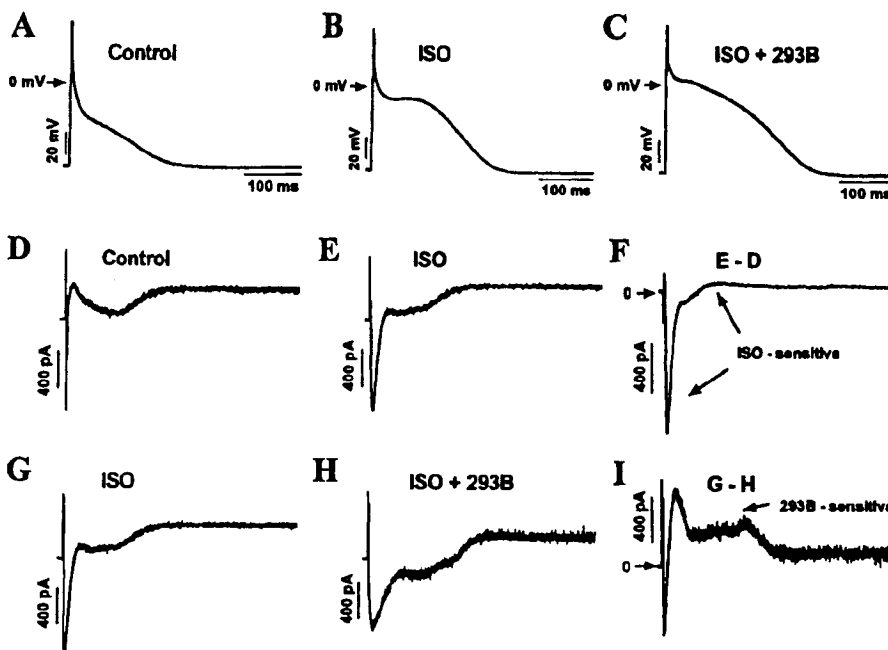


Fig. 3. Influence of 293B, Iso, and 293B + Iso on action potential (AP). Recordings were conducted under current-clamp mode at 37°C. APs were elicited by twice-threshold rectangular pulses at a frequency of 0.1 Hz. *A-C*: representative Purkinje cell APs in the absence (Ctl) and presence of 293B (*A*), Iso alone (*B*), and Iso + 293B (*C*). *D*: changes of AP duration (APD) to 90% repolarization (APD₉₀) in 293B, Iso, and 293B + Iso ($n = 7$ per group). Iso did not significantly change APD vs. control. Each cell was studied under control conditions and after 1 intervention. Control APDs were not significantly different among groups.

Fig. 4. Currents affected by Iso and 293B, as indicated by AP-clamp methods. A–C: APs from 1 cell recorded at 0.1 Hz under control conditions (A) and after the sequential addition of 100 nM Iso (B) and 50 μ M 293B + 100 nM Iso (C). The AP recorded under control conditions (A) was used as a voltage-clamp waveform to elicit currents under control conditions (D) and then in the presence of Iso (E). The subtracted current (F) indicates the Iso-sensitive component flowing during the AP. The AP recorded in the presence of 100 nM Iso (B) was used as a voltage command pulse to record currents in the presence of Iso alone (G) and then in the presence of Iso + 293B (H). The subtracted current (I) gives an indication of the 293B-sensitive current during the AP in the presence of Iso. Similar results were obtained in 3 other experiments.



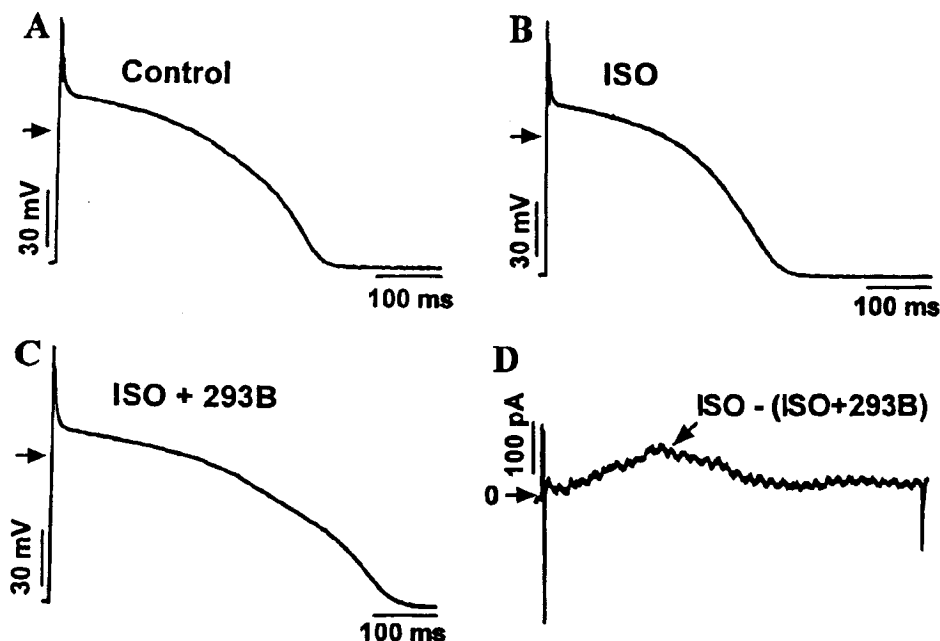
Because we were unable to identify a more selective tool than 293B with which to inhibit PC I_{Ks} , we used 4-AP to study (in the absence of I_{to}) the effects of Iso in the absence and presence of 293B. Figure 5 shows AP recordings from one PC under control (A), Iso (B), and Iso + 293B (C) conditions in the continuous presence of 1 mM 4-AP to suppress I_{to} . Under these conditions, APD at 90% repolarization in eight cells averaged 211 ± 29 and 218 ± 26 ms under control and Iso conditions ($P = NS$) compared with 281 ± 43 ms ($P = 0.02$ vs. Iso alone) in the presence of Iso + 293B. In the absence of Iso, APD at 90% repolarization averaged

190 ± 15 ms in six cells before and 193 ± 12 ms after 293B ($P = NS$). As shown in Fig. 5D, the 293B-sensitive current during AP clamp (current in the presence of Iso alone compared with current in the presence of Iso + 293B) showed a delayed outward current, without any transient component, indicating that the effect of 293B on the AP in the presence of 4-AP is attributable to I_{Ks} inhibition alone.

DISCUSSION

We recorded large I_{Ks} with typical properties in canine PCs. We were unable to demonstrate an effect of

Fig. 5. Effects of Iso and 293B on Purkinje cell APs in the absence of transient outward current (I_{to}). A cell was exposed to each condition during the continuous presence of 1 mM 4-aminopyridine. APs (at 0.1 Hz) from 1 cell are shown under control conditions (A) and after the addition of Iso (B) and Iso + 293B (C). AP clamp was used to record the 293B-sensitive current in the presence of Iso (D). In the presence of Iso, 293B removed an outward component that activated during the plateau and then deactivated on repolarization, consistent with I_{Ks} . Similar results were obtained in 3 other experiments.



I_{Ks} inhibition on PC APD in the absence of β -adrenergic stimulation; however, in the presence of β -adrenergic stimulation, I_{Ks} appeared to contribute to PC repolarization.

Comparison with previous observations regarding I_K in isolated PCs. In contrast to the very clear I_K recorded from multicellular Purkinje fiber preparations (5, 17), studies in isolated PCs have described very small (22) or absent (9, 18) I_K. In the present study, we were able to record large I_{Ks} step and tail currents in PCs from canine false tendons, with properties compatible with those reported for I_{Ks} in multicellular Purkinje preparations (5, 17) and isolated ventricular myocytes (3, 11, 13, 14, 20, 21, 29). The effects of Iso in our study, including increased I_{Ks} density, negative shift in inactivation voltage dependence, and acceleration of activation, are similar to effects in guinea pig ventricular myocytes (29) and bull frog atrial myocytes (11). The presence of clear I_{Ks} in our preparations, in contrast to previous studies in PCs, may be due to species differences (rabbit vs. dog) or the site from which cells are isolated (subendocardial tissues vs. false tendons). An additional very important factor may be differences in isolation technique, to which I_K is particularly sensitive (30). Given the physiological significance of I_K and the importance of I_{Ks} deficiencies in congenital LQTS, the demonstration of clear I_{Ks} in single PCs is, in itself, a significant contribution.

Role of I_{Ks} in PC repolarization and potential importance in LQTS. We were unable to identify a role for I_{Ks} in PC repolarization in the absence of β -adrenergic stimulation. These results are similar to those of Varro et al. (26) and Burashnikov and Antzelevitch (8). The lack of I_{Ks} involvement in PC repolarization is consistent with PC plateau voltage in the range of 0 mV, at which relatively little I_{Ks} is activated. We found three mechanisms through which β -adrenergic stimulation can increase the contribution of I_{Ks} to PC repolarization: 1) increased maximal conductance, 2) accelerated activation, and 3) an activation-voltage shift toward the plateau potential. β -Adrenergic stimulation is well known to enhance L-type I_{Ca} (11), an effect that in itself would tend to delay repolarization and promote arrhythmogenic afterdepolarizations (12, 15). An important functional role of I_{Ks} in PCs might therefore be to act as a "brake" to prevent excessive APD prolongation in the face of β -adrenergic enhancement of L-type I_{Ca}. Varro et al. (26) recently suggested a similar type of I_{Ks} "braking" function against excessive APD prolongation caused by I_{Kr} blockade. I_{Ks} may therefore function more as a physiological safety mechanism protecting against factors prolonging APD than as an important repolarizing current under normal conditions.

Our results point to a possible mechanism whereby Purkinje fibers could participate in producing ventricular tachyarrhythmias in congenital LQTS caused by dysfunctional I_{Ks}, LQTS1 and LQTS5 (1, 3). If I_{Ks} activation by β -adrenergic stimulation serves as a brake for the APD-prolonging effect of adrenergic enhancement of I_{Ca}, unopposed I_{Ca} stimulation in pa-

tients with I_{Ks} dysfunction could provoke excessive APD prolongation, leading to arrhythmogenic afterdepolarizations in PCs. These afterdepolarizations could act as a trigger on the reentrant substrate caused by transmural repolarization abnormalities (25) to produce TdP. This notion is consistent with the preferential occurrence of drug-induced early afterdepolarizations (EADs) in the Purkinje fiber network (16), initiation by subendocardial-triggered activity of reentry in an animal LQTS model (10), and mathematical modeling studies of polymorphic ventricular tachyarrhythmias (6). However, EADs were not recorded in the present study or in the study of Burashnikov and Antzelevitch (8). The in vitro conditions may be suppressing EAD generation, or other mechanisms similar to delayed afterdepolarizations (8) may be provoked by prolonged APs.

Potential limitations. The isolation of PCs is difficult, particularly because of the connective tissue sheath around false tendons. This may account for discrepant results in the literature and increases variability in PC APs. Some of the variability in single-cell APs may also be due to intrinsic differences among cells in ionic current composition (27). Another problem that we encountered was a lack of highly selective I_{Ks} blockers for pharmacological dissection.

We used AP clamp to evaluate the currents responsible for 293B-induced AP prolongation in the presence of Iso. The AP-clamp technique requires that electrophysiological conditions be stable over the course of measurement before and after an intervention. To avoid potential time-dependent confounding factors, we recorded the AP under control conditions before drug superfusion and then used the recorded control AP to perform AP clamp immediately before and immediately after equilibration with a drug (5 min). Nonetheless, some current rundown may still have occurred, with I_{Ca} rundown possibly explaining the small early inward component in Fig. 4I. We did not perform a detailed characterization of all repolarizing currents in PCs and, therefore, cannot exclude Iso- or 293B-mediated effects via processes such as the Ca²⁺-dependent Cl⁻ current, the Na⁺/Ca²⁺ exchanger, Na⁺-K⁺-ATPase, or intracellular Ca²⁺ handling.

The authors thank Chantal St-Cyr for excellent technical assistance and Annie Laprade and France Thériault for secretarial help with the manuscript.

This work was supported by operating grants from the Medical Research Council of Canada and the Quebec Heart Foundation.

REFERENCES

1. Ackerman MJ. The long QT syndrome: ion channel diseases of the heart. *Mayo Clin Proc* 73: 250-269, 1998.
2. Ali RH, Zareba W, Rosero SZ, Moss AJ, Schwartz PJ, Benhorin J, Priori SG, Robinson JL, and Locati EH. Adrenergic triggers and non-adrenergic factors associated with cardiac events in long QT syndrome patients (Abstract). *PACE* 20: 1072, 1997.
3. Barhanin J, Attali B, and Lazdunski M. I_{Ks}, a slow and intriguing cardiac K⁺ channel and its associated long QT diseases. *Trends Cardiovasc Med* 8: 207-214, 1998.

4. Bennett PB and Begenisich TB. Catecholamines modulate the delayed rectifying potassium current (I_K) in guinea pig ventricular myocytes. *Pflügers Arch* 410: 217–219, 1987.
5. Bennett P, McKinney L, Begenisich T, and Kass RS. Adrenergic modulation of the delayed rectifier potassium channel in calf cardiac Purkinje fibers. *Biophys J* 49: 839–848, 1986.
6. Berenfeld O and Jalife J. Purkinje-muscle reentry as a mechanism of polymorphic ventricular arrhythmias in a 3-dimensional model of the ventricles. *Circ Res* 82: 1063–1077, 1998.
7. Bosch RF, Gaspo R, Busch AE, Lang HJ, Li GR, and Nattel S. Effects of the chromanol 293B, a selective blocker of the slow component of the delayed rectifier K^+ current, on repolarization in human and guinea pig ventricular myocytes. *Cardiovasc Res* 38: 441–450, 1998.
8. Burashnikov A and Antzelevitch C. Block of $I(Ks)$ does not induce early afterdepolarization activity but promotes β -adrenergic agonist-induced delayed afterdepolarization activity. *J Cardiovasc Electrophysiol* 11: 458–465, 2000.
9. Cordeiro JM, Spitzer KW, and Giles WR. Repolarizing K^+ currents in rabbit heart Purkinje cells. *J Physiol (Lond)* 503: 811–823, 1998.
10. El-Sherif N, Caref EB, Yin H, and Restivo M. The electrophysiological mechanism of ventricular arrhythmias in the long QT syndrome. Tridimensional mapping of activation and recovery patterns. *Circ Res* 79: 474–492, 1996.
11. Giles W, Nakajima T, Ono K, and Shibata EF. Modulation of the delayed rectifier K^+ current by isoprenaline in bull-frog atrial myocytes. *J Physiol (Lond)* 415: 233–249, 1989.
12. January CT and Riddle JM. Early afterdepolarizations: mechanism of induction and block. A role for L-type Ca^{2+} current. *Circ Res* 64: 977–990, 1989.
13. Li GR, Feng J, Yue L, Carrier M, and Nattel S. Evidence for two components of delayed rectifier K^+ current in human ventricular myocytes. *Circ Res* 78: 689–696, 1996.
14. Liu DW and Antzelevitch C. Characteristics of the delayed rectifier current (I_{Kr} and I_{Ks}) in canine ventricular epicardial, midmyocardial, and endocardial myocytes. A weaker I_{Ks} contributes to the longer action potential of the M cell. *Circ Res* 76: 351–365, 1995.
15. Marban E, Robinson SW, and Wier WG. Mechanisms of arrhythmogenic delayed and early afterdepolarizations in ferret ventricular muscle. *J Clin Invest* 78: 1185–1192, 1986.
16. Nattel S and Quantz MA. Pharmacological response of quinidine-induced early afterdepolarizations in canine cardiac Purkinje fibres: insights into underlying ionic mechanisms. *Cardiovasc Res* 22: 808–817, 1988.
17. Noble D and Tsien RW. Outward membrane currents activated in the plateau range of potentials in cardiac Purkinje fibres. *J Physiol (Lond)* 200: 205–231, 1969.
18. Pinto JMB and Boyden PA. Reduced inward rectifying and increased E-4031-sensitive K^+ current density in arrhythmogenic subendocardial Purkinje myocytes from the infarcted heart. *J Cardiovasc Electrophysiol* 9: 299–311, 1998.
19. Sanguinetti MC. Dysfunction of delayed rectifier potassium channels in an inherited cardiac arrhythmia. *Ann NY Acad Sci* 868: 406–413, 1999.
20. Sanguinetti MC and Jurkiewicz NK. Two components of cardiac delayed rectifier K^+ current. Differential sensitivity to block by class III antiarrhythmic agents. *J Gen Physiol* 96: 195–215, 1990.
21. Sanguinetti MC, Jurkiewicz NK, Scott A, and Siegl PKS. Isoproterenol antagonizes prolongation of refractory period by the class III antiarrhythmic agent E-4031 in guinea pig myocytes. Mechanism of action. *Circ Res* 68: 77–84, 1991.
22. Scamps F and Carmeliet E. Delayed K^+ current and external K^+ in single cardiac Purkinje cells. *Am J Physiol Cell Physiol* 257: C1086–C1092, 1989.
23. Selnick HG, Liverton NJ, Baldwin JJ, Butcher JW, Claramon DA, Elliott JM, Freidinger RM, King SA, Libby BE, McIntyre CJ, Pribush DA, Remy DC, Smith GR, Tebben AJ, Jurkiewicz NK, Lynch JJ, Salata JJ, Sanguinetti MC, Siegl PK, Slaughter DE, and Vyas K. Class III antiarrhythmic activity in vivo by selective blockade of the slowly activating cardiac delayed rectifier potassium current I_{Ks} by (R)-2-(2,4-trifluoromethyl)-N-[2-oxo-5-phenyl-1-(2,2,2-trifluoroethyl)-2,3-dihydro-1H-benzof[e][1,4]diazepin-3-yl]acetamide. *J Med Chem* 40: 3865–3868, 1997.
24. Shi H, Wang H, and Wang Z. Identification and characterization of multiple subtypes of muscarinic acetylcholine receptors and their physiological functions in canine hearts. *Mol Pharmacol* 55: 497–507, 1999.
25. Shimizu W and Antzelevitch C. Cellular basis for the ECG features of the LQT1 form of the long-QT syndrome. Effects of β -adrenergic agonists and antagonists and sodium channel blockers on transmural dispersion of repolarization and torsade de pointes. *Circulation* 98: 2314–2322, 1998.
26. Varro A, Balati B, Iost N, Takacs J, Virag L, Lathrop DA, Casaba L, Talosi L, and Papp JG. The role of the delayed rectifier component I_{Ks} in dog ventricular muscle and Purkinje fibre repolarization. *J Physiol (Lond)* 523: 67–81, 2000.
27. Verkerk AO, Veldkamp MW, Abbate F, Antoons G, Bouman LN, Ravesloot JH, and Van Ginneken ACG. Two types of action potential configuration in single cardiac Purkinje cells of sheep. *Am J Physiol Heart Circ Physiol* 277: H1299–H1310, 1999.
28. Wilde AAM, Jongbloed RJE, Doevendans PA, Düren Hauer RNW, van Langen IM, van Tintelen JP, Smeets HJM, Meyer H, and Geelen JLMC. Auditory stimuli as a trigger for arrhythmic events differentiate *HERG*-related (LQTS2) patients from *KvLQT1*-related patients (LQTS1). *J Am Coll Cardiol* 33: 327–332, 1999.
29. Yazawa K and Kameyama M. Mechanism of receptor-mediated modulation of the delayed outward potassium current in guinea-pig ventricular myocytes. *J Physiol (Lond)* 421: 135–150, 1990.
30. Yue L, Feng J, Li GR, and Nattel S. Transient outward and delayed rectifier currents in canine atrium: properties and role of isolation methods. *Am J Physiol Heart Circ Physiol* 270: H2157–H2168, 1996.

**CHAPTER 5. PURKINJE CELL IONIC REMODELING BY
CONGESTIVE HEART FAILURE**

Ionic Remodeling of Cardiac Purkinje Cells by Congestive Heart Failure

Wei Han, MSc; Denis Chartier, BSc; Danshi Li, MD, PhD; Stanley Nattel, MD

Background—Cardiac Purkinje cells (PCs) are important for the generation of triggered arrhythmias, particularly in association with abnormal repolarization. The effects of congestive heart failure (CHF) on the ionic properties of PCs are unknown.

Methods and Results—PCs were isolated from false tendons of control dogs and dogs with ventricular tachypacing-induced CHF. CHF PCs were hypertrophied (capacitance, mean \pm SEM, 149 ± 4 pF, $n = 130$; versus 128 ± 3 pF, $n = 150$, control; $P < 0.001$). Transient outward current density was reduced in CHF PCs without change in voltage dependence or kinetics. CHF also reduced inward-rectifier current density, with no change in form of the current-voltage relationship. Densities of L- and T-type calcium, rapid and slow delayed rectifier, and Na^+ - Ca^{2+} exchange currents were unaltered by CHF, but L-type calcium current inactivation was slowed at positive potentials. Purkinje fiber action potentials from CHF dogs showed decreased phase 1 amplitudes and elevated plateau voltages and demonstrated twice as much prolongation on exposure to the rapid delayed rectifier blocker E-4031 as control Purkinje fibers.

Conclusions—CHF causes remodeling of important K^+ and Ca^{2+} currents in cardiac PCs, decreasing repolarization reserve and causing an exaggerated repolarization delay in response to a class III drug. These results have important potential implications regarding ventricular arrhythmogenesis, particularly related to triggered activity in PCs, in patients with CHF. (*Circulation*. 2001;104:2095-2100.)

Key Words: ion channels ■ remodeling ■ electrophysiology ■ antiarrhythmia agents ■ heart failure

Congestive heart failure (CHF) predisposes to the generation of ventricular tachyarrhythmias¹ and the occurrence of sudden death.² In addition, CHF promotes drug-induced Torsades de Pointes arrhythmias.³ Abnormal repolarization, related to ion channel remodeling, is important in the arrhythmogenic potential of CHF.^{1,4,5}

CHF-induced remodeling of ionic currents in ventricular⁵ and atrial⁶ myocytes has been studied in detail. Cardiac Purkinje cells (PCs) are believed to play important roles in the generation of ventricular arrhythmias, particularly those related to triggered activity.⁷⁻⁹ Ionic currents are altered in subendocardial PCs in regions of myocardial infarction¹⁰⁻¹²; however, almost nothing is known about PC ionic remodeling in CHF. The present study was designed to evaluate CHF-induced changes in ionic currents and action potentials (APs) in canine cardiac PCs.

Methods

CHF Preparation

CHF was produced as previously described⁶ by pacing the right ventricle at 240 bpm for 3 weeks followed by 2 weeks at 220 bpm. Dogs were then anesthetized with morphine (2 mg/kg SC) and α -chloralose (120 mg/kg IV load, 29.25 mg/kg per hour infusion),

and a median sternotomy was performed. All animal care and handling procedures followed the guidelines of the Canadian Council on Animal Care. Excised hearts were immersed in Tyrode solution at room temperature. Free-running false tendons were excised into modified Eagle's MEM (Gibco-BRL; pH 6.8, HEPES-NaOH) containing collagenase (800 to 900 U/mL, Worthington Type-II) and 1% BSA (Sigma), and single PCs were isolated as previously described.^{13,14}

Solutions

Standard Tyrode solution contained (in mmol/L) NaCl 136, KCl 5.4, MgCl₂ 1, CaCl₂ 1, NaH₂PO₄ 0.33, HEPES 5, and dextrose 10; pH 7.4 (NaOH). High-K⁺ storage solution contained (in mmol/L) KCl 20, KH₂PO₄ 10, dextrose 10, glutamic acid 70, β -hydroxybutyric acid 10, taurine 10, and EGTA 10; 0.1% BSA; pH 7.4 (KOH). Standard pipette solution contained (in mmol/L) K⁺ aspartate 110, KCl 20, MgCl₂ 1, Mg₂ATP 5, HEPES 10, phosphocreatine 5, GTP 0.1, and EGTA 5; pH 7.2 (KOH). Solutions were equilibrated with 100% O₂.

For K⁺ current measurement, the extracellular solution included 1 μ mol/L atropine to eliminate muscarinic K⁺ currents and CdCl₂ (200 μ mol/L) or nimodipine (1 μ mol/L, for I_K studies) to block Ca²⁺ currents. Na⁺ current contamination was prevented by equimolar substitution of choline for extracellular Na⁺. For currents other than transient outward current (I_{to}), 1 mmol/L 4-AP was used to block I_{to}. Rapid delayed rectifier current (I_{Kr}) was studied as 5 μ mol/L E4031-sensitive current and inward rectifier current (I_{K1}) as 1 mmol/L Ba²⁺-sensitive current. Slow delayed rectifier current (I_{Ks})

Received May 17, 2001; revision received July 20, 2001; accepted July 25, 2001.

From the Department of Medicine, Montreal Heart Institute and University of Montreal (W.H., D.C., D.L., S.N.) and the Department of Pharmacology, McGill University (W.H., S.N.), Montreal, Quebec, Canada.

Correspondence to Stanley Nattel, Montreal Heart Institute Research Center, 5000 Belanger St East, Montreal, Quebec, H1T 1C8, Canada. E-mail nattel@icm.umontreal.ca

© 2001 American Heart Association, Inc.

Circulation is available at <http://www.circulationaha.org>

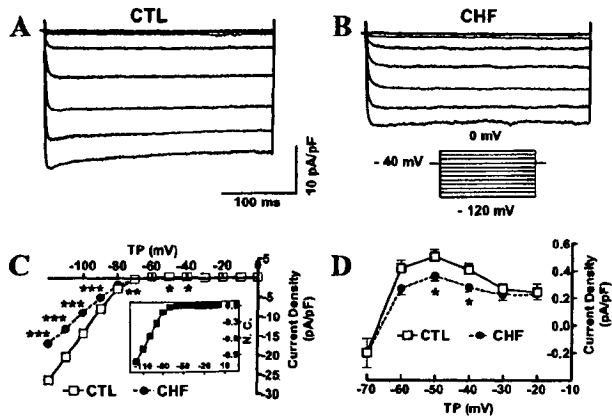


Figure 1. Ba²⁺-sensitive I_{K1} in representative control (A) and CHF (B) PCs (voltage protocol in inset delivered at 0.1 Hz). C, Mean ± SEM I_{K1} density in 29 control and 27 CHF cells. *P < 0.05, **P < 0.01, ***P < 0.001 vs control. Inset, Normalized current-voltage relations overlap. D, Currents between -70 and -20 mV on expanded scale. CTL indicates control; TP, test potential.

was studied in the presence of 1 μmol/L dofetilide to eliminate I_{Kr}. For I_{Ca} recording, the bath solution contained tetraethylammonium chloride, CsCl, and CsOH in place of NaCl, KCl, and NaOH, respectively, and [CaCl₂] was 2 mmol/L. The pipette for I_{Ca} recording contained (in mmol/L) CsCl 20, Cs-aspartate 110, MgCl₂ 1, EGTA 10, GTP 0.1, ATP-Mg 5, HEPES 10, and Na₂ phosphocreatine 5; pH 7.2 (CsOH). Na⁺-Ca²⁺ exchange (NCX) current (I_{NCX}) was recorded with ramp pulses and extracellular (in mmol/L, NaCl 140, CaCl₂ 0 or 5, MgCl₂ 1, CsCl 5, HEPES 5, nimodipine 0.001, ouabain 0.01, and ryanodine 0.005; pH 7.2 CsOH) and pipette (in mmol/L, CsCl 90, NaCl 50, MgATP 5, MgCl₂ 3, EGTA 13, and HEPES 20; pH 7.2, CsOH) solutions designed to suppress K⁺ current, Na⁺-K⁺ ATPase, and sarcoplasmic reticulum Ca²⁺ release.¹⁵

Data Acquisition and Analysis

Whole-cell patch clamp was performed as previously described^{13,14} at 36.5°C. Compensated series resistance and capacitive time constants (τ) averaged 2.5 ± 0.1 MΩ and 290 ± 10 μs. Leakage compensation was not used. The capacitance of CHF cells was increased (149 ± 4 pF, n = 130, versus 128 ± 3 pF in control, n = 150; P < 0.001), so currents are expressed in terms of density.

Standard microelectrode techniques were used to record action potentials (APs). The Tyrode solution contained (in mmol/L) NaCl 120, KCl 1.5, KH₂PO₄ 1.2, MgSO₄ 0.1, NaHCO₃ 25, CaCl₂ 1.25, and dextrose 5; pH 7.4. Purkinje fiber false tendons were superfused with oxygenated (95% O₂ and 5% CO₂) Tyrode solution at 36°C and impaled with 3 mol/L KCl-filled glass microelectrodes (8 to 20 MΩ) connected to a high input-impedance amplifier.

Nonlinear least-square curve-fitting algorithms were used for curve fitting. Nonpaired t tests were used to compare CHF with control cells. P < 0.05 was considered to indicate statistical significance. Group data are expressed as mean ± SEM.

Results

Changes in Ionic Currents

K⁺ Currents

Figure 1 shows representative I_{K1} recordings (panels A and B). CHF significantly reduced I_{K1} (C), including the outward component (D), without altering the form of the I_{K1} current-voltage relation (Figure 1C, inset).

Figures 2A and 2B illustrate I_{to} recordings from control and CHF PCs. I_{to} density was significantly smaller in CHF PCs (Figure 2C); however, there were no differences in the form

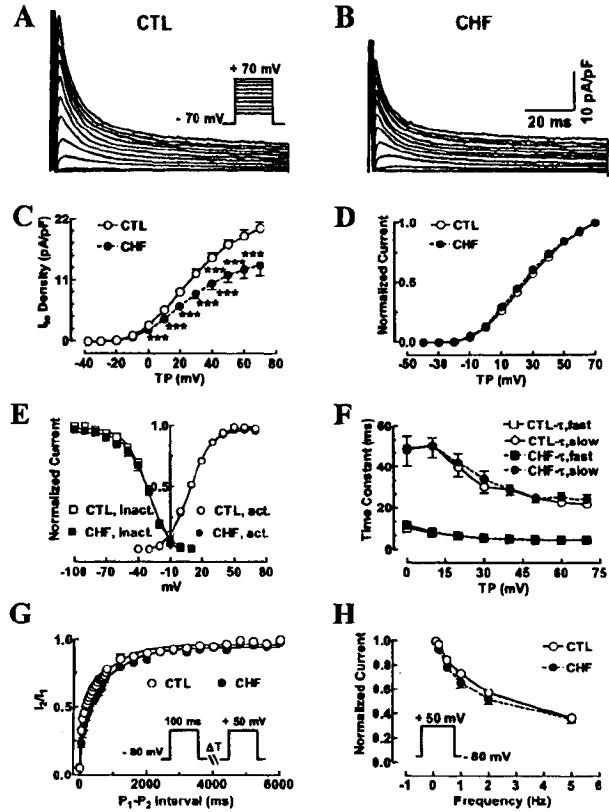


Figure 2. I_{to} recordings obtained with 100-ms test pulses at 0.1 Hz from representative control (A) and CHF (B) PCs. C, Mean ± SEM I_{to} density for 37 cells from 13 control dogs and 34 cells from 14 CHF dogs (*P < 0.05, **P < 0.01, ***P < 0.001 vs control at same test potential). D, Mean ± SEM I_{to}-V relations normalized to maximum current in each cell. E, I_{to} inactivation and activation voltage dependence. Inactivation was evaluated with 1000-ms prepulses followed by a 200-ms test pulse to +50 mV. Activation voltage dependence was analyzed from data obtained with the protocol in panel A according to equation in the text. Data are mean ± SEM (n = 10 cells/group, inactivation; n = 20 cells/group, activation); curves are best-fit Boltzmann relations. F, Mean ± SEM inactivation τs (n = 15 cells/group). G, I_{to} reactivation time course evaluated by ratio of current (I₂) during a 100-ms test pulse (P₂, identical to P₁) to current (I₁) during a conditioning pulse (P₁) with varying P₁ to P₂ interval (protocol delivered at 0.07 Hz). Curves are biexponential fits (n = 10 cells/group). H, I_{to} frequency dependence, determined by ratio of current during the 15th pulse to current during the first pulse of a train of 100-ms depolarizations (n = 15 cells/group). CTL indicates control; TP, test potential.

of the I_{to}-V relation (Figure 2D). The voltage dependence of I_{to} inactivation was tested with a 2-pulse protocol as described in Figure 2E. Activation voltage dependence was evaluated from the relation I_{TP} = a_{TP}G_{max}(V_{TP} - V_R), where I_{TP} and a_{TP} are current and activation variable at test potential V_{TP}, V_R is reversal potential, and G_{max} is maximal conductance. Half-maximal voltage (V_{1/2}) and activation slope factor (Boltzmann fits) were 8.9 ± 0.7 and 10.3 ± 0.4 mV (control) and 8.9 ± 1.0 and 10.9 ± 1.0 mV (CHF, P = NS). V_R obtained from the reversal of I_{to} tail currents after 2-ms activating pulses averaged -75.3 ± 2.2 mV. Inactivation V_{1/2} and slope factor were -30 ± 2 and 11 ± 1 mV (control) and -31 ± 2 and 11 ± 1 mV (CHF, P = NS). I_{to} inactivation kinetics were biexponential, with τs unaltered by CHF (Figure 2F). I_{to} recovery

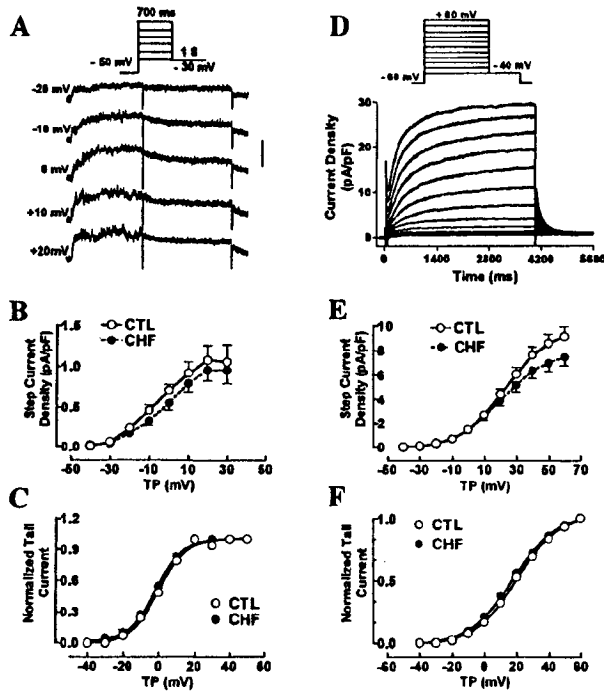


Figure 3. A, Representative E-4031-sensitive I_{Kr} recordings. B, Mean \pm SEM I_{Kr} density voltage relations ($n=11$, control; $n=9$, CHF). C, Mean \pm SEM normalized I_{Kr} tail currents ($n=5$ cells/group) and best-fit Boltzmann relations. D, Representative I_{Ks} recordings with 4-second depolarizing pulses (0.1 Hz) and 2-second repolarizations to -40 mV to record tail currents. E, Mean \pm SEM I_{Ks} density voltage relations ($n=30$, control; $n=25$, CHF). F, Normalized I_{Ks} tail I - V relations and best-fit Boltzmann relations. CTL indicates control; TP, test potential.

(Figure 2G) was biexponential, with τ s averaging 42 ± 8 and 1391 ± 67 ms (control) and 52 ± 11 and 1486 ± 108 ms (CHF, $n=10$ for each, $P=NS$). I_{to} frequency dependence was similarly unaffected by CHF (Figure 2H).

Figure 3 shows results for I_{Kr} (left) and I_{Ks} (right). Representative control recordings are shown at the top, with mean step I - V relations, which were unchanged by CHF, in the middle. Activation voltage dependence based on normalized tail currents is shown in bottom panels and was not altered by CHF for either I_{Kr} or I_{Ks} .

Ca²⁺ Currents

Representative L-type calcium current ($I_{Ca,L}$) recordings are shown in Figures 4A and 4B and point to slowed $I_{Ca,L}$ decay in CHF. $I_{Ca,L}$ density was not significantly different between control and CHF cells (Figure 4C). Inactivation τ s were slowed significantly by CHF at voltages positive to $+10$ mV (Figure 4D). For example, at $+20$ mV, τ_{fast} increased from 6.0 ± 0.3 to 8.2 ± 0.9 ms ($P<0.05$) and τ_{slow} from 38 ± 2 to 66 ± 8 ms ($P<0.01$) in CHF PCs. In addition to a slowing of inactivation τ s, CHF significantly increased the proportion of slow-phase inactivation at positive voltages (Figure 4E). For example, at $+30$ mV, τ_2 accounted for $36 \pm 4\%$ of inactivation in control PCs compared with $51 \pm 5\%$ in CHF ($P<0.05$). $I_{Ca,L}$ inactivation voltage dependence was assessed with a 2-pulse protocol (Figure 4F). Inactivation $V_{1/2}$ and slope factor were -25 ± 2 and -6 ± 1 mV (control) and -26 ± 1 and -7 ± 1 mV

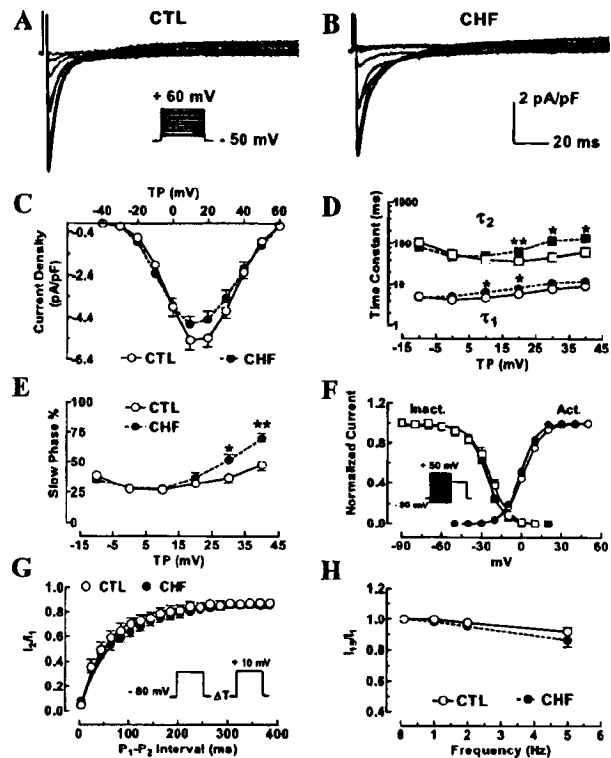


Figure 4. Representative $I_{Ca,L}$ recordings obtained with 250-ms pulses (0.1 Hz) in a control (A) and CHF (B) cell. C, Mean \pm SEM $I_{Ca,L}$ density obtained with the protocol shown in panel A ($n=26$ and 24 cells in control and CHF, respectively). D, Mean \pm SEM $I_{Ca,L}$ inactivation time constants ($n=12$ cells, control; $n=14$, CHF) obtained from recordings with the protocol in panel A. E, Mean \pm SEM percentage of overall inactivation proceeding by the slower time constant at each test potential. $*P<0.05$ and $**P<0.01$ versus control. F, Voltage dependence of $I_{Ca,L}$ inactivation (Inact.) and activation (Act.). Steady-state inactivation was assessed with 1-second conditioning pulses followed by a 300-ms test pulse to $+10$ mV (0.1 Hz). Activation was assessed from data obtained with the protocol shown in panel A, according to the equation in the text. Data are mean \pm SEM from 10 control and 10 CHF cells; curves are best-fit Boltzmann relations. G, $I_{Ca,L}$ reactivation time course, studied with paired 100-ms pulses delivered with varying interpulse intervals at 0.1 Hz. Curves are monoexponential fits ($n=10$ cells/group). H, $I_{Ca,L}$ frequency dependence, determined from the ratio of current during the 15th pulse to current during the first pulse of a train of 100-ms depolarizations from -80 mV to $+10$ mV at frequencies indicated ($n=10$ cells/group). CTL indicates control; TP, test potential.

(CHF, $n=10$ cells/group, $P=NS$). Activation voltage dependence was assessed according to the relation $I_{TP} = a_{TP} G_{max} (V_{TP} - V_R)$, with V_R obtained from a linear fit to the ascending portion of the I - V relation. Resulting mean $V_{1/2}$ and slope factors were 2.0 ± 1.4 and 6.6 ± 0.2 mV (control) and 0.4 ± 1.4 and 6.5 ± 0.1 mV (CHF, $n=10$ /group, $P=NS$). Reactivation kinetics at holding potential (HP) (-80 mV) close to the PC resting potential are shown in Figure 4G. Reactivation was monoexponential, with similar τ s in control (44 ± 7 ms) and CHF PCs (53 ± 6 ms, $n=10$ /group, $P=NS$). $I_{Ca,L}$ showed little frequency dependence between 1 and 5 Hz at a HP of -80 mV, and there were no significant CHF-related differences in $I_{Ca,L}$ frequency dependence (Figure 4H).

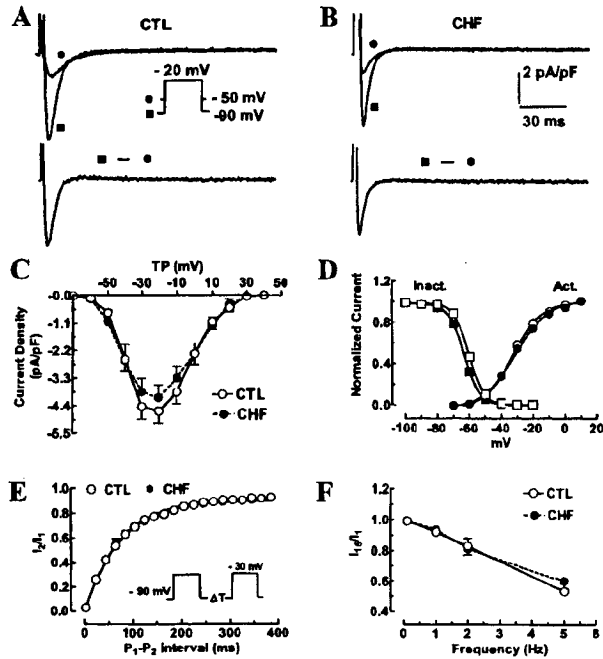


Figure 5. $I_{Ca,T}$ was obtained by subtracting currents recorded during 250-ms depolarizations (0.1 Hz) from a HP of -50 mV from those with the same depolarization and a HP of -90 mV. Examples are shown for control (A) and CHF (B) cells. C, Mean \pm SEM $I_{Ca,T}$ density voltage relation ($n=16$ cells/group). D, Voltage dependence of inactivation (Inact.) and activation (Act.) of $I_{Ca,T}$. Steady-state inactivation was assessed with 1-second prepulses from a HP of -90 mV, followed by a 300-ms test pulse to -30 mV (0.1 Hz). Activation was assessed from currents recorded on 250-ms depolarizations, according to the relation $I_{TP} = a_{TP} G_{max} (V_{TP} - V_R)$, with V_R obtained from a linear fit to the ascending portion of the $I-V$ relation. Data are mean \pm SEM for 10 cells/group; curves are best-fit Boltzmann relations. E, $I_{Ca,T}$ reactivation time course, studied with paired 100-ms pulses with varying interpulse intervals delivered at 0.1 Hz. Data are mean \pm SEM ($n=10$ /group); curves are best-fit monoexponentials. F, Frequency dependence of $I_{Ca,T}$, obtained with 15 100-ms pulses from -90 to -30 mV. Current during the 15th pulse was normalized to current during the first pulse ($n=10$ cells/group). CTL indicates control; TP, test potential.

All PCs possessed a relatively large T-type calcium current ($I_{Ca,T}$) (Figures 5A and B). $I_{Ca,T}$ was obtained as previously described^{16,17} by digital subtraction of I_{Ca} elicited at HP -50 mV from I_{Ca} at a HP of -90 mV. The mean $I_{Ca,T}$ density voltage relation was not altered by CHF (Figure 5C). $I_{Ca,T}$ inactivation $V_{1/2}$ and slope factors averaged -61 ± 2 and 4.1 ± 0.4 mV (control) and -63 ± 2 and 4.9 ± 0.5 mV (CHF, $n=10$ /group, $P=NS$) (Figure 5D). Activation $V_{1/2}$ and slope factors were -32 ± 1 and 10 ± 1 mV (control) and -30 ± 2 and 12 ± 1 mV (CHF), respectively ($n=10$ /group, $P=NS$). The time course of $I_{Ca,T}$ inactivation was monoexponential, and there were no significant differences between groups; for example, at -20 mV (voltage of maximum $I_{Ca,T}$), τ were 4.5 ± 0.2 ms (control, $n=10$) versus 4.6 ± 0.3 ms (CHF, $n=10$, $P=NS$). $I_{Ca,T}$ reactivation was assessed (Figure 5E) at a test potential (-30 mV) at which no $I_{Ca,L}$ is activated (Figure 4C). $I_{Ca,T}$ reactivation τ s averaged 51 ± 3 ms (control) versus 49 ± 4 ms (CHF, $n=10$ cells/group, $P=NS$). The frequency dependence of $I_{Ca,T}$ (Figure 4F) was greater than that of $I_{Ca,L}$ but did not differ between groups.

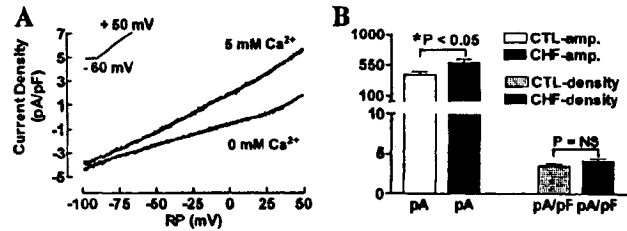


Figure 6. A, Currents recorded during 164-ms ramps from -60 to $+50$ mV in the presence of 0 and 5 mmol/L $[Ca^{2+}]_o$. B, Mean \pm SEM (24 cells/group) I_{NCX} amplitude (left) and density (right). CTL indicates control; RP, ramp potential.

NCX

Figure 6A shows I_{NCX} as determined from current during ramp depolarizations from -60 to $+50$ mV in the presence of 5 and 0 mmol/L $[Ca^{2+}]_o$. Reverse-mode I_{NCX} is substantial in the presence of 5 mmol/L Ca^{2+} and is absent in the presence of 0 mmol/L Ca^{2+} , allowing I_{NCX} to be calculated from the difference between the two current recordings.¹⁵ The results in Figure 6B show that I_{NCX} amplitude was larger in CHF cells but that after correction for cell size (capacitance normalization), there were no significant differences.

Changes in APs

PC AP characteristics were first recorded at a total of 42 sites from 11 control dogs and 37 sites in 8 CHF dogs at 1 Hz. Phase 1 repolarization was less marked in CHF, and the

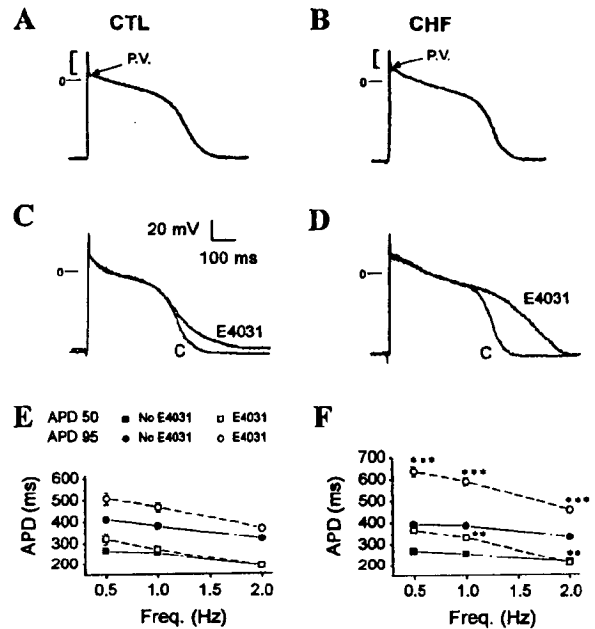


Figure 7. AP results for control (left) and CHF (right) Purkinje fiber preparations. A and B, Typical AP recordings. Vertical line to the left of each AP shows phase-1 amplitude. P.V. indicates the point used to measure voltage at the onset of the plateau. C and D, Effects of E-4031 on APs at 1 Hz in control (C) and CHF (D) PCs. E and F, Effects of E-4031 on mean \pm SEM APD in 20 control (E) and 26 CHF (F) PCs. * $P < 0.05$, ** $P < 0.01$, *** $P < 0.001$ for difference between CHF and control PCs under corresponding conditions with respect to frequency and drug. CTL indicates control.

Comparison of AP Properties in Control and CHF PCs at 1 Hz

	Control (n=42)	CHF (n=37)
RP, mV	-80.5±0.8	-79.0±0.9
APA, mV	111.6±1.4	112.4±1.2
Plateau voltage, mV	2.7±1.4	9.0±1.4*
Phase 1, mV	28.5±1.0	24.4±0.8*
APD ₅₀ , ms	258±8	253±8
APD ₉₀ , ms	373±8	361±8

RP indicates resting potential; APA, AP amplitude; Phase 1, amplitude of phase 1; APD₅₀, APD to 50% repolarization; APD₉₀, APD to 90% repolarization. Plateau voltage was measured at onset of plateau, as shown in Figure 7.

* $P < 0.01$ compared with control.

plateau voltage was higher (Figure 7, top). There were no significant differences in resting potential, AP amplitude, or AP duration (APD) between control and CHF cells, but plateau-voltage was significantly more positive and phase 1 amplitude significantly smaller in CHF PCs (Table).

To evaluate the possibility that the response to an I_{Kr} -blocking class III drug may be altered in CHF PCs, APs were recorded from control and CHF PCs in free-running false tendons with standard microelectrodes before and after exposure to E-4031 (1 $\mu\text{mol/L}$). The results are illustrated in Figures 7C and 7D, and mean data are provided in Figures 7E and 7F. As in the first series of experiments, predrug APDs were not significantly different between control and CHF PCs. However, E-4031 had substantially larger effects on APD in CHF PCs, so that APD₉₅ after the drug was significantly greater in CHF cells at all frequencies ($P < 0.001$ for each). For example, E-4031-induced APD₉₅ increases averaged 103 ± 45 ms ($25 \pm 10\%$) at 1 Hz in control preparations compared with 231 ± 40 ms ($54 \pm 10\%$) in CHF preparations.

Discussion

We have evaluated the effects of CHF on K^+ currents, Ca^{2+} currents, NCX, and AP properties of PCs from free-running ventricular false tendons. CHF decreased PC I_{to} and I_{K1} density and slowed the inactivation of $I_{Ca,L}$ without altering its density. I_{Ks} , I_{Kr} , I_{NCX} , and $I_{Ca,T}$ were unaffected. CHF reduced the amplitude of phase 1 repolarization, increased plateau voltage, and enhanced the APD-prolonging effect of E-4031.

Comparison with Previous Studies of CHF-Induced Ionic Remodeling

There have been extensive studies of the ionic remodeling of K^+ and Ca^{2+} channels in ventricular myocytes of patients and experimental animals with CHF.^{5,18,19} I_{to} is quite consistently reduced^{5,20-22} by an average of $\approx 35\%$ in ventricular myocytes of patients with CHF.¹⁸ I_{K1} also tends to be decreased by $\approx 25\%$.¹⁸ Although there is some variability in the results for $I_{Ca,L}$,^{5,23} overall there seems to be no change in $I_{Ca,L}$ density or kinetics. Recent studies point to downregulation of I_{Ks} and possibly I_{Kr} in ventricular myocytes of rabbits with tachypacing-induced CHF.²⁴ Atrial ionic remodeling in CHF has been studied to a lesser extent, but recent studies suggest that I_{to} , I_{Ks} , and I_{Ca} are all decreased and I_{NCX} is increased, with

no change in kinetics or voltage dependence and no change in I_{K1} or I_{Kr} .⁶

Several aspects of PC ionic remodeling resemble previously reported findings in ventricular myocytes: I_{to} and I_{K1} were reduced and $I_{Ca,L}$ density was unchanged. These observations suggest that the mechanisms leading to CHF-induced I_{to} and I_{K1} downregulation at the ventricular level also likely operate on free-running Purkinje fiber false tendons. The CHF-induced slowing of I_{Ca} inactivation that we observed has not, to our knowledge, been reported in ventricular myocytes. We did not observe changes in I_{Kr} or I_{Ks} , suggesting that PCs may be spared from the I_{K} downregulation occurring with CHF in ventricular myocytes²⁴ and possibly explaining why overall APD was not prolonged in CHF PCs. Unlike typical findings in ventricular⁵ and atrial⁶ myocytes, I_{NCX} density was not increased by CHF in PCs.

Relationship to Other Studies in PCs

I_{to} , I_{Ca} , I_{K1} , and E-4031-sensitive current have been studied in PCs from the subendocardial Purkinje fiber network overlying 24- to 48-hour-old myocardial infarctions.¹⁰⁻¹² I_{to} density was reduced by $> 50\%$ in the infarct zone, with no change in voltage dependence but a slowing in reactivation.¹⁰ PCs from free-running false tendons had normal I_{to} properties. Both $I_{Ca,L}$ and $I_{Ca,T}$ were reduced in subendocardial PCs from the infarct zone, with no changes in voltage dependence or inactivation kinetics.¹¹ I_{K1} was reduced in PCs from the infarct zone, and a very rapidly activating E-4031-sensitive current was increased, with no classical I_{K} noted in either normal or infarct zone PCs.¹² In general, the abnormalities noted in infarct zone PCs were more severe than those we observed. There are, however, some qualitative similarities in terms of decreases in I_{K1} and I_{to} . In contrast to our findings, myocardial infarction did not affect the electrophysiology in PCs from free-running false tendons, suggesting that myocardial infarction produces severe but localized ionic remodeling in infarct zone PCs whereas CHF produces more generalized but less severe remodeling.

Potential Significance

The present study constitutes the first detailed analysis of CHF-induced ionic remodeling in PCs. PCs are believed to play an important role in ventricular arrhythmogenesis, particularly in the generation of early afterdepolarization-induced arrhythmias.^{7,8} The CHF-induced ionic abnormalities we noted in PCs may contribute to promoting the occurrence of arrhythmogenic afterdepolarizations in patients with CHF, particularly in response to interventions such as I_{Kr} -blocking antiarrhythmic drugs and hypokalemia that prolong APD. Downregulation of I_{to} , along with slowed inactivation of I_{Ca} , is likely responsible for the positive shift in the plateau voltage of PCs. The positive shift in plateau voltage and slowed $I_{Ca,L}$ inactivation at positive voltages would act to promote the occurrence of $I_{Ca,L}$ -dependent early afterdepolarizations under conditions that delay repolarization.²⁵

The CHF-induced decreases in I_{to} and I_{K1} are likely to reduce the repolarization reserve, the ability of myocardial cells to repolarize when normal repolarizing currents are reduced by drugs, metabolic or electrolyte imbalances, or

intercurrent diseases. Consistent with this notion, PCs from dogs with CHF showed twice as great APD prolongation in response to I_{Kr} blockade with E-4031 compared with control PCs. CHF significantly increases the risk of drug-induced Torsades de Pointes arrhythmias.³ The CHF-induced ionic remodeling that we observed in PCs could clearly play an important role in this clinically important phenomenon.

Potential Limitations

The isolation of PCs from free-running Purkinje fibers is technically challenging, requiring prolonged periods of bath exposure to cell-dissociating enzymes (chuck method). This likely explains the absence of studies of PC remodeling in CHF, despite the large number of studies that have evaluated ventricular myocyte remodeling. I_{Kr} is particularly sensitive to isolation technique²⁶ and has been difficult to record in isolated PCs.^{12,27} We were able to record robust I_{Kr} s in isolated PCs, but I_{Kr} was smaller and more difficult to record; therefore, our results regarding I_{Kr} should be interpreted with caution. The properties of the currents we recorded from normal PCs were generally similar to those reported for studies with other preparations; however, we cannot exclude the possibility that cell isolation might have affected the currents we evaluated. Isolation of PCs uncouples them from other PCs and from ventricular myocytes, removing an important modulator of electrophysiologic function present in vivo. This consideration does not apply to the multicellular preparations we studied, which maintain attachments to both false tendon PCs and underlying muscle intact. We measured currents in the presence of heavily buffered $[Ca^{2+}]_i$. $[Ca^{2+}]_i$ buffering was necessary to preserve cell viability under our recording conditions; however, CHF-induced changes in $[Ca^{2+}]_i$ could importantly affect currents like the NCX. Such changes would not have been detected in the present study.

Acknowledgments

This work was supported by operating grants from the Canadian Institutes for Health Research and the Quebec Heart and Stroke Foundation. Dr Li was a Heart and Stroke Corporation of Canada/AstraZeneca Fellow. The authors thank Essai and Pfizer Pharmaceuticals for providing E-4031 and dofetilide, Chantal St-Cyr and Chantal Maltais for technical assistance, and Annie Laprade for secretarial help.

References

- Nuss HB, Kaab S, Kass DA, et al. Cellular basis of ventricular arrhythmias and abnormal automaticity in heart failure. *Am J Physiol*. 1999;277:H80-H91.
- Cohn JN, Archibald DG, Ziesche S, et al. Effect of vasodilator therapy on mortality in chronic congestive heart failure: results of a Veterans Administration cooperative study. *N Engl J Med*. 1986;314:1547-1552.
- Lehmann MH, Hardy S, Archibald D, et al. Sex difference in risk of torsade de pointe with d,l-sotalolol. *Circulation*. 1996;94:2535-2541.
- Pak PH, Nuss HB, Tunin RS, et al. Repolarization abnormalities, arrhythmia and sudden death in canine tachycardia-induced cardiomyopathy. *J Am Coll Cardiol*. 1997;30:576-584.
- Tomaselli GF, Marbán E. Electrophysiological remodeling in hypertrophy and heart failure. *Cardiovasc Res*. 1999;42:270-283.
- Li D, Melnyk P, Feng J, et al. Effects of experimental heart failure on atrial cellular and ionic electrophysiology. *Circulation*. 2000;101:2631-2638.
- Nattel S, Quantz MA. Pharmacological response of quinidine induced early afterdepolarisations in canine cardiac Purkinje fibres: insights into underlying ionic mechanisms. *Cardiovasc Res*. 1988;22:808-817.
- El Sherif N, Caref EB, Yin H, et al. The electrophysiological mechanism of ventricular arrhythmias in the long QT syndrome: tridimensional mapping of activation and recovery patterns. *Circ Res*. 1996;79:474-492.
- Berenfeld O, Jalife J. Purkinje-muscle reentry as a mechanism of polymorphic ventricular arrhythmias in a 3-dimensional model of the ventricles. *Circ Res*. 1998;82:1063-1077.
- Jeck C, Pinto JM, Boyden PA. Transient outward currents in subendocardial Purkinje myocytes surviving in the 24 and 48 hr infarcted heart. *Circulation*. 1995;92:465-473.
- Boyden PA, Pinto JM. Reduced calcium currents in subendocardial Purkinje myocytes that survive in the 24- and 48-hour infarcted heart. *Circulation*. 1994;89:2747-2759.
- Pinto JM, Boyden PA. Reduced inward rectifying and increased E-4031-sensitive K^+ current density in arrhythmogenic subendocardial Purkinje myocytes from the infarcted heart. *J Cardiovasc Electrophysiol*. 1998;9:299-311.
- Han W, Wang Z, Nattel S. A comparison of transient outward currents in canine cardiac Purkinje cells and ventricular myocytes. *Am J Physiol*. 2000;279:H466-H474.
- Han W, Wang Z, Nattel S. Slow delayed rectifier current and repolarization in canine cardiac Purkinje cells. *Am J Physiol*. 2001;280:H1075-H1080.
- Hattori Y, Matsuda N, Kimura J, et al. Diminished function and expression of the cardiac Na^+-Ca^{2+} exchanger in diabetic rats: implication in Ca^{2+} overload. *J Physiol (Lond)*. 2000;527:85-94.
- Hirano Y, Fozzard HA, January CT. Characteristics of L- and T-type Ca^{2+} currents in canine cardiac Purkinje cells. *Am J Physiol*. 1989;256:H1478-H1492.
- Tseng GN, Boyden PA. Multiple types of Ca^{2+} currents in single canine Purkinje cells. *Circ Res*. 1989;65:1735-1750.
- Priebe L, Beuckelmann DJ. Simulation study of cellular electric properties in heart failure. *Circ Res*. 1998;82:1206-1223.
- Nabauer M, Kaab S. Potassium channel down-regulation in heart failure. *Cardiovasc Res*. 1998;37:324-334.
- Kaab S, Nuss HB, Chiamvimonvat N, et al. Ionic mechanism of action potential prolongation in ventricular myocytes from dogs with pacing-induced heart failure. *Circ Res*. 1996;78:262-273.
- Beuckelmann DJ, Nabauer M, Erdmann E. Alterations of K^+ currents in isolated human ventricular myocytes from patients with terminal heart failure. *Circ Res*. 1993;73:379-385.
- Thüringer D, Coulombe A, Deroubaix E, et al. Depressed transient outward current density in ventricular myocytes from cardiomyopathic Syrian hamsters of different ages. *J Mol Cell Cardiol*. 1996;28:387-401.
- Mukherjee R, Spinale FG. L-type calcium channel abundance and function with cardiac hypertrophy and failure: a review. *J Mol Cell Cardiol*. 1998;30:1899-1916.
- Tsuji Y, Ophof T, Kamiya K, et al. Pacing-induced heart failure causes a reduction of delayed rectifier potassium currents along with decreases in calcium and transient outward currents in rabbit ventricle. *Cardiovasc Res*. 2000;48:300-309.
- Viswanathan PC, Rudy Y. Pause induced early afterdepolarizations in the long QT syndrome: a simulation study. *Cardiovasc Res*. 1999;42:530-542.
- Yue L, Feng J, Li GR, et al. A characterization of transient outward and delayed rectifier currents in canine atrial myocytes: properties of currents and role of cell isolation methods. *Am J Physiol*. 1996;270:H2157-H21683.
- Cordeiro JM, Spitzer KW, Giles WR. Repolarizing K^+ currents in rabbit heart Purkinje cells. *J Physiol*. 1998;508:811-823.

CHARTER 6. GENERAL DISCUSSION

The present chapter will mainly focus on the novel findings of our studies, the significance of these findings and future directions of research.

6.1 Summary of novel findings in the thesis and significance of this work in context of the literature

Prior to the present thesis, there were no studies in the literature characterizing in detail the ionic properties of repolarizing currents in isolated PCs and comparing them directly with properties of VM. There were no studies of human PC electrophysiology, none examining PC ionic remodeling by CHF and no reports of ion-channel subunit expression in PCs. We have characterized repolarizing currents in canine cardiac PCs in terms of electrophysiology, molecular biology and pathophysiology. In particular, we have studied in detail the electrophysiological, pharmacological and molecular properties of canine Purkinje I_{to} in comparison to canine ventricular myocyte I_{to} . We also characterized K^+ currents in human PCs. In addition, we characterized a wide range of ion channel expression underlying Purkinje repolarization, and conducted the first detailed analyses of the potential role of I_{Ks} in abnormal repolarization-related arrhythmogenesis and CHF-induced ionic remodeling in PCs.

6.1.1 Unique properties and potential molecular basis of Purkinje I_{to}

As described in chapters 2-5, Purkinje fibers have very small mass (< 100 mg per dog heart). They also have a thick fibrous sheath, posing technical problems in terms of single cell isolation and single cell-based methodologies like immunocytochemistry. Consequently, relatively little work with modern patch clamp and molecular biological techniques has been done in PCs compared to the extensive studies performed in working myocytes.

The presence of I_{to} was first recognized in 1964 in cardiac multicellular preparations of PFs with the use of early dual-microelectrode voltage-clamp techniques (Deck and Trautwein 1964). Although Kenyon and Gibbons (1979a and 1979b) showed in 1979 that Purkinje I_{to} could be suppressed by the K^+ channel blockers 4-AP and TEA, and I_{to} recovery in PFs could be relatively slow, studies of multicellular PF preparations with

dual-microelectrode voltage-clamp were limited by great technical difficulty, potential problems of voltage control, and issues of slow (in the range of hours) and uneven distribution of drugs requiring diffusion across superfused multicellular preparations. A couple of patch-clamp studies were performed in canine subendocardial PCs (Jeck et al. 1995) and rabbit PCs from free-running false tendons (Cordeiro et al. 1998) showing a substantial I_{to} , with strong inhibition by 2mM 4AP. Neither studies performed detailed concentration–response analyses for TEA or 4AP effects on Purkinje I_{to} , direct comparisons between I_{to} properties in Purkinje and muscle tissues were not obtained, and the effects of probes like flecainide, oxidative stress, blood-depressing substance (BDS) or dendrotoxin (DTX) on Purkinje I_{to} were not assessed. Our results reveal that Purkinje I_{to} has some important properties differing from those of working myocytes, in that Purkinje I_{to} has slow inactivation and a large, very slowly recovering component, is more sensitive to 4AP, is sensitive to TEA, and inactivation is slowed by H_2O_2 , suggesting a different molecular basis from that of working myocyte I_{to} .

It is now clear that the Kv4.2 and / or Kv4.3 play a prominent role in encoding pore-forming I_{to} channel-subunits in mammalian working myocytes (Barry et al. 1998; Fiset et al. 1997; Dixon et al. 1996) and Kv1.4 also likely contributes to a slowly recovering I_{to} component in rabbit atrial myocytes (Wang et al. 1999), rat ventricular septum (Xu et al. 1999) and ferret ventricular subendocardium (Brahmajothi et al. 1999). However, the properties of Purkinje I_{to} do not match those of I_{to} carried by any of these cloned subunits. In particular, Purkinje I_{to} is sensitive to TEA, whereas I_{to} carried by Kv1.4 or Kv4 subunits is not. TEA sensitivity is a property of I_{to} -like current carried by Kv3.4 (Rettig et al. 1992; Schroter et al. 1991) but this subunit had not been known to be expressed in the heart.

We employed a combination of competitive RT-PCR, Western blot and immunocytochemistry to define the potential molecular composition of Purkinje I_{to} , using VM as the comparator tissue. We found that Kv4.3 protein is predominantly expressed and the immunostaining is stronger in VM, whereas Kv3.4 protein is predominantly expressed and the immunostaining is stronger in PFs. Kv1.4 expression is limited and Kv4.2 is undetectable. Interestingly, we also found that expression of KChIP2, the isoform 2 of Kv channel interacting proteins reportedly involved in the transmural heterogeneity of I_{to} in

canine and human hearts through interaction with Kv4 channels (An et al. 2000; Rosati et al. 2001), is around 25 fold higher in VM than PFs at the mRNA levels. These results indicate that Kv3.4 and low-level KCHIP2 expression may play an important role in PCs, contributing to the slowly recovering component of I_{to} and accounting for rate-dependent notch known for PFs.

Figure 1 is a summary of some important electrophysiological properties of the Purkinje cell repolarization and the underlying ionic and molecular basis based on our work.

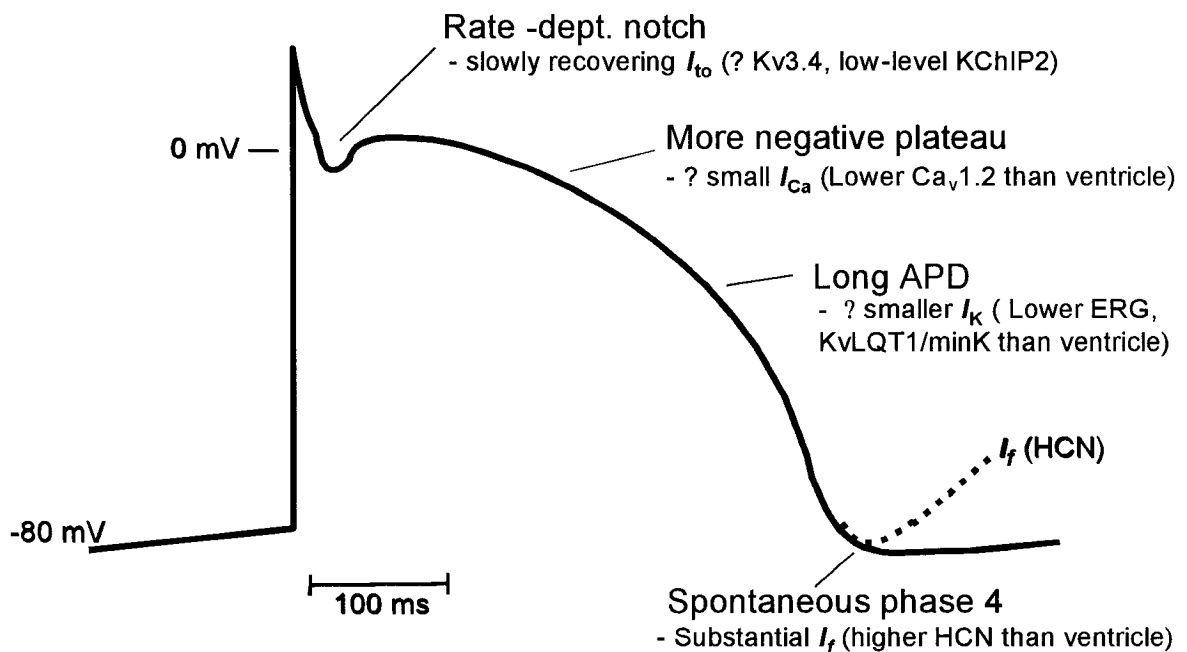


Figure 1. Ionic determinants of the Purkinje cell repolarization.

6.1.2 Characterization of some K^+ currents in human Purkinje cells

The only electrophysiological study in human PFs was performed by Dangman et al in 1982 with the use of standard microelectrode techniques and multicellular preparations. They found that the PFs from the hearts of five patients with CHF and coronary artery disease have a significantly bigger V_{max} than that of ventricular myocardium. Both epinephrine and digitalis-induced delayed afterdepolarizations were seen in human PFs, but not in the human ventricle. Clinical observations demonstrate that reentry initiated from (His)-Purkinje fibers is a mechanism of ventricular tachycardia (Lai et al. 1998; Blanck and Akhtar 1993; Nakagawa et al. 1993; Tada et al. 1998; Sasano et al. 1999; Tomokuni et al. 1998) and AV block in the Purkinje network is associated with the congenital LQT syndrome (Pruvot et al. 1999). However, prior to our work there has been no exploration of the ionic properties of human cardiac PCs.

Our results demonstrate that a substantial I_{to} is present in human PCs, with properties different from those of human ventricular I_{to} but similar to those of canine Purkinje I_{to} , suggesting a similar molecular basis of human Purkinje I_{to} to that of canine Purkinje I_{to} and different from those previously described in working atrium or ventricle. The detection of a large I_f in PCs but not in VM points to the ionic basis of pacemaking in human PCs. Our observation that I_{K1} is substantial in human PCs contradicts earlier results in rabbit (Cordeiro et al. 1998), with important potential implications for understanding excitability in human PCs. Finally, our demonstration of the apparent lack of a Kv1.5-equivalent current in PCs supports the notion of developing Kv1.5-blockers as human atrial-specific antiarrhythmic agents.

6.1.3 Demonstration of the presence of I_K in canine cardiac Purkinje cells and characterization of the expression profiles of Ca^{2+} , NCX and HCN channels

The presence of two forms of I_K , I_{Kr} and I_{Ks} has been demonstrated in SA node cells, atrial and ventricular myocytes of many species. However, the study of I_K in PCs has been proven to be much more difficult because I_K is particularly sensitive to the cell isolation process (Yue et al. 1996). In isolated rabbit PCs, Scamps and Carmeliet (1989) described a very small I_K without separating I_{Kr} and I_{Ks} , whereas Cordeiro et al (1998) failed to record I_K directly, despite the observation that APD was prolonged by specific

I_{Kr} and I_{Ks} blockers. In canine subendocardial PCs, Pinto and Boyden (1998) described a very rapidly activating E4030-sensitive current, with no properties of classical I_K .

We were able to show a clear but small I_{Kr} and robust I_{Ks} , with classical properties of I_{Kr} and I_{Ks} as noted in cardiac cells of other regions. The presence of I_K in our study, in contrast to the results of previous studies described above, may be due to species differences (rabbit vs dog) or to the sites from which cells are isolated (subendocardial vs false tendon Purkinje fibers). In addition, our detection of I_K electrophysiologically has been further strengthened by our molecular studies of I_K subunit expression. We have found HERG, KvLQT1 and minK are all expressed in PFs, albeit with significant lower protein levels than those in VM. These results suggest that I_{Kr} and I_{Ks} are present in PCs, but at lower levels than in VM, which may be important in explaining longer Purkinje fiber action potential durations (APDs) and their greater tendency to generate EADs.

We also characterized the expression profiles of Ca^{2+} , NCX1 and HCN channels. To our best knowledge, this is the first molecular study of ion channel subunit expression in PFs. Our results reveal that PFs have far less $Ca_v1.2$ protein expression than VM. This result may account for the less positive plateau of the AP in PFs (Fig 1), and is likely related to the much greater importance of contractile function in VM compared to PFs. NCX1, encoding the cardiac Na/Ca exchanger, was also significantly less expressed in PCs than VM. In addition to differences in absolute protein quantity, the distinct pattern of NCX1 immunolocalization in PCs compared to ventricular myocytes (localized to the membrane surface of PCs but absent in t-tubules) points to functionally important differences in subcellular localization. Purkinje fibers have greater expression of all cardiac isoforms of HCN channels than VM, consistent with the observation of a large I_f in previous reports (DiFrancesco 1981a; DiFrancesco 1981b) and our study of human PCs. This specialization of HCN expression is likely important for PC pacemaking function. In addition, Purkinje fibers have also greater expression of all three α subunits of T-type Ca^{2+} channels, in agreement with the recording of a large $I_{Ca,T}$ in PCs (Tseng and Boyden 1989), and consistent with the observation that T-type I_{Ca} tends to be differentially-expressed in pacemaking tissue (Schram et al. 2002).

6.1.4 Identification of I_{Ks} and potential role of I_{Ks} in abnormal repolarization-related arrhythmogenesis

We have demonstrated the presence of I_{Ks} in PCs where this current has been reported to be absent or small. We have also studied its potential role in PC repolarization, especially in the face of β -adrenergic stimulation. The importance of I_{Ks} in repolarization of APs has been reinforced by the demonstration of the importance of genetic defects in I_{Ks} channels in LQTS. Defects in KvLQT1, which encodes the pore-forming subunit of I_{Ks} channels, cause LQT1, in which the occurrence of Torsades de Pointes (TdP) ventricular tachyarrhythmias is particularly adrenergically-dependent (Wilde et al. 1999). Furthermore, β -adrenergic stimulation has been shown to cause a substrate for TdP in the presence of I_{Ks} inhibition with chromanol 293B (Shimizu and Antzelevitch 1998).

We have found that without β -adrenergic stimulation, I_{Ks} plays little role in PC repolarization, because little I_{Ks} is activated at the PC plateau voltage range of 0 mV. With β -adrenergic stimulation, I_{Ks} contributes to repolarization in order to balance the increased L-type I_{Ca} , thus it seems that an important role of I_{Ks} may act as a “brake” to prevent excessive APD prolongation in the face of β -adrenergic enhancement of I_{Ca} . Such a role of I_{Ks} is similar to the report of I_{Ks} “brake” function against excessive APD prolongation caused by I_{Kr} blockade (Varro et al. 2000). Our study leads us to speculate that lack of I_{Ks} in LQT1 may exaggerate β -adrenergic effects to delayed PC repolarization, leading to arrhythmogenesis.

6.1.5 Ionic remodeling of Purkinje cells by congestive heart failure

Congestive heart failure (CHF) is a very strong risk factor for LQT proarrhythmias. It has been reported there is a 3-fold increase in risk of LQT-associated TdP with I_{Kr} blockers (Lehmann et al. 1996) and a high incidence of lethal ventricular tachycardia (Bayes et al. 1989; Nuss et al. 1999; Packer 1985) in CHF patients. In diverse animal models, CHF has been shown to cause discrete atrial and ventricular ionic remodeling (Li et al. 2000; Nabauer and Kaab 1998; Tsuji et al. 2000) with a general pathophysiological hallmark of delayed repolarization. However, there is no information available about effects of CHF on cardiac Purkinje tissue.

We have investigated CHF effects on the repolarizing ionic currents and APs of PCs, as well as on the response to the I_{Kr} blocker E4031 in PFs. We found that CHF caused a significant reduction in I_{K1} and I_{to} without altering voltage-dependence and kinetics, consistent with observations in atrial and ventricular remodeling (Nabauer et al. 1993; Kaab et al. 1996; Schroder et al. 1998; Thuringer et al. 1996; Tomaselli and Marban 1999). Furthermore, CHF caused a slowing of I_{Ca} inactivation with no changes in density. Unlike findings regarding ionic remodeling of ventricular (Tsuji et al. 2000) and atrial (Li et al. 2000) myocytes, in which I_{Ks} and possibly I_{Kr} are decreased while I_{NCX} is increased, no changes in I_{Kr} , I_{Ks} and I_{NCX} were observed in CHF PCs, which may explain why overall APD was not prolonged in CHF PCs. However, when CHF PCs were exposed to E4031, the APs were prolonged twice as strongly as in normal PCs. Although CHF did not cause APD prolongation, CHF reduced “repolarization reserve” due to decreased I_{to} and I_{K1} , sensitized PCs to I_{Kr} blockade. As mentioned above, CHF significantly increases the risk of drug-induced Torsade de Pointes arrhythmias (Lehmann et al. 1996). It is therefore reasonable to speculate that the CHF-induced ionic remodeling in PCs could play an important role in this clinically important phenomenon.

6.2 Directions for future research

The present studies have helped to achieve a better understanding of PC molecular electrophysiology, but many important issues remain to be explored. Some that I feel to be key are outlined below.

6.2.1 Purkinje I_{to} and Kv3.4

We have obtained the evidence suggesting that Kv3.4 may play an important role in the molecular composition of Purkinje I_{to} channels. However, there are some observations that argue against this notion, including the fact that Kv3.4 sensitivity to TEA is about one order of magnitude greater than that of Purkinje I_{to} and that the specific Kv3.4 blocker BDS had no effect on Purkinje I_{to} .

It is known that nerve I_{Na} and cardiac I_{Na} are quite different in terms of kinetics, sensitivity to TTX, divalent ions such as Cd^{2+} and Zn^{2+} and the local anesthetic lidocaine. This is believed to be the case because nerve and cardiac I_{Na} are encoded by different

isoforms of Na⁺ channels. Kv3.4 was first cloned from brain (Rettig et al. 1992; Schroter et al. 1991) and later found to be expressed in skeletal muscle (Vullhorst et al. 1998). It is possible that there is a cardiac-specific Kv3.4 isoform. In fact, we have cloned and sequenced a partial-length cardiac Kv3.4 clone (339 bp) and shown that it is not fully identical to the brain form. We thus first hypothesize that the attributes of Purkinje I_{to} may be determined by a new isoform of Kv3.4. Another clue comes from a recent report (Abbott et al. 2001) that MiRP2 forms K⁺ channels with Kv3.4 in skeletal muscle and is associated with periodic paralysis, in which MiRP2 not only altered the voltage-dependent activation, single channel conductance and kinetics, and also changed the sensitivity of Kv3.4 channels to BDS; MiRP2-Kv3.4 channels was ~30-fold less sensitive to BDS than Kv3.4 channels alone. We can therefore suggest a second hypothesis that the attributes of Purkinje I_{to} may be due to coassembly of Kv3.4 with MiRP2-like accessory subunits.

Future studies should focus on cloning the full-length cardiac Kv3.4 subunit isoform, followed by heterologous expression and characterization. Yeast-2 hybridization should be used to screen and identify potential interacting proteins for Kv3.4. Once identified, those interacting proteins will need to be characterized biophysically and functionally. Eventually, heterologous expression of cardiac Kv3.4 alone and Kv3.4 with interacting proteins, characterization and comparison with native Purkinje I_{to} will be needed to further define the relation between the expressed currents and Purkinje I_{to} . This relation will finally need to be tested by the methods of specific antisense (Wang et al. 1999; Bou-Abboud and Nerbonne 1999), mutation or knockout (Barry et al. 1998; Kuo et al. 2001; London et al. 1998).

6.2.2 Molecular mechanisms underlying big maximal upstroke velocity (V_{max}) of Purkinje depolarization

Purkinje fibers (PFs) have a very big V_{max} upon depolarization. At physiological temperature, 300-600 V/s has been reported for PFs in animals (Munger et al. 1994; Fozzard 1993) and humans (Dangman et al. 1982), which is significantly greater than the value of 180-390 V/s for ventricular muscle (Dangman et al. 1982; Gintant and Liu 1992; Krishnan and Antzelevitch 1991). This phenomenon lends us to hypothesize that the

underlying molecular mechanism in PFs and VM may be different. It is known that inward I_{Na} is responsible for the fast depolarization of APs. A larger I_{Na} is believed to account for larger V_{max} in PFs. However, the molecular basis is not clear. As a first step, we have quantified the expression of the Na^+ channel α subunit- $Na_v1.5$ ($SCN5\alpha$). Our preliminary data show that the mRNA expression of $Na_v1.5$ in PFs is not different from that in VM. A specific anti- $Na_v1.5$ antibody is not commercially available. Western blot with anti-pan- Na^+ antibody unfortunately did not reveal any significant bands in PFs, suggesting Purkinje Na^+ channels may be different, so that they are not recognized by anti-pan- Na^+ antibody. Recently, a study of $Na_v1.5$ regional distribution in sheep heart showed that $Na_v1.5$ mRNA is more strongly expressed in left atria (LA), right atria (RA) and left ventricle (LV) than in PFs and right ventricle (RV). However, at the protein level, $Na_v1.5$ (measured with anti-pan- Na^+ antibody) is higher in LA and LV than in RA and RV- results for PF were not provided (Fahmi et al. 2001). Another study of regional $Na_v1.5$ immunolocalization in rat heart with specific rH1 (rat Na^+ channel α subunit) antibody showed that $Na_v1.5$ staining is localized to the surface membrane and t-tubular system and that there is no large variation across different regions, other than for somewhat enhanced labeling at the intercalated disks of ventricular myocytes. This localization is thought to be responsible for fast conduction in ventricular myocardium (Cohen 1996). More information is needed about the specific I_{Na} content (both qualitatively and quantitatively) in PFs, and the $Na_v1.5$ distribution in PFs and VM.

In addition, the expressions of all Na^+ channel-associated β subunits including $\beta1$, $\beta1A$, $\beta2$, and $\beta3$, needs to be characterized in PFs and compared with VM, because β subunits modify Na^+ channel expression and properties (An et al. 1998; Dhar et al. 2001; Fahmi et al. 2001; Kupersmidt et al. 1998; Makielski et al. 1996; Malhotra et al. 2000; Nuss et al. 1995; Qu et al. 1995)

Finally, the expression of atypical Na^+ channels (Na_x) will need to be investigated, because they are abundantly expressed in the heart (Felipe et al. 1994; George, Jr. et al. 1992; Plummer and Meisler 1999), although they are reportedly functionally quiescent (Akopian et al. 1997; George, Jr. et al. 1992). Atypical Kv channels such as Kv5.1, Kv6.1, Kv8 and Kv9 associate with Kv2.1 channels and alter their biophysical properties

(Kramer et al. 1998; Salinas et al. 1997), similar mechanisms may operate for Na⁺ channels.

6.2.3 Molecular mechanisms underlying ionic remodeling of Purkinje cells by congestive heart failure.

To understand the molecular mechanisms of Purkinje ionic remodeling, a comparison of mRNA expressions of ion channels between control and CHF PCs is first required. A comparison of ion channel subunit protein expression will also be needed, because of the effects of post-transcriptional and translation modulation. Finally subcellular distributions should be studied because the trafficking and insertion of ion channel proteins to the surface membrane may be changed (Baroudi et al. 2001).

6.3 General conclusions

Cardiac Purkinje fibers have a variety of unique ionic properties important for their specialized function and role in arrhythmogenesis. However, much remains to be explored. An improved understanding of Purkinje fiber molecular electrophysiology may provide new insights into the prevention of lethal cardiac arrhythmias

6.4 References

- Abbott, G. W., Butler, M. H., Bendahhou, S., Dalakas, M. C., Ptacek, L. J., and Goldstein, S. A. (2001). MiRP2 forms potassium channels in skeletal muscle with Kv3.4 and is associated with periodic paralysis. *Cell* **104**, 217-231.
- Akopian, A. N., Souslova, V., Sivillotti, L., and Wood, J. N. (1997). Structure and distribution of a broadly expressed atypical sodium channel. *FEBS Lett.* **400**, 183-187.
- An, R. H., Wang, X. L., Kerem, B., Benhorin, J., Medina, A., Goldmit, M., and Kass, R. S. (1998). Novel LQT-3 mutation affects Na⁺ channel activity through interactions between alpha- and beta1-subunits. *Circ.Res.* **83**, 141-146.
- An, W. F., Bowlby, M. R., Betty, M., Cao, J., Ling, H. P., Mendoza, G., Hinson, J. W., Mattsson, K. I., Strassle, B. W., Trimmer, J. S., and Rhodes, K. J. (2000). Modulation of A-type potassium channels by a family of calcium sensors. *Nature* **403**, 553-556.
- Baroudi, G., Pouliot, V., Denjoy, I., Guicheney, P., Shrier, A., and Chahine, M. (2001). Novel mechanism for Brugada syndrome: defective surface localization of an SCN5A mutant (R1432G). *Circ.Res.* **88**, E78-E83.
- Barry, D. M., Xu, H., Schuessler, R. B., and Nerbonne, J. M. (1998). Functional knockout of the transient outward current, long-QT syndrome, and cardiac remodeling in mice expressing a dominant-negative Kv4 alpha subunit. *Circ.Res.* **83**, 560-567.
- Bayes, d. L., Coumel, P., and Leclercq, J. F. (1989). Ambulatory sudden cardiac death: mechanisms of production of fatal arrhythmia on the basis of data from 157 cases. *Am.Heart J.* **117**, 151-159.
- Blanck, Z. and Akhtar, M. (1993). Ventricular tachycardia due to sustained bundle branch reentry: diagnostic and therapeutic considerations. *Clin.Cardiol.* **16**, 619-622.
- Bou-Abboud, E. and Nerbonne, J. M. (1999). Molecular correlates of the calcium-independent, depolarization- activated K⁺ currents in rat atrial myocytes. *J.Physiol* **517** (Pt 2), 407-420.
- Brahmajothi, M. V., Campbell, D. L., Rasmusson, R. L., Morales, M. J., Trimmer, J. S., Nerbonne, J. M., and Strauss, H. C. (1999). Distinct transient outward potassium current (I_{to}) phenotypes and distribution of fast-inactivating potassium channel alpha subunits in ferret left ventricular myocytes. *J.Gen.Physiol* **113**, 581-600.
- Cohen, S. A. (1996). Immunocytochemical localization of rHI sodium channel in adult rat heart atria and ventricle. Presence in terminal intercalated disks. *Circulation* **94**, 3083-3086.
- Cordeiro, J. M., Spitzer, K. W., and Giles, W. R. (1998). Repolarizing K⁺ currents in rabbit heart Purkinje cells. *J.Physiol* **508** (Pt 3), 811-823.
- Dangman, K. H., Danilo, P., Jr., Hordof, A. J., Mary-Rabine, L., Reder, R. F., and Rosen, M. R. (1982). Electrophysiologic characteristics of human ventricular and Purkinje fibers. *Circulation* **65**, 362-368.

- Deck, K.A. and Trautwein, W.** (1964). Ionic currents in cardiac excitation. *Pflügers.Arch.* **280**, 63- 80.
- Dhar, M. J., Chen, C., Rivolta, I., Abriel, H., Malhotra, R., Mattei, L. N., Brosius, F. C., Kass, R. S., and Isom, L. L.** (2001). Characterization of sodium channel alpha- and beta-subunits in rat and mouse cardiac myocytes. *Circulation* **103**, 1303-1310.
- DiFrancesco, D.** (1981a). A new interpretation of the pace-maker current in calf Purkinje fibres. *J.Physiol* **314**, 359-376.
- DiFrancesco, D.** (1981b). A study of the ionic nature of the pace-maker current in calf Purkinje fibres. *J.Physiol* **314**, 377-393.
- Dixon, J. E., Shi, W., Wang, H. S., McDonald, C., Yu, H., Wymore, R. S., Cohen, I. S., and McKinnon, D.** (1996). Role of the Kv4.3 K⁺ channel in ventricular muscle. A molecular correlate for the transient outward current. *Circ.Res.* **79**, 659-668.
- Fahmi, A. I., Patel, M., Stevens, E. B., Fowden, A. L., John, J. E., Lee, K., Pinnock, R., Morgan, K., Jackson, A. P., and Vandenberg, J. I.** (2001). The sodium channel beta-subunit SCN3b modulates the kinetics of SCN5a and is expressed heterogeneously in sheep heart. *J.Physiol* **537**, 693-700.
- Felipe, A., Knittle, T. J., Doyle, K. L., and Tamkun, M. M.** (1994). Primary structure and differential expression during development and pregnancy of a novel voltage-gated sodium channel in the mouse. *J.Biol.Chem.* **269**, 30125-30131.
- Fiset, C., Clark, R. B., Shimoni, Y., and Giles, W. R.** (1997). Shal-type channels contribute to the Ca²⁺-independent transient outward K⁺ current in rat ventricle. *J.Physiol* **500** (Pt 1), 51-64.
- Fozzard, HA.** (1993). Cardiac electrogenesis and the sodium channel. In Spooner PM, Brown AM, Catterall WA, Kaczorowski GJ, and Strauss HC, eds. Ion channel in the cardiovascular system, Function and dysfunction, New York, Future Publishing Company, Inc. 81-100.
- George, A. L., Jr., Knittle, T. J., and Tamkun, M. M.** (1992). Molecular cloning of an atypical voltage-gated sodium channel expressed in human heart and uterus: evidence for a distinct gene family. *Proc.Natl.Acad.Sci.U.S.A* **89**, 4893-4897.
- Gintant, G. A. and Liu, D. W.** (1992). Beta-adrenergic modulation of fast inward sodium current in canine myocardium. Syncytial preparations versus isolated myocytes. *Circ.Res.* **70**, 844-850.
- Jeck, C., Pinto, J., and Boyden, P.** (1995). Transient outward currents in subendocardial Purkinje myocytes surviving in the infarcted heart. *Circulation* **92**, 465-473.
- Kaab, S., Nuss, H. B., Chiamvimonvat, N., O'Rourke, B., Pak, P. H., Kass, D. A., Marban, E., and Tomaselli, G. F.** (1996). Ionic mechanism of action potential prolongation in ventricular myocytes from dogs with pacing-induced heart failure. *Circ.Res.* **78**, 262-273.
- Kenyon, J. L. and Gibbons, W. R.** (1979b). 4-Aminopyridine and the early outward current of sheep cardiac Purkinje fibers. *J.Gen.Physiol* **73**, 139-157.

- Kenyon, J. L. and Gibbons, W. R. (1979a).** Influence of chloride, potassium, and tetraethylammonium on the early outward current of sheep cardiac Purkinje fibers. *J.Gen. Physiol* **73**, 117-138.
- Kramer, J. W., Post, M. A., Brown, A. M., and Kirsch, G. E. (1998).** Modulation of potassium channel gating by coexpression of Kv2.1 with regulatory Kv5.1 or Kv6.1 alpha-subunits. *Am.J.Physiol* **274**, C1501-C1510.
- Krishnan, S. C. and Antzelevitch, C. (1991).** Sodium channel block produces opposite electrophysiological effects in canine ventricular epicardium and endocardium. *Circ.Res.* **69**, 277-291.
- Kuo, H. C., Cheng, C. F., Clark, R. B., Lin, J. J., Lin, J. L., Hoshijima, M., Nguyen-Tran, V. T., Gu, Y., Ikeda, Y., Chu, P. H., Ross, J., Giles, W. R., and Chien, K. R. (2001).** A defect in the Kv channel-interacting protein 2 (KCHIP2) gene leads to a complete loss of I(to) and confers susceptibility to ventricular tachycardia. *Cell* **107**, 801-813.
- Kupershmidt, S., Yang, T., and Roden, D. M. (1998).** Modulation of cardiac Na⁺ current phenotype by beta1-subunit expression. *Circ.Res.* **83**, 441-447.
- Lai, L. P., Lin, J. L., Hwang, J. J., and Huang, S. K. (1998).** Entrance site of the slow conduction zone of verapamil-sensitive idiopathic left ventricular tachycardia: evidence supporting macroreentry in the Purkinje system. *J.Cardiovasc.Electrophysiol.* **9**, 184-190.
- Lehmann, M. H., Hardy, S., Archibald, D., quart, B., and MacNeil, D. J. (1996).** Sex difference in risk of torsade de pointes with d,l-sotalol. *Circulation* **94**, 2535-2541.
- Li, D., Melnyk, P., Feng, J., Wang, Z., Petrecca, K., Shrier, A., and Nattel, S. (2000).** Effects of experimental heart failure on atrial cellular and ionic electrophysiology. *Circulation* **101**, 2631-2638.
- London, B., Wang, D. W., Hill, J. A., and Bennett, P. B. (1998).** The transient outward current in mice lacking the potassium channel gene Kv1.4. *J.Physiol* **509** (Pt 1), 171-182.
- Makielski, J. C., Limberis, J. T., Chang, S. Y., Fan, Z., and Kyle, J. W. (1996).** Coexpression of beta 1 with cardiac sodium channel alpha subunits in oocytes decreases lidocaine block. *Mol.Pharmacol.* **49**, 30-39.
- Malhotra, J. D., Kazen-Gillespie, K., Hortsch, M., and Isom, L. L. (2000).** Sodium channel beta subunits mediate homophilic cell adhesion and recruit ankyrin to points of cell-cell contact. *J.Biol.Chem.* **275**, 11383-11388.
- Munger, T. M., Johnson, S. B., and Packer, D. L. (1994).** Voltage dependence of beta-adrenergic modulation of conduction in the canine Purkinje fiber. *Circ.Res.* **75**, 511-519.
- Nabauer, M., Beuckelmann, D. J., and Erdmann, E. (1993).** Characteristics of transient outward current in human ventricular myocytes from patients with terminal heart failure. *Circ.Res.* **73**, 386-394.
- Nabauer, M. and Kaab, S. (1998).** Potassium channel down-regulation in heart failure. *Cardiovasc.Res.* **37**, 324-334.

- Nakagawa, H., Beckman, K. J., McClelland, J. H., Wang, X., Arruda, M., Santoro, I., Hazlitt, H. A., Abdalla, I., Singh, A., Gossinger, H., and .** (1993). Radiofrequency catheter ablation of idiopathic left ventricular tachycardia guided by a Purkinje potential. *Circulation* **88**, 2607-2617.
- Nuss, H. B., Chiamvimonvat, N., Perez-Garcia, M. T., Tomaselli, G. F., and Marban, E.** (1995). Functional association of the beta 1 subunit with human cardiac (hH1) and rat skeletal muscle (μ 1) sodium channel alpha subunits expressed in *Xenopus* oocytes. *J.Gen.Physiol* **106**, 1171-1191.
- Nuss, H. B., Kaab, S., Kass, D. A., Tomaselli, G. F., and Marban, E.** (1999). Cellular basis of ventricular arrhythmias and abnormal automaticity in heart failure. *Am.J.Physiol* **277**, H80-H91.
- Packer, M.** (1985). Sudden unexpected death in patients with congestive heart failure: a second frontier. *Circulation* **72**, 681-685.
- Pinto, J. M. and Boyden, P. A.** (1998). Reduced inward rectifying and increased E-4031-sensitive K^+ current density in arrhythmogenic subendocardial Purkinje myocytes from the infarcted heart. *J.Cardiovasc. Electrophysiol.* **9**, 299-311.
- Plummer, N. W. and Meisler, M. H.** (1999). Evolution and diversity of mammalian sodium channel genes. *Genomics* **57**, 323-331.
- Pruvot, E., De Torrente, A., De Ferrari, G. M., Schwartz, P. J., and Goy, J. J.** (1999). Two-to-one AV block associated with the congenital long QT syndrome. *J.Cardiovasc.Electrophysiol.* **10**, 108-113.
- Qu, Y., Isom, L. L., Westenbroek, R. E., Rogers, J. C., Tanada, T. N., McCormick, K. A., Scheuer, T., and Catterall, W. A.** (1995). Modulation of cardiac Na^+ channel expression in *Xenopus* oocytes by beta 1 subunits. *J.Biol.Chem.* **270**, 25696-25701.
- Rettig, J., Wunder, F., Stocker, M., Lichtinghagen, R., Mastiaux, F., Beckh, S., Kues, W., Pedarzani, P., Schroter, K. H., Ruppertsberg, J. P., and .** (1992). Characterization of a Shaw-related potassium channel family in rat brain. *EMBO J.* **11**, 2473-2486.
- Rosati, B., Pan, Z., Lypen, S., Wang, H. S., Cohen, I., Dixon, J. E., and McKinnon, D.** (2001). Regulation of KChIP2 potassium channel beta subunit gene expression underlies the gradient of transient outward current in canine and human ventricle. *J.Physiol* **533**, 119-125.
- Salinas, M., Duprat, F., Heurteaux, C., Hugnot, J. P., and Lazdunski, M.** (1997). New modulatory alpha subunits for mammalian Shab K^+ channels. *J.Biol.Chem.* **272**, 24371-24379.
- Sasano, T., Okishige, K., Azegami, K., Ohira, H., Yamashita, K., and Satake, S.** (1999). Transient complete atrioventricular block provoked by ventricular pacing in a patient with nonsustained ventricular tachycardia. *J.Electrocardiol.* **32**, 185-190.
- Scamps, F. and Carmeliet, E.** (1989). Delayed K^+ current and external K^+ in single cardiac Purkinje cells. *Am.J.Physiol* **257**, C1086-C1092.

- Schram, G., Pourrier, M., Melnyk, P., and Nattel, S. (2002). Differential distribution of cardiac ion channel expression as a basis for regional specialization in electrical function. *Circ.Res.* **90**, 939-950.
- Schroder, F., Handrock, R., Beuckelmann, D. J., Hirt, S., Hullin, R., Priebe, L., Schwinger, R. H., Weil, J., and Herzig, S. (1998). Increased availability and open probability of single L-type calcium channels from failing compared with nonfailing human ventricle. *Circulation* **98**, 969-976.
- Schroter, K. H., Ruppertsberg, J. P., Wunder, F., Rettig, J., Stocker, M., and Pongs, O. (1991). Cloning and functional expression of a TEA-sensitive A-type potassium channel from rat brain. *FEBS Lett.* **278**, 211-216.
- Shimizu, W. and Antzelevitch, C. (1998). Cellular basis for the ECG features of the LQT1 form of the long-QT syndrome: effects of beta-adrenergic agonists and antagonists and sodium channel blockers on transmural dispersion of repolarization and torsade de pointes. *Circulation* **98**, 2314-2322.
- Tada, H., Nogami, A., Naito, S., Tomita, T., Oshima, S., Taniguchi, K., Aonuma, K., and Iesaka, Y. (1998). Retrograde Purkinje potential activation during sinus rhythm following catheter ablation of idiopathic left ventricular tachycardia. *J.Cardiovasc.Electrophysiol.* **9**, 1218-1224.
- Thuringer, D., Coulombe, A., Deroubaix, E., Coraboeuf, E., and Mercadier, J. J. (1996). Depressed transient outward current density in ventricular myocytes from cardiomyopathic Syrian hamsters of different ages. *J.Mol.Cell Cardiol.* **28**, 387-401.
- Tomaselli, G. F. and Marban, E. (1999). Electrophysiological remodeling in hypertrophy and heart failure. *Cardiovasc.Res.* **42**, 270-283.
- Tomokuni, A., Igawa, O., Yamanouchi, Y., Adachi, M., Suga, T., Yano, A., Miake, J., Inoue, Y., Fujita, S., Hisatome, I., and Shigemasa, C. (1998). Idiopathic left ventricular tachycardia with block between purkinje potential and ventricular myocardium. *Pacing Clin.Electrophysiol.* **21**, 1824-1827.
- Tseng, G. N. and Boyden, P. A. (1989). Multiple types of Ca²⁺ currents in single canine Purkinje cells. *Circ.Res.* **65**, 1735-1750.
- Tsuji, Y., Opthof, T., Kamiya, K., Yasui, K., Liu, W., Lu, Z., and Kodama, I. (2000). Pacing-induced heart failure causes a reduction of delayed rectifier potassium currents along with decreases in calcium and transient outward currents in rabbit ventricle. *Cardiovasc.Res.* **48**, 300-309.
- Varro, A., Balati, B., Iost, N., Takacs, J., Virag, L., Lathrop, D. A., Csaba, L., Talosi, L., and Papp, J. G. (2000). The role of the delayed rectifier component IKs in dog ventricular muscle and Purkinje fibre repolarization. *J.Physiol* **523 Pt 1**, 67-81.
- Vullhorst, D., Klocke, R., Bartsch, J. W., and Jockusch, H. (1998). Expression of the potassium channel KV3.4 in mouse skeletal muscle parallels fiber type maturation and depends on excitation pattern. *FEBS Lett.* **421**, 259-262.

- Wang, Z., Feng, J., Shi, H., Pond, A., Nerbonne, J. M., and Nattel, S. (1999).** Potential molecular basis of different physiological properties of the transient outward K⁺ current in rabbit and human atrial myocytes. *Circ.Res.* **84**, 551-561.
- Wilde, A. A., Jongbloed, R. J., Doevendans, P. A., Duren, D. R., Hauer, R. N., van Langen, I. M., van Tintelen, J. P., Smeets, H. J., Meyer, H., and Geelen, J. L. (1999).** Auditory stimuli as a trigger for arrhythmic events differentiate HERG- related (LQTS2) patients from KVLQT1-related patients (LQTS1). *J.Am.Coll.Cardiol.* **33**, 327-332.
- Xu, H., Guo, W., and Nerbonne, J. M. (1999).** Four kinetically distinct depolarization-activated K⁺ currents in adult mouse ventricular myocytes. *J.Gen.Physiol* **113**, 661-678.
- Yue, L., Feng, J., Li, G. R., and Nattel, S. (1996).** Transient outward and delayed rectifier currents in canine atrium: properties and role of isolation methods. *Am.J.Physiol* **270**, H2157-H2168.



Hotmail®

wshanj1@hotmail.com

Inbox | Previous Page

From : Dennis Martin
To : 'wei Han' <wsl
Subject : RE: PERMISSIONS REQUEST again
Date : Tue, 17 Dec 2002 08:57:07 -0600

Thank you for your recent copyright permissions request. We have received your request for the journal articles. I have forwarded this onto our scientific publications for approval. You should hear from them in a few days. Thank you for your patience.

Dennis Martin
Copyright Permissions Coordinator

-----Original Message-----
From: wei Han [mailto:wsl
Sent: Tuesday, December 17, 2002 8:46 AM
To: I
Subject: PERMISSIONS REQUEST again

Dear Dennis Martin,

I wondered if you received my request dated on Dec 4, 2002 (more than 10 business days already). I could not get the certificate of acceptability of the thesis until I get your copyright permission. If I don't get the certificate, I can't register as postdoc, and consequently my postdoc fellowship can't be activated and it will be void after 1 Jan. 2003. So, could you please to consider my case and process as soon as possible?

I greatly appreciate you.

Wei Han

Protect your PC - get McAfee.com VirusScan Online
<http://clinic.mcafee.com/clinic/ibuy/campaign.asp?cid=3963>

**Order Confirmation
Republication Licensing Service
Copyright Clearance Center**

RECEIVED

02/20/2003

Account Name: WEI HAN
Order Number: 913529
Date to be Published: 01/15/2003

Account Number: 2000133448
Order Date: 12/4/2002
Est. Invoice Date: 2/2/2003

Document Reference:

Title: MOLECULAR ELECTROPHYSIOLOGY UNDERLYING REPOLARIZATION IN CANINE CARDIAC PURKINJE CELLS: CHARACTERIZATION AND SIGNIFICANCE

Publisher Name: MCGILL UNIVERSITY

Republication Format: Dissertation

Circulation/Distribution: 2

Order Detail Number: 9180103

Requested Title: AMERICAN JOURNAL OF PHYSIOLOGY. HEART AND CIRCULATORY PHYSIOLOGY

Requested Content: Full Article

Content Description: PROPERTIES OF POTASSIUM CURRENTS IN PURK

From: 2495 **To:** 2503

Response Status: Yes

Total Fee: \$0.00

Order Detail Number: 9180168

Requested Title: AMERICAN JOURNAL OF PHYSIOLOGY. HEART AND CIRCULATORY PHYSIOLOGY

Requested Content: Figure

Content Description: FIG1-7 AND TABLE1

From: 2495 **To:** 2503

Response Status: Yes

Total Fee: \$0.00

Order Detail Number: 9180178

Requested Title: AMERICAN JOURNAL OF PHYSIOLOGY. HEART AND CIRCULATORY PHYSIOLOGY

Requested Content: Full Article

Content Description: SLOW DELAYED RECTIFIER CURRENT AND REPOL

From: 1075 **To:** 1080

Response Status: Yes

Total Fee: \$0.00

Order Detail Number: 9180194

Requested Title: AMERICAN JOURNAL OF PHYSIOLOGY. HEART AND CIRCULATORY PHYSIOLOGY

Requested Content: Figure

Content Description: FIG1-5

From: 1075 **To:** 1080

Response Status: Yes

Total Fee: \$0.00

Order Detail Number: 9180220

Requested Title: AMERICAN JOURNAL OF PHYSIOLOGY. HEART AND CIRCULATORY PHYSIOLOGY

Requested Content: Full Article

Content Description: A COMPARISON OF TRANSIENT OUTWARD CURREN

From: 466 **To:** 474

Response Status: Yes

Total Fee: \$0.00

Order Detail Number: 9180230

Requested Title: AMERICAN JOURNAL OF PHYSIOLOGY. HEART AND CIRCULATORY PHYSIOLOGY

Requested Content: Figure

Content Description: FIG1-10

From: 466.

To: 474

Response Status: Yes

Total Fee: \$0.00